Agro-ecological control of a spatio-temporal parasite-host system. Preventing spreading and optimising the harvest.

Baptiste Maucourt

Institut Camille Jordan

Laboratoire de recherche en mathématiques Lyon/Saint-Étienne

Contrôle agro-écologique d'un système parasite-hôte spatio-temporel

Prévention de la propagation et optimisation de la récolte

Baptiste Maucourt

Thèse de doctorat

Université Claude Bernard Lyon 1

Université Claude Bernard Lyon 1
École doctorale **InfoMath**, ED 512
Spécialité : **Mathématiques**

Agro-ecological control of a spatio-temporal parasite-host system

Preventing spreading and optimising the harvest

Thèse de doctorat

Soutenue publiquement le 11 juillet 2024 par

Baptiste Maucourt

devant le Jury composé de:

Mme Magali Ribot	Université d'Orléans	Rapporteuse
M. Nicolas Vauchelet	Université Sorbonne Paris Nord	Rapporteur
M. Bastien Boussau	CNRS Lyon	
Mme Cécile Carrère	Université d'Orléans	
Mme Anne-Laure Fougères	Université Lyon 1	
M. Léo Girardin	CNRS Lyon	
M. Thomas Lepoutre	INRIA Lyon	Directeur de thèse
M. Idriss Mazari	Université Paris-Dauphine	

Remerciements

S'il y a une chose importante que ces trois ans de thèse m'ont appris, c'est qu'une thèse, ça ne se fait pas tout seul, au sens propre comme figuré. Que ce soit vos encadrants, vos collègues, vos amis, votre famille, les rencontres faites au cours de divers conférences, professionnelles ou amicales, et même les actuels ou anciens mathématiciens experts de votre domaine que vous ne rencontrerez jamais, via la bibliographie qu'ils mettront à votre disposition ; tous vous aideront à leur manière à arriver au bout de votre thèse.

Je tente alors ici de leur rendre un minuscule fragment de ce que ces personnes m'ont apporté, en leur écrivant, chaudement et sincèrement, merci.

À mon premier encadrant, Léo Girardin. Tu as su porter cette thèse et son doctorant avec brio et professionnalisme, au travers toutes ses difficultés. Il va sans dire que sans toi, cette thèse n'existerait pas. J'ai conscience qu'encadrer quelqu'un comme moi ne doit pas être tâche aisée ; tu l'as pourtant fait, tu m'as transmis ta motivation, même dans les moments les plus difficiles, où la mienne me paraissait bien loin. Tu t'es tellement investi ! Dès les premiers jours de stage, dans un contexte particulier de confinement, tu m'as accompagné avec patience et pédagogie dans la théorie des mathématiques que j'allais utiliser. Tu t'es montré disponible au-delà de mes espérances et prêt à répondre à mes questions avec une bienveillance que j'admire. Tu as continué sans relâche, au cours de ces trois ans, à m'accompagner avec excellence dans cette thèse, à passer des après-midi avec moi au tableau de ton bureau, à m'orienter vers les bonnes pistes, les bonnes références, les bonnes personnes, à m'aider à naviguer dans l'administration parfois longue et répétitive, à m'indiquer les conférences les plus adéquates, allant même jusqu'à me présenter à de grands noms que je n'aurai sinon jamais osé aborder, et à me prouver, via notre travail accompli, que je suis moi aussi capable d'apporter ma pierre, si petite soit-elle, à l'édifice. Tu m'as montré, petit à petit, le chemin vers l'indépendance dans la recherche. Travailler avec toi a été une expérience formidable. Je suis heureux et fier d'avoir été ton doctorant.

À mes deux autres encadrants, Bastien Boussau et Thomas Lepoutre. Bastien, pour ton expertise et tes connaissances biologiques évidemment, mais aussi pour ta gentillesse et ta bienveillance. Merci d'avoir donné vie au projet, de m'avoir fait confiance lors de notre premier entretien, et de m'avoir même suivi dans une analyse que j'aurais été incapable de conduire seul, et qui trouvera peut-être (qui sait ?) un point final lors d'une prochaine aventure thésienne. Thomas, pour tes généreux conseils et ton expérience, accompagnés de ta présence chaleureuse. Tu as apporté à cette thèse le regard neuf et aiguisé dont elle avait besoin.

Aux membres de mon jury de thèse, Magali Ribot, Nicolas Vauchelet, Anne-Laure Fougères, Cécile Carrère, et Idriss Mazari pour avoir pris le temps de lire ce manuscrit et d'assister à ma soutenance. Votre temps est précieux et je suis honoré que vous m'en accordiez. À mon

comité de suivi, Louis Dupaigne et Jérôme Coville, pour vos commentaires enrichissants, et l'inspiration qu'ils m'ont donné pour progresser dans ma recherche.

Au bureau 109E, mes plus proches collègues et amis de ces dernières années. Merci d'avoir égayé toutes mes journées, et transformé mes matinées de flemme en hâte de me rendre au laboratoire pour vous voir. Luca (s ?), ta bonne humeur et gentillesse sont un réconfort au quotidien (ton rire restera gravé dans ma mémoire pendant longtemps !). Wissam, pour reprendre les mots d'un grand ami, tu es le soleil du 109E. J'ai pu découvrir avec joie ton sens de l'humour ces derniers mois, et toi aussi, tu vas me manquer. Mariane, pour une fois, je ne moquerai ! Je n'oublierai pas tous ces dramas, les funny blagues, et bien sûr le chaos. Merci pour ta présence aussi divertissante qu'indispensable. Thibault, j'ai hésité à ne rien écrire du tout, puisque que tu ne vas peut-être pas lire ceci. Au cas où, prépare-toi, ça va être cringe. Je n'ai pas besoin de tout écrire, il y a des choses qui se communiquent autrement. Tu es de loin la personne avec qui je me suis le plus rapproché cette année. Je devrais aussi remercier Terraria par la même occasion... Je ne pensais pas trouver en toi, la première fois que je t'ai rencontré, un meilleur ami. Et pourtant, plus j'apprends à te connaître, plus j'aime te connaître. Merci d'être là.

Aux doctorants du bâtiment Braconnier. À Simon, pour avoir été mon grand frère de thèse. Pour m'avoir redonné goût aux échecs et avoir été le premier à initier la pause post-domus (qui je l'espère, se perpétuera de génération en génération !). Merci pour ton amitié généreuse et sincère. À Louna, mon ancienne co-bureau 131, pour avoir animé les journées un peu solitaire de l'époque. Merci d'avoir organisé toutes ces belles soirées libanaises, je n'oublierai pas tous ces bons plats (sauf le Knafé). À Tibo, pour m'avoir offert ta présence complice durant ces longues après-midi, et tes bonnes idées pour craquer n'importe quel exo. J'aurais aimé grimper avec toi, maintenant que j'y pense ! À Sébastien, pour ta gentillesse, ta bonté, ta présence et tes mots réconfortants, lorsque j'avais le plus besoin de les entendre. À Docteure Louise, même si elle n'est pas en Braconnier mais presque, de me forcer à sortir, et à ta fat relecture / commentaires marrants dont mon manuscrit avait besoin (j'ai même pas eu le choix). À la team pause, Goumgoum, Pablito, Yvono, Antwain, Nouti, Rémi, Martín, Moxmox, Fanch (cimer pour l'image), Matthieu, Luca, Lorenzo, Paul, Layoush, Raphaël et les autres. Merci d'apporter la vie dans ce bureau, merci de rendre le quotidien si agréable.

Aux rencontres que j'ai pu faire pendant les conférences auxquelles j'ai assisté à Paris, Marseille, Toulouse, Héraklion : Luis Almeida, merci pour ton entrain et ton intérêt pour mon sujet, Idriss Mazari pour avoir répondu à mes nombreux appels à l'aide à Paris, par téléphone, et par mail, Grégoire Nadin pour ta précieuse expérience, Toyo, Elisa, Samuel, Chiara, Giorgia, Noemi, Emma, Laura, Thomas & Afonso (mbmciuuu), Odile, Vasiliki (thank you again for bringing me to the hospital when I carelessly hit my toe), Vasilis (efkolakiii), Tom, Maxime (oui, tu es si peu venu au labo que je te mets dans cette catégorie), Charlotte, Arsène, Céline, et encore beaucoup, beaucoup d'autres que j'oublie sans doute. Merci de rendre ces expériences uniques et inoubliables.

À mes amis, de si longue date qu'il paraît qu'ils sont là depuis toujours. À Dalmo, mon colocataire à distance, pour ta grande singerie. Merci pour toutes ces soirées, toutes ces heures de jeux dogs, de streams aléatoires et de séries discutables. Grâce à toi, je ne suis jamais seul. Merci pour tous ces fous rires. À Alex, pour ton amitié, nos longues discussions philosophiques et zététiques, et ton goût pour les mathématiques qui me donne presque envie de faire de la géométrie algébrique. La prochaine fois, je te donnerai un double de mes clés promis. À Jules, tranquille ce soir. À Lanlan, Susu (désinstalle ton appli), Constance (t'es drôle), Tara, Clarence,

Armand, Mattis, Paul, Alexandre, Stéphane, Charlotte, Yann, Nicolas, Marlène, Melchior, à tout ceux que je n'ai pas cité parce que mon cerveau est si petit, merci à vous, merci pour tous ces bons moments, merci de rendre la ville de Lyon si belle à mes yeux.

À mes amis théatreux, et au théâtre en général qui m'a offert l'échappatoire dont j'avais parfois besoin. À Clémentine, Flore, Célia, Clément, Bastien, Flo, Hugo, Julie, Ombeline, Quentin, Alix, Natacha, Victor, Élia, Anthony, Axel, Louise, Lise, Lou, Vianney, Jean, Romain, Virgile, Pierre, à ceux que je n'ai pas cité, à vous tous qui ont partagé toutes ces émotions uniques à la scène, à tous ces jeux et à ces phrases d'articulations qui n'ont aucun sens, au Dindon, au Portrait d'une femme, à la Cantatrice Chauve, aux yeux des autres, à Alice in Wonderland, à Amaryllis, au Tramway nommé Désir, merci pour toutes ces aventures, ces répétitions, ces amitiés uniques et inoubliables qui m'ont construit et enrichi.

Aux enseignants de ma vie, collège, lycée, prépa, et université, qui m'ont marqué, qui m'ont appris à aimer les maths et à me donner envie de les enseigner aussi bien qu'eux. Mention spéciale à Philippe Caldero pour ce projet musical qui a illuminé mon confinement !

À l'association du piano d'or et sa convivialité, qui m'a donné envie de sortir de ma chambre et de partager ma musique avec vous. À Adrien pour porter cette association, à Bianca pour m'avoir fait découvrir ce merveilleux bar jam qu'est l'Âne sans queue (merci à Yoann et Russel au passage !), à Romain pour cette super soirée musique, et à tous les autres, Hamza, Nabaz, Gab, Walid, Victor, à ceux qui ne font que passer, à ceux qui nous écoute, à ceux qui nous encourage, et à ceux qui nous pousse à nous améliorer. Merci de donner vie à cette passion qui m'anime, merci pour toutes ces après-midi et ces soirées qui me paraissent toujours trop courtes.

À mes climbing buddys, aux gens aléatoires toujours amicaux et leurs conseils avisés, et à l'escalade, l'évasion qu'elle m'apporte, à l'adrénaline des jetés, et à la dalle qui remonte mon égo quand le dévert m'épuise. À Renard pour m'avoir accompagné tant de fois et à me pousser à faire du statique de l'enfer.

À mes amis du Corbier, Baptiste, Capucine et vos super pizzas, Guillaume, Sophie, Joy, Alice et Cap Dantoche, Alice Midol, Charles, Juliette, Anne, Arthur, Alizée, Jacques et Flo pour m'avoir emmené un week-end, merci à Olive et sa sympathie envers ma gaucherie et à Flo pour écouter ma magnifique musique en étant presque pas gênée, merci à Carole et à Marco pour tous tes conseils qui remontent le moral, et ta bonne humeur à tout épreuve, et aux températures encore froides qui permettent à la neige de tomber. Merci pour toutes ces descentes, ces burgers, ces nouvels ans en altitude, merci à vous de rendre ces séjours riches en souvenirs.

À Julie, pour cette rencontre aussi belle qu'inattendue. J'ai hâte du futur, et encore plus d'y aller à tes côtés.

À ma famille de cœur, la Croix-Valmer. À Caroline, Marie-Lou, Cindy, Hugo, Claire, Madeleine, JB, Denis, Françoise, Annie, Philippe et tous les autres, pour tous ces moments inoubliables à la plage, toutes ces soirées à faire des loup-garous ou à simplement manger, boire, parler et rire. Vous avez gagné une place toute spéciale dans mon cœur que seuls des gens exceptionnels comme vous peuvent atteindre. Merci d'avoir été là et d'être là. Mention spéciale à Marie-Lou pour tes gyozas, et encore merci de m'avoir fait aimer l'escalade. Je vous aime, les potes <3

À ma famille, tout court. Tout d'abord, à celle que je ne vois pas souvent, mais que je suis

toujours ravi de retrouver pendant nos réunions de famille, à Pâques, à la Pentecôte, ou encore à Noël. À ma marraine qui m'a épaulé dans des moments clés de ma vie et m'a donné confiance en moi. À mes oncles et mes tantes, Christelle, Bénédicte, Sophie, Jérôme et Audrey, pour tout cet amour que vous partagez autour de vous pendant nos retrouvailles. À mes cousins, Raphaël, Charlotte, Tom, Martin, Charlie, Yoël et Léo, pour avoir rendu magique chaque fête familiale, décidément toujours trop courte. À Léo de nouveau, pour être aussi beau, pour ton amitié, pour ces longues soirées sources d'anecdotes, et pour être encore plus beau.

À mes grands-parents. À mon grand-père qui reste présent dans mon cœur. À ma grand-mère, pour tes mots réconfortants, ton amour, ton sourire et ta présence chaleureuse. À ma mamie, pour ton écoute, ton support, ton énergie débordante, ton excellente cuisine et ta générosité. À mon Papi, pour toutes nos discussions complices, pour m'avoir fait découvrir la disparition par la méthode de l'eau, m'avoir fait ramasser des fraises vivantes, et pour l'intérêt touchant que tu portes à mes passions. Vous êtes un pilier inébranlable de ma vie et me remplissez de joie. À mon frère, avec qui ça n'a pas toujours été facile, mais dont la présence aujourd'hui m'égaye et me rassure. Merci de m'avoir supporté pendant mon adolescence, merci de m'avoir fait découvrir la musique et de participer à alimenter mon amour pour elle. Merci pour tous ces souvenirs, merci d'avoir toujours été là, dans le meilleur et dans le pire de ma vie. Merci à Léna de le rendre si heureux.

Et enfin,

À mes parents. Pour votre amour infini et inconditionnel. Pour votre investissement sans égal dans ma vie et mes projets. Pour votre support, votre écoute, votre bienveillance et votre confiance. Pour m'avoir accompagné, porté, aidé et conseillé, depuis le début, dans chaque moment important ou moins important. Votre présence est unique et irremplaçable, elle m'apaise et me remplit d'amour. Merci d'exister. Merci d'être les deux personnes les plus importantes de ma vie. Je vous aime.

Résumé

Cette thèse est consacrée à l'exploration du système agro-écologique de la betterave sucrière, à sa modélisation grâce à des équations aux dérivées partielles, et à l'optimisation de l'utilisation d'une méthode de protection sans pesticide contre le virus de la jaunisse de la betterave. Ce virus se propage au sein des champs de betteraves sucrières par des pucerons, et constitue une menace pour le rendement des champs. Dans notre modèle, nous introduisons des prédateurs naturels des pucerons afin de contrôler leur population, et plaçons des «refuges» de biodiversité à l'intérieur du champ, désormais hétérogène en espace (c'est-à-dire dont les propriétés dépendent de la position). Au chapitre 2, notre premier article se penche sur ce système, en étudiant la valeur propre principale d'un opérateur spécifique représentant l'évolution de la population de pucerons. Si celle-ci est strictement positive, la population de pucerons converge uniformément vers 0, et la population de prédateurs converge uniformément vers leur capacité de charge strictement positive. Nous fournissons alors des estimations pour la population de pucerons et la récolte restante. Inversement, lorsque cette valeur propre principale est strictement négative, les pucerons persistent en tout point de l'espace et du temps, ce qui se traduit par une récolte nulle. Au chapitre 3, le deuxième article explore le même système, établissant la convergence de la récolte vers celle du système homogénéisé lorsque la fréquence des refuges tend vers l'infini. Nous étudions l'optimalité d'un refuge homogénéisé pour maximiser une quantité appelée récolte linéarisée sous des hypothèses spécifiques concernant la condition initiale de la population de pucerons infectés. Lorsqu'elle est constante, nous identifions une valeur explicite pour le refuge homogénéisé optimal. Le chapitre 4 présente des idées et des conjectures sur les vitesses de propagation de toutes les populations au cours d'une invasion de pucerons, ainsi qu'un résultat d'homogénéisation potentiel lié à ces vitesses de propagation. La discussion s'appuie sur des résultats établis sur les ondes progressives. Le dernier chapitre 5 fournit des valeurs numériques biologiquement cohérentes et dérivées des expériences de la littérature pour les paramètres. Cela nous permet d'effectuer des simulations numériques du système, illustrant l'évolution de la population et les calculs de récolte pour une gamme de paramètres.

Mots clés: réaction–diffusion; environnements hétérogènes; distribution libre idéale; contrôle optimal; système proie-prédateur; maladie à transmission vectorielle.

Abstract

This thesis is dedicated to exploring the sugar-beet agro-ecological system, modeling it thanks to partial differential equations, and optimising the use of a pesticide-free method of protection from the beet yellows virus. This virus is spread in sugar beet fields by aphids, and poses a threat to field yield. In our model, we introduce natural aphid predators to control aphid populations, and place biodiversity "refuges" within the now spatially heterogeneous field (i.e. whose properties depend on position). In Chapter 2, our first paper delves into this system, by studying the principal eigenvalue of a specific operator representing the evolution of the aphid population. If it is positive, the population of aphids uniformly converges to 0, and the population of predators uniformly converges to their positive carrying capacity. We then provide estimates for aphid population and the remaining harvest. Conversely, when this principal eigenvalue is negative, aphids persist at all points of space and time, resulting in a null harvest. In Chapter 3, the second paper explores the same system, establishing the convergence of the harvest to that of the homogenized system as the frequency of refuges goes to infinity. We investigate the optimality of a homogenized refuge for maximizing a quantity called linearized harvest under specific assumptions about the initial condition of the infected aphid population. When it is constant, we identify an explicit value for the optimal homogenized refuge. Chapter 4 presents insights and conjectures on the spreading speeds of all populations during an aphid invasion, and a potential homogenization result related to these spreading speeds. The discussion draws from established results on traveling waves. The final chapter 5 provides biologically consistent numerical values derived from literature experiments for parameters of the model. This allows for numerical simulations of the system, demonstrating population evolution and harvest computations across a range of parameters.

Keywords: reaction–diffusion; heterogeneous environments; ideal free distribution; optimal control; prey-predator system; vector-borne disease.

Contents

Chapter 1

Introduction

1.1 Contexte biologique

1.1.1 Utilisation de pesticides dans l'agriculture

L'utilisation de pesticides dans l'agriculture a fait l'objet à la fois d'un usage intensif et de nombreux débats [40], notamment en ce qui concerne les implications environnementales et sanitaires associées à certains composés chimiques. Les néonicotinoïdes, un groupe d'insecticides systémiques largement utilisés dans les cultures agricoles, constituent une classe de pesticides qui a fait l'objet d'un examen approfondi [13], [60], [34], [18]. Nous nous concentrons sur le contexte spécifique de l'utilisation des néonicotinoïdes dans les champs de betteraves sucrières.

Le terme «néonicotinoïdes» englobe une classe d'insecticides neuro-actifs mis au point pour lutter contre une série d'organismes nuisibles affectant diverses cultures. La particularité de ces pesticides réside dans leur nature systémique, puisqu'ils sont absorbés par les plantes et distribués dans leurs tissus, assurant ainsi une protection contre les ravageurs à différents stades de la croissance de la culture. Dans les champs de betteraves sucrières, les néonicotinoïdes sont couramment utilisés [38] pour lutter contre les ravageurs tels que les pucerons, qui peuvent causer des dommages considérables à la culture [52].

Cependant, l'impact de ces pesticides sur l'environnement et la santé humaine est considérable. Nous soulignons ici l'urgence et l'importance d'identifier des alternatives viables et moins nocives pour les écosystèmes et le bien-être humain. En effet, malgré leur efficacité dans la lutte contre les ravageurs, les néonicotinoïdes ont été associés à de graves conséquences environnementales. L'une des principales préoccupations est leur rôle dans le déclin des pollinisateurs, en particulier pour des espèces cruciales comme les abeilles [60]. Les néonicotinoïdes peuvent persister dans le sol et l'eau, ce qui présente des risques pour les organismes non ciblés et peut entrer dans la chaîne alimentaire. Doris Klingelhöfer et al. [34] ont mis en évidence les effets néfastes sur la biodiversité, la qualité de l'eau et l'écosystème au sens large.

Les risques potentiels des néonicotinoïdes vont au-delà de l'environnement et touchent la santé humaine. Des résidus de ces pesticides ont été détectés dans des produits alimentaires [74], ce qui soulève des questions quant à leur impact sur les consommateurs. Des recherches récentes [18] lient l'exposition chronique aux néonicotinoïdes à des problèmes de santé, notamment à des effets neurotoxiques, soulignant la nécessité d'une évaluation complète des risques.

Compte tenu de la prise de conscience croissante des risques environnementaux et sanitaires posés par les néonicotinoïdes, l'attention se tourne de plus en plus vers la recherche d'approches alternatives pour la lutte contre les ravageurs dans l'agriculture. Certaines recherches en cours

Figure 1.1: Feuille de betterave sucrière présentant des symptômes du virus de la jaunisse de la betterave (source: Farmers weekly).

[33] visent à identifier des alternatives durables et respectueuses de l'environnement aux néonicotinoïdes. Ces alternatives englobent des méthodologies non chimiques telles que l'utilisation de micro-organismes, de produits sémiochimiques ou la mise en œuvre de revêtements de surface. Cette thèse contribue à la recherche actuelle d'alternatives aux pesticides. Dans le contexte de l'agro-écosystème de la betterave sucrière, notre recherche concerne une méthode de contrôle agro-écologique sans pesticide des insectes ravageurs des cultures : l'utilisation de prédateurs naturels spécialisés.

1.1.2 L'agroécosystème de la betterave sucrière

Dans les champs de betteraves, les pucerons (à savoir *Myzus Persicae* et *Aphis Fabae*) sont les vecteurs de quatre virus de la jaunisse. Selon l'Institut Technique de la Betterave [10] (which is the reference for all this subsection), deux de ces virus, appartenant au genre polerovirus, sont étroitement liés génétiquement et induisent des symptômes de jaunisse modérée : Beet mild yellowing virus (BMYV) et Beet chlorosis virus (BChV). Le virus de la jaunisse de la betterave (BYV), qui provoque des symptômes de jaunisse sévère, est une espèce plus éloignée appartenant au genre closterovirus. Le virus de la mosaïque (BtMV), plus rare, appartient au genre potyvirus. Ces virus sont transmis exclusivement par des pucerons vecteurs lorsqu'ils se nourrissent des feuilles de betterave, le puceron vert du pêcher *Myzus persicae* étant le principal vecteur. La transmission est non propagative : ces virus ne peuvent pas être transmis à la descendance des pucerons virulifères. En 2020, l'Institut technique de la betterave a effectué une analyse du virus en France, révélant une prévalence du BYV supérieure à 90% parmi tous les virus de la jaunisse. Le BYV possède une phase d'acquisition virale allant de quelques minutes à quelques heures. Toutefois, le virus ne peut être conservé que pendant 48 heures au maximum dans les pièces buccales de l'insecte, les taux de transmission diminuant significativement après 24 heures. Il peut être retransmis immédiatement après son acquisition, mais il est perdu lors de la mue du puceron.

Les premiers symptômes se manifestent sous la forme de petits points pâles sur le limbe de la feuille, qui évoluent ensuite vers un éclaircissement des nervures secondaires, ressemblant à une gravure sur feuille, caractéristique de la maladie. Finalement, des taches jaune citron apparaissent. Dans les stades plus avancés, ces taches peuvent évoluer vers des taches brun-rouge qui peuvent fusionner, pouvant conduire à une teinte rougeâtre dominante (voir figure 1.1).

En ce qui concerne l'impact sur le rendement, des expériences menées en Angleterre ont

Figure 1.2: Une coccinelle se nourrissant de pucerons (source: Quora).

révélé des pertes de productivité substantielles allant de 40 à 50% dans les zones infectées.

Actuellement, les pesticides constituent le principal outil de protection des betteraves, utilisé par une grande majorité d'agriculteurs. Dans l'approche alternative que nous étudions, les prédateurs naturels des pucerons, tels que les coccinelles (*Hippodamia variegata* ou *Chnootriba similis*), servent de méthode agro-écologique pour gérer la population de pucerons, et par conséquent la propagation du virus de la jaunisse de la betterave.

Généralement, l'absence de plantes ou de fleurs crée un environnement défavorable pour ces prédateurs. Nous allouons une partie de l'espace du champ à la culture de fleurs, formant ainsi ce que nous appelons des refuges de biodiversité. Dans ces zones florales, nous prévoyons une prolifération d'insectes dont les coccinelles peuvent se nourrir, ce qui accélère leur reproduction. Bien que ces refuges aident les prédateurs à prospérer et à lutter contre les pucerons, deux inconvénients potentiels sont à considérer. D'abord, le refuge pourrait potentiellement accélérer la croissance des pucerons, étant donné que les betteraves sucrières sont initialement trop peu développées pour que les pucerons puissent s'en nourrir. Ensuite, et cela est la contrainte principale, aucune betterave ne peut être cultivée dans les zones où le refuge a été établi. Dans le cas où le refuge ralentirait l'invasion des pucerons, il est donc nécessaire de trouver un compromis quant à la quantité de refuge à mettre en place.

La base de notre thèse se centre sur ce système agro-écologique : un champ de betteraves sucrières avec des refuges de biodiversité aménagés en parcelles fleuries, où les pucerons constituent une menace en envahissant potentiellement le champ, exposant ainsi les betteraves au risque de contamination par le virus de la jaunisse, tandis que les coccinelles agissent en tant que prédateurs naturels, se nourrissant des pucerons et arrêtant potentiellement la propagation de la maladie. La question centrale qui guide l'ensemble de notre thèse est la suivante :

Dans le champ de betteraves, quelle est la disposition de refuge optimale pour limiter au mieux la propagation du virus de la jaunisse de la betterave et maximiser le rendement ?

Pour répondre à cette question, nous utiliserons un modèle mathématique de ce système.

1.2 Modélisation mathématique, quelques exemples

La modélisation mathématique est un outil puissant et polyvalent qui comble le fossé entre les concepts théoriques et les phénomènes du monde réel. Il s'agit d'une approche systématique de la représentation, de l'analyse et de la compréhension de systèmes complexes à l'aide de structures et de techniques mathématiques. Elle implique la création de représentations mathéma-

tiques qui simulent le comportement d'un système ou d'un processus. Ces modèles sont conçus pour capturer les caractéristiques et les relations essentielles au sein du système, ce qui permet de faire des prédictions, des analyses et de prendre des décisions. Ils comprennent des variables représentant différents aspects du système et des paramètres fixés qui définissent ses caractéristiques. Généralement, les relations mathématiques sont exprimées par des équations décrivant l'interaction des variables dans le temps ou l'espace. Les modèles s'appuient souvent sur des hypothèses et des contraintes pour simplifier les systèmes complexes et les rendre plus accessibles. Nous allons nous pencher sur un type spécifique de modèle mathématique : le système de réaction-diffusion.

1.2.1 Comprendre les systèmes de réaction-diffusion

Les systèmes de réaction-diffusion constituent une classe de modèles mathématiques qui décrivent l'interaction dynamique entre les réactions locales et la diffusion spatiale d'une ou plusieurs substances ou populations en interaction. Ces systèmes sont caractérisés par un ensemble d'équations aux dérivées partielles (EDP) qui régissent l'évolution temporelle des concentrations ou des densités des entités impliquées dans un domaine spatial. Formellement, supposons que Ω soit un sous-ensemble ouvert de $\mathbb{R}^d$. Un système de réaction-diffusion est un système d'EDP de la forme

$$\partial_t \mathbf{u} + \sigma \mathcal{L} \mathbf{u} = f(\mathbf{u}, x, t),$$

où σ est une matrice diagonale à coefficients strictement positifs appelée matrice de diffusion,

$$f : \mathbb{R}^k \times \Omega \times \mathbb{R}_+^* \to \mathbb{R}^k$$

est appelé le terme de réaction et

$$\mathbf{u} : \Omega \times \mathbb{R}_+^* \to \mathbb{R}^k$$

est l'inconnue (k est un entier naturel non nul). ∂_t désigne la dérivée partielle temporelle, et $\mathcal{L}$ désigne un opérateur du second ordre qualifié d'elliptique [22], c'est-à-dire un opérateur de la forme $\mathcal{L} = \sum_{|\alpha| \leq 2} a_\alpha(x) \partial^\alpha$, où pour tout x dans Ω et pour tout ξ dans $\mathbb{R}^d \setminus \{0\}$, on a $\sum_{|\alpha|=2} a_\alpha(x) \xi^\alpha \neq 0$. Dans beaucoup d'exemples, nous prendrons $\mathcal{L} = -\Delta$, où Δ désigne le laplacien, qui est la somme des dérivées partielles spatiales de second ordre.

Les systèmes de réaction-diffusion trouvent des applications dans divers domaines scientifiques, ce qui témoigne de leur polyvalence et de leur importance. En biologie du développement, dans le développement embryonnaire, les modèles de réaction-diffusion élucident la formation de modèles spatiaux, guidant l'agencement des structures biologiques [49]. En neurobiologie, les systèmes de réaction-diffusion sont utilisés pour étudier la dynamique spatiale des signaux neuronaux, ce qui permet de mieux comprendre le fonctionnement du cerveau et la formation de modèles dans les réseaux neuronaux [59]. En écologie et dynamique des populations, ces systèmes contribuent à la compréhension de la distribution spatiale des espèces, des interactions prédateur-proie et de l'émergence de modèles de biodiversité dans les écosystèmes [19]. Appliqués aux processus chimiques, ces modèles aident à analyser la distribution spatiale des réactifs et des produits [65]. En science de l'environnement, les systèmes de réaction-diffusion aident à modéliser la propagation des polluants et la dispersion des substances dans les environnements naturels [58].

Un système générique unidimensionnel de réaction-diffusion à deux espèces peut être exprimé comme suit :

$$\begin{cases} \partial_t u - \sigma_u \partial_{xx}^2 u = r(u, v) \\ \partial_t v - \sigma_v \partial_{xx}^2 v = s(u, v) \end{cases}$$

où :

- $u(x,t)$ et $v(x,t)$ représentent les concentrations ou les densités de substances ou de populations en interaction à la position x et au temps t.
- σ_u et σ_v sont des coefficients de diffusion strictement positifs, déterminant la vitesse à laquelle u et v se propagent dans l'espace, respectivement. Le terme «diffusion» désigne ici un mouvement uniforme, sans direction privilégiée. Les valeurs les plus élevées indiquent une diffusion plus rapide, tandis que les valeurs les plus faibles indiquent une diffusion plus lente.
- $r(u,v)$ et $s(u,v)$ sont des termes de réaction, encapsulant les interactions locales entre u et v. Ces termes définissent comment les concentrations de u et v changent en raison de leur influence mutuelle. La forme spécifique de r et s dépend de la nature des interactions et des réactions dans le système. Par exemple, dans les modèles écologiques, r et s peuvent représenter les taux de naissance, de mortalité et de prédation dans un système proie-prédateur.

Nous complétons généralement le système par des conditions initiales :

$$\begin{cases} u(\cdot,0) = u_0 \\ v(\cdot,0) = v_0, \end{cases}$$

u_0 et v_0 étant des fonctions données, généralement positives dans un cadre biologique. Le domaine de la variable spatiale est soit l'ensemble non borné $\mathbb{R}$, soit un intervalle borné Ω de $\mathbb{R}$. Dans ce dernier cas, des conditions aux bords sont nécessaires pour décrire le comportement des entités aux bords de l'intervalle :

$$\begin{cases} \alpha_u u + \beta_u \dfrac{\partial u}{\partial n} = 0 & \text{sur } \partial\Omega \\ \alpha_v v + \beta_v \dfrac{\partial v}{\partial n} = 0 & \text{sur } \partial\Omega, \end{cases}$$

où α_u, β_u, α_v, β_v sont positifs, avec $\alpha_u + \beta_u > 0$ et $\alpha_v + \beta_v > 0$. Le scénario dans lequel $\beta_u = \beta_v = 0$ est appelé conditions limites homogènes de Dirichlet. Cette configuration établit que la concentration d'entités devient fixe à zéro à la frontière. Dans le contexte de l'évolution de la densité de population, cette condition peut être comparée à une zone de mort ou à un gouffre, éliminant effectivement tout individu au contact. D'autre part, lorsque $\alpha_u = \alpha_v = 0$, cela correspond à des conditions limites homogènes de Neumann ou à des conditions limites d'absence de flux. Cette condition garantit qu'aucune entité ne peut entrer ou sortir de l'ensemble Ω. Elle fonctionne comme un mur imperméable, obligeant les populations à rebondir et à se déplacer dans la direction opposée lorsqu'elles le rencontrent. Dans les cas où les coefficients α_u, β_u, α_v, β_v sont tous non nuls, les conditions sont connues sous le nom de conditions aux limites de Robin ou mixtes.

1.2.2 Un théorème de comparaison pour les équations de réaction-diffusion

Dans cette thèse, nous allons être amené à comparer des solutions d'équations de réaction-diffusion. Pour cela, nous présentons un théorème très utile, en suivant le chapitre 2, troisième section de [69]. Considérons l'équation scalaire de réaction-diffusion

$$\partial_t u - \sigma \Delta u = f(u,x,t) \tag{1.1}$$

dans un domaine $\Omega \subset \mathbb{R}^d$. Soit $T > 0$ et $D = \Omega \times (0, T)$. Nous supposons que u est continue dans $\overline{D}$, que sa dérivée seconde par rapport à x et sa dérivée première par rapport à t sont bornées et continues dans D. La fonction f et sa dérivée $\partial f / \partial u$ sont bornées et continues dans $\overline{D}$ par rapport à toutes les variables u, x, t.

Théorème 1.2.1. *(Théorème de comparaison). Soit $u(x,t)$ et $v(x,t)$ des solutions de l'équation 1.1 dans un domaine borné Ω. Si $u(x,t) \geq v(x,t)$ sur $\partial D \cap \{t < T\}$, alors $u(x,t) \geq v(x,t)$ dans D.*

1.2.3 L'équation de Fisher-KPP

Les équations de Fisher-KPP (KPP pour Kolmogorov, Petrovsky et Piskunov) constituent un modèle de réaction-diffusion, spécialement conçu pour décrire la propagation des caractères avantageux dans les populations. Nommées d'après les mathématiciens qui les ont introduites pour la première fois dans les années 1930 [23], [35], ces équations ont trouvé des applications dans divers domaines, notamment l'écologie, la dynamique des populations et la biologie mathématique. Par la suite, nous utiliserons ce modèle pour étudier l'évolution de nos populations. L'équation de Fisher-KPP se présente généralement sous la forme suivante :

$$\partial_t u - \sigma \Delta u = ru - su^2.$$

Ici, le terme de réaction représente la croissance logistique de la population. Le facteur ru décrit la croissance exponentielle, et $-su^2$ introduit un effet d'autolimitation, empêchant la population de dépasser une certaine valeur. Les paramètres strictement positifs r et s sont appelés, respectivement, le taux de croissance malthusien de la population et le taux de saturation de la population. Le terme de diffusion $-\sigma\Delta$ modélise un mouvement uniforme de la population, sans direction privilégiée. Nous pouvons comprendre la diffusion laplacienne d'une densité de population de la manière suivante : n individus se déplaçant aléatoirement dans l'espace suivant un mouvement brownien, et $n \to +\infty$.

Si les paramètres sont indépendants de la variable d'espace et de temps (ou homogènes en espace et en temps), et si la condition initiale positive fournie pour résoudre le système est également homogène en espace, alors le système devient un système différentiel ordinaire de Cauchy :

$$\begin{cases} u' = ru - su^2 \\ u(0) = u_0 > 0, \end{cases}$$

dont la solution peut être calculée explicitement : pour tout $t \geq 0$,

$$u(t) = \frac{r/s}{1 + (r/(su_0) - 1)e^{-t}}.$$

La figure 1.5 présente cette solution pour différents ensembles de paramètres et de conditions initiales.

La limite de toutes les solutions, c'est-à-dire la quantité r/s, est appelée capacité de charge de la population. Il s'agit de la taille maximale de la population qu'un environnement particulier peut supporter sur une période prolongée. Ce concept est un élément fondamental des études écologiques et de la dynamique des populations. La capacité de charge est influencée par la disponibilité des ressources, les conditions environnementales et les interactions entre les espèces [63]. Il est important de noter que dans le cas hétérogène en espace, qui est le cas que nous allons étudier par la suite, r/s n'est pas une solution stationnaire en raison de la présence du laplacien dans l'équation. La solution stationnaire de l'équation de Fisher-KPP, dans ce cas, est la solution de $-\sigma\Delta u = ru - su^2$. Nous traçons diverses solutions stationnaires u pour un

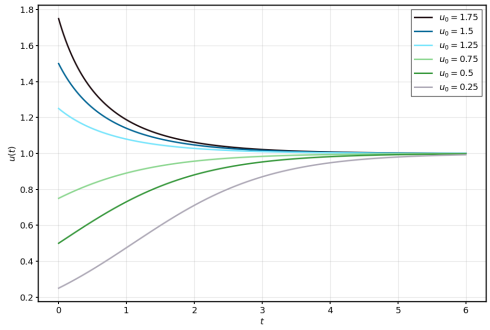

Figure 1.3: Solutions analytiques de l'équation de Fisher-KPP pour diverses valeurs des conditions initiales, avec $r = s = 1$.

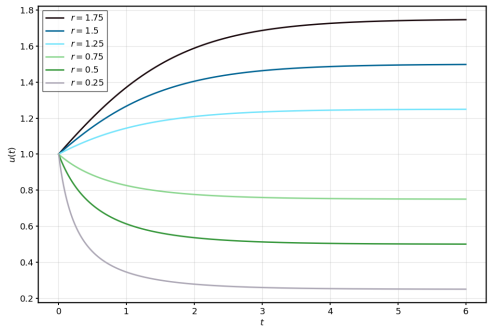

Figure 1.4: Solutions analytiques de l'équation de Fisher-KPP pour différentes valeurs de r, avec $u_0 = s = 1$.

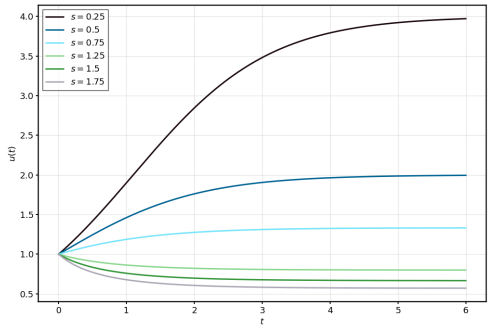

Figure 1.5: Solutions analytiques du l'équation de Fisher-KPP pour différentes valeurs de s, avec $u_0 = r = 1$.

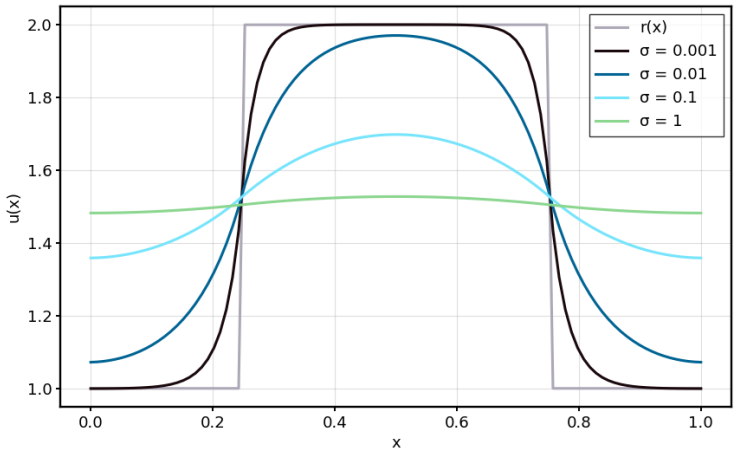

Figure 1.6: Solutions de $-\sigma\Delta u = r(x)u - su^2$, conditions aux limites de Neumann, pour diverses valeurs de σ, avec r une fonction porte et $s = 1$.

coefficient hétérogène $r(x)$, dans l'intervalle $[0,1]$, avec des conditions aux limites de Neumann, pour une gamme de σ, dans la Figure 1.6. Lorsque σ diminue, u converge vers $r(x)/s$. Lorsque σ augmente, u converge vers $\int_0^1 r/s$. La limite $\sigma \to +\infty$ est communément appelée homogénéisation, et sera un concept clé dans cette thèse pour déterminer la disposition optimale du refuge.

1.2.4 Méthode numérique pour les équations de réaction-diffusion

Nous prenons l'exemple de l'équation de Fisher-KPP complétée par des conditions aux limites de Neumann

$$\begin{cases} \partial_t u - \sigma\Delta u = ru - su^2 & \text{dans } (0,1)\times\mathbb{R}_+^*, \\ u(\cdot,0) = u_0 & \text{dans } [0,1], \\ \dfrac{\partial u}{\partial n} = 0 & \text{dans } \{0,1\}\times\mathbb{R}_+^*, \end{cases} \tag{1.2}$$

pour introduire une méthode numérique de base de résolution de ce système : le schéma semi-implicite de différences finies. Puisque nous ne pouvons pas calculer de solution pour des temps infinis, il faut définir un temps final $T > 0$. Nous discrétisons l'espace et le temps avec une grille finie dans $[0,1]\times[0,T]$: en fixant un nombre de pas de temps $N+1 \in \mathbb{N}^*$ et un nombre de pas d'espace $J+1 \in \mathbb{N}^*$. Notre domaine discrétisé est alors

$$\mathcal{G} := \left\{ j\frac{1}{J},\ j \in [0,J] \right\} \times \left\{ n\frac{T}{N},\ n \in [0,N] \right\},$$

et l'objectif est de calculer une solution approchée $\mathfrak{u} : \mathcal{G} \to \mathbb{R}$. Nous désignons les quantités $\mathrm{d}x = 1/J$ et $\mathrm{d}t = T/N$, et pour tout $(j\mathrm{d}x, n\mathrm{d}t) \in \mathcal{G}$, $\mathfrak{u}(j\mathrm{d}x, n\mathrm{d}t) = u_j^n$. La méthode des différences finies consiste à approximer la dérivée temporelle $\partial_t u(x,t)$ par $\dfrac{u_j^{n+1} - u_j^n}{\mathrm{d}t}$ et le laplacien spatial $\Delta u(x,t)$ (qui est simplement la dérivée de second ordre dans notre cas unidimensionnel)

par

$$\frac{u_{j-1}^{n+1} - 2u_j^{n+1} + u_{j+1}^{n+1}}{\mathrm{d}x^2}.$$

L'équation devient

$$\frac{u_j^{n+1} - u_j^n}{\mathrm{d}t} - \sigma \frac{u_{j-1}^{n+1} - 2u_j^{n+1} + u_{j+1}^{n+1}}{\mathrm{d}x^2} = ru_j^n - s(u_j^n)^2.$$

On dit que la partie réactionnelle est résolue explicitement : les termes ne dépendent pas des temps futurs et on peut résoudre explicitement $\frac{u_j^{n+1} - u_j^n}{\mathrm{d}t} = ru_j^n - s(u_j^n)^2$ en injectant simplement $u_j^{n+1} = u_j^n + \mathrm{d}t(ru_j^n - s(u_j^n)^2)$ pour chaque j, d'un pas de temps à l'autre. On dit que la partie diffusion est résolue implicitement, car les termes dépendent des temps futurs.

Pour gérer le terme $\frac{u_{j-1}^n - 2u_j^n + u_{j+1}^n}{\mathrm{d}x^2} = 0$ dans l'équation, on ne peut pas calculer les valeurs de u un pas spatial à la fois, puisqu'elles dépendent des emplacements $j+1$, j et $j-1$. Au lieu de cela, nous écrivons, pour $n \in [0, N]$,

$$\frac{1}{\mathrm{d}x^2} L U^n,$$

où

$$L = \begin{pmatrix} -1 & 1 & 0 & 0 & 0 & \cdots & 0 \\ 1 & -2 & 1 & 0 & 0 & \cdots & 0 \\ 0 & 1 & -2 & 1 & 0 & \cdots & 0 \\ \vdots & 0 & \ddots & \ddots & \ddots & 0 & \vdots \\ 0 & \cdots & 0 & 1 & -2 & 1 & 0 \\ 0 & \cdots & 0 & 0 & 1 & -2 & 1 \\ 0 & \cdots & 0 & 0 & 0 & 1 & -1 \end{pmatrix} \in \mathcal{M}_{J+1}(\mathbb{R}),$$

et

$$U^n = \begin{pmatrix} u_0^n \\ u_1^n \\ \\ \vdots \\ \\ u_{J-2}^n \\ u_J^n \end{pmatrix},$$

qui est une représentation matricielle des termes $\frac{u_{j-1}^n - 2u_j^n + u_{j+1}^n}{\mathrm{d}x^2}$ pour tout $j \in [1, J-1]$, et, conformément aux conditions aux limites de Neumann, $\frac{-u_0^n + u_1^n}{\mathrm{d}x^2} = 0$ et $\frac{u_{J-1}^n - u_J^n}{\mathrm{d}x^2} = 0$.

Nous écrivons ici la représentation matricielle suivante de notre système : pour tout $n \in [0, N-1]$, en notant $R^n = (ru_j^n - s(u_j^n)^2)_{j \in [0,J]}$,

$$\left(I_{J+1} - \frac{\sigma \mathrm{d}t}{\mathrm{d}x^2} L\right) U^{n+1} = U^n + \mathrm{d}t R^n,$$

où I_{J+1} désigne la matrice identité de taille $(J+1)\times(J+1)$. On inverse ensuite numériquement la matrice $I_{J+1} - \dfrac{\sigma \mathrm{d}t}{\mathrm{d}x^2} L$ et on en déduit, pour tout $n \in [0, N-1]$,

$$U^{n+1} = \left(I_{J+1} - \frac{\sigma \mathrm{d}t}{\mathrm{d}x^2} L \right)^{-1} (U^n + \mathrm{d}t R^n).$$

1.3 Homogénéisation

L'homogénéisation est une technique mathématique utilisée pour étudier le comportement d'un matériau ou d'un milieu hétérogène à plus grande échelle. Elle implique l'analyse d'un système d'EDP dans un domaine dont les coefficients oscillent rapidement. L'idée principale est de dériver une équation dite homogénéisée à une plus grande échelle, capturant le comportement moyen du milieu. Cette équation macroscopique est souvent plus facile à analyser que le système d'EDP original, fortement oscillatoire. L'homogénéisation trouve de multiples applications [44], [5], et sert d'outil efficace pour aborder la modélisation mathématique à l'interface des échelles micro et macro. L'objectif mathématique de cette technique est de prouver que la solution du modèle initial converge vers la solution du macro-modèle.

Le problème peut être énoncé comme suit. Pour un paramètre $\varepsilon > 0$ que nous appelons période, nous considérons une équation de réaction-diffusion de la forme

$$\partial_t u_\varepsilon + \mathcal{L}_\varepsilon u_\varepsilon = f_\varepsilon$$

avec des conditions initiales et au bord appropriées. Ici, $\mathcal{L}_\varepsilon$ est un opérateur elliptique, et $\mathcal{L}_\varepsilon$ et f_ε dépendent de la période d'oscillation ε. Nous définissons ensuite l'équation homogénéisée :

$$\partial_t u + \mathcal{L} u = f.$$

L'objectif principal est de répondre à la question suivante.

Lorsque ε tend vers 0, la solution u_ε converge-t-elle vers u ? Dans quel sens ?

Soyons plus précis et examinons un exemple simple d'homogénéisation. Soit r appartenant à $\mathcal{C}^2((0,1),\mathbb{R})$, étendons cette fonction périodiquement sur tout $\mathbb{R}$, et définissons $r_\varepsilon : x \mapsto r(x/\varepsilon)$. Ainsi définie, la fonction $r_\varepsilon : (0,1) \mapsto \mathbb{R}$ a une période de ε, et oscille rapidement lorsque ε tend vers 0. Considérons le problème de Cauchy–Neumann

$$\begin{cases} \partial_t u_\varepsilon - \sigma \Delta u_\varepsilon = r_\varepsilon u - s u_\varepsilon^2 & \text{dans } (0,1)\times\mathbb{R}_+^* \\ u_\varepsilon(\cdot,0) = u_0 & \text{dans } [0,1] \\ \dfrac{\partial u_\varepsilon}{\partial n} = 0 & \text{sur } \{0,1\}\times\mathbb{R}_+^*. \end{cases}$$

Il est bien connu que r_ε converge faiblement dans $\mathrm{L}^2((0,1))$ vers $\int_0^1 r$, la moyenne de la fonction r. Le problème homogénéisé est le suivant.

$$\begin{cases} \partial_t u - \sigma \Delta u = \int_0^1 r u - s u^2 & \text{dans } (0,1)\times\mathbb{R}_+^* \\ u(\cdot,0) = u_0 & \text{dans } [0,1] \\ \dfrac{\partial u}{\partial n} = 0 & \text{sur } \{0,1\}\times\mathbb{R}_+^*. \end{cases}$$

Pour $T > 0$, en dérivant des estimations sur la solution u_ε et en obtenant donc de la compacité sur la suite (u_ε), on peut prouver la forte convergence de u_ε dans $\mathrm{L}^2((0,1)\times[0,T])$ et presque partout dans $(0,1)\times[0,T]$ vers u lorsque ε tend vers 0. Dans notre modèle, nous utiliserons l'homogénéisation sur les emplacements des refuges dans le champ.

1.4 Le théorème de Krein-Rutman

L'étude des valeurs propres et des vecteurs propres joue un rôle fondamental dans la compréhension du comportement des opérateurs linéaires et des systèmes dans diverses branches des mathématiques. Un domaine important où les problèmes de valeurs propres se posent est le contexte des opérateurs compacts sur les espaces de Banach. Dans ce domaine, le théorème de Krein-Rutman est un outil puissant pour comprendre l'existence et la stabilité de solutions positives dans divers modèles mathématiques, en donnant un aperçu des propriétés spectrales des opérateurs compacts positifs. Il a été prouvé par Krein et Rutman en 1948 [37]. Ce théorème a des applications très étendues, en particulier dans l'analyse de problèmes non linéaires [62], [48] et de modèles mathématiques dans divers domaines [57].

Le théorème de Krein-Rutman généralise le théorème de Perron-Frobenius et traite des propriétés spectrales des opérateurs compacts positifs définis sur un espace de Banach de dimension potentiellement infinie. Plus précisément, supposons que T soit un opérateur compact non nul avec un rayon spectral positif $r(T)$ dans un espace de Banach X, et un cône convexe K avec $K \cap -K = \{0\}$ et $K - K$ dense dans X, tel que $T(K) \subset K$. Alors, $r(T)$ est une valeur propre simple (strictement positive) de T :

$$T(u) = r(T)u,$$

avec un vecteur propre u associé strictement positif, et est la seule valeur propre de T associée à un vecteur propre strictement positif [66].

La conséquence la plus importante de ce théorème est, dans cette thèse, le théorème suivant : [62].

Théorème 1.4.1. *Soit $\mathcal{L}$ un opérateur elliptique sur un domaine borné Ω de $\mathbb{R}^d$ à bord lisse. On considère le problème de valeur propre suivant :*

$$\begin{cases} \mathcal{L}u + \lambda u = 0 & \text{dans } \Omega \\ \alpha u + \beta \dfrac{\partial u}{\partial n} = 0 & \text{sur } \partial\Omega. \end{cases} \tag{1.3}$$

Alors 1.3 a une valeur propre réelle simple λ_1 associée à une fonction propre strictement positive, et est la seule valeur propre associée à une fonction propre strictement positive. En outre, pour toute valeur propre λ de $-\mathcal{L}$, $\lambda_1 \leq \mathrm{Re}(\lambda)$.

La valeur propre λ_1 est appelée *valeur propre principale* de l'opérateur $-\mathcal{L}$, et constitue un concept clé dans notre analyse : son signe détermine l'extinction ou non des pucerons.

1.5 Modélisation de notre système

Dans cette section, nous présentons les choix de modélisation que nous avons faits pour aborder le système agro-écologique de la betterave sucrière. Nous utilisons les notations suivantes pour nos différentes populations :

- La population de betteraves : H, pour les hôtes.
- La population de betteraves infectées : I.
- La population de betteraves sensibles : S (nous avons donc $H = I + S$).
- La population de pucerons : V, pour les vecteurs.

- La population de pucerons infectés : V_i.
- La population de pucerons sensibles : V_s (nous avons donc $V = V_i + V_s$).
- La population de coccinelles : P, pour les prédateurs.

Nous supposons que la variation au cours du temps d'une population infectée par le virus de la jaunisse de la betterave est uniquement proportionnelle au produit de la population sensible et de la population infectée. Nous appelons la constante de proportionnalité de la transmission des vecteurs aux hôtes $\beta_{VH} > 0$ et la constante de proportionnalité de la transmission des hôtes aux vecteurs $\beta_{HV} > 0$. En outre, nous supposons que la population totale de pucerons guérissent du virus proportionnellement à la population de pucerons infectés, avec une constante de proportionnalité que nous notons $\alpha > 0$, appelée taux de récupération. Puisque les betteraves ne guérissent pas du virus, elles n'en guérissent pas non plus dans notre modèle. Le modèle épidémiologique est donc le suivant :

$$\begin{cases} \partial_t I = \beta_{VH} S V_i \\ \partial_t S = -\beta_{VH} S V_i \\ \partial_t V_i = \beta_{HV} I V_s - \alpha V_i \\ \partial_t V_s = -\beta_{HV} I V_s + \alpha V_i. \end{cases}$$

Nous avons implicitement supposé, avec ce modèle, que la population de betteraves $H = I + S$ est indépendante du temps : $\partial_t H = \partial_t I + \partial_t S = \beta_{VH} S V_i - \beta_{VH} S V_i = 0$ (mais dépend de l'espace, car le fait d'avoir un refuge à un endroit implique l'absence de betteraves à ce même endroit). Nous pouvons réécrire ce système en supposant que H est indépendant du temps et en supprimant une équation :

$$\begin{cases} \partial_t I = \beta_{VH} (H(x) - I) V_i \\ \partial_t V_i = \beta_{HV} I V_s - \alpha V_i \\ \partial_t V_s = -\beta_{HV} I V_s + \alpha V_i. \end{cases} \tag{1.4}$$

Il sera explicité dans la suite que nous supposons que les pucerons ne transmettent pas le virus à leur progéniture. Le terme de naissance figurera donc uniquement dans l'équation sur V_s.

Ensuite, nous estimons la propagation et la reproduction des pucerons et des coccinelles à l'aide d'un modèle de Fisher-KPP. En l'absence de prédateurs,

$$\partial_t V - \sigma_V \Delta V = r_V(x) V - s_V V^2,$$

où $\sigma_V > 0$ est leur taux de diffusion, $r_V(x) > 0$ leur taux de croissance malthusien, et $s_V > 0$ leur taux de saturation. Nous avons supposé ici que seul le taux de croissance malthusien est une fonction de l'espace, affectée par la présence du refuge dans le champ.

En l'absence de pucerons, le modèle du prédateur serait le suivant

$$\partial_t P - \sigma_P \Delta P = r_P(x) P - s_P P^2,$$

avec $\sigma_P > 0$, $r_P(x) > 0$, et $s_P > 0$ étant respectivement le taux de diffusion, le taux de croissance malthusien, et le taux de saturation, avec la même hypothèse sur la dépendance spatiale de $r_P(x)$. Il est important de noter que les prédateurs sont génériques dans notre modèle : ils peuvent survivre et se développer même en l'absence de pucerons. Cependant, comme nous l'avons vu dans la section précédente, la solution stationnaire de cette équation P^* n'est pas explicite. Pour des raisons techniques, notamment pour avoir un contrôle direct sur la valeur

propre principale de l'opérateur $\mathcal{L} = -\sigma_V \Delta - r_V + hP^*$ (ce qui s'avérera crucial dans notre premier article [1]), nous supposons que la stratégie de diffusion des coccinelles est différente. De plus, d'un point de vue biologique, les coccinelles devraient être capables d'avoir une vision plus large du champ puisqu'elles volent, donc une dispersion uniforme n'est probablement pas le modèle le plus précis. Nous tenons à souligner que les larves de coccinelles sont également de grandes consommatrices de pucerons, mais elles ne volent évidemment pas. Par souci de simplification du modèle, nous ne prenons en compte qu'un seul type de prédateur : la coccinelle adulte. Nous supposons donc que les coccinelles ont une connaissance parfaite de la distribution des ressources dans le champ (les ressources désignent ici toute nourriture du champ à l'exception des pucerons) et qu'elles peuvent adapter leur configuration spatiale de manière optimale. Cette stratégie est appelée «stratégie idéale de dispersion libre». Il a été prouvé dans [16] que, dans le contexte du modèle Fisher-KPP 1.2 de la section précédente, une stratégie de diffusion-advection de la forme $u \mapsto \nabla \cdot (\nabla u - u\nabla(\ln r)) = \nabla \cdot (r\nabla (u/r))$ est stable du point de vue de l'évolution, stable par convergence, et conduit à ce que l'on appelle une «distribution libre idéale», où la distribution spatiale de la densité de population à l'équilibre est exactement proportionnelle à la distribution spatiale des ressources. Nous adoptons cette stratégie de diffusion-advection exacte pour notre population de prédateurs, de sorte qu'en l'absence de pucerons, l'équation est la suivante

$$\partial_t P - \sigma_P \nabla \cdot (r_P(x) \nabla (P/r_P(x))) = r_P(x)P - s_P P^2.$$

Il est facile de voir ici que $r_P(x)/s_P$ est une solution stationnaire, et même la seule solution stationnaire strictement positive de cette équation [1] : les coccinelles peuvent parfaitement s'adapter à leur environnement et se disposer de manière optimale dans le champ. Cependant, nous soulignons qu'en présence de pucerons, leur distribution peut ne pas être optimale, puisqu'elles ne sont pas attirées par les pucerons. Ce type de dispersion, appelé chimiotaxie, n'entre pas dans le cadre de cette thèse mais constitue une amélioration potentielle du modèle. Pour alléger l'écriture, nous notons

$$\overline{\mathcal{L}}(P) = \nabla \cdot (r_P(x) \nabla (P/r_P(x))) .$$

De plus, nous supposons que la prédation est préjudiciable à la population de pucerons et proportionnelle au produit de leur population par la population de prédateurs, avec une constante de proportionnalité $h > 0$ appelée taux de prédation. La prédation est modélisée comme étant bénéfique pour la population de coccinelles et proportionnelle au produit de leur population et de la population de pucerons, avec une constante de proportionnalité $\gamma h > 0$, γ étant appelé l'efficacité de la prédation. Enfin, nous supposons que nos prédateurs se nourrissent indifféremment de pucerons, qu'ils soient infectés ou non. Le modèle complet proie-prédateur est donc le suivant :

$$\begin{cases} \partial_t V - \sigma_V \Delta V = r_V(x)V - s_V V^2 - hPV \\ \partial_t P - \sigma_P \overline{\mathcal{L}}(P) = r_P(x)P - s_P P^2 + \gamma hVP. \end{cases} \tag{1.5}$$

Dans notre modèle complet, nous combinons le modèle épidémiologique 1.4 et le modèle proie-prédateur 1.5 pour obtenir

$$\begin{cases} \partial_t I = \beta_{VH}(H(x) - I)V_i \\ \partial_t V_i - \sigma_V \Delta V_i = \beta_{HV} I V_s - \alpha V_i - d_V(x)V_i - s_V V V_i - hPV_i \\ \partial_t V_s - \sigma_V \Delta V_s = -\beta_{HV} I V_s + \alpha V_i - d_V(x)V_s - s_V V V_s - hPV_s + b_V(x)V \\ \partial_t P - \sigma_P \overline{\mathcal{L}}(P) = r_P(x)P - s_P P^2 + \gamma hVP. \end{cases}$$

Nous avons supposé ici que la maladie ne se transmettait pas à la progéniture des pucerons, de sorte que le taux de croissance malthusien $r_V(x)$ est divisé entre un taux de naissance $b_V(x) >$

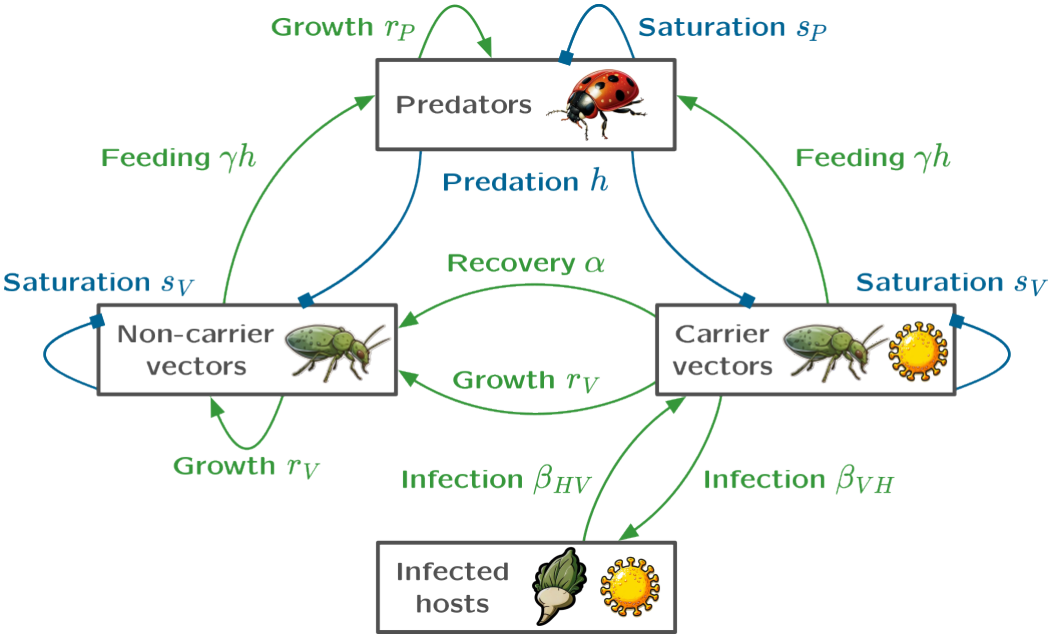

Figure 1.7: Représentation visuelle de la modélisation mathématique de l'agroécosystème de la betterave sucrière.

0 et un taux de mortalité $d_V(x) > 0 : r_V(x) = b_V(x) - d_V(x)$, et que le taux de naissance n'apparaît que dans l'équation V_s. Les interactions entre nos quatre populations I, V_i, V_s et P sont résumées dans la figure 1.7.

En dernière hypothèse, les paramètres β_{VH}, β_{HV}, α, σ_V, s_V, σ_P, s_V, h et γ ne sont pas affectés par la présence du refuge, ce qui les rend spatialement homogènes, et tous nos paramètres β_{VH}, β_{HV}, α, σ_V, b_V, σ_V, s_V, σ_P, r_P, s_V, h et γ sont strictement positifs et homogènes en temps. L'indépendance temporelle peut être justifiée biologiquement par la dynamique rapide des populations : dans les simulations numériques, en un mois ou moins, les populations V et P (et, par conséquent, I) tendent à atteindre l'équilibre. Cela peut également être confirmé par des données réelles, où les coccinelles, par exemple, mangent jusqu'à cinquante pucerons par jour [36], et se diffusent à un rythme élevé [72]. Par conséquent, nous négligeons les changements saisonniers et environnementaux potentiels qui se produiraient sur une longue période.

Pour démontrer nos résultats principaux, nous utilisons des conditions de Neumann au bord de notre domaine spatial (le champ de betteraves), que nous appelons Ω.

Maintenant que notre modèle mathématique est posé, nous pouvons reformuler rigoureusement notre question de recherche. Puisque nous avons supposé un printemps éternel, la quantité que nous avons appelé «rendement», que nous notons η, est égale à

$$\eta = \int_\Omega H - I_\infty = \lim_{t \to +\infty} \int_\Omega H - I(\cdot, t).$$

Cette quantité dépend donc du refuge R choisi, puisque ce refuge affecte certains paramètres de notre système. Notons X l'ensemble des refuges admissibles. Le «refuge optimal» que nous recherchons est alors

$$\operatorname{argmax}_{R \in X} \eta(R).$$

Évidemment, puique nous ne pouvons pas calculer explicitement les solutions de notre système, il paraît trop difficile d'obtenir une expression explicite de ce refuge optimal. Cependant, il est possible d'accéder à certaines propriétés de ce refuge.

1.6 Principaux résultats

Dans le chapitre 2, nous introduisons notre premier article traitant du système présenté ci-dessus. Nous démontrons, dans un premier temps, le caractère bien posé (c'est-à-dire l'existence et l'unicité de la solution) du problème de Cauchy–Neumann que nous avons posé, dans le cas où nos paramètres hétérogènes en espace sont des fonctions dans $\mathcal{C}^{2+\alpha}(\overline{\Omega})$. Sans cette hypothèse de régularité, le problème devrait toujours être bien posé, et nécessite de bonnes estimations de régularité des solutions pour conclure. Ces estimations sont techniques, notamment la gestion du terme de dispersion idéal libre de la population P. Ce théorème d'existence et d'unicité avec des paramètres dans, par exemple, $\mathrm{L}^\infty(\Omega)$ n'a pas été démontré dans cette thèse. Dans un deuxième temps, sous la condition que la valeur propre principale de l'opérateur $-\sigma_V\Delta - r_V(x) + hr_P(x)/s_P$ soit strictement positive, nous prouvons la convergence uniforme de notre population (V,P) vers $(0, r_P(x)/s_P)$, et nous obtenons des estimations de la population de pucerons et de la récolte restante, qui est la quantité

$$\eta = \lim_{t\to+\infty} \int_\Omega H - I(\cdot,t),$$

(Ω étant le domaine spatial). Dans le cas où cette valeur propre principale est strictement négative, nous prouvons que les pucerons persistent en tout point de l'espace et du temps dans le champ, et que la récolte est nulle. Plus précisément, soit $\mathcal{L}_{V_s} = -\sigma_V\Delta - r_V(x) + hr_P(x)/s_P$, $\mathcal{L}_{V_i} = -\sigma_V\Delta + \alpha + d_V(x) + hr_P(x)/s_P$ et soit $\lambda_1(\mathcal{L}_{V_s})$, $\lambda_1(\mathcal{L}_{V_i})$ leurs principales valeurs propres avec des conditions aux limites de Neumann sur $\partial\Omega$. Notons $\varphi_{s,1}$ et $\varphi_{i,1}$, les fonctions propres principales associées, respectivement, à $\lambda_1 s, 1$ et $\varphi_{i,1}$, à $\lambda_1(\mathcal{L}_{V_s})$ et $\lambda_1(\mathcal{L}_{V_i})$, avec les normalisations $\min_\Omega \varphi_{s,1} = 1$ et $\max_\Omega \varphi_{i,1} = 1$. Le résultat principal de notre premier article est donc le suivant.

Théorème 1.6.1. *(i) Cas d'extinction: on suppose que $P_0 \not\equiv 0$ et $\lambda_1(\mathcal{L}_{V_s}) > 0$. Soit $V = V_i + V_s$. Dans ce cas, les affirmations suivantes sont vraies.*

- *$(V,P)(x,t) \to (0, r_P(x)/s_P)$ lorsque $t \to +\infty$, uniformément dans Ω.*
- *Si on suppose aussi que $V_{i,0} \not\equiv 0$, alors $\liminf_{t\to+\infty} \inf_{x\in\Omega} I(x,t) > 0$.*
- *Plus précisément, nous disposons des estimations suivantes. Pour tout $\varepsilon > 0$ tel que $\lambda_1(\mathcal{L}_{V_s}) - h\varepsilon > 0$, si $|P_0 - r_P/s_P| \le \varepsilon$ et $V_0 := V_{i,0} + V_{s,0} \le \varepsilon$, alors pour tout $x \in \Omega$, $t \ge 0$,*

$$V(x,t) \le \max_\Omega V_0 \max_\Omega \varphi_{s,1} e^{-(\lambda_1(\mathcal{L}_{V_s}) - h\varepsilon)t},$$

$$\frac{I(x,t)}{H(x)} \le 1 - \exp\left(-\beta_{VH} \frac{\max_\Omega V_0 \max_\Omega \varphi_{s,1}}{\lambda_1(\mathcal{L}_{V_s}) - h\varepsilon}\right),$$

$$1 - \exp\left(-\beta_{VH} \min_\Omega V_{i,0} \min_\Omega \varphi_{i,1} \frac{1 - e^{-(\lambda_1(\mathcal{L}_{V_i}) + s_V\varepsilon + h\varepsilon)t}}{\lambda_1(\mathcal{L}_{V_i}) + s_V\varepsilon + h\varepsilon}\right) \le \frac{I(x,t)}{H(x)}.$$

(ii) Cas de persistance: on suppose que $V_{i,0} \not\equiv 0$ et $\lambda_1(\mathcal{L}_{V_s}) < 0$. Alors,

- $\liminf_{t\to+\infty} \inf_{x\in\Omega} V_i(x,t) > 0$;
- $\lim_{t\to+\infty} I(x,t) = H(x)$ *uniformément dans* Ω.

Ce théorème suggère que la maximisation de $\lambda_1(\mathcal{L}_{V_s})$ (qui peut être réalisée en augmentant la fréquence des refuges, conséquence directe de la formulation variationnelle de $\lambda_1(\mathcal{L}_{V_s})$) est une stratégie efficace pour maximiser la récolte, puisqu'elle doit être positive pour éradiquer les pucerons. De plus, les estimations sur les différentes populations conduisent à l'estimation suivante de la récolte :

Corollaire 1.6.1. *On suppose que $\lambda_1(\mathcal{L}_{V_s}) > 0$. Alors, pour tout $\varepsilon > 0$ tel que $\lambda_1(\mathcal{L}_{V_s}) - h\varepsilon > 0$, si $|P_0 - r_P/s_P| \le \varepsilon$ et $V_0 \le \varepsilon$, alors*

$$e^{-\beta_{VH}\frac{\max_\Omega V_0 \max_\Omega \varphi_{s,1}}{\lambda_1(\mathcal{L}_{V_s}) - h\varepsilon}} \le \frac{\int_\Omega (H - I_\infty)}{\int_\Omega H} \le e^{-\beta_{VH}\frac{\min_\Omega V_{i,0} \min_\Omega \varphi_{i,1}}{\lambda_1(\mathcal{L}_{V_i}) + s_V\varepsilon + h\varepsilon}}.$$

On suppose que $\lambda_1(\mathcal{L}_{V_s}) < 0$. Alors

$$\int_\Omega (H - I_\infty) = 0.$$

Cette estimation suggère une possible monotonie de l'application $\lambda_1(\mathcal{L}_{V_s}) \mapsto \eta$. Néanmoins, il apparaît que cette hypothèse de monotonie est probablement incorrecte, comme nous l'expliquerons dans le second article.

Dans le chapitre 3, nous introduisons notre deuxième article, qui examine également le système discuté ci-dessus. Nous prouvons la convergence de la récolte vers la récolte du système homogénéisé lorsque la fréquence du refuge tend vers l'infini (la fréquence du refuge étant le nombre de petites parcelles uniformément réparties dans le champ). Plus précisément, soit $R \in \mathrm{L}^\infty(\Omega)$, étendu périodiquement dans $\mathbb{R}^d$. Nous appelons «refuge de fréquence n» l'application $R_n : x \mapsto R(nx)$. Nous désignons sa moyenne sur le champ $\mathcal{R} = \langle R_n \rangle_\Omega = 1/|\Omega| \int_\Omega R_n$ (qui ne dépend pas de n). Nous supposons que nos paramètres hétérogènes en espace sont de la forme suivante :

$$\begin{aligned}
&H_n = H^0(1 - R_n) \text{ d'intégrale également indépendante de } n\\
&b_V^n = (b_V^r - b_V^f)R_n + b_V^f\\
&d_V^n = (d_V^r - d_V^f)R_n + d_V^f\\
&r_V^n = b_V^n - d_V^n\\
&r_P^n = (r_P^r - r_P^f)R_n + r_P^f.
\end{aligned}$$

Nous considérons un problème de Cauchy–Neumann similaire à celui décrit ci-dessus, avec un refuge R_n, pour lequel le système se réécrit

$$\begin{cases}
\partial_t I &= \beta_{VH}(H_n - I)V_i\\
\partial_t V_i &= \sigma_V \Delta V_i + \beta_{HV} I V_s - (\alpha + d_V^n + s_V(V_s + V_i) + hP)V_i\\
\partial_t V_s &= \sigma_V \Delta V_s + (\alpha + b_V^n)V_i + (r_V^n - \beta_{HV} I - s_V(V_s + V_i) - hP)V_s\\
\partial_t P &= \sigma_P \nabla \cdot \left(r_P^n \nabla \left(\frac{P}{r_P^n} \right) \right) + (\gamma h(V_s + V_i) + r_P^n - s_P P)P.
\end{cases} \tag{1.6}$$

avec des conditions initiales positives $(I, V_i, V_s, P)(\cdot, 0) = (I_0^n, V_{i,0}^n, V_{s,0}^n, P_0^n) \quad \text{dans } \Omega.$

Notons (I_n, V_i^n, V_s^n, P_n), l'unique solution de ce nouveau problème, et

$$\eta_n = \left(\int_\Omega H - I_\infty\right)_n = \int_\Omega H_n e^{-\beta_{VH}\int_0^{+\infty} V_i^n}$$

la récolte associée.

Nous notons également

$$\begin{array}{rll} H_\infty & = \langle H_n\rangle_\Omega & = H^0(1-\mathcal{R}) \\ b_V^\infty & = \langle b_V^n\rangle_\Omega & = (b_V^r - b_V^f)\mathcal{R} + b_V^f \\ d_V^\infty & = \langle d_V^n\rangle_\Omega & = (d_V^r - d_V^f)\mathcal{R} + d_V^f \\ r_V^\infty & = \langle r_V^n\rangle_\Omega & = b_V^\infty - d_V^\infty \\ r_P^\infty & = \langle r_P^n\rangle_\Omega & = (r_P^r - r_P^f)\mathcal{R} + r_P^f \\ (r_P^\infty)_2 & = \langle (r_P^n)^2\rangle_\Omega & = (r_P^r - r_P^f)^2\mathcal{R}_2 + 2(r_P^r - r_P^f)r_P^f\mathcal{R} + (r_P^f)^2, \end{array}$$

et $r^* \in \mathcal{M}_d(\mathbb{R})$ la dite «conductivité homogénéisée» définie dans [4].

Le problème de Cauchy–Neumann homogénéisé est le suivant:

$$\begin{cases} \partial_t I & = \beta_{VH}(H_\infty - I)V_i \\ \partial_t V_i & = \sigma_V \Delta V_i + \beta_{HV} I V_s - (\alpha + d_V^\infty + s_V(V_s+V_i) + hP)V_i \\ \partial_t V_s & = \sigma_V \Delta V_s + (\alpha + b_V^\infty)V_i + (r_V^\infty - \beta_{HV} I - s_V(V_s+V_i) - hP)V_s \\ \partial_t P & = \sigma_P \nabla\cdot\left(r^*\nabla\left(\frac{P}{r_P^\infty}\right)\right) + (\gamma h(V_s+V_i) + \frac{(r_P^\infty)_2}{r_P^\infty} - s_P\frac{(r_P^\infty)_2}{(r_P^\infty)^2}P)P. \end{cases} \tag{1.7}$$

avec des conditions initiales positives $(I, V_i, V_s, P)(\cdot, 0) = (I_0^\infty, V_{i,0}^\infty, V_{s,0}^\infty, P_0^\infty)$ dans Ω. Nous supposons la convergence faible dans $L^2(\Omega)$ de I_0^n, $V_{i,0}^n$, $V_{s,0}^n$, P_0^n vers I_0^∞, $V_{i,0}^\infty$, $V_{s,0}^\infty$, P_0^∞, respectivement.

Notons $(I^\infty, V_i^\infty, V_s^\infty, P^\infty)$, l'unique solution de ce problème, et

$$\eta_\infty = \left(\int_\Omega H - I_\infty\right)_\infty = \int_\Omega H_\infty e^{-\beta_{VH}\int_0^{+\infty} V_i^\infty}$$

la récolte associée. Nous avons alors le théorème suivant.

Théorème 1.6.2. *On suppose que $\lambda_1(\mathcal{L}_{V_s}) > 0$.*

La récolte $\eta_n = \left(\int_\Omega H - I_\infty\right)_n$ converge vers $\eta_\infty = \left(\int_\Omega H - I_\infty\right)_\infty$ lorsque $n \to +\infty$.

Ce théorème est essentiel pour répondre à notre question de recherche car il relie la stratégie d'homogénéisation (c'est-à-dire l'augmentation de la fréquence des refuges) à l'optimalité du refuge homogénéisé (qui est le dernier théorème principal de cet article).

Notons

- $m = \dfrac{h}{s_P}(r_P^r - r_P^f) + d_V^r - d_V^f$,
- $\xi = \alpha + d_V^f + \dfrac{h}{s_P} r_P^f > 0$.

Nous prouvons que, quand $\Omega = [-L, L]$ pour $L > 0$, sous une hypothèse spécifique sur la forme de la condition initiale de la population de pucerons $V_{i,0}$, un refuge homogénéisé n'est pas optimal pour maximiser une quantité η_L que nous appelons *récolte linéarisée* :

$$\eta_L(R, V_{i,0}) = H^0 \left(|\Omega| - \int_\Omega R \right) + \frac{\beta_{VH} H^0}{m} \left(\int_\Omega V_{i,0} - (\xi + m) \int_\Omega \varphi_R V_{i,0} \right),$$

dont nous observons numériquement qu'elle est très proche de la récolte non linéarisée η lorsque la valeur propre $\lambda_1(\mathcal{L}_{V_s})$ est strictement positive. La forme à laquelle nous faisons référence est appelée «réarrangement de Schwarz» d'une fonction (notée f_* pour une fonction f). Il s'agit d'une fonction symétrique, radialement décroissante, qui préserve les mesures des ensembles de niveaux de la fonction initiale. Le théorème en question est le suivant.

Théorème 1.6.3. *Notons, pour $c > 0$,*
$\mathcal{M}_c(\Omega) = \left\{ f \in \mathcal{C}^{2+\alpha}(\overline{\Omega}, [0,1]),\ \|f\|_{\mathrm{L}^1} = c \right\}$.
Fixons $V_{i,0} \in \mathcal{C}^{2+\alpha}(\Omega)$ et $\mathcal{R} > 0$. Supposons que $V_{i,0} = (V_{i,0})_*$ et est radialement décroissant. Alors,

$$\eta_L(\mathcal{R}, V_{i,0}) \neq \max_{R \in \mathcal{M}_{|\Omega|\mathcal{R}}(\Omega)} \eta_L(R, V_{i,0}).$$

De plus, il existe $R \in \mathcal{M}_{|\Omega|\mathcal{R}}(\Omega)$ tel que $R = R_*$ et $\eta_L(R, V_{i,0}) > \eta_L(\mathcal{R}, V_{i,0})$.

Le théorème sert de contre-exemple à la stratégie d'homogénéisation. Si nous supposons que la condition initiale des pucerons infectés est symétrique et radialement strictement décroissante, alors le refuge homogénéisé (qui peut être approché, comme l'indique le théorème précédent, en augmentant la fréquence des refuges) n'est pas optimal. Dans ce cas, il existe un refuge symétrique et radialement décroissant qui produit une récolte linéarisée supérieure à celle du refuge homogénéisé. Cependant, sous une hypothèse différente, à savoir si $V_{i,0}$ est constant en espace, nous prouvons qu'un refuge homogénéisé est optimal pour la récolte linéarisée, et nous fournissons une formule explicite de ce refuge homogénéisé :

Théorème 1.6.4. *Supposons que $x \mapsto V_{i,0}$ est constant.*
Soit $\mathcal{R} = \left(\dfrac{\sqrt{\beta_{VH}(\xi + m) V_{i,0}} - \xi}{m} \right)^+$. Alors

$$\eta_L(\mathcal{R}, V_{i,0}) = \max_{R \in \mathcal{C}_b^{2+\alpha}(\Omega, \mathbb{R})} \eta_L(R, V_{i,0}).$$

En fait, nous prouvons ce théorème en supposant que *la moyenne de $V_{i,0}$* est constante en espace (dans un cadre de probabilité délibérément vague). Cette condition est purement biologique et ne sert qu'à alléger l'hypothèse stricte d'une condition initiale constante sur la population de pucerons infectés. Elle ne change rien à la preuve. Si cette hypothèse sur $V_{i,0}$ est satisfaite, alors la stratégie d'homogénéisation maximise la récolte linéarisée.

Dans le chapitre 4, nous proposons des idées et des conjectures, s'inspirant des résultats établis sur les ondes progressives, concernant les vitesses de propagation des populations I, V_i, V et P dans le contexte de l'invasion de pucerons. Concrètement, nous conjecturons que la vitesse de propagation des populations V et P est, si elle est bien définie,

$$c_*^V = c_*^P = \min_{\mu > 0} \frac{-\lambda_1(-\sigma_V \partial_{xx} + 2\sigma_V \mu \partial_x - \sigma_V \mu^2 - r(x) + h r_P(x)/s_P)}{\mu},$$

et la vitesse de propagation de I et V_i est

$$\min_{\mu>0} \frac{-\lambda_1(\mathcal{L}_\mu)}{\mu}$$

où $\lambda_1(\mathcal{L}_\mu)$ désigne la valeur propre principale de l'opérateur

$$\mathcal{L}_\mu = -\begin{pmatrix} 0 & 0 \\ 0 & \sigma_V \end{pmatrix} \partial_{xx} + 2\mu \begin{pmatrix} 0 & 0 \\ 0 & \sigma_V \end{pmatrix} \partial_x - \mu^2 \begin{pmatrix} 0 & 0 \\ 0 & \sigma_V \end{pmatrix} - A.$$

En outre, nous conjecturons un résultat d'homogénéisation potentiel concernant la convergence de ces vitesses de propagation vers celles du système homogénéisé lorsque la fréquence du refuge tend vers l'infini.

Au chapitre 5, nous fournissons des valeurs numériques biologiquement cohérentes pour tous nos paramètres, dérivées d'expériences documentées dans la littérature. Cela nous permet d'effectuer des simulations numériques de notre système, de tracer l'évolution des populations et de calculer la récolte pour une gamme de paramètres variables. Il est important de noter qu'avec le jeu de paramètres que nous avons choisi, les valeurs propres principales des opérateurs $-r_V^R + hr_P^R/s_V$ et $-r_V^F + hr_P^F/s_V$ sont positives, où r_V^R, r_V^F, r_P^R, r_P^R sont les valeurs de r_V et r_P dans le refuge et dans le champ, respectivement. Ainsi, même en l'absence de refuge, la population de pucerons converge vers 0 dans nos simulations numériques.

Introduction (English version)

1.7 Biological context

1.7.1 Pesticide use in agriculture

Pesticide use in agriculture has been a subject of both intensive use and heated debate [40], particularly as it pertains to environmental and health implications associated with certain chemical compounds. One class of pesticides that has come under intense scrutiny is neonicotinoids, a group of systemic insecticides widely employed in agro-cultures [13], [60], [34], [18]. We focus on the specific context of neonicotinoid use in sugar beet fields.

The term "neonicotinoids" encompasses a class of neuro-active insecticides developed to combat a range of pests affecting various crops. The unique feature of these pesticides lies in their systemic nature, as they are absorbed by plants and distributed throughout their tissues, providing protection against pests at various stages of the crop's growth. In sugar beet fields, neonicotinoids are commonly used [38] to control pests such as aphids, which can cause considerable damage to the crop [52].

However, the impact of these pesticides on the environment and human health is significant. We emphasize the urgency and importance of identifying viable alternatives that are less harmful to both ecosystems and human well-being. Indeed, despite their efficacy in pest management, neonicotinoids have been linked to severe environmental consequences. One of the primary concerns is their role in pollinator decline, particularly impacting crucial species like bees [60]. Neonicotinoids can persist in soil and water, posing risks to non-target organisms and potentially entering the food chain. Doris Klingelhöfer et al. [34] have highlighted their adverse effects on biodiversity, water quality, and the broader ecosystem.

The potential risks of neonicotinoids extend beyond the environment to human health. Residues of these pesticides have been detected in food items [74], raising questions about their impact on human consumers. Recent research [18] link chronic neonicotinoid exposure to various health issues, including neurotoxic effects, emphasizing the need for a comprehensive assessment of risks.

In light of the growing awareness of the environmental and health risks posed by neonicotinoids, there is an increasing emphasis on finding alternative approaches to pest management in agriculture. Some ongoing research [33] aims at identifying sustainable, eco-friendly alternatives to neonicotinoids. These alternatives encompass non-chemical methodologies like leveraging microorganisms, semiochemicals, or implementing surface coatings. This thesis contributes to the ongoing search for pesticide alternatives. In the context of the sugar-beet agro-ecosystem, our research is concerned with a pesticide-free agro-ecological method of controlling insect crop pests: the employement of natural specialized predators.

Figure 1.8: A sugar beet leaf presenting symptoms of the beet yellows virus (source: Farmers weekly).

1.7.2 The sugar-beet agro-ecosystem

In the beet field, aphids (namely, *Myzus Persicae* and *Aphis Fabae*) are vectors of four yellows viruses. According to the Institut Technique de la Betterave [10] (qui est la référence de toute cette sous-section), two of these viruses, belonging to the polerovirus genus, are closely related genetically and induce symptoms of moderate jaundice: Beet mild yellowing virus (BMYV) and Beet chlorosis virus (BChV). Beet yellows virus (BYV), causing severe jaundice symptoms, is a more distantly related species belonging to the closterovirus genus. The rarer mosaic virus (BtMV) belongs to the potyvirus genus. These viruses are transmitted exclusively by aphid vectors when they feed on beet leaves, with the green peach aphid *Myzus persicae* being the primary vector. Transmission is non-propagative: these viruses cannot be transmitted to the offspring of viruliferous aphids. In 2020, the Institut Technique de la Betterave conducted a virus analysis in France, revealing a prevalence of BYV exceeding 90 percent among all yellows viruses. The BYV has a viral acquisition phase ranging from a few minutes to a few hours. However, the virus can only be retained for a maximum of 48 hours in the insect's mouthparts, with transmission rates significantly dropping after 24 hours. It can be retransmitted immediately after acquisition but is lost when the aphid molts.

The initial symptoms manifest as small, pale dots on the leaf blade, subsequently progressing to a lightening of the secondary veins, resembling leaf engraving, which is characteristic of the disease. Eventually, lemon-yellow spots develop. In the later stages, these spots may evolve into reddish-brown patches that can merge, potentially leading to a dominant reddish hue (see figure 1.8).

Regarding the impact on yield, experiments conducted in England unveiled substantial productivity losses ranging between 40-50 percent within the infected areas.

Currently, pesticides stand as the primary tool for beet protection, employed by a significant majority of farmers. In our alternative approach of interest, natural predators of aphids, such as ladybugs (*Hippodamia variegata* or *Chnootriba similis*), serve as a biological method of managing the aphid population, and consequently the spread of the beet yellows virus.

Typically, the absence of plants or flowers creates an unfavorable environment for these predators. We allocate a portion of the field for the cultivation of flowers, forming what we refer to as biodiversity refuges. Within these floral patches, we anticipate a proliferation of insects that ladybugs can feed on, accelerating their reproduction. While these refuges aid the predators in flourishing and managing the aphids, there are two potential drawbacks to consider. Firstly, the refuge could potentially accelerate aphid growth, given that the sugar beets

Figure 1.9: A ladybug feeding on aphids (source: Quora).

are initially too underdeveloped for aphids to feed on. Secondly, and this is the main constraint, no beet can be grown in the areas where the refuges have been established. In the case when the refuge slows down the invasion of aphids, it is therefore necessary to find a compromise in terms of the quantity of refuge to be set up.

The foundation for our thesis revolves around this agro-ecological system: a sugar beet field with designated biodiversity refuges in the form of flower patches, where aphids pose a threat by potentially invading the field, putting the beets at risk of contamination with the yellows virus, while ladybugs act as natural predators, feeding on the aphids and potentially halting the spread of the disease. The central question guiding our entire thesis is:

In the beet field, what refuge layout is optimal to best limit the spread of the beet yellows virus and to maximize the harvest ?

To help answer this question, we will use a mathematical model of this system.

1.8 Mathematical modeling, some examples

Mathematical modeling is a powerful and versatile tool that bridges the gap between theoretical concepts and real-world phenomena. It is a systematic approach to representing, analyzing, and understanding complex systems using mathematical structures and techniques. It involves the creation of mathematical representations that simulate the behavior of a system or process. These models are designed to capture essential features and relationships within the system, allowing for predictions, analysis, and decision-making. They include variables representing different aspects of the system and fixed parameters that define its characteristics. Typically, mathematical relationships are expressed through equations describing how variables interact over time or space. Models often rely on assumptions and constraints to simplify complex systems and make them more tractable. We will delve into a specific type of mathematical model: the reaction-diffusion system.

1.8.1 Understanding reaction-diffusion systems

Reaction-diffusion systems constitute a class of mathematical models that describe the dynamic interplay between the local reactions and the spatial diffusion of one or more interacting substances or populations. These systems are characterized by a set of partial differential equations (PDE) that govern the temporal evolution of concentrations or densities of the involved entities

across a spatial domain. Formally, let Ω be an open subset of $\mathbb{R}^d$. A reaction-diffusion system is a system of PDE of the form

$$\partial_t \mathbf{u} + \sigma \mathcal{L} \mathbf{u} = f(\mathbf{u}, x, t),$$

where σ is a diagonal matrix with positive coefficients called diffusion matrix,

$$f : \mathbb{R}^k \times \Omega \times \mathbb{R}_+^* \to \mathbb{R}^k$$

is called the reaction term and

$$\mathbf{u} : \Omega \times \mathbb{R}_+^* \to \mathbb{R}^k$$

is the unknown (k is a non-zero natural number). ∂_t designates the partial derivative in time, and $\mathcal{L}$ denotes a second order operator qualified as elliptic [22], i.e an operator of the form $\mathcal{L} = \sum_{|\alpha| \leq 2} a_\alpha(x) \partial^\alpha$, where for all x in Ω and for all ξ in $\mathbb{R}^d \setminus \{0\}$, we have $\sum_{|\alpha|=2} a_\alpha(x) \xi^\alpha \neq 0$. In many examples, we will take $\mathcal{L} = -\Delta$, where Δ denotes the Laplacian, which is the sum of the second order spatial partial derivatives.

Reaction-diffusion systems find applications across diverse scientific domains, showcasing their versatility and significance. In developmental biology, in embryonic development, reaction-diffusion models elucidate the formation of spatial patterns, guiding the arrangement of biological structures [49]. In neurobiology, reaction-diffusion systems are used to study the spatial dynamics of neural signals, leading to a better understanding of brain function and pattern formation in neural networks [59]. In ecology and population dynamics, these systems contribute to the understanding of the spatial distribution of species, predator-prey interactions, and the emergence of biodiversity patterns in ecosystems [19]. Applied to chemical processes, these models help analyze the spatial distribution of reactants and products [65]. In environmental science, reaction-diffusion systems help to model the propagation of pollutants and the dispersion of substances in natural environments [58].

A generic one-dimensional two-species reaction-diffusion system can be expressed as follows:

$$\begin{cases} \partial_t u - \sigma_u \partial_{xx}^2 u = r(u, v) \\ \partial_t v - \sigma_v \partial_{xx}^2 v = s(u, v) \end{cases}$$

where:

- $u(x, t)$ and $v(x, t)$ represent the concentrations or densities of interacting substances or populations at position x and time t.
- σ_u and σ_v are positive diffusion coefficients, determining the rate at which u and v spread through space, respectively. The term "diffusion" refers here to uniform movement, with no preferred direction. Higher values indicate faster diffusion, while smaller values indicate slower diffusion.
- $r(u, v)$ and $s(u, v)$ are reaction terms, encapsulating the local interactions between u and v. These terms define how the concentrations of u and v change due to their mutual influence. The specific form of r and s depends on the nature of the interactions and reactions in the system. For example, in ecological models, r and s might represent birth, death, and predation rates in a prey-predator system.

We typically supplement the system with initial conditions:

$$\begin{cases} u(\cdot, 0) = u_0 \\ v(\cdot, 0) = v_0, \end{cases}$$

u_0 and v_0 being given functions, usually nonnegative in a biological framework. The domain of the space variable is either the unbounded set $\mathbb{R}$, or a bounded interval Ω of $\mathbb{R}$. In the latter case, boundary conditions are required to describe the behaviour of the entities at the boundary of the interval:

$$\begin{cases} \alpha_u u + \beta_u \dfrac{\partial u}{\partial n} = 0 & \text{on } \partial\Omega \\ \alpha_v v + \beta_v \dfrac{\partial v}{\partial n} = 0 & \text{on } \partial\Omega, \end{cases}$$

where α_u, β_u, α_v, β_v are nonnegative, with $\alpha_u + \beta_u > 0$ and $\alpha_v + \beta_v > 0$. The scenario where $\beta_u = \beta_v = 0$ is called homogeneous Dirichlet boundary conditions. This configuration establishes that the concentration of entities becomes fixed to zero at the boundary. In the context of population density evolution, this condition can be likened to a death zone or a chasm, effectively eliminating any individual upon contact. On the other hand, when $\alpha_u = \alpha_v = 0$, it corresponds to homogeneous Neumann boundary conditions or no-flux boundary conditions. This condition ensures that no entities can traverse in or out of the set Ω. It functions like an impermeable wall, causing populations to rebound and move in the opposite direction when they encounter it. In cases where the coefficients α_u, β_u, α_v, β_v are all non-zero, the conditions are known as Robin, or mixed, boundary conditions.

1.8.2 A comparison theorem for reaction-diffusion equations

In this thesis, we will be comparing solutions of reaction-diffusion equations. For this purpose, we present a very useful theorem, following the chapter 2, third section of [69]. Consider the scalar reaction-diffusion equation

$$\partial_t u - \sigma \Delta u = f(u, x, t) \tag{1.8}$$

in a domain $\Omega \subset \mathbb{R}^d$. Let $T > 0$ and $D = \Omega \times (0, T)$. We assume that u is continuous in $\overline{D}$, its second derivative with respect to x and first derivative with respect to t are bounded and continuous in D. The function f and its derivative $\partial f / \partial u$ are bounded and continuous in $\overline{D}$ with respect to all variable u, x, t.

Theorem 1.8.1. *(Comparison theorem). Let $u(x,t)$ and $v(x,t)$ be solutions of equation 1.8 in a bounded domain Ω. If $u(x,t) \geq v(x,t)$ on $\partial D \cap \{t < T\}$, then $u(x,t) \geq v(x,t)$ in D.*

1.8.3 The Fisher-KPP equation

The Fisher-KPP (KPP stands for Kolmogorov, Petrovsky, and Piskunov) equations constitute a reaction-diffusion model, specifically designed to describe the spread of advantageous traits in populations. Named after the mathematicians who first introduced them in the 1930s [23], [35], these equations have found applications in various fields, including ecology, population dynamics, and mathematical biology. We will later use this model to study the evolution of our populations. The Fisher-KPP equation typically takes the form:

$$\partial_t u - \sigma \Delta u = ru - su^2.$$

Here, the reaction term represents the logistic growth of the population. The factor ru describes the exponential growth, and $-su^2$ introduces a self-limiting effect, preventing the population from exceeding a certain value. The positive parameters r and s are called, respectively, the Malthusian growth rate of the population, and the saturation rate of the population. The diffusion term $-\sigma\Delta$ modelizes a uniform movement of the population, with no favored direction

to go. We can understand the laplacian diffusion of a population density with the following: n individuals moving randomly in space following a Brownian motion, and $n \to +\infty$.

If the parameters are independent of the space and time variable (or space-time homogeneous), and if the positive initial condition provided to solve the system is also space homogeneous, then the system becomes an ordinary differential Cauchy system:

$$\begin{cases} u' = ru - su^2 \\ u(0) = u_0 > 0, \end{cases}$$

whose solution can be computed explicitely: for all $t \geq 0$,

$$u(t) = \frac{r/s}{1 + (r/(su_0) - 1)e^{-t}}.$$

We plot this solution for different sets of parameters and initial condition in Figure 1.12.

The time limit of all the solutions, i.e the quantity r/s, is called the carrying capacity of the population. It refers to the maximum population size that a particular environment can sustain over an extended period. This concept is a fundamental component in ecological studies and population dynamics. The carrying capacity is influenced by the availability of resources, environmental conditions, and interactions between species [63]. It is important to note that in the space-heterogeneous case, which is going to be our case of interest, r/s is not a stationary solution due to the presence of the laplacian in the equation. The stationary solution of the Fisher-KPP equation, in this case, is the solution of $-\sigma\Delta u = ru - su^2$. We plot various stationary solutions u for a heterogeneous coefficient $r(x)$, in the interval $[0,1]$, with Neumann boundary conditions, for a range of σ, in Figure 1.13. As σ gets smaller, u converges to $r(x)/s$. As σ gets bigger, u converges to $\int_0^1 r/s$. The limit $\sigma \to +\infty$ is commonly referred to as homogenization, and will be a key concept in this thesis in determining the optimal refuge layout.

1.8.4 Numerical method for reaction-diffusion equations

We use the example of the Fisher-KPP equation supplemented with Neumann boundary conditions

$$\begin{cases} \partial_t u - \sigma\Delta u = ru - su^2 & \text{in } (0,1) \times \mathbb{R}_+^*, \\ u(\cdot, 0) = u_0 & \text{in } [0,1], \\ \dfrac{\partial u}{\partial n} = 0 & \text{in } \{0,1\} \times \mathbb{R}_+^*, \end{cases} \tag{1.9}$$

to introduce a basic numerical method to solve this system: the semi-implicit finite difference scheme. Since we cannot compute a solution for infinite times, one needs to define an ending time $T > 0$. We discretise space and time with a finite grid in $[0,1] \times [0,T]$: we fix a number of time steps $N+1 \in \mathbb{N}^*$ and a number of space steps $J+1 \in \mathbb{N}^*$. Our discretised domain is then

$$\mathcal{G} := \left\{ j\frac{1}{J},\, j \in [0,J] \right\} \times \left\{ n\frac{T}{N},\, n \in [0,N] \right\},$$

and the goal is to compute an approximated solution $\mathfrak{u} : \mathcal{G} \to \mathbb{R}$. We define the quantities $\mathrm{d}x = 1/J$ and $\mathrm{d}t = T/N$, and for all $(j\mathrm{d}x, n\mathrm{d}t) \in \mathcal{G}$, $\mathfrak{u}(j\mathrm{d}x, n\mathrm{d}t) = u_j^n$. The finite difference method consists in approximating the time derivative $\partial_t u(x,t)$ with $\dfrac{u_j^{n+1} - u_j^n}{\mathrm{d}t}$ and the spatial

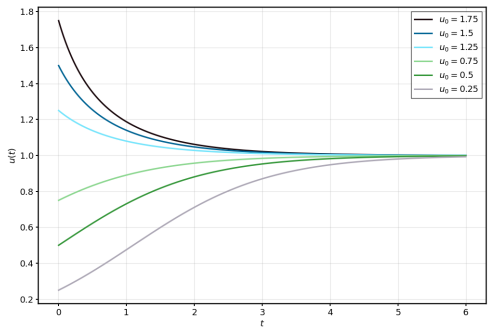

Figure 1.10: Fisher-KPP analytical solutions for various values of initial conditions, with $r = s = 1$.

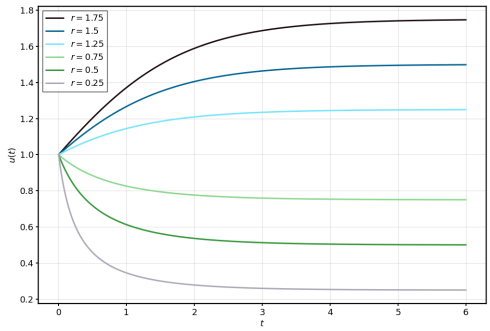

Figure 1.11: Fisher-KPP analytical solutions for various values of r, with $u_0 = s = 1$.

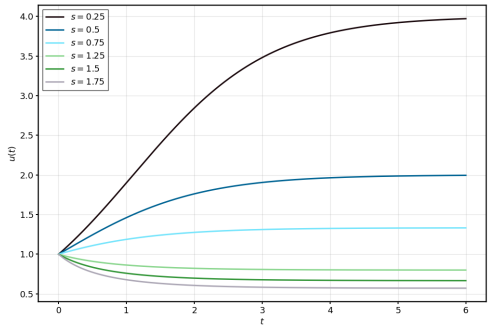

Figure 1.12: Fisher-KPP analytical solutions for various values of s, with $u_0 = r = 1$.

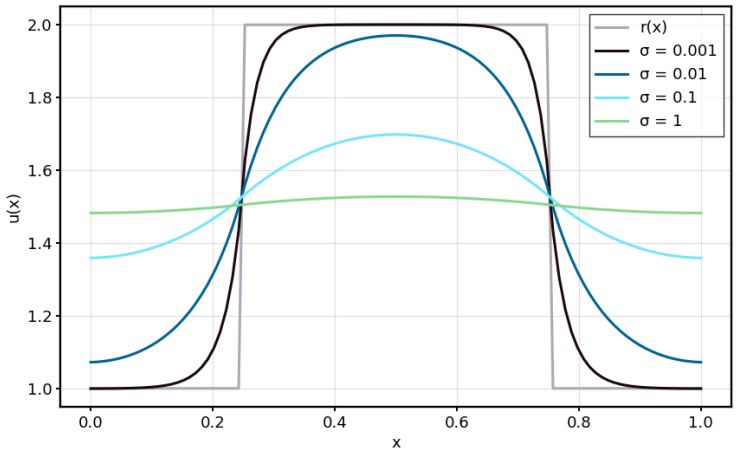

Figure 1.13: Solutions of $-\sigma\Delta u = r(x)u - su^2$, Neumann boundary conditions, for various values of σ, with r a rectangular function and $s = 1$.

laplacian $\Delta u(x,t)$ (which is simply the second-order derivative in our one-dimensional case) with $\dfrac{u_{j-1}^{n+1} - 2u_j^{n+1} + u_{j+1}^{n+1}}{\mathrm{d}x^2}$. The equation becomes

$$\frac{u_j^{n+1} - u_j^n}{\mathrm{d}t} - \sigma \frac{u_{j-1}^{n+1} - 2u_j^{n+1} + u_{j+1}^{n+1}}{\mathrm{d}x^2} = ru_j^n - s(u_j^n)^2.$$

The reaction part is solved explicitely, meaning that the terms do not depend on future times. One can explicitely solve $\dfrac{u_j^{n+1} - u_j^n}{\mathrm{d}t} = ru_j^n - s(u_j^n)^2$ by simply plugging $u_j^{n+1} = u_j^n + \mathrm{d}t(ru_j^n - s(u_j^n)^2)$ for every j, one time step at a time. The diffusion part is solved implicitely, meaning that the terms depend on future times.

To deal with the term $\dfrac{u_{j-1}^n - 2u_j^n + u_{j+1}^n}{\mathrm{d}x^2}$ in the equation, one cannot compute values of u one spatial step at a time, since they depend on the locations $j+1$, j, and $j-1$. Instead, we write, for $n \in [0, N]$,

$$\frac{1}{\mathrm{d}x^2} LU^n,$$

where

$$L = \begin{pmatrix} -1 & 1 & 0 & 0 & 0 & \cdots & 0 \\ 1 & -2 & 1 & 0 & 0 & \cdots & 0 \\ 0 & 1 & -2 & 1 & 0 & \cdots & 0 \\ \vdots & 0 & \ddots & \ddots & \ddots & 0 & \vdots \\ 0 & \cdots & 0 & 1 & -2 & 1 & 0 \\ 0 & \cdots & 0 & 0 & 1 & -2 & 1 \\ 0 & \cdots & 0 & 0 & 0 & 1 & -1 \end{pmatrix} \in \mathcal{M}_J(\mathbb{R}),$$

and

$$U^n = \begin{pmatrix} u_0^n \\ u_1^n \\ \\ \vdots \\ \\ u_{J-2}^n \\ u_{J-1}^n \end{pmatrix},$$

which is a matricial representation of the terms $\frac{u_{j-1}^n - 2u_j^n + u_{j+1}^n}{\mathrm{d}x^2}$ for all $j \in [1, J-1]$, and, according to the Neumann boundary conditions, $\frac{-u_0^n + u_1^n}{\mathrm{d}x^2} = 0$ and $\frac{u_{J-1}^n - u_J^n}{\mathrm{d}x^2} = 0$.

Here, we write the following matricial representation of our system: for all $n \in [0, N-1]$, denoting $R^n = (ru_j^n - s(u_j^n)^2)_{j\in[0,J]}$,

$$\left(I_{J+1} - \frac{\sigma \mathrm{d}t}{\mathrm{d}x^2} L\right) U^{n+1} = U^n + \mathrm{d}t R^n,$$

with I_{J+1} designating the identity $(J+1) \times (J+1)$ matrix. We then numerically invert the matrix $I_{J+1} - \frac{\sigma \mathrm{d}t}{\mathrm{d}x^2} L$ and deduce that, for all $n \in [0, N-1]$,

$$U^{n+1} = \left(I_{J+1} - \frac{\sigma \mathrm{d}t}{\mathrm{d}x^2} L\right)^{-1} (U^n + \mathrm{d}t R^n).$$

1.9 Homogenization

Homogenization is a mathematical technique used to study the behavior of a heterogeneous material or medium at a larger scale. It involves the analysis of a PDE system in a domain with rapidly oscillating coefficients. The key idea is to derive a so-called homogenized equation at a larger scale, capturing the averaged behavior of the medium. This macroscopic equation is often easier to analyze than the original, highly oscillatory PDE system. Homogenization has broad applications [44], [5], providing a powerful tool to bridge the gap between micro and macro scales in mathematical modeling. The mathematical goal of this technique is to prove that the solution of the initial model converges to the solution of the macro model.

The problem can be stated as follows. For a parameter $\varepsilon > 0$ we call period, we consider a reaction-diffusion equation of the form

$$\partial_t u_\varepsilon + \mathcal{L}_\varepsilon u_\varepsilon = f_\varepsilon$$

with appropriate initial and boundary conditions. Here, $\mathcal{L}_\varepsilon$ is an elliptic operator, and both $\mathcal{L}_\varepsilon$ and f_ε depend on the period of oscillations ε. Next, we define the homogenized equation:

$$\partial_t u + \mathcal{L} u = f.$$

The main goal is to answer the following question.

When ε goes to 0, does the solution u_ε converge to u ? In what sense ?

Let us be more specific on the matter by considering a simple example of homogenization. Let $r \in \mathcal{C}^2((0,1),\mathbb{R})$, extend periodically this function in all $\mathbb{R}$ and define $r_\varepsilon : x \mapsto r(x/\varepsilon)$. Defined like so, the function $r_\varepsilon : (0,1) \mapsto \mathbb{R}$ has a period of ε, and is rapidly oscillating as ε goes to 0. Consider the Cauchy–Neumann problem

$$\begin{cases} \partial_t u_\varepsilon - \sigma \Delta u_\varepsilon = r_\varepsilon u - s u_\varepsilon^2 & \text{in } (0,1) \times \mathbb{R}_+^* \\ u_\varepsilon(\cdot, 0) = u_0 & \text{in } [0,1] \\ \dfrac{\partial u_\varepsilon}{\partial n} = 0 & \text{on } \{0,1\} \times \mathbb{R}_+^*. \end{cases}$$

It is well known that r_ε converges weakly in $\mathrm{L}^2((0,1))$ to $\int_0^1 r$, the average of the function r. The homogenized problem is the following.

$$\begin{cases} \partial_t u - \sigma \Delta u = \int_0^1 r u - s u^2 & \text{in } (0,1) \times \mathbb{R}_+^* \\ u(\cdot, 0) = u_0 & \text{in } [0,1] \\ \dfrac{\partial u}{\partial n} = 0 & \text{on } \{0,1\} \times \mathbb{R}_+^*. \end{cases}$$

For $T > 0$, by deriving estimates on the solution u_ε and therefore obtaining some compactness on the sequence (u_ε), one can prove the strong convergence of u_ε in $\mathrm{L}^2((0,1) \times [0,T])$ and almost everywhere in $(0,1) \times [0,T]$ to u as ε goes to 0. In our model, we will use homogenization on the locations of refuges in the field.

1.10 The Krein-Rutman theorem

The study of eigenvalues and eigenvectors plays a fundamental role in understanding the behavior of linear operators and systems in various branches of mathematics. One important area where eigenvalue problems arise is in the context of compact operators on Banach spaces. In this realm, the Krein-Rutman theorem stands out as a powerful tool in understanding the existence and stability of positive solutions in various mathematical models, providing insights into the spectral properties of positive compact operators. It was proved by Krein and Rutman in 1948 [37]. This theorem has far-reaching applications, particularly in the analysis of nonlinear problems [62], [48] and mathematical models in diverse fields [57].

The Krein-Rutman theorem generalizes the Perron-Frobenius theorem, and addresses the spectral properties of positive compact operators defined on a potentially infinite-dimensional Banach space. Specifically, let T be a non-zero compact operator with positive spectral radius $r(T)$ in a Banach space X, and a convex cone K with $K \cap -K = \{0\}$ and $K - K$ dense in X, such that $T(K) \subset K$. Then, $r(T)$ is a (positive) simple eigenvalue of T:

$$T(u) = r(T)u,$$

with a positive associated eigenvector u, and is the only eigenvalue of T associated with a positive eigenvector [66].

The most important consequence of this theorem, in this thesis, is the following theorem: [62].

Theorem 1.10.1. *Let $\mathcal{L}$ be an elliptic operator on a bounded domain Ω in $\mathbb{R}^d$ with smooth boundary. Consider the eigenvalue problem*

$$\begin{cases} \mathcal{L}u + \lambda u = 0 & \text{in } \Omega \\ \alpha u + \beta \dfrac{\partial u}{\partial n} = 0 & \text{on } \partial\Omega. \end{cases} \tag{1.10}$$

Then 1.10 has a simple real eigenvalue λ_1 associated to a positive eigenfunction, and is the only eigenvalue associated to a positive eigenfunction. Additionally, for all eigenvalues λ of $\mathcal{L}$, $\lambda_1 \leq \mathrm{Re}(\lambda)$.

The eigenvalue λ_1 is called the *principal eigenvalue* of the operator $-\mathcal{L}$, and is a key concept in our analysis: its sign determines whether aphids go extinct or not.

1.11 Modeling our system

In this section, we present the modeling choices we employed to approach the sugar-beet agro-ecological system. Below are the notations we use for our different populations:

- The population of beets: H, for hosts.
- The population of infected beets: I.
- The population of susceptible beets: S (we then have $H = I + S$).
- The population of aphids: V, for vectors.
- The population of infected aphids: V_i.
- The population of susceptible aphids: V_s (we then have $V = V_i + V_s$).
- The population of ladybugs: P, for predators.

We suppose that the variation over time of a population infected with the beet yellows virus is solely proportional to the product of the population of susceptible and infected population. We call the proportionality constant of the transmission from vectors to hosts $\beta_{VH} > 0$ and the proportionality constant of the transmission from hosts to vectors $\beta_{HV} > 0$. Additionaly, we assume that the total population of aphids recover the virus proportionally to the infected aphid population, with a proportionality constant we denote $\alpha > 0$, called the recovery rate. Since the beets do not cure the virus, they do not either in our model. The epidemiological model is then the following:

$$\begin{cases} \partial_t I = \beta_{VH} S V_i \\ \partial_t S = -\beta_{VH} S V_i \\ \partial_t V_i = \beta_{HV} I V_s - \alpha V_i \\ \partial_t V_s = -\beta_{HV} I V_s + \alpha V_i. \end{cases}$$

We have implicitely assumed, with this model, that the population of beets $H = I + S$ is independent of time: $\partial_t H = \partial_t I + \partial_t S = \beta_{VH} S V_i - \beta_{VH} S V_i = 0$ (but is dependent of space, as having a refuge in one location implies the absence of beet in that same spot). We can rewrite this system by assuming that H is independent of time and removing one equation:

$$\begin{cases} \partial_t I = \beta_{VH} (H(x) - I) V_i \\ \partial_t V_i = \beta_{HV} I V_s - \alpha V_i \\ \partial_t V_s = -\beta_{HV} I V_s + \alpha V_i. \end{cases} \tag{1.11}$$

It will later be made explicit that we assume aphids do not transmit the virus to their offspring. The birth term will therefore only appear in the equation for V_s.

Next, we describe the aphids and ladybugs spread and reproduction with a Fisher-KPP model. In the absence of predators,

$$\partial_t V - \sigma_V \Delta V = r_V(x) V - s_V V^2,$$

where $\sigma_V > 0$ is their diffusion rate, $r_V(x) > 0$ their Malthusian growth rate, and $s_V > 0$ their saturation rate. We assumed here that only the Malthusian growth rate is a function of space, affected by the presence of the refuge in the field.

In the absence of aphids, the predator model would be

$$\partial_t P - \sigma_P \Delta P = r_P(x)P - s_P P^2,$$

with $\sigma_P > 0$, $r_P(x) > 0$, and $s_P > 0$ being the respective diffusion rate, Malthusian growth rate, and saturation rate, with the same assumption on the space-dependency of $r_P(x)$. It is important to note that the predators are generic in our model: they can survive and thrive even in the absence of aphids. However, as we saw in the previous section, the stationary solution of this equation P^* is not explicit. For technical reasons, namely to have direct control over the principal eigenvalue of the operator $\mathcal{L} = -\sigma_V \Delta - r_V + hP^*$ (which will prove to be crucial in our first paper [1]), we assume that the diffusion strategy of the ladybugs is different. Plus, biologically, ladybugs should be able to have a broader view of the field since they fly, therefore a uniform dispersion is likely to not be the most precise model. We would like to point out that ladybug larvae are also great consumers of aphids, but of course they do not fly. To simplify the model, we have only included one type of predator: the adult ladybug. We therefore assume that the ladybugs have perfect knowledge of the distribution of resources in the field (resources here refer to any food in the field, with the exception of aphids), and can adapt their spatial configuration optimally. This strategy is called an "ideal free dispersal strategy". It was proven in [16] that, in the context of the Fisher-KPP model 1.9 of the previous section, a diffusion–advection strategy of the form $u \mapsto \nabla \cdot (\nabla u - u \nabla(\ln r)) = \nabla \cdot (r \nabla (u/r))$ is evolutionary stable, convergent stable, and leads to a so-called "ideal free distribution" where the spatial distribution of the population density at equilibrium is exactly proportional to the spatial distribution of resources. We adopt this exact diffusion–advection strategy for our population of predators, hence, in the absence of aphids, the equation is

$$\partial_t P - \sigma_P \nabla \cdot (r_P(x) \nabla (P/r_P(x))) = r_P(x)P - s_P P^2.$$

It is easy to see here that $r_P(x)/s_P$ is a stationary solution, and in fact the only positive stationary solution of this equation [1]: the ladybugs can perfectly adapt to their environment and arrange themselves optimally in the field. However, we point out that in the presence of aphids, their distribution might not be optimal, since they are not attracted by aphids in any manner. Such a type of dispersion is called chemotaxis and is out of a scope of this thesis, but is a potential improvement of the model. To lighten the writing, we denote

$$\overline{\mathcal{L}}(P) = \nabla \cdot (r_P(x) \nabla (P/r_P(x))).$$

Moreover, we assume that the predation is detrimental to the population of aphids and proportional to the product of their population and the population of predators, with a proportionality constant $h > 0$ called predation rate. The predation is modeled as beneficial for the population of ladybugs and proportional to the product of their population and the population of aphids, with a proportionality constant $\gamma h > 0$, γ being called the efficiency of predation. Finally, we assume that our predators feed indifferently on aphids, whether infected or not. The complete prey-predator model is then:

$$\begin{cases} \partial_t V - \sigma_V \Delta V = r_V(x)V - s_V V^2 - hPV \\ \partial_t P - \sigma_P \overline{\mathcal{L}}(P) = r_P(x)P - s_P P^2 + \gamma h V P. \end{cases} \tag{1.12}$$

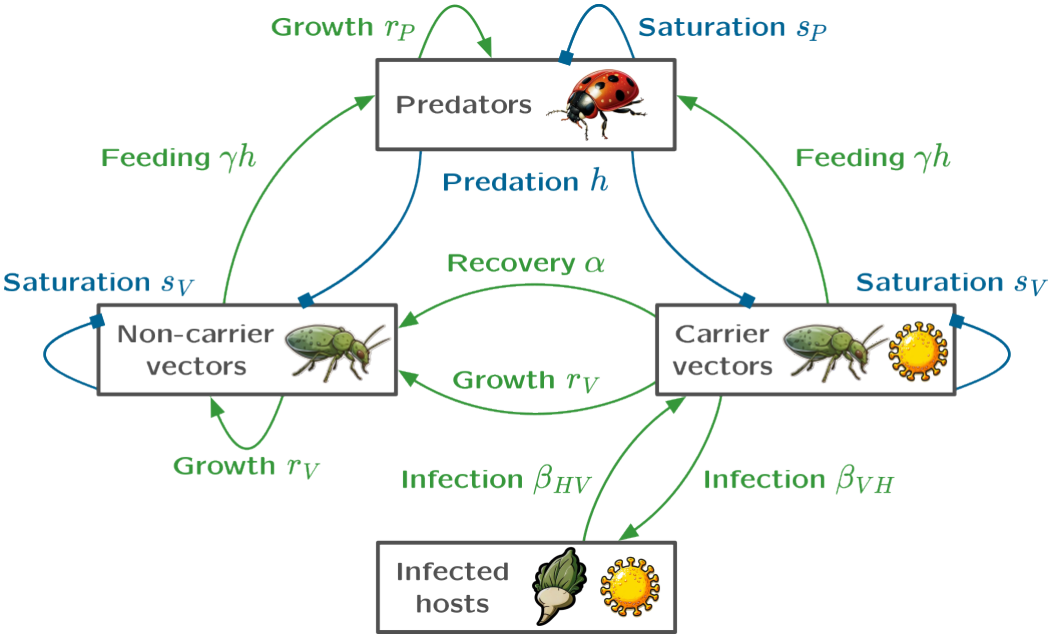

Figure 1.14: A visual representation of the mathematical modeling of the sugar-beet agro-ecosystem.

In our complete model, we mix the epidemiological model 1.11 and the prey–predator model 1.12 to get

$$\begin{cases} \partial_t I = \beta_{VH}(H(x) - I)V_i \\ \partial_t V_i - \sigma_V \Delta V_i = \beta_{HV} I V_s - \alpha V_i - d_V(x) V_i - s_V V V_i - hPV_i \\ \partial_t V_s - \sigma_V \Delta V_s = -\beta_{HV} I V_s + \alpha V_i - d_V(x) V_s - s_V V V_s - hPV_s + b_V(x)V \\ \partial_t P - \sigma_P \overline{\mathcal{L}}(P) = r_P(x)P - s_P P^2 + \gamma h V P. \end{cases}$$

We assumed here that the disease does not transmit to the offspring of the aphids, so the Malthusian growth rate $r_V(x)$ is split between a birth rate $b_V(x) > 0$ and a death rate $d_V(x) > 0$, so that $r_V(x) = b_V(x) - d_V(x)$, and the birth rate appears only in the V_s equation. The interactions between our four populations I, V_i, V_s, and P are summarized in Figure 1.14.

As a last assumption, the parameters β_{VH}, β_{HV}, α, σ_V, s_V, σ_P, s_V, h and γ remain unaffected by the presence of the refuge, making them spatially homogeneous, and all of our parameters β_{VH}, β_{HV}, α, σ_V, b_V, d_V, s_V, σ_P, r_P, s_V, h and γ are positive and time-homogeneous. The time-independency can be biologically justified with the rapid population dynamic: in numerical simulations, within a month or less, the populations V and P (and, as a consequence, I) tend to reach equilibrium. This can also be supported by real-life data, where ladybugs, for instance, eat up to fifty aphids a day [36], and diffuse at a high pace [72]. Therefore, we neglect the potential seasonal and environmental changes that would occur over a long period of time.

To demonstrate our main results, we use Neumann boundary conditions at the boundaries of our spatial domain (the beet field), which we call Ω.

Now that our mathematical model is in place, we can rigorously reformulate our research question. Since we've assumed an eternal spring, the quantity we've called "harvest", which

we denote η, is equal to

$$\eta = \int_\Omega H - I_\infty = \lim_{t\to+\infty} \int_\Omega H - I(\cdot,t).$$

This quantity therefore depends on the refuge R chosen, since this refuge affects certain parameters of our system. Let us denote X the set of admissible refuges. The "optimal refuge" we're looking for is then

$$\text{argmax}_{R\in X}\, \eta(R).$$

Obviously, since we can't explicitly compute the solutions of our system, it seems too difficult to obtain an explicit expression for this optimal refuge. However, it is possible to access certain properties of this refuge.

1.12 Main results

In Chapter 2, we introduce our first paper dealing with the system presented above. We begin by establishing the well-posedness, i.e., the existence and uniqueness of the solution, of the Cauchy-Neumann problem we have formulated, assuming that our spatially heterogeneous parameters are functions in $\mathcal{C}^{2+\alpha}(\overline{\Omega})$. Without this regularity assumption, the problem should still be well-posed, and requires adequate estimates on the regularity of the solutions in order to conclude. These estimates are technical, in particular the handling of the ideal free dispersion term of the population P. This theorem concerning existence and uniqueness, with parameters in, for example, $\mathrm{L}^\infty(\Omega)$ has not been proved in this thesis. Then, under the condition that the principal eigenvalue of the operator $-\sigma_V\Delta - r_V(x) + hr_P(x)/s_P$ is positive, we prove the uniform convergence of our population (V,P) to $(0, r_P(x)/s_P)$, and we derive estimates for the population of aphids, and the remaining harvest $\lim_{t\to+\infty}\int_\Omega H - I(\cdot,t)$. In the case where this principal eigenvalue is negative, we prove that the aphids persist at all times and everywhere in the field, and that the harvest is null. More precisely, let $\mathcal{L}_{V_s} = -\sigma_V\Delta - r_V(x) + hr_P(x)/s_P$, $\mathcal{L}_{V_i} = -\sigma_V\Delta + \alpha + d_V(x) + hr_P(x)/s_P$ and let $\lambda_1(\mathcal{L}_{V_s})$, $\lambda_1(\mathcal{L}_{V_i})$ be their principal eigenvalues with Neumann boundary conditions on $\partial\Omega$. Denote $\varphi_{s,1}$ and $\varphi_{i,1}$, the principal eigenfunctions associated, respectively, to $\lambda_1(\mathcal{L}_{V_s})$ and $\lambda_1(\mathcal{L}_{V_i})$, with normalizations $\min_\Omega \varphi_{s,1} = 1$ and $\max_\Omega \varphi_{i,1} = 1$. Then, the main result of our first paper is the following.

Theorem 1.12.1. *(i) Case of extinction: assume that $P_0 \not\equiv 0$ and $\lambda_1(\mathcal{L}_{V_s}) > 0$. Let $V = V_i + V_s$. Then, the following statements are true.*

- *$(V,P)(x,t) \to (0, r_P(x)/s_P)$ as $t \to +\infty$, uniformly in Ω.*
- *If we also assume $V_{i,0} \not\equiv 0$, then $\liminf_{t\to+\infty} \inf_{x\in\Omega} I(x,t) > 0$.*
- *More precisely, we have the following estimates. For any $\varepsilon > 0$ such that $\lambda_1(\mathcal{L}_{V_s}) - h\varepsilon > 0$, if $|P_0 - r_P/s_P| \le \varepsilon$ and $V_0 := V_{i,0} + V_{s,0} \le \varepsilon$, then for all $x \in \Omega$, $t \ge 0$,*

$$V(x,t) \le \max_\Omega V_0 \max_\Omega \varphi_{s,1} e^{-(\lambda_1(\mathcal{L}_{V_s})-h\varepsilon)t},$$

$$\frac{I(x,t)}{H(x)} \le 1 - \exp\left(-\beta_{VH}\frac{\max_\Omega V_0 \max_\Omega \varphi_{s,1}}{\lambda_1(\mathcal{L}_{V_s}) - h\varepsilon}\right),$$

$$1 - \exp\left(-\beta_{VH}\min_\Omega V_{i,0}\min_\Omega \varphi_{i,1}\frac{1 - e^{-(\lambda_1(\mathcal{L}_{V_i})+s_V\varepsilon+h\varepsilon)t}}{\lambda_1(\mathcal{L}_{V_i}) + s_V\varepsilon + h\varepsilon}\right) \le \frac{I(x,t)}{H(x)}.$$

(ii) Case of persistence: assume that $V_{i,0} \not\equiv 0$ and $\lambda_1(\mathcal{L}_{V_s}) < 0$. Then,

- $\liminf_{t\to+\infty} \inf_{x\in\Omega} V_i(x,t) > 0$;
- $\lim_{t\to+\infty} I(x,t) = H(x)$ *uniformly in* Ω.

This theorem suggests that maximizing $\lambda_1(\mathcal{L}_{V_s})$ (which can be achieved by increasing the refuge frequency, as a direct consequence of the variational formulation of $\lambda_1(\mathcal{L}_{V_s})$) is an effective strategy for maximizing the harvest, as it must be positive to eradicate the aphids. Furthermore, the estimates on the different populations lead to the following estimate of the harvest:

Corollary 1.12.2. *Assume that $\lambda_1(\mathcal{L}_{V_s}) > 0$. Then, for any $\varepsilon > 0$ such that $\lambda_1(\mathcal{L}_{V_s}) - h\varepsilon > 0$, if $|P_0 - r_P/s_P| \le \varepsilon$ and $V_0 \le \varepsilon$, then*

$$e^{-\beta_{VH}\frac{\max_\Omega V_0 \max_\Omega \varphi_{s,1}}{\lambda_1(\mathcal{L}_{V_s}) - h\varepsilon}} \le \frac{\int_\Omega (H - I_\infty)}{\int_\Omega H} \le e^{-\beta_{VH}\frac{\min_\Omega V_{i,0} \min_\Omega \varphi_{i,1}}{\lambda_1(\mathcal{L}_{V_i}) + s_V\varepsilon + h\varepsilon}}.$$

Assume that $\lambda_1(\mathcal{L}_{V_s}) < 0$. Then

$$\int_\Omega (H - I_\infty) = 0.$$

This estimate hints toward a potential monotonicity of the application $\lambda_1(\mathcal{L}_{V_s}) \mapsto \eta$. However, it turns out that this monotonicity is likely incorrect, as we will discuss in the second paper.

In Chapter 3, we introduce our second paper, which also delves into the system discussed above. We prove the convergence of the harvest to the harvest of the homogenized system when the frequency of the refuge goes to infinity (the frequency of the refuge being the number of uniformly distributed small patches in the field). Specifically, let $R \in \mathrm{L}^\infty(\Omega)$, periodically extended in $\mathbb{R}^d$. We call "refuge of frequency n" the application $R_n : x \mapsto R(nx)$. We denote its average over the field $\mathcal{R} = \langle R_n \rangle_\Omega = 1/|\Omega| \int_\Omega R_n$ (which does not depend on n). We assume that our space-heterogeneous parameters are of the following form:

$$\begin{aligned}
&H_n = H^0(1 - R_n) \text{ of integral also independent of } n\\
&b_V^n = (b_V^r - b_V^f)R_n + b_V^f\\
&d_V^n = (d_V^r - d_V^f)R_n + d_V^f\\
&r_V^n = b_V^n - d_V^n\\
&r_P^n = (r_P^r - r_P^f)R_n + r_P^f.
\end{aligned}$$

We consider a similar Cauchy–Neumann problem as the one described above, with a refuge R_n, for which the system rewrites itself

$$\begin{cases}
\partial_t I &= \beta_{VH}(H_n - I)V_i\\
\partial_t V_i &= \sigma_V \Delta V_i + \beta_{HV} I V_s - (\alpha + d_V^n + s_V(V_s + V_i) + hP)V_i\\
\partial_t V_s &= \sigma_V \Delta V_s + (\alpha + b_V^n)V_i + (r_V^n - \beta_{HV} I - s_V(V_s + V_i) - hP)V_s\\
\partial_t P &= \sigma_P \nabla \cdot \left(r_P^n \nabla \left(\frac{P}{r_P^n} \right) \right) + (\gamma h(V_s + V_i) + r_P^n - s_P P)P.
\end{cases} \tag{1.13}$$

with nonnegative initial condition $(I, V_i, V_s, P)(\cdot, 0) = (I_0^n, V_{i,0}^n, V_{s,0}^n, P_0^n) \quad \text{in } \Omega.$

Denote (I_n, V_i^n, V_s^n, P_n), the unique solution of this new problem, and

$$\eta_n = \left(\int_\Omega H - I_\infty\right)_n = \int_\Omega H_n e^{-\beta_{VH}\int_0^{+\infty} V_i^n}$$

the associated harvest.

We also denote

$$\begin{array}{rll} H_\infty & = \langle H_n\rangle_\Omega & = H^0(1-\mathcal{R}) \\ b_V^\infty & = \langle b_V^n\rangle_\Omega & = (b_V^r - b_V^f)\mathcal{R} + b_V^f \\ d_V^\infty & = \langle d_V^n\rangle_\Omega & = (d_V^r - d_V^f)\mathcal{R} + d_V^f \\ r_V^\infty & = \langle r_V^n\rangle_\Omega & = b_V^\infty - d_V^\infty \\ r_P^\infty & = \langle r_P^n\rangle_\Omega & = (r_P^r - r_P^f)\mathcal{R} + r_P^f \\ (r_P^\infty)_2 & = \langle (r_P^n)^2\rangle_\Omega & = (r_P^r - r_P^f)^2\mathcal{R}_2 + 2(r_P^r - r_P^f)r_P^f\mathcal{R} + (r_P^f)^2, \end{array}$$

and $r^* \in \mathcal{M}_d(\mathbb{R})$ the so-called "homogenized conductivity" defined in [4].

The homogenized Cauchy–Neumann problem is the following:

$$\begin{cases} \partial_t I & = \beta_{VH}(H_\infty - I)V_i \\ \partial_t V_i & = \sigma_V \Delta V_i + \beta_{HV} I V_s - (\alpha + d_V^\infty + s_V(V_s+V_i) + hP)V_i \\ \partial_t V_s & = \sigma_V \Delta V_s + (\alpha + b_V^\infty)V_i + (r_V^\infty - \beta_{HV} I - s_V(V_s+V_i) - hP)V_s \\ \partial_t P & = \sigma_P \nabla\cdot\left(r^*\nabla\left(\frac{P}{r_P^\infty}\right)\right) + (\gamma h(V_s+V_i) + \frac{(r_P^\infty)_2}{r_P^\infty} - s_P\frac{(r_P^\infty)_2}{(r_P^\infty)^2}P)P. \end{cases} \tag{1.14}$$

with nonnegative initial condition $(I, V_i, V_s, P)(\cdot, 0) = (I_0^\infty, V_{i,0}^\infty, V_{s,0}^\infty, P_0^\infty)$ in Ω. We assume the weak convergence in $\mathrm{L}^2(\Omega)$ of I_0^n, $V_{i,0}^n$, $V_{s,0}^n$, P_0^n to I_0^∞, $V_{i,0}^\infty$, $V_{s,0}^\infty$, P_0^∞, respectively.

Denote $(I^\infty, V_i^\infty, V_s^\infty, P^\infty)$, the unique solution of this problem, and

$$\eta_\infty = \left(\int_\Omega H - I_\infty\right)_\infty = \int_\Omega H_\infty e^{-\beta_{VH}\int_0^{+\infty} V_i^\infty}$$

the associated harvest. Then, we have the following theorem.

Theorem 1.12.3. *Suppose that* $\lambda_1(\mathcal{L}_{V_s}) > 0$.

The harvest $\eta_n = \left(\int_\Omega H - I_\infty\right)_n$ *converges to* $\eta_\infty = \left(\int_\Omega H - I_\infty\right)_\infty$ *as* $n \to +\infty$.

This theorem is central in answering our research question because it links the homogenization strategy (i.e increasing the refuge frequency) with the optimality of the homogenized refuge (which is the last main theorem of this paper).

Let us denote

- $m = \dfrac{h}{s_P}(r_P^r - r_P^f) + d_V^r - d_V^f$,
- $\xi = \alpha + d_V^f + \dfrac{h}{s_P} r_P^f > 0$.

We prove that, when $\Omega = [-L, L]$ for $L > 0$, under a specific assumption on the shape of the initial condition of the infected population of aphids $V_{i,0}$, a homogenized refuge is not optimal for maximizing a quantity η_L we call *linearized harvest*:

$$\eta_L(R, V_{i,0}) = H^0\left(|\Omega| - \int_\Omega R\right) + \frac{\beta_{VH}H^0}{m}\left(\int_\Omega V_{i,0} - (\xi+m)\int_\Omega \varphi_R V_{i,0}\right),$$

which we numerically observe to be very close to the non linearized harvest η when the eigenvalue $\lambda_1(\mathcal{L}_{V_s})$ is positive. The shape we are refering to is called a "Schwarz rearrangement" of a function (denoted f_* for a function f), and is a symmetric, radially nonincreasing function that preserves the measures of the level sets of the initial function. The theorem in question is as follows.

Theorem 1.12.4. *Denote, for $c > 0$,*
$\mathcal{M}_c(\Omega) = \left\{ f \in \mathcal{C}^{2+\alpha}(\overline{\Omega}, [0,1]),\ \|f\|_{\mathrm{L}^1} = c \right\}$.
Fix $V_{i,0} \in \mathcal{C}^{2+\alpha}(\Omega)$ and $\mathcal{R} > 0$. Let us assume that $V_{i,0} = (V_{i,0})_*$ and is radially decreasing. Then,

$$\eta_L(\mathcal{R}, V_{i,0}) \neq \max_{R \in \mathcal{M}_{|\Omega|\mathcal{R}}(\Omega)} \eta_L(R, V_{i,0}).$$

Moreover, there exists $R \in \mathcal{M}_{|\Omega|\mathcal{R}}(\Omega)$ such that $R = R_*$ and $\eta_L(R, V_{i,0}) > \eta_L(\mathcal{R}, V_{i,0})$.

The theorem serves as a counterexample to the homogenization strategy. If we assume that the initial condition of the infected aphids is symmetric and radially decreasing, then the homogenized refuge (which can be approached, as indicated by the previous theorem, by increasing the refuge frequency) is not optimal. In this case, a symmetric, radially nonincreasing refuge exists that produces a superior linearized harvest compared to the homogenized refuge. However, under a different assumption, namely if $V_{i,0}$ is constant in space, we prove that a homogenized refuge is optimal for the linearized harvest, and we provide an explicit formula of this homogenized refuge:

Theorem 1.12.5. *Suppose that $x \mapsto V_{i,0}$ is constant.*
Let $\mathcal{R} = \left(\dfrac{\sqrt{\beta_{VH}(\xi + m)V_{i,0}} - \xi}{m} \right)^+$. Then

$$\eta_L(\mathcal{R}, V_{i,0}) = \max_{R \in \mathcal{C}_b^{2+\alpha}(\Omega, \mathbb{R})} \eta_L(R, V_{i,0}).$$

In fact, we prove this theorem assuming that *the mean of* $V_{i,0}$ is constant in space (in a deliberately vague probability framework). This condition is purely biologically motivated, and only serves to alleviate the strict assumption of a constant initial condition on the population of infected aphids. It does not change the proof. If this assumption on $V_{i,0}$ is satisfied, then the homogenization strategy maximises the linearized harvest.

In Chapter 4, we offer insights and conjectures, drawing from established findings on traveling waves, regarding the spreading speeds of the populations I, V_i, V, and P in the context of aphid invasion. Concretely, we conjecture that the spreading speed of both the populations V and P is, if well-defined,

$$c_*^V = c_*^P = \min_{\mu > 0} \frac{-\lambda_1(-\sigma_V \partial_{xx} + 2\sigma_V \mu \partial_x - \sigma_V \mu^2 - r(x) + h r_P(x)/s_P)}{\mu},$$

and the spreading speed of I and V_i is

$$\min_{\mu > 0} \frac{-\lambda_1(\mathcal{L}_\mu)}{\mu}$$

where $\lambda_1(\mathcal{L}_\mu)$ designates the principal eigenvalue of the operator

$$\mathcal{L}_\mu = -\begin{pmatrix} 0 & 0 \\ 0 & \sigma_V \end{pmatrix} \partial_{xx} + 2\mu \begin{pmatrix} 0 & 0 \\ 0 & \sigma_V \end{pmatrix} \partial_x - \mu^2 \begin{pmatrix} 0 & 0 \\ 0 & \sigma_V \end{pmatrix} - A.$$

Additionally, we conjecture a potential homogenization result concerning the convergence of these spreading speeds to those of the homogenized system when the frequency of the refuge goes to infinity.

In Chapter 5, we provide biologically consistent numerical values for all our parameters, derived from experiments documented in the literature. This enables us to conduct numerical simulations of our system, plotting the evolution of the populations, and calculating the harvest across a range of varying parameters. It is important to note that, with the set of parameters we chose, the principal eigenvalues of the operators $-r_V^R + hr_P^R/s_V$ and $-r_V^F + hr_P^F/s_V$ are positive, where r_V^R, r_V^F, r_P^R, r_P^R are the values of r_V and r_P in the refuge and in the field, respectively. Therefore, even in the absence of refuge, the population of aphids converges to 0 in our numerical simulations.

Chapter 2

Agro-ecological control of a pest–host system: preventing the spreading

This article was published in the SIAM Journal on Applied Mathematics [1].

2.1 Abstract

We consider an agro-ecologically motivated coupling between a prey–predator system and a vector-borne epidemic system. The coupled system contains one ODE, two reaction–diffusion PDEs and one reaction–diffusion–advection PDE; it has no complete variational or monotonic structure and coefficients are spatially heterogeneous. We study the long-time behavior of solutions of the Cauchy–Neumann problem, which turns out to be largely decided by a linear stability criterion but still involves nonlinear subtleties. Then we consider an optimal control problem. Although it remains elusive analytically, we show numerically the variety of outcomes and the strong impact of the initial conditions.

2.2 Introduction

We are interested in the sugar beet agro-ecosystem. In the beet field (which is typically a rectangle), aphids (namely, Myzus Persicae and Aphis Fabae) are vectors of four yellows viruses: the beet mild yellowing virus (BMYV), the beet chlorosis virus (BChV), the beet yellows virus (BYV) and the beet mosaic virus (BtMV). The spread of these viruses in a field can be an economic disaster if left uncontrolled, as the sugar concentration in an infected beet decreases by about 50%.

To date, pesticides are the main tool to protect beets, and are used by a large majority of farmers. However, these pesticides have been proven to be a threat to biodiversity and human health. Finding effective alternatives to their use is a major challenge for a modern and sustainable world.

In our system, natural predators of the aphids (for instance, ladybugs Hippodamia variegata or Chnootriba similis) act as a biological method to control the aphid population. Usually, the lack of plants or flowers creates an unsuitable environment for such predators. We sacrifice a portion of the sugar beets in favor of flowers that will form what we call biodiversity refuges. In these flower patches, we expect an abundance of insects that ladybugs can feed on and use to reproduce faster. These refuges should help the predators to thrive and control the aphids, but might also help the aphids to grow faster, as the sugar beets are initially not developped enough for the aphids to feed on them. If this turns out to be biologically incorrect, the analysis we have done works just the same (the growth rate in the refuges would just be smaller than in the field). The refuges will in any case reduce the quantity of beets in the field. Therefore we expect conditions on the ecological properties of these refuges as well as the existence of an optimal refuge geometry. We understand this problem as an optimal control problem.

Many other agro-ecosystems have a similar predator–pest–host structure and can benefit from our analysis.

The mathematical model we use is built upon the ODE model of [50]:

$$\begin{cases} I' &= \beta_{VH}(H-I)V_i - \alpha_I I \\ V_i' &= \beta_{HV} I V_s - d_V V_i - s_V(V_s+V_i)V_i - hPV_i \\ V_s' &= -\beta_{HV} I V_s - d_V V_s - s_V(V_s+V_i)V_s - hPV_s + b_V(V_s+V_i) \\ P' &= \gamma h(V_s+V_i)P - d_P P. \end{cases}$$

Here, the notations I, V_i, V_s, P stand respectively for the population density of infected hosts, infected vectors, susceptible vectors and predators. The various parameters (all positive constants) are biologically meaningful: H is the total population of hosts, β_{VH} and β_{HV} are the transmission rates (from vectors to hosts and vice-versa), α_I is the recovery rate of the hosts, b_V is the birth rate of the vectors, d_V and d_P are the death rates of the vectors and the predators respectively, s_V is the saturation rate of vectors (intraspecific competition for space or resources leading to logistic growth), h is the predation rate and γ is a coefficient measuring the efficiency of predation.

To better account for the sugar beet agro-ecosystem, we modify this model as follows:

- since infected beets never recover, we remove the recovery term $-\alpha_I I$;
- on the contrary, aphids can recover, whence we add a recovery term with rate α for vectors;
- since we are interested in generalist predators, able to survive in the absence of aphids because of other prey populations present in the environment, we add a birth term with rate b_P and a saturation term with rate s_P so that predator growth in the absence of aphids is logistic;
- the field is an open bounded connected set Ω with smooth boundary $\partial\Omega$ in a Euclidean space $\mathbb{R}^d$;
- the spatial heterogeneity in the field due to the biodiversity refuges changes the Malthusian parameters $r_V = b_V - d_V$, $r_P = b_P - d_P$ and the total host population H into positive functions in $\mathcal{C}^{2+\alpha}(\overline{\Omega})$;
- vectors and predators are able to move and disperse in this heterogeneous field: vectors use Brownian motion and diffuse with rate σ_V whereas predators use a non-standard "ideal free dispersal strategy" [16, 15] with rate σ_P that will be commented in more details below.

Our interest is therefore in the following parabolic–ordinary differential system:

$$\begin{cases} \partial_t I &= \beta_{VH}(H(x)-I)V_i \\ \partial_t V_i &= \sigma_V \Delta V_i + \beta_{HV} I V_s - \alpha V_i - d_V(x)V_i - s_V(V_s+V_i)V_i - hPV_i \\ \partial_t V_s &= \sigma_V \Delta V_s - \beta_{HV} I V_s + \alpha V_i - d_V(x)V_s - s_V(V_s+V_i)V_s - hPV_s \\ & \quad + b_V(x)(V_s+V_i) \\ \partial_t P &= \sigma_P \nabla \cdot \left(r_P(x) \nabla \left(\frac{P}{r_P(x)} \right) \right) + \gamma h (V_s+V_i)P + r_P(x)P - s_P P^2 \end{cases} \tag{2.1}$$

in $\Omega \times \mathbb{R}_+^*$, where we ommited the dependency on (x,t) for I, V_i, V_s and P. We supplement it with initial conditions:

$$(I, V_i, V_s, P)(\cdot, 0) = (0, V_{i,0}, V_{s,0}, P_0) \quad \text{in } \Omega,$$

where $V_{i,0}$, $V_{s,0}$, P_0 are nonnegative functions in $L^\infty(\overline{\Omega})$, and with "no-flux" boundary conditions:

$$\frac{\partial V_i}{\partial n} = \frac{\partial V_s}{\partial n} = \frac{\partial (P/r_P)}{\partial n} = 0 \quad \text{on } \partial\Omega.$$

Note that the condition $\partial_n(P/r_P) = 0$ reduces to $\partial_n P = 0$ under the biologically relevant assumption $\partial_n r_P = 0$, that will be a standing assumption from now on. Hence, we actually have homogeneous Neumann boundary conditions for all three animal populations V_i, V_s and P.

At least formally, the ideal free dispersal strategy $\nabla \cdot (r_P \nabla (P/r_P))$ can be rewritten as $\nabla \cdot (\nabla P - P\nabla(\ln r_P))$. Diffusion–advection strategies of the form $u \mapsto \nabla \cdot (\nabla u - u\mathbf{q})$ with u a population density subjected to a logistic growth of the form $u \mapsto u(r-u)$ with r the spatially heterogeneous distribution of resources were compared in [16]. It was proved that choosing an advection strategy of the form $\mathbf{q} = \nabla(\ln r)$ leads to a so-called "ideal free distribution" where the spatial distribution of the population density at equilibrium is exactly proportional to the spatial distribution of resources. In contrast, it is well-known that if $\mathbf{q} = \mathbf{0}$, that is if the population density is subjected to pure Laplacian diffusion, the equilibrium will not be proportional to the distribution of resources. The choice $\mathbf{q} = \nabla(\ln r_P)$, referred to as an "ideal free dispersal strategy", is both evolutionary stable and convergent stable [16]. Thus natural selection should favor such strategies, as conjectured by theoretical ecologists. Many other forms of ideal free dispersal strategies have been studied mathematically in the last few years. We emphasize in particular the case of patchy environments with edge behavior [46] since this is the kind of environments we actually have in mind and will simulate numerically. In the present model, the ideal free distribution of the predators at equilibrium in the absence of aphids will be a key component of our attempt at an analysis of the optimal control problem. Indeed, the biodiversity refuges will act on the harvest through the population density V_i, which will itself be impacted by the refuges through r_V on one hand and through the predator equilibrium on the other hand. Precise knowledge of this equilibrium is therefore very helpful, and actually quite necessary. We emphazise the fact that r_P/s_P is an equilibrium only in the absence of aphids: to avoid complicated cross-diffusion terms, the ideal free distribution of the predators does not take into account the vector population $V_i + V_s$, only the other resources.

Since the predators we consider may typically have a broad view of the field, it is natural to assume that they will tend to optimize their spatial distribution based on resources. In contrast, vectors are aphids, and their movement is mostly governed by the wind, which could be approximated by a Brownian motion if we consider that, on average, the wind blows uniformly in all directions. Taking a Brownian motion for the predators would mean that their equilibrium

state is no longer proportional to their resources, and would invalidate the optimization of the principal eigenvalue of Section 2.6, but not the main theorem of this paper. One could also take an ideal free dispersal strategy for the vectors and the result of Theorem 2.2.1 would still be valid.

In the sugar beet agro-ecosystem, these equations correspond to the spring, when the beets are susceptible to the disease. It is known that in this system, the population dynamics are much faster than the seasonal flow, which means that by the end of spring, the system will have reached a steady state. This is consistent with our numerical simulations and with the parameter values we found in the literature (cf. Supplementary Materials). This is why we simplify by considering an eternal spring.

With this set of notations and assumptions, our optimal control problem can be recasted as follows: assuming that $r_V = r_V^{\text{field}} + r_V^{\text{refuge}} R$, $r_P = r_P^{\text{field}} + r_P^{\text{refuge}} R$, $H = H^{\text{field}}(1-R)$ with $R : \Omega \to [0,1]$ a spatial distribution of biodiversity refuges and with positive constants r_V^{field}, r_V^{refuge}, r_P^{field}, r_P^{refuge}, H^{field}, characterize the set of optimal R such that the harvest of healthy beets $\lim_{t\to+\infty} \int_\Omega H - I(\cdot,t)$ is maximized.

2.2.1 Organization of the paper

In the next subsection, we present our main result. In Section 2, we verify the well-posedness of the Cauchy–Neumann problem. In Section 3, we prove our main result. In Section 4, we establish estimates on the harvest. Finally, in Section 5, we study numerically the optimal control problem.

2.2.2 Main result

Let $\mathcal{L}_{V_s} = -\sigma_V \Delta - r_V + h\dfrac{r_P}{s_P}$, $\mathcal{L}_{V_i} = -\sigma_V \Delta + \alpha + d_V + h\dfrac{r_P}{s_P}$ and let $\lambda_1(\mathcal{L}_{V_s})$, $\lambda_1(\mathcal{L}_{V_i})$ be their principal eigenvalues with Neumann boundary conditions on $\partial\Omega$. $\lambda_1(\mathcal{L}_{V_i})$ is positive thanks to its Rayleigh quotient and the positivity of $\alpha + d_V + hr_P/s_P$ (see proof of Corollary 2.4.7); however, $\lambda_1(\mathcal{L}_{V_s})$ can be of any sign. Denote $\varphi_{s,1}$ and $\varphi_{i,1}$, the principal eigenfunctions associated, respectively, to $\lambda_1(\mathcal{L}_{V_s})$ and $\lambda_1(\mathcal{L}_{V_i})$, with normalizations $\min_\Omega \varphi_{s,1} = 1$ and $\max_\Omega \varphi_{i,1} = 1$.

Our main result is the following.

Theorem 2.2.1. *(i) Case of extinction: assume that $P_0 \not\equiv 0$ and $\lambda_1(\mathcal{L}_{V_s}) > 0$. Let $V = V_i + V_s$. Then, the following statements are true.*

- $(V,P)(x,t) \to (0, r_P(x)/s_P)$ *as* $t \to +\infty$, *uniformly in* Ω.
- *If we also assume* $V_{i,0} \not\equiv 0$, *then* $\liminf_{t\to+\infty} \inf_{x\in\Omega} I(x,t) > 0$.
- *More precisely, we have the following estimates. For any* $\varepsilon > 0$ *such that* $\lambda_1(\mathcal{L}_{V_s}) - h\varepsilon > 0$, *if* $|P_0 - r_P/s_P| \le \varepsilon$ *and* $V_0 := V_{i,0} + V_{s,0} \le \varepsilon$, *then for all* $x \in \Omega$, $t \ge 0$,

$$V(x,t) \le \max_\Omega V_0 \max_\Omega \varphi_{s,1} e^{-(\lambda_1(\mathcal{L}_{V_s}) - h\varepsilon)t},$$

$$\frac{I(x,t)}{H(x)} \le 1 - \exp\left(-\beta_{VH} \frac{\max_\Omega V_0 \max_\Omega \varphi_{s,1}}{\lambda_1(\mathcal{L}_{V_s}) - h\varepsilon}\right),$$

$$1 - \exp\left(-\beta_{VH} \min_\Omega V_{i,0} \min_\Omega \varphi_{i,1} \frac{1 - e^{-(\lambda_1(\mathcal{L}_{V_i}) + s_V\varepsilon + h\varepsilon)t}}{\lambda_1(\mathcal{L}_{V_i}) + s_V\varepsilon + h\varepsilon}\right) \le \frac{I(x,t)}{H(x)}.$$

(ii) Case of persistence: assume that $V_{i,0} \not\equiv 0$ and $\lambda_1(\mathcal{L}_{V_s}) < 0$. Then,

- $\liminf_{t\to+\infty} \inf_{x\in\Omega} V_i(x,t) > 0$;
- $\lim_{t\to+\infty} I(x,t) = H(x)$ *uniformly in* Ω.

This theorem, that does not require any particular relations between r_V, r_P, H and the refuge distribution R, links the non-linear stability of the equilibrium $U_P = (0,0,0,r_P/s_P)^T$ with its linear stability. The proof combines linear stability arguments, supersolutions and subsolutions and a parabolic Harnack inequality in simultaneous time due to Huska [32]. In the persistence case, the control strategy fails and the whole field ends up being contaminated. On the contrary, in the extinction case, there might still be a salvageable harvest in the end. We point out that, although the persistence versus extinction criterion is classically the sign of some principal eigenvalue, the nonlinearities of the system still play a role in the extinction property. In a purely linearly determined extinction scenario, the equilibrium U_P would attract trajectories. This is for instance what happens classically in Fisher–KPP-type equations or systems. Here, in contrast, (V_i, V_s, P) converges indeed to $(0,0,r_P/s_P)$ but I ends up being at positive distance from 0. We point out right now that the quantity of infected beets I is nondecreasing in time. Moreover, when $V_i = V_s = 0$ and $P = r_P/s_P$, any function I_∞ of the spatial variable x gives an equilibrium: the final quantity of infected beets cannot be figured out simply by calculating equilibria. Still, we provide estimates that bound the neighborhood of U_P in which the evolution is trapped when initial conditions are well-prepared. The conditions $|P_0 - r_P/s_P| \leq \varepsilon$ and $V_{i,0} + V_{s,0} \leq \varepsilon$ are biologically natural in a context of biological invasion by aphids in a territory where predators were previously close to equilibrium. Nevertheless, as will be shown by the proof, we can still provide estimates for ill-prepared initial conditions; these are just slightly more complicated.

As a by-product of these estimates, we can derive estimates for the harvest when initial conditions are well-prepared (i.e close to the equilibrium $V = 0$, $P = r_P(x)/s_P$). We denote I_∞ the pointwise limit of $I(t,x)$ as $t \to +\infty$ (which is well-defined since I is monotonic with respect to time and globally bounded).

Corollary 2.2.2. *Assume that $\lambda_1(\mathcal{L}_{V_s}) > 0$. Then, for any $\varepsilon > 0$ such that $\lambda_1(\mathcal{L}_{V_s}) - h\varepsilon > 0$, if $|P_0 - r_P/s_P| \leq \varepsilon$ and $V_0 \leq \varepsilon$, then*

$$e^{-\beta_{VH}\frac{\max_\Omega V_0 \max_\Omega \varphi_{s,1}}{\lambda_1(\mathcal{L}_{V_s}) - h\varepsilon}} \leq \frac{\int_\Omega (H - I_\infty)}{\int_\Omega H} \leq e^{-\beta_{VH}\frac{\min_\Omega V_{i,0} \min_\Omega \varphi_{i,1}}{\lambda_1(\mathcal{L}_{V_i}) + s_V\varepsilon + h\varepsilon}}.$$

Assume that $\lambda_1(\mathcal{L}_{V_s}) < 0$. Then

$$\int_\Omega (H - I_\infty) = 0.$$

2.3 Existence and uniqueness of the solution

Proposition 2.3.1. *The system (2.1) admits a unique classical solution defined in $\overline{\Omega} \times \mathbb{R}_+^*$.*

Proof. The local Lipschitz continuity of the functions involved in system (2.1) and [54, Page 447, Theorem 11.2] yield the existence of a unique classical solution in $\overline{\Omega} \times [0, T_0)$, for some $T_0 \leq +\infty$. This solution either exists globally or blows up in finite time. It is left to show that the solution is bounded independently of T_0.

First of all, because of the nonnegativity of the initial conditions $V_{i,0}, V_{s,0}$ and P_0, 0 is a trivial subsolution of each equation, hence the solutions V_i, V_s and P are nonnegative.

I can be computed explicitly, at least for $t \in [0, T_0)$:

$$0 \leq I(x,t) = H(x)\left(1 - \exp\left(-\beta_{VH}\int_0^t V_i(x,s)\mathrm{d}s\right)\right).$$

Since $\beta_{VH} > 0$ and $V_i \geq 0$, it follows that $0 \leq I(x,t) \leq H(x)$ for all $(x,t) \in \Omega \times [0,T_0)$: I is bounded. Let us point out that this integral formula for $I(x,t)$ also confirms the time monotonicity and the fact that the final value of I is not easily figured out, as it depends upon the whole trajectory of V_i, and in particular upon the initial condition $V_{i,0}$.

Denote $V := V_i + V_s$. The function V solves

$$\partial_t V - \sigma_V \Delta V = r_V V - s_V V^2 - hPV.$$

Let $\overline{V}$ be a solution of

$$\begin{cases} \overline{V}(\cdot,0) = \max\limits_{x\in\Omega} V_0 := \max\limits_{x\in\Omega}(V_{i,0} + V_{s,0}) & \text{in } \Omega \\ \partial_t \overline{V} = \max\limits_{x\in\Omega}(r_V)\overline{V} - s_V\overline{V}^2 & \text{in } \Omega \times \mathbb{R}_+^* \\ \dfrac{\partial \overline{V}}{\partial n} = 0 & \text{on } \partial\Omega \times \mathbb{R}_+^*. \end{cases}$$

By nonnegativity of h, P, V, $\overline{V}$ is a supersolution of the Cauchy–Neumann scalar problem of which V is a solution. Moreover, $\overline{V}$ converges to

$$\max_{x\in\Omega} r_V(x)/s_V$$

when $t \to +\infty$ (the solution can be computed explicitly), therefore is bounded. We then deduce the global boundedness of V_i, V_s: $0 \leq V_i(x,t), V_s(x,t) \leq \overline{V}(x,t)$ for all $(x,t) \in \Omega \times [0,T_0)$, independently of T_0.

Let $\mu \in \mathbb{R}$ be large enough so that $\overline{P} := \mu r_P \geq P_0$ and $(r_P^2 + \gamma h \overline{V} r_P)\mu - s_P r_P^2 \mu^2 \leq 0$. This is possible because s_P, r_P are positive everywhere on the compact $\overline{\Omega}$. Then

$$\begin{aligned} \partial_t \overline{P} - \sigma_P \nabla \cdot \left(r_P \nabla\left(\frac{\overline{P}}{r_P}\right)\right) = 0 \quad &\geq (r_P^2 + \gamma h \overline{V} r_P)\mu - s_P r_P^2 \mu^2 \\ &= \gamma h V \overline{P} + r_P \overline{P} - s_P \overline{P}^2, \end{aligned}$$

hence $\overline{P} = \mu r_P$ is a supersolution of the Cauchy–Neumann scalar problem of which P is a solution. Hence, P is globally bounded, independently of T_0.

□

2.4 Stability of the predator-only equilibrium

2.4.1 Existence and uniqueness

We are interested in studying the stability of the predator-only equilibrium $U_P := (0,0,0,P^*)^T$, where P^* is the nonnegative nonzero solution of

$$-\sigma_P \overline{\mathcal{L}}(P^*) = r_P P^* - s_P (P^*)^2 \text{ in } \Omega. \tag{2.2}$$

where we denote $\overline{\mathcal{L}} := \overline{\mathcal{L}}(r_P) := \nabla \cdot \left(r_P \nabla\left(\frac{\cdot}{r_P}\right)\right)$.

Proposition 2.4.1. *$P^* = \dfrac{r_P}{s_P}$ is the unique nonnegative nonzero solution of (2.2).*

Proof. First of all, an easy computation shows that r_P/s_P is a solution of (2.2).

According to [14, Proposition 3.3], the nonnegative nonzero solution P^* is unique if and only if the principal eigenvalue associated to the linearized operator around 0, $\lambda_1(\mathcal{L}_0)$, is negative.

We remind that r_P is positive everywhere on $\overline{\Omega}$. Using the variational formulation of the elliptic principal eigenvalue $\lambda_1(\mathcal{L}_0)$,

$$\begin{aligned}\lambda_1(\mathcal{L}_0) &= \inf_{\varphi\in\mathcal{C}^{2+\alpha}(\Omega),\|\varphi\|_{L^2}=1}\int_\Omega \sigma_P r_P\nabla\left(\frac{\varphi}{r_P}\right)\cdot\nabla\varphi - r_P\varphi^2\\ &\leq -\frac{\int_\Omega r_P^3}{\int_\Omega r_P^2} \quad (\text{with } \varphi = r_P/\|r_P\|_{L^2})\\ &< 0.\end{aligned}$$

This ends the proof. □

2.4.2 Linear stability

Denote $\varphi(x,t) := (I(x,t), V_i(x,t), V_s(x,t), P(x,t) - P^*(x))^T$.

From (2.1), a formal Taylor expansion at first order around

$$U_P = (0,0,0,r_P/s_P)^T$$

yields

$$\partial_t\varphi + \mathcal{L}\varphi = o(\|(I,V_i,V_s,P-P^*)\|)(1,1,1,1)^T$$

where

$$\begin{aligned}\mathcal{L} &:= \begin{pmatrix}\mathcal{L}_I & -\beta_{VH}H & 0 & 0\\ 0 & \mathcal{L}_{V_i} & 0 & 0\\ 0 & -\alpha - b_V & \mathcal{L}_{V_s} & 0\\ 0 & -\gamma h\dfrac{r_P}{s_P} & -\gamma h\dfrac{r_P}{s_P} & \mathcal{L}_P\end{pmatrix}\\ &:= \begin{pmatrix}0 & -\beta_{VH}H & 0 & 0\\ 0 & -\sigma_V\Delta + \alpha + d_V + h\dfrac{r_P}{s_P} & 0 & 0\\ 0 & -\alpha - b_V & -\sigma_V\Delta - r_V + h\dfrac{r_P}{s_P} & 0\\ 0 & -\gamma h\dfrac{r_P}{s_P} & -\gamma h\dfrac{r_P}{s_P} & -\sigma_P\overline{\mathcal{L}} + r_P\end{pmatrix}.\end{aligned}$$

We look for solutions of the form $\varphi(x,t) = e^{-\lambda t}\psi(x)$, where (λ,ψ) is an eigenpair of $\mathcal{L}$. Hence, we are focused on the linear elliptic eigenvalue problem

$$\mathcal{L}\psi = \lambda\psi.$$

In the following, we will write $\mathrm{eig}(\mathcal{L})$ the set of eigenvalues of an operator $\mathcal{L}$, and $\sigma(\mathcal{L})$ its spectrum.

It is well known that any scalar elliptic operator $\mathcal{L}$ admits a unique principal eigenvalue. The Krein-Rutman theorem (see [66]) gives an associated positive principal eigenfunction to the principal eigenvalue.

Definition 2.4.2. *Let $\mathcal{L}$ be a scalar elliptic operator. The principal eigenvalue of $\mathcal{L}$, noted $\lambda_1(\mathcal{L})$, is the only eigenvalue associated to a positive eigenfunction.*

We also need a different definition that applies to more general operators.

Definition 2.4.3. *Let $\mathcal{L}$ be a linear operator with eigenvalues. We set*

$$\Lambda(\mathcal{L}) := \inf \ \mathrm{Re}(\mathrm{eig}(\mathcal{L})).$$

We are interested in the stability of U_P. We will use the following terminology:

Definition 2.4.4. *U_P is :*

- *linearly unstable if $\Lambda(\mathcal{L}) < 0$;*
- *linearly marginally stable if $\Lambda(\mathcal{L}) = 0$;*
- *linearly stable if $\Lambda(\mathcal{L}) > 0$.*

The spectral problem $\mathcal{L}\psi = \lambda\psi$ is non-scalar, non-monotonous and non-compact (the equation on I is not elliptic), hence difficult to study. In what follows, we take advantage of the specific form of the operator $\mathcal{L}$: a block triangular matrix, with each block being itself triangular.

We first need the following lemma.

Lemma 2.4.5. *Let $\mathcal{E}$ a scalar elliptic operator with coefficients in $\mathcal{C}^\alpha(\overline{\Omega})$. Then, for any $K > 0$ large enough, the spectrum of $\mathcal{E} + K$ is exactly the set of eigenvalues of $\mathcal{E} + K$.*

Proof. We consider the problem $(\mathcal{E} + K)u = f$, for a given $f \in \mathcal{C}^\alpha(\overline{\Omega})$, where the solution u belongs to $\mathcal{C}^{2+\alpha}(\overline{\Omega})$. Given Neumann boundary conditions, the existence and uniqueness theorem (see [54, Page 447, Theorem 1.3]) shows that, for $K > 0$ large enough, $\mathcal{E} + K : \mathcal{C}^{2+\alpha}(\overline{\Omega}) \to \mathcal{C}^\alpha(\overline{\Omega})$ is bijective (and continuous). Furthermore, its inverse $(\mathcal{E} + K)^{-1} : \mathcal{C}^\alpha(\overline{\Omega}) \to \mathcal{C}^{2+\alpha}(\overline{\Omega})$ is classically continuous. Hence, one can define $\iota : \mathcal{C}^{2+\alpha}(\overline{\Omega}) \to \mathcal{C}^\alpha(\overline{\Omega})$ the canonical injection (which is compact, as a consequence of Arzela–Ascoli theorem), and $T := \iota \circ (\mathcal{E} + K)^{-1} : \mathcal{C}^\alpha(\overline{\Omega}) \to \mathcal{C}^\alpha(\overline{\Omega})$, so that T is a compact operator.

Let $\lambda \in \sigma(\mathcal{E} + K)$ ($\lambda \neq 0$). We claim the following:

$$\mathcal{E} + K - \lambda \text{ is invertible } \Leftrightarrow (\mathcal{E} + K)^{-1} - \frac{1}{\lambda} \text{ is invertible.}$$

Indeed, suppose that $\mathcal{E} + K - \lambda$ is invertible. With $(\mathcal{E} + K)^{-1}$ invertible, their product $1 - \lambda(\mathcal{E} + K)^{-1} = -\lambda((\mathcal{E} + K)^{-1} - 1/\lambda)$ is also invertible. The proof of the converse is very similar.

We deduce that $1/\lambda \in \sigma((\mathcal{E} + K)^{-1})$.

If $1/\lambda \in \mathrm{eig}((\mathcal{E} + K)^{-1})$, then from $(\mathcal{E} + K)^{-1}u = (1/\lambda)u$ we deduce $\iota \circ (\mathcal{E} + K)^{-1}u = (1/\lambda)\iota \circ u = (1/\lambda)u$, hence $1/\lambda \in \sigma(T)$.

If $1/\lambda \notin \mathrm{eig}((\mathcal{E} + K)^{-1})$, then $(\mathcal{E} + K)^{-1} - 1/\lambda$ is not surjective. Let $u \in \mathcal{C}^{2+\alpha}(\overline{\Omega})$ not attained by $(\mathcal{E} + K)^{-1} - 1/\lambda$. Suppose we can find $f \in \mathcal{C}^\alpha(\overline{\Omega})$ such that $(T - 1/\lambda)f = \iota \circ u$. Then $\iota \circ ((\mathcal{E} + K)^{-1} - 1/\lambda)f = (\iota \circ (\mathcal{E} + K)^{-1} - (1/\lambda)\iota)f = \iota \circ u$. By injectivity of ι, $((\mathcal{E} + K)^{-1} - 1/\lambda)f = u$, which contradicts our assumption on u. Therefore $T - 1/\lambda$ is not surjective, and $1/\lambda \in \sigma(T)$.

In both cases, $1/\lambda \in \sigma(T)$.

By Fredholm's alternative, $1/\lambda \in \mathrm{eig}(T)$. By injectivity of ι, $1/\lambda \in \mathrm{eig}((\mathcal{E} + K)^{-1})$. This shows that $\lambda \in \mathrm{eig}(\mathcal{E} + K)$, therefore $\sigma(\mathcal{E} + K) = \mathrm{eig}(\mathcal{E} + K)$. □

With this result, we are ready to assert the link between the eigenvalues of $\mathcal{L}$ and the eigenvalues of the other scalar operators.

Proposition 2.4.6. $\mathrm{eig}(\mathcal{L}) = \bigcup_{Y \in \{I, V_i, V_s, P\}} \mathrm{eig}(\mathcal{L}_Y)$.

Proof. Let $K > 0$ so large that Lemma 2.4.5 can be applied with $\mathcal{E} = \mathcal{L}_{V_i}, \mathcal{L}_{V_s}, \mathcal{L}_P$. Let λ be an eigenvalue of $\mathcal{L} + K$ and $\Phi(x) = (I(x), V_i(x), V_s(x), P(x))^T$ an eigenvector associated to it.

From the second line of $(\mathcal{L} + K)\Phi(x) = \lambda\Phi(x)$, we deduce

$$(\mathcal{L}_{V_i} + K)V_i(x) = \lambda V_i(x),$$

hence λ is an eigenvalue of $\mathcal{L}_{V_i} + K$, or $V_i(x) = 0$.

If $V_i(x) = 0$, looking at the first line of $(\mathcal{L} + K)\Phi(x) = \lambda\Phi(x)$, we deduce

$$(\mathcal{L}_I + K)I(x) = \lambda I(x),$$

hence λ is an eigenvalue of $\mathcal{L}_I + K$, or $I(x) = 0$.

If $V_i(x) = 0$ and $I(x) = 0$, looking at the third line of $(\mathcal{L} + K)\Phi(x) = \lambda\Phi(x)$, we deduce

$$(\mathcal{L}_{V_s} + K)V_s(x) = \lambda V_s(x),$$

hence λ is an eigenvalue of $\mathcal{L}_{V_s} + K$, or $V_s(x) = 0$.

If $V_i(x) = 0$, $I(x) = 0$ and $V_s(x) = 0$, looking at the fourth line of $(\mathcal{L} + K)\Phi(x) = \lambda\Phi(x)$, we deduce

$$(\mathcal{L}_P + K)P(x) = \lambda P(x),$$

hence λ is an eigenvalue of $\mathcal{L}_P + K$, and P cannot be null, otherwise Φ would be null.

Thus, necessarily, λ is an eigenvalue of one of the four operators $\mathcal{L}_I + K$, $\mathcal{L}_{V_i} + K$, $\mathcal{L}_{V_s} + K$, or $\mathcal{L}_P + K$.

Reciprocally, let us show that if λ is an eigenvalue of one of the four operators $\mathcal{L}_I + K$, $\mathcal{L}_{V_i} + K$, $\mathcal{L}_{V_s} + K$, $\mathcal{L}_P + K$, then λ is an eigenvalue of $\mathcal{L} + K$. By Lemma 2.4.5, for $K > 0$ large enough and for all $Y \in \{V_i, V_s, P\}$, the spectrum of $\mathcal{L}_Y + K$ is exactly its set of eigenvalues. Also, $\mathcal{L}_I + K - \lambda = K - \lambda$ is trivially invertible for $\lambda \neq K$, hence $\mathrm{eig}(\mathcal{L}_I + K) = \sigma(\mathcal{L}_I + K) = \{K\}$.

First case:

Let λ be an eigenvalue of $\mathcal{L}_I + K$, and $\varphi(x)$ an eigenfunction associated to it.

Then we have $(\mathcal{L} + K)(\varphi(x), 0, 0, 0)^T = \lambda(\varphi(x), 0, 0, 0)^T$ and λ is an eigenvalue of $\mathcal{L} + K$.

Second case:

Let λ be an eigenvalue of $\mathcal{L}_{V_i} + K$, and $\psi(x)$ an eigenfunction associated to it. We are going to construct three functions φ, η and μ such that

$(\mathcal{L} + K)(\varphi(x), \psi(x), \eta(x), \mu(x))^T = \lambda(\varphi(x), \psi(x), \eta(x), \mu(x))^T$.

First of all, as seen in the first case, if $\lambda \in \mathrm{eig}(\mathcal{L}_I + K)$, we have an obvious eigenvector showing that λ is an eigenvalue of $\mathcal{L} + K$. Supposing now that $\lambda \notin \mathrm{eig}(\mathcal{L}_I + K) = \sigma(\mathcal{L}_I + K)$. $\mathcal{L}_I + K - \lambda$ is invertible, hence we can define $\varphi(x) = -(\mathcal{L}_I + K - \lambda)^{-1}\beta_{HV}H\psi(x)$.

If $\lambda \in \mathrm{eig}(\mathcal{L}_P + K)$, again we have a obvious eigenvector of $\mathcal{L} + K$:

$$(0, 0, 0, \mu(x))^T$$

with μ an eigenfunction of $\mathcal{L}_P + K$ associated to λ. We suppose now that $\lambda \notin \mathrm{eig}(\mathcal{L}_P + K) = \sigma(\mathcal{L}_P + K)$.

If $\lambda \in \mathrm{eig}(\mathcal{L}_{V_s} + K)$, we pose η an eigenfunction of $\mathcal{L}_{V_s} + K$ associated to it, and $\mu(x) = (\mathcal{L}_P + K - \lambda)^{-1}\gamma h P^* \eta(x)$. This way, we have

$$(\mathcal{L} + K)(0, 0, \eta(x), \mu(x))^T = \lambda(0, 0, \eta(x), \mu(x))^T.$$

We suppose now that $\lambda \notin \text{eig}(\mathcal{L}_{V_s} + K) = \sigma(\mathcal{L}_{V_s} + K)$.
We define $\eta(x) = (\mathcal{L}_{V_s} + K - \lambda)^{-1}(\alpha + b_V)\psi(x)$ and

$$\mu(x) = (\mathcal{L}_P + K - \lambda)^{-1}\gamma h P^*(\psi(x) + \eta(x)).$$

With φ, ψ, η and μ defined as such, we have

$$(\mathcal{L} + K)(\varphi(x), \psi(x), \eta(x), \mu(x))^T = \lambda(\varphi(x), \psi(x), \eta(x), \mu(x))^T,$$

thus λ is an eigenvalue of $\mathcal{L} + K$.

Third case:

Let λ be an eigenvalue of $\mathcal{L}_{V_s} + K$, and $\eta(x)$ an eigenfunction associated to it. If $\lambda \in \text{eig}(\mathcal{L}_P + K)$, as seen before, we have an obvious eigenvector of $\mathcal{L} + K$. Suppose that $\lambda \notin \text{eig}(\mathcal{L}_P + K) = \sigma(\mathcal{L}_P + K)$. We define $\mu(x) = (\mathcal{L}_P + K - \lambda)^{-1}\gamma h P^* \eta(x)$, and we have $(\mathcal{L} + K)(0, 0, \eta(x), \mu(x))^T = \lambda(0, 0, \eta(x), \mu(x))^T$, and λ is an eigenvalue of $\mathcal{L} + K$.

Fourth case:

Let λ be an eigenvalue of $\mathcal{L}_P + K$, and $\mu(x)$ an eigenfunction associated to it. $(0, 0, 0, \mu(x))^T$ is an eigenvector of $\mathcal{L} + K$ associated to λ.

We showed that:

$$\text{eig}(\mathcal{L} + K) = \bigcup_{Y \in \{I, V_i, V_s, P\}} \text{eig}(\mathcal{L}_Y + K).$$

Therefore

$$\begin{aligned} \text{eig}(\mathcal{L}) &= \text{eig}(\mathcal{L} + K) - K \\ &= \bigcup_{Y \in \{I, V_i, V_s, P\}} \text{eig}(\mathcal{L}_Y + K) - K \\ &= \bigcup_{Y \in \{I, V_i, V_s, P\}} \text{eig}(\mathcal{L}_Y). \end{aligned}$$

□

With Proposition 2.4.6 in mind, the sign of the principal eigenvalues (in our case, the minimum of all eigenvalues) of the scalar operators actually yields a more precise result.

Corollary 2.4.7. *$\Lambda(\mathcal{L}) \in \text{eig}(\mathcal{L})$ and $\Lambda(\mathcal{L}) = \min(0, \lambda_1(\mathcal{L}_{V_s}))$.*

Proof. By Proposition 2.4.6, and by definition of $\Lambda(\mathcal{L})$, $\Lambda(\mathcal{L}) = \min_{Y \in \{I, V_i, V_s, P\}} \Lambda(\mathcal{L}_Y)$. Also, by Lemma 2.4.5, and by the fact that $\mathcal{L}_I = 0$, for $K > 0$ large enough, $\text{eig}(\mathcal{L}_Y + K) = \sigma(\mathcal{L}_Y + K)$ for any $Y \in \{I, V_i, V_s, P\}$.

Hence, for all $Y \in \{V_i, V_s, P\}$, $\Lambda(\mathcal{L}_Y + K) = \lambda_1(\mathcal{L}_Y + K)$, which yields $\Lambda(\mathcal{L}_Y) = \lambda_1(\mathcal{L}_Y)$. Moreover, as $-\lambda\text{Id}$ is not invertible if and only if $\lambda = 0$, $\sigma(0) = \{0\}$, whence $\Lambda(\mathcal{L}_I) = 0$. Thus we only have to prove that $\lambda_1(\mathcal{L}_{V_i}) > 0$ and $\lambda_1(\mathcal{L}_P) > 0$.

Using the variational formulation of the principal eigenvalue,

$$\lambda_1(\mathcal{L}_{V_i}) = \inf_{\varphi \in \mathcal{C}^{2+\alpha}(\Omega), \|\varphi\|_{L^2} = 1} \int_\Omega \sigma_V |\nabla \varphi|^2 + (\alpha + d_V + h\frac{r_P}{s_P})\varphi^2 > 0.$$

Finally, eigenelements (λ, φ) of $\mathcal{L}_P$ verify

$$-\sigma_P \nabla \cdot \left(r_P \nabla \left(\frac{\varphi}{r_P} \right) \right) + r_P \varphi = \lambda \varphi,$$

hence, multiplying the equation by φ / r_P and integrating over Ω,

$$\begin{aligned}\lambda \int_\Omega \frac{\varphi^2}{r_P} &= \int_\Omega -\sigma_P \nabla \cdot \left(r_P \nabla \left(\frac{\varphi}{r_P} \right) \right) \frac{\varphi}{r_P} + \varphi^2 \\ &= \int_\Omega \sigma_P r_P \left| \nabla \frac{\varphi}{r_P} \right|^2 + \varphi^2.\end{aligned}$$

By definition, the principal eigenfunction φ_1 of $\mathcal{L}_P$ is not identically 0, therefore $\int_\Omega (\varphi_1^2/r_P) \neq 0$. φ_1 being defined up to a multiplicative constant, we can choose it so that $\int_\Omega (\varphi_1^2/r_P) = 1$. It yields $\lambda_1(\mathcal{L}_P) > 0$. □

2.4.3 Nonlinear stability

We now link the linear stability with the nonlinear stability of U_P, or in other words we prove Theorem 2.2.1. As Corollary 2.4.7 shows, U_P is marginally linearly stable if and only if $\lambda_1(\mathcal{L}_{V_s})$ is nonnegative. With the help of [14, Proposition 3.2] and a uniform Harnack inequality of [32, Theorem 2.5], we can make precise the large-time behaviour of our solution depending on the sign of $\lambda_1(\mathcal{L}_{V_s})$.

Proof of Theorem 2.2.1. (i) First of all, 0 being an obvious subsolution of (2.1), we have $P, V_i, V_s \geq 0$.

P and $V := V_i + V_s$ are solutions of the system

$$\begin{cases} \partial_t V - \sigma_V \Delta V &= r_V V - s_V V^2 - hPV \\ \partial_t P - \sigma_P \overline{\mathcal{L}}(P) &= r_P P - s_P P^2 + \gamma h V P, \end{cases} \tag{2.3}$$

for $(x,t) \in \Omega \times \mathbb{R}_+^*$, with Neumann boundary conditions and initial conditions $P(\cdot,0) = P_0$, $V(\cdot,0) = V_0 := V_{i,0} + V_{s,0}$.

Let $\underline{P}$ be a solution of

$$\begin{cases} \underline{P}(\cdot,0) = P_0 & \text{in } \Omega \\ \partial_t \underline{P} - \sigma_P \overline{\mathcal{L}}(\underline{P}) = r_P \underline{P} - s_P \underline{P}^2 & \text{in } \Omega \times \mathbb{R}_+^* \\ \dfrac{\partial \underline{P}}{\partial n} = 0 & \text{on } \partial\Omega \times \mathbb{R}_+^*. \end{cases}$$

By the nonnegativity of γ, h, V and $\underline{P}$, $\underline{P}$ is a subsolution of the second equation of (2.3). Moreover, a linearization of the associated elliptic problem around the steady state 0 yields the spectral problem

$$(-\sigma_P \overline{\mathcal{L}} - r_P)\varphi = \lambda \varphi.$$

By monotonicity of the principal eigenvalue with respect to the zeroth order term,

$$\lambda_1(-\sigma_P \overline{\mathcal{L}} - r_P) \leq \lambda_1(-\sigma_P \overline{\mathcal{L}} - \min_{x \in \overline{\Omega}} r_P) \leq -\min_{x \in \overline{\Omega}} r_P < 0.$$

We used the fact that $(\lambda,\varphi)=(-\min_{x\in\overline{\Omega}} r_P, r_P)$ are eigenelements of the operator $-\sigma_P \overline{\mathcal{L}} - \min_{x\in\overline{\Omega}} r_P$.

[14, Proposition 3.2] and Proposition 2.4.1 yield the uniform convergence of $\underline{P}$ towards $\dfrac{r_P}{s_P}$.

Let $\varepsilon > 0$. There exists $t_0 > 0$ such that for all $x \in \Omega$ and $t \geq t_0$, $P(x,t) \geq \underline{P}(x,t) \geq \dfrac{r_P(x)}{s_P} - \varepsilon$. Denote $V_{t_0} := V(\cdot, t_0)$, from the solution of (2.1) taken at time $t = t_0$.

Let $\overline{V}$ be a solution of

$$\begin{cases} \overline{V}(\cdot,t_0) = V_{t_0} & \text{in } \Omega \\ \partial_t \overline{V} - \sigma_V \Delta \overline{V} = r_V \overline{V} - h(\frac{r_P}{s_P} - \varepsilon)\overline{V} & \text{in } \Omega \times [t_0, +\infty) \\ \dfrac{\partial \overline{V}}{\partial n} = 0 & \text{on } \partial\Omega \times [t_0, +\infty). \end{cases}$$

By our choice of t_0, $\overline{V}$ is a supersolution of the first equation of (2.3) with V_{t_0} as initial condition. Moreover, $\overline{V}$ is below

$$\max_{x\in\Omega} V(x,t_0) \max_{x\in\Omega} \varphi_{s,1}(x) e^{-(\lambda_1(\mathcal{L}_{V_s})-h\varepsilon)(t-t_0)},$$

where $\varphi_{s,1}$ and $\lambda_1(\mathcal{L}_{V_s})$ satisfy

$$(-\sigma_V \Delta + h(\frac{r_P}{s_P} - \varepsilon) - r_V)\varphi_{s,1} = (\lambda_1(\mathcal{L}_{V_s}) - h\varepsilon)\varphi_{s,1}.$$

with $\min_{x\in\Omega} \varphi_{s,1}(x) = 1$.

By positivity of $\lambda_1(\mathcal{L}_{V_s})$, one can choose $\varepsilon > 0$ small enough so that $\lambda_1(\mathcal{L}_{V_s}) - h\varepsilon > 0$.

Hence, one has the uniform convergence of

$\overline{V} \leq \max_{x\in\Omega} V(x,t_0) \max_{x\in\Omega} \varphi_{s,1}(x) e^{-(\lambda_1(\mathcal{L}_{V_s})-h\varepsilon)(t-t_0)}$ to 0 when $t \to +\infty$, yielding the uniform convergence of

$$0 \leq V_i, V_s \leq V \leq \overline{V} \leq \max_{x\in\Omega} V(x,t_0) \max_{\Omega} \varphi_{s,1} e^{-(\lambda_1(\mathcal{L}_{V_s})-h\varepsilon)(t-t_0)}$$

to 0. It is useful to point out that the uniform convergence of V to 0 demonstrates a control of the infection, and not the end of it.

Now, take $t_0' > 0$ such that for all $x \in \Omega$ and $t \geq t_0'$, $V(x,t) \leq \dfrac{\varepsilon}{\gamma h} \min_{x\in\overline{\Omega}}(r_P(x))$. Denote $P_{t_0'} := P(\cdot, t_0')$, from the solution of (2.1) taken at time $t = t_0'$.

Let $\overline{P}$ be a solution of

$$\begin{cases} \overline{P}(\cdot,t_0') = P_{t_0'} & \text{in } \Omega \\ \partial_t \overline{P} - \sigma_P \overline{\mathcal{L}}(\overline{P}) = r_P \overline{P} - s_P \overline{P}^2 + \varepsilon r_P \overline{P} & \text{in } \Omega \times [t_0', +\infty) \\ \dfrac{\partial \overline{P}}{\partial n} = 0 & \text{on } \partial\Omega \times [t_0', +\infty). \end{cases}$$

By our choice of t_0', $\overline{P}$ is a supersolution of the second equation of (2.3) with $P_{t_0'}$ as initial condition. Moreover, a linearization of the associated elliptic problem around the steady state 0 yields the spectral problem

$$(-\sigma_P \overline{\mathcal{L}} - (1+\varepsilon) r_P)\varphi = \lambda\varphi.$$

By monotonicity of the principal eigenvalue with respect to the zeroth order term,

$$\lambda_1(-\sigma_P \overline{\mathcal{L}} - (1+\varepsilon) r_P) \leq \lambda_1(-\sigma_P \overline{\mathcal{L}} - (1+\varepsilon) \min_{x\in\overline{\Omega}} r_P) \leq -(1+\varepsilon) \min_{x\in\overline{\Omega}} r_P < 0.$$

We used the fact that (λ,φ)=$(-(1+\varepsilon)\min_{x\in\overline{\Omega}} r_P, r_P)$ are eigenelements of the operator $-\sigma_P \overline{\mathcal{L}} - (1+\varepsilon)\min_{x\in\overline{\Omega}} r_P$.

[14, Theorem 3.2] and a very similar version of Proposition 2.4.1 (with $(1+\varepsilon)r_P$ instead of r_P) yield the uniform convergence of $\overline{P}$ towards $(1+\varepsilon)\frac{r_P}{s_P}$. Combining the convergence of $\underline{P}$ and $\overline{P}$, there exist a $t_1 > 0$ large enough so that, for all $x \in \Omega$ and $t \geq t_1$, $\frac{r_P(x)}{s_P} - \varepsilon \leq \underline{P}(x,t) \leq P(x,t) \leq \overline{P} \leq (1+\varepsilon)\frac{r_P(x)}{s_P} + \varepsilon$.

Since ε is arbitrary, this shows the uniform convergence of P to r_P/s_P.

Finally, assume $V_{i,0} \not\equiv 0$ and let $\delta > 0$. Suppose by contradiction that $\min_{x\in\Omega} V_i(x,\delta) = 0$. By the uniform Harnack inequality (see [32, Theorem 2.5]), there exists $C_\delta > 0$ such that $\max_{x\in\Omega} V_i(x,\delta) \leq C_\delta \min_{x\in\Omega} V_i(x,\delta) = 0$ for all $x \in \Omega$, therefore we would have $V_i(x,\delta) = 0$ for all $x \in \Omega$. By uniqueness of the Cauchy–Neumann problem, V would be identically 0 for all time, which contradicts the fact that $V_{i,0} \not\equiv 0$. Therefore, for all $x \in \Omega$,

$$I(x,\delta) = H(x)\left(1 - \exp\left(-\beta_{VH}\int_0^\delta V_i(x,s)\mathrm{d}s\right)\right) > 0.$$

By the Hopf boundary lemma and the homogeneous Neumann boundary conditions, for all $t \in (0,\delta)$, $\inf_{x\in\Omega} V_i(x,t) > 0$. Then, for all $x \in \Omega$, $\int_0^\delta V_i(x,s)\mathrm{d}s \geq \int_0^\delta \inf_{x\in\Omega} V_i(x,s)\mathrm{d}s$, which yields $\inf_{x\in\Omega}\int_0^\delta V_i(x,s)\mathrm{d}s > 0$. By positivity of H on the compact $\overline{\Omega}$, $\inf_{x\in\Omega} I(x,\delta) > 0$. By increasingness of $t \mapsto I(x,t)$,

$$\liminf_{t\to+\infty} \inf_{x\in\Omega} I(x,t) \geq \inf_{x\in\Omega} I(x,\delta) > 0.$$

Let $t_\varepsilon > 0$ such that, for all $x \in \Omega$ and $t \geq t_\varepsilon$, $V(x,t) \leq \varepsilon$ and $|P(x,t) - r_P/s_P| \leq \varepsilon$. Denote $\underline{V_i}$, the solution of

$$\begin{cases} \underline{V_i}(x,t_\varepsilon) = V_{i,t_\varepsilon} & \text{in } \Omega \\ \partial_t \underline{V_i} - \sigma_V \Delta \underline{V_i} = (-\alpha - d_V - s_V\varepsilon - h(r_P/s_P + \varepsilon))\underline{V_i} & \text{in } \Omega \times [t_\varepsilon, +\infty) \\ \dfrac{\partial \underline{V_i}}{\partial n} = 0 & \text{on } \partial\Omega \times [t_\varepsilon, +\infty) \end{cases}$$

Denote $\varphi_{i,1}$ the principal eigenfunction associated to $\lambda_1(\mathcal{L}_{V_i})$ (which is positive, by the Krein-Rutman theorem), with $\max_{x\in\Omega}\varphi_{i,1}(x) = 1$. By our choice of t_ε, $\underline{V_i}$ is a subsolution of the Cauchy–Neumann scalar system verified by V_i, and for all $x \in \Omega$, $t \geq t_\varepsilon$,

$$V_i(x,t) \geq \min_{x\in\Omega} V_i(x,t_\varepsilon)\min_{\Omega}\varphi_{i,1}\exp\left(-(\lambda_1(\mathcal{L}_{V_i}) + s_V\varepsilon + h\varepsilon)(t - t_\varepsilon)\right).$$

We denote $C_s = \max_{x\in\Omega} V(x,t_\varepsilon)\max_{\Omega}\varphi_{s,1}$ and $C_i = \min_{x\in\Omega} V_i(x,t_\varepsilon)\min_{\Omega}\varphi_{i,1}$. By the supersolution of V_i we have exibited before, for all $x \in \Omega$, $t \geq t_\varepsilon$,

$$\begin{aligned} & I(x,t)/H(x) \\ = \;& 1 - \exp\left(-\beta_{VH}\int_0^t V_i(x,s)\mathrm{d}s\right) \\ \leq \;& 1 - \exp\left(-\beta_{VH}\left(\int_0^{t_\varepsilon} V_i(x,s)\mathrm{d}s + C_s\int_{t_\varepsilon}^t e^{-(\lambda_1(\mathcal{L}_{V_s})-h\varepsilon)(s-t_\varepsilon)}\mathrm{d}s\right)\right) \\ \leq \;& 1 - \exp\left(-\beta_{VH}\left(\int_0^{t_\varepsilon} V_i(x,s)\mathrm{d}s + \frac{C_s}{\lambda_1(\mathcal{L}_{V_s}) - h\varepsilon}\right)\right). \end{aligned}$$

By the subsolution of V_i we have exibited before, for all $x \in \Omega,\ t \geq t_\varepsilon$,

$$\begin{aligned} & I(x,t)/H(x) \\ \geq\ & 1 - \exp\left(-\beta_{VH}\left(\int_0^{t_\varepsilon} V_i(x,s)\mathrm{d}s + C_i \int_{t_\varepsilon}^{t} e^{-(\lambda_1(\mathcal{L}_{V_i})+s_V\varepsilon+h\varepsilon)(s-t_\varepsilon)}\mathrm{d}s\right)\right) \\ =\ & 1 - \exp\left(-\beta_{VH}\left(\int_0^{t_\varepsilon} V_i(x,s)\mathrm{d}s + C_i \frac{1-e^{-(\lambda_1(\mathcal{L}_{V_i})+s_V\varepsilon+h\varepsilon)(t-t_\varepsilon)}}{\lambda_1(\mathcal{L}_{V_i})+s_V\varepsilon+h\varepsilon}\right)\right). \end{aligned}$$

If $|P_0 - r_P/s_P| \leq \varepsilon$ and $V_0 \leq \varepsilon$, then $t_\varepsilon = 0$ and the proof is completed.

(ii) Let us first prove that

$$\liminf_{t\to+\infty} \inf_{x\in\Omega} V(x,t) > 0.$$

We are going to need the following lemma:

Lemma 2.4.8. *Let $\varepsilon > 0$, and let $[t_0, T)$ be any interval of time where V is lower than or equal to ε. There exists $S_\varepsilon > 0$ such that $T \leq S_\varepsilon$.*

Proof. Let $\varepsilon > 0$ be fixed. During the course of the proof, we will make a smallness assumption on its value that could have been made from the start without loss of generality. Let $[t_0, T)$ be an interval of time where $V(x,t) \leq \varepsilon$ for all $x \in \Omega$. We are going to prove that $T \leq S_\varepsilon$, and we are going to give an explicit formula for S_ε. Let us suppose, by contradiction, that $T = +\infty$.

We can consider $\overline{P}$, the solution of the Cauchy scalar problem

$$\begin{cases} \overline{P}(t_0) = m_{P_0} := \max\limits_{x\in\Omega}\left(\dfrac{P_{t_0}}{r_P}\right) \\ \partial_t \overline{P} = \max\limits_{x\in\Omega}(r_P)(\overline{P} - s_P\overline{P}^2) + \gamma h\varepsilon\overline{P} \quad \text{in } [t_0, T). \end{cases}$$

One easily checks that $\overline{P}$ is a supersolution of

$$\begin{cases} \tilde{P}(.,t_0) = \dfrac{P_{t_0}}{r_P} & \text{in } \Omega \\ \partial_t\tilde{P} - \dfrac{\sigma_P}{r_P}\nabla\cdot\left(r_P\nabla(\tilde{P})\right) = r_P(\tilde{P} - s_P\tilde{P}^2) + \gamma h V\tilde{P} & \text{in } \Omega\times[t_0,T) \\ \dfrac{\partial\tilde{P}}{\partial n} = 0 & \text{on } \partial\Omega\times[t_0,T). \end{cases}$$

Hence, $P = r_P\tilde{P} \leq r_P\overline{P}$ on this interval. Moreover, one can compute explicitly

$$\overline{P}(t) = K_\varepsilon \frac{1}{1 + \left(K_\varepsilon/m_{P_0} - 1\right)e^{-(\max\limits_{x\in\Omega}(r_P)+\gamma h\varepsilon)(t-t_0)}},$$

which converges to $K_\varepsilon := \dfrac{\max\limits_{x\in\Omega}(r_P) + \gamma h\varepsilon}{\max\limits_{x\in\Omega}(r_P)s_P}$. Hence, there exists $t_1 \geq t_0$ such that

$$\overline{P}(t) \leq K_\varepsilon + \varepsilon$$

for all $t \geq t_1$. Assume t_1 is minimal.

If $m_{P_0}s_P \leq 1$, then $\overline{P}$ is increasing in time and $\overline{P}(t) \leq K_\varepsilon$ for all $t \geq t_0$, hence $t_1 = t_0$.

If $m_{P_0}s_P > 1$, then $\overline{P}$ is decreasing in time, $\overline{P}(t) \leq m_{P_0}$ for all $t \geq t_0$, and t_1 is given by

$$\overline{P}(t_1) = K_\varepsilon + \varepsilon,$$

hence

$$e^{-(\max\limits_{x\in\Omega}(r_P)+\gamma h\varepsilon)(t-t_0)} = \frac{1}{(1+K_\varepsilon/\varepsilon)\left(1-K_\varepsilon/m_{P_0}\right)},$$

and

$$t_1 = t_0 + \frac{\ln\left(1+K_\varepsilon/\varepsilon\right) + \ln\left(1-K_\varepsilon/m_{P_0}\right)}{\max\limits_{x\in\Omega}(r_P)+\gamma h\varepsilon}.$$

Denote $\overline{\mathcal{P}} := \max\limits_{x\in\Omega}(r_P)\max\left(K_\varepsilon, m_{P_0}\right)$, so that, for all $x\in\Omega$ and $t\geq t_0$, $P(x,t)\leq\overline{\mathcal{P}}$. We can construct a subsolution $\underline{U}$ of the Cauchy–Neumann scalar problem verified by V on $[t_0,T)$:

$$\begin{cases} \underline{U}(t_0) = \min\left(\min\limits_{x\in\Omega} V_{t_0}, \dfrac{\min\limits_{x\in\Omega} r_V}{s_V}\right) \\ \partial_t\underline{U} = -h\overline{\mathcal{P}}\underline{U} & \text{in } [t_0,T), \end{cases}$$

which gives us, for all $x\in\Omega$, the following inequality:

$$V(x,t_1)\geq C := \min\left(\min_{x\in\Omega} V_{t_0}, \frac{\min\limits_{x\in\Omega} r_V}{s_V}\right) e^{-h\overline{\mathcal{P}}(t_1-t_0)}.$$

Now, let $\underline{V}$ be the solution of

$$\begin{cases} \underline{V}(\cdot,t_1) = V_{t_1} & \text{in } \Omega \\ \partial_t\underline{V} - \sigma_V\Delta\underline{V} = r_V\underline{V} - 2s_V\varepsilon\underline{V} - hr_P\left(K_\varepsilon+\varepsilon\right)\underline{V} & \text{in } \Omega\times[t_1,T) \\ \dfrac{\partial\underline{V}}{\partial n} = 0 & \text{on } \partial\Omega\times[t_1,T). \end{cases}$$

By construction of t_1, $\underline{V}$ is a subsolution of the Cauchy–Neumann scalar problem verified by V on this interval, as long as $\underline{V}\leq 2\varepsilon$. Say that $\underline{V}\leq 2\varepsilon$ in an interval $[t_1,t^*]$ ($t^*>t_1$ exists by the assumption $V\leq\varepsilon$ and by continuity of $\underline{V}$). By negativity of $\lambda_1(\mathcal{L}_{V_s})$ and by continuity of the principal eigenvalue with respect to the zeroth order term, one can take ε small enough such that

$$\lambda_1^\varepsilon := \lambda_1\left(-\sigma_V\Delta - r_V + 2s_V\varepsilon + hr_P\left(K_\varepsilon+\varepsilon\right)\right) < 0$$

(recall that $K_\varepsilon\to 1/s_P$ as $\varepsilon\to 0$).

Even if it means reducing it, take ε satisfying this condition.

The subsolution $\underline{V}$ is above $C\varphi_1^\varepsilon(x)e^{-\lambda_1^\varepsilon(t-t_1)}$ for all $x\in\Omega$ and $t\geq t_1$, φ_1^ε being the principal eigenvalue associated to λ_1^ε (which is positive, by the Krein-Rutman theorem) with $\max\limits_{x\in\Omega}\varphi_1^\varepsilon = 1$. Therefore, for all $x\in\Omega$ and $t\in[t_1,t^*]$,

$$\begin{aligned} V(x,t) &\geq \underline{V}(x,t) \\ &\geq C\varphi_1^\varepsilon(x)e^{-\lambda_1^\varepsilon(t-t_1)} \\ &\geq \min\left(\min_{x\in\Omega} V_{t_0}, \frac{\min\limits_{x\in\Omega} r_V}{s_V}\right) e^{-h\overline{\mathcal{P}}(t_1-t_0)}\min_\Omega\varphi_1^\varepsilon e^{-\lambda_1^\varepsilon(t-t_1)}, \end{aligned}$$

hence $\underline{V}$ is above an increasing function until the finite time t^* where $\underline{V}(x,t^*)=2\varepsilon$ for all $x\in\Omega$. According to the previous inequality, one has, for all $x\in\Omega$, $V(x,t^*)\geq 2\varepsilon>\varepsilon$, which contradicts the assumption on T. T is hereby finite, and we can compute S_ε:

$$\min\left(\min_{x\in\Omega} V_{t_0}, \frac{\min\limits_{x\in\Omega} r_V}{s_V}\right) e^{-h\overline{\mathcal{P}}(t_1-t_0)}\min_\Omega\varphi_1^\varepsilon e^{-\lambda_1^\varepsilon(t_0+S_\varepsilon-t_1)} = \varepsilon,$$

hence

$$S_\varepsilon = \frac{\ln\left(\min\left(\min_{x\in\Omega} V_{t_0}, \dfrac{\min_{x\in\Omega} r_V}{s_V}\right) e^{-h\overline{\mathcal{P}}(t_1-t_0)} \min_{\Omega} \varphi_1^\varepsilon\right) - \ln(\varepsilon)}{\lambda_1^\varepsilon} + t_1 - t_0,$$

with the value of $t_1 - t_0$ given above. □

First of all, let us prove that, for any $\delta > 0$, $\min_{x\in\Omega} V(x,\delta) > 0$. Let $\delta > 0$. Suppose by contradiction that $\min_{x\in\Omega} V(x,\delta) = 0$. By the uniform Harnack inequality (see [32, Theorem 2.5]), there exists $C_\delta > 0$ such that $\max_{x\in\Omega} V(x,\delta) \leq C_\delta \min_{x\in\Omega} V(x,\delta) = 0$ for all $x \in \Omega$, therefore we would have $V(x,\delta) = 0$ for all $x \in \Omega$. By uniqueness of the Cauchy–Neumann problem, V would be identically 0 for all time, which contradicts the fact that $V_0 \not\equiv 0$.

Let $\varepsilon > 0$. We are going to consider two cases:

Case 1: there exists $t^* > 0$ such that, for all $t \geq t^*$, $\max_{x\in\Omega} V(x,t) \geq \varepsilon$. By the uniform Harnack inequality (see [32, Theorem 2.5]), there exists $C_{t^*} > 0$ so that, for all $t \geq t^*$, $\min_{x\in\Omega} V(x,t) \geq C_{t^*} \max_{x\in\Omega} V(x,t) \geq C_{t^*}\varepsilon$. The proof is then completed.

Case 2: for all $t^* > 0$, there exists $t \geq t^*$ such that $\max_{x\in\Omega} V(x,t) < \varepsilon$. By the lemma, we can deduce the existence of an increasing sequence of times $(t_n)_{n\in\mathbb{N}}$, $t_0 > 0$, $t_n \underset{n\to+\infty}{\longrightarrow} +\infty$, where, for all $n \in \mathbb{N}$,

$$\begin{cases} 0 < \max_{x\in\Omega} V(x,t) \leq \varepsilon & \forall t \in [t_{2n}, t_{2n+1}] \\ \max_{x\in\Omega} V(x,t) \geq \varepsilon & \forall t \in [t_{2n+1}, t_{2n+2}]. \end{cases}$$

By the uniform Harnack inequality (see [32, Theorem 2.5]), there exists $C_{t_0} > 0$ so that, for all $t \geq t_0$, $\min_{x\in\Omega} V(x,t) \geq C_{t_0} \max_{x\in\Omega} V(x,t)$.

Hence, for all $n \in \mathbb{N}$ and all $t \in [t_{2n+1}, t_{2n+2}]$, $\min_{x\in\Omega} V(x,t) \geq C_{t_0} \max_{x\in\Omega} V(x,t) \geq C_{t_0}\varepsilon$.

Again by the lemma, we know that, for all $n \in \mathbb{N}$, $|t_{2n+1} - t_{2n}| \leq S_\varepsilon$. Therefore, for all $n \in \mathbb{N}$ and all $t \in [t_{2n}, t_{2n+1}]$,

$$\min_{x\in\Omega} V(x,t) \geq \min_{t\in[t_{2n}, t_{2n}+S_\varepsilon]} \min_{x\in\Omega} V(x,t)$$

Denote $\overline{\mathcal{P}} := \max_{x\in\Omega}(r_P) \max\left(\dfrac{\max_{x\in\Omega}(r_P) + \gamma h\varepsilon}{\max_{x\in\Omega}(r_P) s_P}, \max_{x\in\Omega}\left(\dfrac{P_{t_0}}{r_P}\right)\right)$. Without detailing more (see the proof of the lemma), we have for all $x \in \Omega$ and $t \geq t_0$, $P(x,t) \leq \overline{\mathcal{P}}$. We can construct, for all $n \in \mathbb{N}$, a subsolution $\underline{U}$ of the Cauchy–Neumann scalar problem verified by V on $[t_{2n}, t_{2n} + S_\varepsilon]$:

$$\begin{cases} \underline{U}(t_0) = C_{t_0}\varepsilon \\ \partial_t \underline{U} = -h\overline{\mathcal{P}}\underline{U} \quad \text{in } [t_{2n}, t_{2n} + S_\varepsilon], \end{cases}$$

which yields, for all $n \in \mathbb{N}$ and all $t \in [t_{2n}, t_{2n} + S_\varepsilon]$,

$$\min_{x\in\Omega} V(x,t) \geq C_{t_0}\varepsilon e^{-h\overline{\mathcal{P}}S_\varepsilon},$$

hence

$$\min_{t\in[t_{2n}, t_{2n}+S_\varepsilon]} \min_{x\in\Omega} V(x,t) \geq C_{t_0}\varepsilon e^{-h\overline{\mathcal{P}}S_\varepsilon}.$$

Finally, combining the inequalities on all segments, for all $t \geq t_0$,

$$\min_{x\in\Omega} V(x,t) \geq \underline{\mathcal{V}} := \min\left(C_{t_0}\varepsilon, C_{t_0}\varepsilon e^{-h\overline{\mathcal{P}}S_\varepsilon}\right),$$

which proves that

$$\liminf_{t\to+\infty} \inf_{x\in\Omega} V(x,t) > 0.$$

V_i satisfies

$$\begin{cases} V_i(\cdot,0) = V_{i,0} \not\equiv 0 & \text{in } \Omega \\ \partial_t V_i - \sigma_V \Delta V_i = \beta_{HV} I V_s - \alpha V_i - d_V V_i & \\ \qquad\qquad -s_V(V_s+V_i)V_i - hPV_i & \text{in } \Omega\times\mathbb{R}_+^* \\ \dfrac{\partial V_i}{\partial n} = 0 & \text{on } \partial\Omega\times\mathbb{R}_+^*. \end{cases}$$

By classical arguments presented before, for all $\delta > 0$, all $t \geq \delta$ and all $x \in \Omega$, $V_i(x,t) > 0$. In particular, $\min_{x\in\Omega} V_i(x,t_0) > 0$.

The equation on V_i can be rewritten as

$$\begin{aligned} \partial_t V_i - \sigma_V \Delta V_i &= \beta_{HV} I(V - V_i) - \alpha V_i - d_V V_i - s_V V V_i - hPV_i \\ &= \beta_{HV} H\left(1 - \exp\left(-\beta_{VH}\int_0^t V_i\right)\right) V \\ &\quad -(\beta_{HV} I + \alpha + d_V + s_V V + hP) V_i. \end{aligned}$$

I, V and P being bounded, there exists a constant $C > 0$ large enough so that $\beta_{HV} I + \alpha + d_V + s_V V + hP \leq C$. Define $\underline{V_i}$, the solution of

$$\begin{cases} \max_{x\in\Omega} V(x,t_0) \max_{x\in\Omega} \varphi_{s,1}(x) e^{-(\lambda_1(\mathcal{L}_{V_s})-h\varepsilon)(t-t_0)} \underline{V_i}(t_0) = \min_{x\in\Omega} V_i(x,t_0) \\ \partial_t \underline{V_i} = \beta_{HV} \min_{x\in\Omega} H(x) \left(1 - \exp\left(-\beta_{VH}\int_0^{t_0} \min_{x\in\Omega} V_i(x,s)\mathrm{d}s\right)\right) \underline{\mathcal{V}} - C\underline{V_i} \end{cases}$$

in $[t_0, +\infty)$. One easily checks that $\underline{V_i}$ is a subsolution of the Cauchy–Neumann scalar system verified by V_i, and has

$$\underline{V_i}(t) = a + (\min_{x\in\Omega} V_i(x,t_0) - a) e^{-C(t-t_0)},$$

where

$$a = \frac{1}{C}\beta_{HV} \min_{x\in\Omega} H(x) \left(1 - \exp\left(-\beta_{VH}\int_0^{t_0} \min_{x\in\Omega} V_i(x,s)\mathrm{d}s\right)\right) \underline{\mathcal{V}} > 0,$$

hence

$$\liminf_{t\to+\infty} \inf_{x\in\Omega} V_i(x,t) \geq \lim_{t\to+\infty} \underline{V_i}(t) = a > 0.$$

Moreover, for all $x \in \Omega$ and $t \geq t_0$, denoting $\underline{V_{i,t_0}} = \min_{x\in\Omega} V_i(x,t_0)$ and $C_a = \underline{V_{i,t_0}} - a$,

$$\begin{aligned} & |I(x,t) - H(x)| \\ = \;& H(x) \exp\left(-\beta_{VH}\int_0^t V_i(x,s)\mathrm{d}s\right) \\ \leq \;& H(x) \exp\left(-\beta_{VH}\left(\int_0^{t_0} V_i(x,s)\mathrm{d}s + \int_{t_0}^t a + \int_{t_0}^t C_a e^{-C(s-t_0)}\mathrm{d}s\right)\right) \\ = \;& H(x) \exp\left(-\beta_{VH}\left(\int_0^{t_0} V_i(x,s)\mathrm{d}s + (t-t_0)a + C_a\frac{1-e^{-C(t-t_0)}}{C}\right)\right). \end{aligned}$$

By boundedness of H and V_i, $H\exp\left(-\beta_{VH}\left(\int_0^{t_0} V_i(\cdot,s)\mathrm{d}s\right)\right)$ is bounded, say by a constant $C'>0$. Therefore, for all $t\geq t_0$,

$$\begin{aligned}\|I(\cdot,t)-H\|_\infty &\leq C'\exp\left(-\beta_{VH}\left((t-t_0)a+(\underline{V_{i,t_0}}-a)\frac{1-e^{-C(t-t_0)}}{C}\right)\right)\\ &\underset{t\to+\infty}{\longrightarrow} 0.\end{aligned}$$

□

2.5 Estimations of the harvest

Assume that $\lambda_1(\mathcal{L}_{V_s})>0$ and fix $\varepsilon>0$ such that $\lambda_1(\mathcal{L}_{V_s})-h\varepsilon>0$. By theorem 2.2.1, there exists $t_\varepsilon>0$ such that, for all $x\in\Omega$, $t\geq t_\varepsilon$, denoting $C_i=\min_{x\in\Omega} V_i(x,t_\varepsilon)\min_{\Omega}\varphi_{i,1}$ and $C_s=\max_{x\in\Omega} V(x,t_\varepsilon)\max_{\Omega}\varphi_{s,1}$,

$$\begin{aligned}&1-\exp\left(-\beta_{VH}\left(\int_0^{t_\varepsilon} V_i(x,s)\mathrm{d}s+C_i\frac{1-e^{-(\lambda_1(\mathcal{L}_{V_i})+s_V\varepsilon+h\varepsilon)(t-t_\varepsilon)}}{\lambda_1(\mathcal{L}_{V_i})+s_V\varepsilon+h\varepsilon}\right)\right)\\ &\leq I(x,t)/H(x)\\ &\leq 1-\exp\left(-\beta_{VH}\left(\int_0^{t_\varepsilon} V_i(x,s)\mathrm{d}s+\frac{C_s}{\lambda_1(\mathcal{L}_{V_s})-h\varepsilon}\right)\right),\end{aligned}$$

hence, letting $t\to+\infty$ and integrating over Ω,

$$\begin{aligned}&\int_\Omega H\exp\left(-\beta_{VH}\left(\int_0^{t_\varepsilon} V_i(\cdot,s)\mathrm{d}s+\frac{C_s}{\lambda_1(\mathcal{L}_{V_s})-h\varepsilon}\right)\right)\\ \leq\ &\int_\Omega H-I_\infty\\ \leq\ &\int_\Omega H\exp\left(-\beta_{VH}\left(\int_0^{t_\varepsilon} V_i(\cdot,s)\mathrm{d}s+\frac{C_i}{\lambda_1(\mathcal{L}_{V_i})+s_V\varepsilon+h\varepsilon}\right)\right).\end{aligned}$$

If $|P_0-r_P/s_P|\leq\varepsilon$ and $V_0\leq\varepsilon$, then $t_\varepsilon=0$ and the estimates follow.
If $\lambda_1(\mathcal{L}_{V_s})<0$, by Theorem 2.2.1, $I_\infty=H$, hence $\int_\Omega H-I_\infty=0$.

2.6 Numerical analysis of the optimal control problem

Recall that the optimal control problem is enunciated as follows: assuming that $r_V=r_V^{\text{field}}+r_V^{\text{refuge}}R$, $r_P=r_P^{\text{field}}+r_P^{\text{refuge}}R$, $H=H^{\text{field}}(1-R)$ with $R:\Omega\to[0,1]$ a spatial distribution of biodiversity refuges and with positive constants r_V^{field}, r_V^{refuge}, r_P^{field}, r_P^{refuge}, H^{field}, characterize the set of optimal R such that the harvest of healthy beets $\lim_{t\to+\infty}\int_\Omega H(x)-I(x,t)\mathrm{d}x$ is maximized.

Although we worked in the previous analytical sections in a smooth setting (smooth domain, smooth functions r_V, r_P and H, classical solutions) for the sake of simplicity, we actually have in mind, application-wise, a slightly less regular setting, where $\Omega\subset\mathbb{R}^2$ is a rectangle $[0,l_1]\times[0,l_2]$, where R is an indicator function and where solutions are weak solutions. The extension of the preceding analytical sections to this setting by regularization procedures is a

classical but technical issue and is deliberately not written in this paper. Our numerical simulations below will illustrate, quite unambiguously, that the analytical study of the optimal control problem with purely deterministic tools is likely vain, independently of the spatial dimension and the smoothness of the setting: indeed, the main issue lies in the strong dependency on the initial conditions. Therefore, in this section, we only present numerical simulations of the biologically more realistic setting.

2.6.1 First insights

Theorem 2.2.1 established the importance of the principal eigenvalue $\lambda_1(\mathcal{L}_{V_s})$. For the agro-ecological control strategy to succeed, this eigenvalue must be larger than 0. Moreover, when this sign condition is satisfied, the rate of exponential decay of the vector population is, roughly speaking, $-\lambda_1(\mathcal{L}_{V_s})$: the larger the eigenvalue, the faster the eradication of vectors. Therefore it is natural to consider the maximization of this eigenvalue as the spatial distribution of refuges R varies. Since R is in all cases an indicator function $\mathbf{1}_A$, with A the refuge subdomain, the problem reduces to maximizing the eigenvalue as A varies. Also, thanks to the ideal free distribution of predators which makes their equilibrium equal to r_P/s_P, the principal eigenvalue $\lambda_1(\mathcal{L}_{V_s}) = \lambda_1(A)$ depends on A in a completely explicit way:

$$\begin{aligned}\lambda_1(A) &= \lambda_1\left(-\sigma_V\Delta - \left(r_V^{\text{field}} - \frac{h}{s_P}r_V^{\text{field}}\right) - \left(r_V^{\text{refuge}} - \frac{h}{s_P}r_V^{\text{refuge}}\right)\mathbf{1}_A\right)\\ &= -\left(r_V^{\text{field}} - \frac{h}{s_P}r_V^{\text{field}}\right) + \lambda_1\left(-\sigma_V\Delta - \left(r_V^{\text{refuge}} - \frac{h}{s_P}r_V^{\text{refuge}}\right)\mathbf{1}_A\right).\end{aligned}$$

The first remark to be made on this spectral optimization concerns the effect of fragmentation. Is a unique big connected refuge better than a multitude of small disconnected uniformly distributed refuges? The answer is negative: the eigenvalue $\lambda_1(A)$ is increasing with the frequency of the refuge A (in dimension 1, the frequency is the number of connected components, we will provide a preciser definition of the frequency later). This can be easily proved by periodically extending A in $\mathbb{R}^2$ (recall that Ω is now a rectangle), by a change of spatial variable and by using the variational formula for $\lambda_1(A)$: calling $\mu = -r_V^{\text{refuge}} + \frac{h}{s_P}r_V^{\text{refuge}}$, and up to an additive constant, the principal eigenvalue corresponding to the refuges A_n of frequency n we denote $\lambda_1(A_n)$ is

$$\lambda_1(A_n) = \inf_{\varphi\in H^1(\Omega),\|\varphi\|_{L^2}=1}\int_\Omega n^2\sigma_V|\nabla\varphi|^2 + \mu\mathbf{1}_{A_1}\varphi^2.$$

The monotonicity of $\lambda_1(A_n)$ with respect to the frequency n is hereby clear.

Moreover, the limit as the frequency becomes infinite while the area is fixed is identified thanks to a well-known homogenization result (Theorem 2.1 of [17]): indeed it is

$$-r_V^{\text{field}} + \frac{hr_P^{\text{field}}}{s_P} + \frac{|A|}{|\Omega|}\left(-r_V^{\text{refuge}} + \frac{hr_P^{\text{refuge}}}{s_P}\right) = \left(1 - \frac{|A|}{|\Omega|}\right)\lambda_1(\emptyset) + \frac{|A|}{|\Omega|}\lambda_1(\Omega).$$

This limit tells, on a linear level, that the system with a refuge of high frequency behaves like it would if flowers and beets had been perfectly mixed together, and that this is the best configuration of flowers one can hope for.

The second remark follows naturally from this explicit limit: in the high frequency asymptotic regime, the exact shape of the connected components of A does not matter and increasing the area of the refuge is beneficial.

Nevertheless, the quantity we actually want to maximize is not λ_1 but rather the harvest $\Phi = \lim_{t\to+\infty} \int_\Omega H(x) - I(x,t)\mathrm{d}x$. Even though Theorem 2.2.1 hints toward a monotonic relationship between λ_1 and Φ, it turns out this is false. The following argument makes it clear: the best possible eigenvalue corresponds to $A = \Omega$; however, in such a case, there is no beets to harvest anymore whence $\Phi = 0$. Therefore the optimal refuge area is intermediate: $0 < |A| < |\Omega|$. An even more subtle fact is the following: our numerical simulations show that Φ is hugely impacted by the initial conditions P_0 and V_0. For instance, when $P_0 = r_P/s_P$ and V_0 is supported inside a connected component of the refuge, say A_{init}, it is actually better to have A_{init} as large as possible, which means that A_{init} should be the only connected component of A, or in other words A should have a low frequency.

In our understanding of the sugar beet agro-ecosystem, the initial condition for the aphids cannot be predicted and is mostly random. A natural perspective is then the probabilistic study of the expected harvest. However this is way outside the scope of this paper, and we leave it for future work. In particular, a more precise knowledge of the law of this random initial condition is necessary. Preliminary numerical simulations assuming a uniform law tend to indicate that the expected harvest is indeed increasing with the frequency of the refuge.

2.6.2 Numerical framework

We simulate the Cauchy–Neumann system (2.1) with a classical semi-explicit scheme with finite differences (details can be found in the supplementary materials).

The script is written in Python, using the numpy `https://numpy.org/` package, the scipy `https://scipy.org/` package and the matplotlib `https://pypi.org/project/matplotlib/` package. For longer computations, this work was performed using the computing facilities of the CC LBBE/PRABI. Details on the computation of the parameters can be found in the supplementary materials.

The refuge has area $\mathcal{A} \in (0, |\Omega|)$ and we consider a sequence $(A_n)_{n\in\mathbb{N}}$ of uniformly distributed refuges:

$$A_n := \left(\bigcup_{m=0}^{n-1} \left[\frac{m}{n} L, \frac{m}{n} L + \frac{\sqrt{\mathcal{A}}}{n} \right] \right)^2 .$$

For our simulation, we take $N = 4000$ time steps, $J = 80$ spatial steps, $T = 365/4$ days, $\Omega = [0, L]^2$ with $L = 300$ meters, $\mathcal{A} = \dfrac{|\Omega|}{5^2}$, $r_P = (r_R - r_F)\mathbf{1}_{A_4} + r_F$ and the initial conditions $I_0 = 0$, $V_{i,0} = (1/100)(r_V/s_V)$ distributed in 3 patches of different sizes, $V_{s,0} = (9/100)(r_V/s_V)$ distributed in the same patches than $V_{i,0}$, $P_0 = r_P/s_P$.

2.6.3 A remark on the ideal free dispersal strategy

The growth rate r_P is now a piecewise-constant function. This could appear as a difficulty, as the ideal free dispersal strategy $\nabla \cdot (r_P \nabla(P/r_P))$ is *a priori* defined in [16] for r_P at least of class $\mathcal{C}^2$. For piecewise-constant r_P, an alternative ideal free dispersal strategy with interface conditions is suggested in [46]. However, when the space is discretized, even regular functions become piecewise-constant. In fact, it can be verified that an ideal free dispersal strategy of the form $\nabla \cdot (r_P \nabla(P/r_P))$ corresponds, after spatial discretization, to the interface conditions in [46]. Note also that the potential overflow issues can be overcome with a change of variable $\tilde{P} = P/r_P$.

2.6.4 Snapshots of the evolution

Using the package animation https://pypi.org/project/animation/, we produce a video of the simulation (figures 2.1, 2.2).

At the end of the simulation, the total number of healthy beets is 1013554 out of 1016470. In the video, we can see that a very small portion of the beets are infected by aphids in their starting patches, while the aphids are quickly eradicated by the predators.

2.6.5 The optimal control problem

In the numerical simulations, we will refer to certain positionning of the populations as defined in the following.

Definition 2.6.1.
- *"Frequency of the refuges": the integer n, where $R = \mathbf{1}_{A_n}$, i.e n^2 squares uniformly distributed in the field, whose areas sum up to $\mathcal{A}$.*
- *"Random patches": the 3 patches one can see in the snapshot of the video at the initial condition.*
- *"Centered patch" = the frequency 1 square.*

As we explained before, there is no monotonicity of the harvest with respect to $\lambda_1(\mathcal{L}_{V_s})$. To illustrate, we use the fact that increasing the frequency of the refuges increases $\lambda_1(\mathcal{L}_{V_s})$, as shown in [17]. Figure 2.3 displays the harvest $\int_\Omega H - I_\infty$ as a function of the frequency of the refuges, with the same set of parameters and initial conditions as before. Here, the frequencies 8 and 16 are clearly worse than the lower frequencies. The phenomenon can be even clearer: to obtain Figure 2.4, we use a single centered patch as the initial condition for V, at the same location as the refuges at frequency 1. Obviously, in this case, the best strategy is to use the refuges of frequency 1, in order to place the predators exactly where the aphids are at the beginning of the simulation. However, when V_0 is homogeneous in space, as seen in Figure 2.5, the harvest seems to be increasing with $\lambda_1(\mathcal{L}_{V_s})$, which could be an interesting perspective of this paper.

To illustrate the important effect of the initial conditions, we numerically study the optimal quantity of refuges. Say R is a real parameter in $[0,1]$. r_V, r_P and H are now homogeneous in space, and the problem is to find $R_{\text{opt}} \in [0,1)$ to maximize the quantity $\int_\Omega H - I_\infty$. In Figure 2.6 and 2.7, we took the same set of parameters as in the supplementary materials, with the same initial conditions as in the numerical framework except that we took a uniform initial condition on V. In Figure 2.6, $V_{i,0}$ is quite small, and the simulation hints that it is best not to put any resources in the field: $R_{\text{opt}} = 0$. We can interpret this by saying that the predators handle the small quantity of aphids well enough so that they do not need more resources to eradicate the aphid population in a very short amount of time. On the contrary, in Figure 2.7, $V_{i,0}$ is large, and the predators actually need resources for some beets to be saved: R_{opt} is at a great distance from 0. Depending on the initial conditions, it seems that R_{opt} can be located at any point of $[0,1)$.

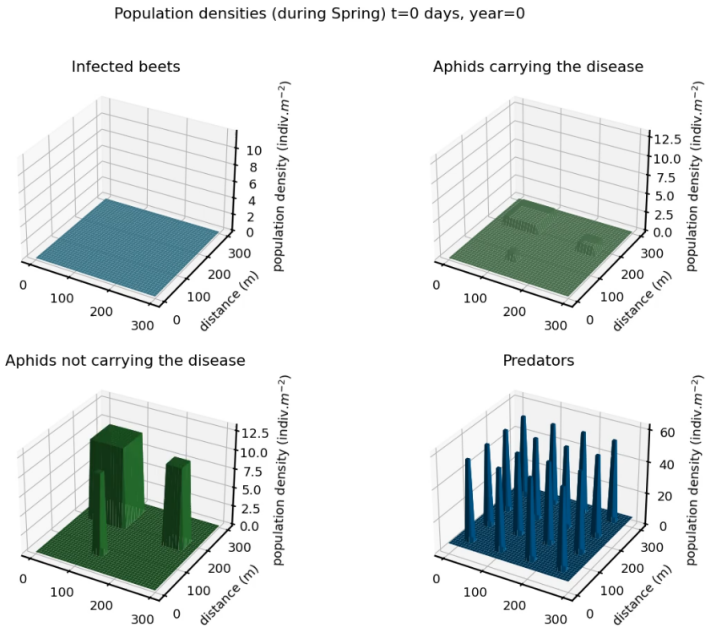

Figure 2.1: Video of the numerical simulation at the initial condition

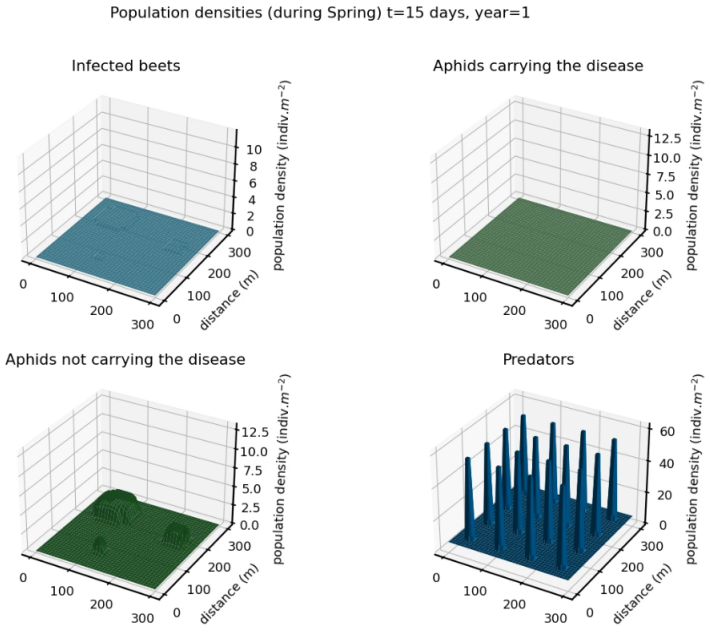

Figure 2.2: Video of the numerical simulation at 15 days

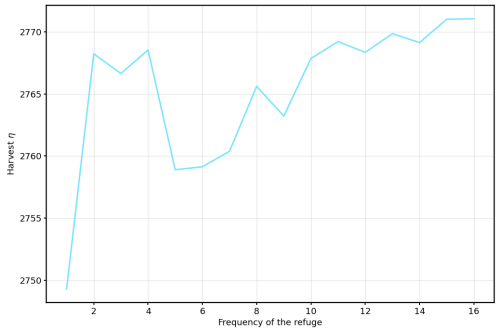

Figure 2.3: Healthy beets in function of the frequency of the refuges, with the initial condition of the aphids V_0 in random patches

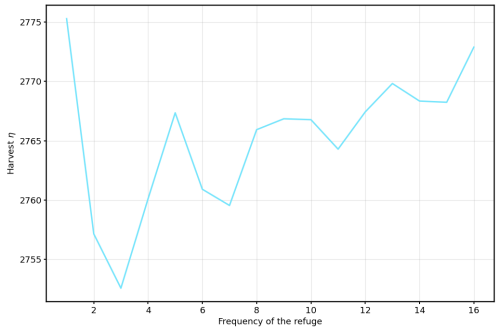

Figure 2.4: Healthy beets in function of the frequency of the refuges, with the initial condition of the aphids V_0 in a centered patch

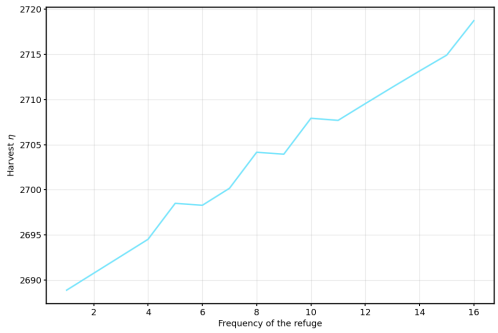

Figure 2.5: Healthy beets in function of the frequency of the refuges, with the initial condition of the aphids V_0 homogeneous in space

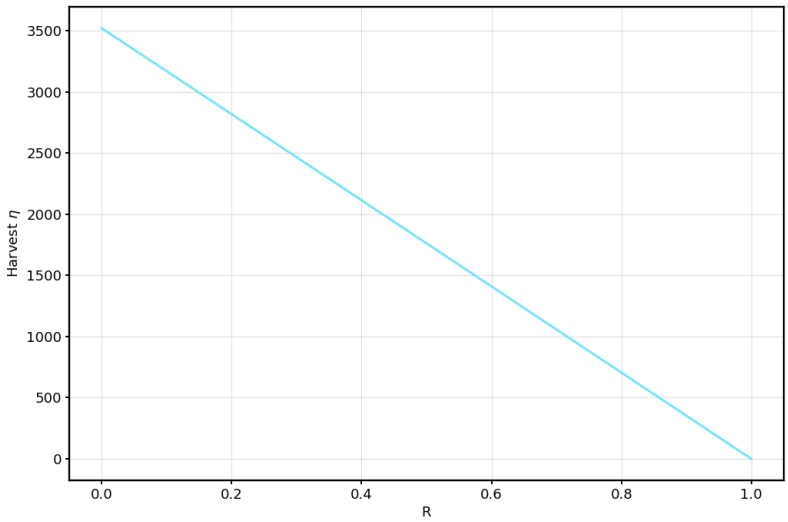

Figure 2.6: Healthy beets in function of the quantity of resources, with the initial condition of the infected aphids $V_{i,0} = \dfrac{r_V}{100 s_V}$ and the refuges R both homogeneous in space

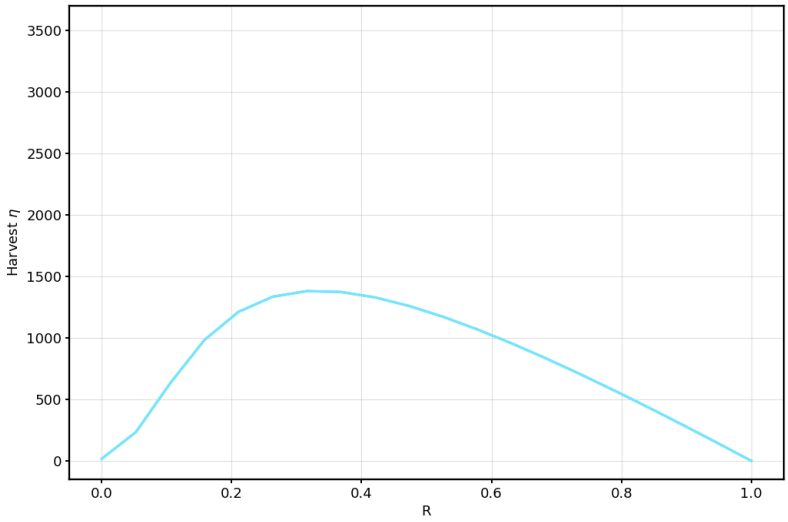

Figure 2.7: Healthy beets in function of the quantity of resources, with the initial condition of the infected aphids $V_{i,0} = \dfrac{2r_V}{s_V}$ and the refuges R both homogeneous in space

Supplementary Materials for chapter 2

2.7 Discretization of the system using finite differences

Let $N \in \mathbb{N}^*$ be the number of time stamps, and $J \in \mathbb{N}^*$ the number of space stamps. The discretized domain is a $J \times J$ square.

Let $T > 0$, $\mathrm{d}t := \dfrac{T}{N}$, $L > 0$, and $\mathrm{d}x := \dfrac{L}{J}$.

From

$$\begin{cases} \partial_t I &= \beta_{VH}(H-I)V_i \\ \partial_t V_i &= \sigma_V \Delta V_i + \beta_{HV} I V_s - \alpha V_i - d_V V_i - s_V(V_s+V_i)V_i - hPV_i \\ \partial_t V_s &= \sigma_V \Delta V_s - \beta_{HV} I V_s + \alpha V_i - d_V V_s - s_V(V_s+V_i)V_s - hPV_s \\ & \quad + b_V(V_s+V_i) \\ \partial_t P &= \sigma_P \nabla \cdot \left(r_P \nabla \left(\frac{P}{r_P} \right) \right) + \gamma h (V_s+V_i)P + r_P P - s_P P^2, \end{cases}$$

we deduce

$$\frac{I_{i,j}^{n+1} - I_{i,j}^n}{\mathrm{d}t} = f(I_{i,j}^n, (V_i)_{i,j}^n),$$

$$\begin{aligned} &\frac{(V_i)_{i,j}^{n+1} - (V_i)_{i,j}^n}{\mathrm{d}t} \\ &-\sigma_V \frac{(V_i)_{i-1,j}^{n+1} + (V_i)_{i,j-1}^{n+1} - 4(V_i)_{i,j}^{n+1} + (V_i)_{i+1,j}^{n+1} + (V_i)_{i,j+1}^{n+1}}{\mathrm{d}x^2} \\ &= g(I_{i,j}^n, (V_i)_{i,j}^n, (V_s)_{i,j}^n, P_{i,j}^n), \end{aligned}$$

and

$$\begin{aligned} &\frac{(V_s)_{i,j}^{n+1} - (V_s)_{i,j}^n}{\mathrm{d}t} \\ &-\sigma_V \frac{(V_s)_{i-1,j}^{n+1} + (V_s)_{i,j-1}^{n+1} - 4(V_s)_{i,j}^{n+1} + (V_s)_{i+1,j}^{n+1} + (V_s)_{i,j+1}^{n+1}}{\mathrm{d}x^2} \\ &= h(I_{i,j}^n, (V_i)_{i,j}^n, (V_s)_{i,j}^n, P_{i,j}^n), \end{aligned}$$

for all $n \in \{0, ..., N-2\}$, $i, j \in \{1, ..., J-2\}$, where

$$\begin{aligned} f(I, V_i) &= \beta_{VH}(H-I)V_i \\ g(I, V_i, V_s, P) &= \beta_{HV} I V_s - \alpha V_i - d_V V_i - s_V(V_s+V_i)V_i - hPV_i \\ h(I, V_i, V_s, P) &= -\beta_{HV} I V_s + \alpha V_i - d_V V_s - s_V(V_s+V_i)V_s - hPV_s \\ & \quad + b_V(V_s+V_i). \end{aligned}$$

The Neumann boundary conditions are:

$$\begin{array}{rclrcl} (V_i)^n_{-1,j} &=& (V_i)^n_{0,j}\ \forall j & (V_s)^n_{-1,j} &=& (V_s)^n_{0,j}\ \forall j \\ (V_i)^n_{i,-1} &=& (V_i)^n_{i,0}\ \forall i & (V_s)^n_{i,-1} &=& (V_s)^n_{i,0}\ \forall i \\ (V_i)^n_{J,j} &=& (V_i)^n_{J-1,j}\ \forall j & (V_s)^n_{J,j} &=& (V_s)^n_{J-1,j}\ \forall j \\ (V_i)^n_{i,J} &=& (V_i)^n_{i,J-1}\ \forall i & (V_s)^n_{i,J} &=& (V_s)^n_{i,J-1}\ \forall i \end{array}$$

which yields the following scheme:

$$\begin{cases} I^{n+1} = I^n + \mathrm{d}t\, f(I^n, V_i^n) \\ (Id_{J^2} - \sigma_V \dfrac{\mathrm{d}t}{\mathrm{d}x^2} A) V_i^{n+1} = V_i^n + \mathrm{d}t\, g(I^n, V_i^n, V_s^n, P^n) \\ (Id_{J^2} - \sigma_V \dfrac{\mathrm{d}t}{\mathrm{d}x^2} A) V_s^{n+1} = V_s^n + \mathrm{d}t\, h(I^n, V_i^n, V_s^n, P^n) \end{cases}$$

where

$$A = \begin{pmatrix} A_1 & I_J & 0 & 0 & 0 & \cdots & 0 \\ I_J & A_2 & I_J & 0 & 0 & \cdots & 0 \\ 0 & I_J & A_3 & I_J & 0 & \cdots & 0 \\ \vdots & 0 & \ddots & \ddots & \ddots & 0 & \vdots \\ 0 & \cdots & 0 & I_J & A_{J-2} & I_J & 0 \\ 0 & \cdots & 0 & 0 & I_J & A_{J-1} & I_J \\ 0 & \cdots & 0 & 0 & 0 & I_J & A_J \end{pmatrix} \in \mathcal{M}_{J^2}(\mathbb{R})$$

with

$$A_1 = A_J = \begin{pmatrix} -2 & 1 & 0 & 0 & 0 & \cdots & 0 \\ 1 & -3 & 1 & 0 & 0 & \cdots & 0 \\ 0 & 1 & -3 & 1 & 0 & \cdots & 0 \\ \vdots & 0 & \ddots & \ddots & \ddots & 0 & \vdots \\ 0 & \cdots & 0 & 1 & -3 & 1 & 0 \\ 0 & \cdots & 0 & 0 & 1 & -3 & 1 \\ 0 & \cdots & 0 & 0 & 0 & 1 & -2 \end{pmatrix} \in \mathcal{M}_J(\mathbb{R})$$

and

$$A_k = \begin{pmatrix} -3 & 1 & 0 & 0 & 0 & \cdots & 0 \\ 1 & -4 & 1 & 0 & 0 & \cdots & 0 \\ 0 & 1 & -4 & 1 & 0 & \cdots & 0 \\ \vdots & 0 & \ddots & \ddots & \ddots & 0 & \vdots \\ 0 & \cdots & 0 & 1 & -4 & 1 & 0 \\ 0 & \cdots & 0 & 0 & 1 & -4 & 1 \\ 0 & \cdots & 0 & 0 & 0 & 1 & -3 \end{pmatrix} \in \mathcal{M}_J(\mathbb{R})$$

$\forall k \in \{2, ..., J-1\}$.

Denote $\tilde{P} = \dfrac{P}{r_P}$. The last equation becomes

$$\partial_t \tilde{P} - \sigma_P \left(\Delta \tilde{P} + \nabla \tilde{P} \cdot \nabla (\ln r_P) \right) = u(V_i, V_s, \tilde{P})$$

(we recall that r_P is independant of time), where $u(V_i, V_s, \tilde{P}) = \gamma h(V_s + V_i)\tilde{P} + r_P(\tilde{P} - s_P\tilde{P}^2)$, with Neumann boundary conditions:

$$\frac{\partial \tilde{P}}{\partial n} = 0 \text{ (we suppose that } \frac{\partial r_P}{\partial n} = 0).$$

We need a way to discretize

$$\nabla \tilde{P} \cdot \nabla \ln(r_P) = \frac{\partial \tilde{P}}{\partial x}\frac{\partial \ln(r_P)}{\partial x} + \frac{\partial \tilde{P}}{\partial y}\frac{\partial \ln(r_P)}{\partial y}.$$

We define 2 matrices:

$$B\text{diff}x = \begin{pmatrix} 0 & 0 & 0 & 0 & 0 & \cdots & 0 \\ -\frac{1}{2}I_J & 0 & \frac{1}{2}I_J & 0 & 0 & \cdots & 0 \\ 0 & -\frac{1}{2}I_J & 0 & \frac{1}{2}I_J & 0 & \cdots & 0 \\ \vdots & 0 & \ddots & \ddots & \ddots & 0 & \vdots \\ 0 & \cdots & 0 & -\frac{1}{2}I_J & 0 & \frac{1}{2}I_J & 0 \\ 0 & \cdots & 0 & 0 & -\frac{1}{2}I_J & 0 & \frac{1}{2}I_J \\ 0 & \cdots & 0 & 0 & 0 & 0 & 0 \end{pmatrix} \in \mathcal{M}_{J^2}(\mathbb{R}),$$

$$B\text{diff}y = \begin{pmatrix} B_1 & 0 & 0 & 0 & 0 & \cdots & 0 \\ 0 & B_2 & 0 & 0 & 0 & \cdots & 0 \\ 0 & 0 & B_3 & 0 & 0 & \cdots & 0 \\ \vdots & 0 & 0 & \ddots & 0 & 0 & \vdots \\ 0 & \cdots & 0 & 0 & B_{J-2} & 0 & 0 \\ 0 & \cdots & 0 & 0 & 0 & B_{J-1} & 0 \\ 0 & \cdots & 0 & 0 & 0 & 0 & B_J \end{pmatrix} \in \mathcal{M}_{J^2}(\mathbb{R}).$$

with

$$B_k = \begin{pmatrix} 0 & 0 & 0 & 0 & 0 & \cdots & 0 \\ -\frac{1}{2} & 0 & \frac{1}{2} & 0 & 0 & \cdots & 0 \\ 0 & -\frac{1}{2} & 0 & \frac{1}{2} & 0 & \cdots & 0 \\ \vdots & 0 & \ddots & \ddots & \ddots & 0 & \vdots \\ 0 & \cdots & 0 & -\frac{1}{2} & 0 & \frac{1}{2} & 0 \\ 0 & \cdots & 0 & 0 & -\frac{1}{2} & 0 & \frac{1}{2} \\ 0 & \cdots & 0 & 0 & 0 & 0 & 0 \end{pmatrix} \in \mathcal{M}_J(\mathbb{R})$$

for all $k \in \{1, ..., J\}$,

so that for $y = \begin{pmatrix} y_{0,0} \\ \vdots \\ y_{0,J-1} \\ y_{1,0} \\ \vdots \\ y_{1,J-1} \\ \vdots \\ y_{J-1,J-1} \end{pmatrix} \in \mathcal{M}_{J^2,1}(\mathbb{R})$,

$$B\text{diff}x.y = \frac{1}{2}\begin{pmatrix} 0 \\ \vdots \\ 0 \\ y_{1,0} - y_{0,0} \\ \vdots \\ y_{1,J-1} - y_{0,J-1} \\ \vdots \\ y_{J-1,J-1} - y_{J-2,J-1} \\ 0 \\ \vdots \\ 0 \end{pmatrix} = \frac{1}{2}\begin{pmatrix} 0 \\ y_{i+1,j} - y_{i-1,j} \\ 0 \end{pmatrix}_{\substack{1 \leq i \leq J-2 \\ 0 \leq j \leq J-1}},$$

and

$$B\text{diff}y.y = \frac{1}{2}\begin{pmatrix} 0 \\ y_{0,1} - y_{0,0} \\ \vdots \\ y_{0,J-1} - y_{0,J-2} \\ 0 \\ \vdots \\ 0 \\ y_{J-1,1} - y_{J-1,0} \\ \vdots \\ y_{J-1,J-1} - y_{J-1,J-2} \\ 0 \end{pmatrix} = \frac{1}{2}\begin{pmatrix} 0 \\ y_{i,j+1} - y_{i,j-1} \\ 0 \end{pmatrix}_{\substack{0 \leq i \leq J-1 \\ 1 \leq j \leq J-2}}.$$

$B\text{diff}x$ (respectively $B\text{diff}y$) is a discretization of $\dfrac{\partial}{\partial x}$ (respectively $\dfrac{\partial}{\partial y}$).
For $r_P \in \mathcal{M}_{J^2,1}(\mathbb{R})$, we then define the matrix

$$B\text{diff}r = B\text{diff}x.\text{diag}(B\text{diff}x.\ln(r_P)) + B\text{diff}y.\text{diag}(B\text{diff}y.\ln(r_P)),$$

so that for $\tilde{P} \in \mathcal{M}_{J^2,1}(\mathbb{R})$,

$$Bdiffr.\tilde{P} = \frac{1}{2}\begin{pmatrix} 0 \\ (\tilde{P}_{i+1,j} - \tilde{P}_{i-1,j})(\ln(r_P)_{i+1,j} - \ln(r_P)_{i-1,j}) \\ 0 \end{pmatrix}_{\substack{1\le i\le J-2 \\ 0\le j\le J-1}}$$
$$+\frac{1}{2}\begin{pmatrix} 0 \\ (\tilde{P}_{i,j+1} - \tilde{P}_{i,j-1})(\ln(r_P)_{i,j+1} - \ln(r_P)_{i,j-1}) \\ 0 \end{pmatrix}_{\substack{0\le i\le J-1 \\ 1\le j\le J-2}},$$

which (by multiplying by $\frac{1}{dx^2}$) is the discretization of $\nabla P \cdot \nabla \ln(r_P)$ we use.
Hence, our scheme is:

$$\left(I_{J^2} - \sigma_P \frac{dt}{dx^2}(A + Bdiffr)\right)\tilde{P}^{n+1} = \tilde{P}^n + dt\, u(V_i^n, V_s^n, \tilde{P}^n),$$

and we come back to our original variable $P = r_P\tilde{P}$.

2.8 Computation of the parameters

2.8.1 Formulas used to convert field data into parameter values

- For the diffusion rates, $\sigma = \frac{d(t)^2}{4t}$, where $d(t)$ is the average displacement during a time t.
  Unit : $m^2.\text{day}^{-1}$.

- For the Malthusian growth rates, $r = \frac{\ln(N)}{\tau}$, where N is the number of offsprings of an individual during its lifetime τ (with abundant resources).
  Unit : day^{-1}.
  For the birth rates, $b = \ln(1 + N)$, where N is the number of offsprings of an individual per day.
  Unit : day^{-1}.

- For the saturation rates, $s = \frac{r}{N}\Sigma$, where N is the average number of individuals in an overgrown field of area Σ.
  Unit : $m^2.\text{individual}^{-1}.\text{day}^{-1}$.

- For the predation rate h : let N_V be the average number of killed prey by a population of predators $P = \frac{N_P}{\sigma_P T}$ over a time T, on a surface $\sigma_P T$, with a total number of prey equal to $\frac{r_V}{s_V}\sigma_P T$. We can approximate the equation and get $V' = -hPV$, therefore $V(t) = \frac{r_V}{s_V}\sigma_P T e^{-hPt}$. We deduce $h = -\frac{\sigma_P}{N_P}\ln(1 - \frac{N_V s_V}{r_V \sigma_P T})$. Unit : $m^2.\text{individual}^{-1}.\text{day}^{-1}$.

- For the "efficiency of predation" rate γ : let N_V be the number of prey needed for the reproduction of one predator egg, during a generation time T. We can approximate the equation and get $P' = \gamma hVP$, therefore $P(t) = \frac{r_P}{s_P}e^{\gamma hVt}$. We deduce $\gamma = \frac{s_P \ln(2)}{hN_V r_P T}$.

Parameter	Value	Unit	Reference
H	11.7647	m^{-2}	Fields of Laon
σ_V	1	$m^2.day^{-1}$	[55]
σ_P	10	$m^2.day^{-1}$	[72, 73]
β_{VH}	0.0379	$m^2.individual^{-1}.day^{-1}$	[9]
β_{HV}	0.003	$m^2.individual^{-1}.day^{-1}$	ITB
α	0.0909	day^{-1}	[10]
b_V	1.6	day^{-1}	[9, 10, 41]
d_V	1.47	day^{-1}	[10, 41]
s_V	0.0011	$m^2.individual^{-1}.day^{-1}$	[61], ITB
r_R	0.0562	day^{-1}	[36]
r_F	0.00562	day^{-1}	[36]
s_P	0.001	$m^2.individual^{-1}.day^{-1}$	[11]
h	0.0421	$m^2.individual^{-1}.day^{-1}$	[21]
γ	0.0008	No unit	[75]

Table 2.1: Parameter values used for the numerical simulation

γ is without unit.

- For the recovery rate, $\alpha = \frac{1}{\tau}$, where τ is the average duration of an infection.

  Unit : day^{-1}.

- For the transmission rates β : let N_B be the average number of contaminated beets by a population of aphids $V = \frac{N_V}{\sigma_V T}$ over a time T, on a surface $\sigma_V T$, with a total number of beets equal to $H\sigma_V T$. We have $I' = \beta_{VH}(H - I)V$, therefore $I(t) = H(1 - e^{-\beta_{VH} V t})$. We deduce $\beta_{VH} = -\frac{\sigma_V}{N_V} \ln(1 - \frac{N_B}{H\sigma_V T})$.

  The same reasonning yields $\beta_{HV} = -\frac{\sigma_V}{N_B} \ln(1 - \frac{N_V s_V}{\sigma_V T r_V})$.

  Unit : $m^2.individual^{-1}.day^{-1}$.

2.8.2 Data used and computation

We use the parameter values indicated on Table 2.8.2.

- H : total beet population density ($H = I + S$).
  Value used : 11.7647 m^{-2}.
  In the fields of Laon, beets are planted in rows, with a 17 cm space between each beet. Two rows are 50 cm apart. Hence the value of $H = \frac{100}{17} \cdot \frac{100}{50} \approx 11.7647\ m^{-2}$.

- σ_V, σ_P : dispersal/diffusion rate in space.
  Value used : $\sigma_V = 1$, and $\sigma_P = 10\ m^2.day^{-1}$.
  Finding the value of the dispersal rate of the aphids is difficult. The apterous aphids actually do not move on their own once they are on a beet. They are only transported by

the wind or the rain. If the wind and rain are not sufficient, they develop wings to avoid saturation. This complex mechanism does not ease the task of modelizing their diffusion with a Brownian motion.

According to [55], "apterous (wingless) aphids move from plant to plant very small distances, at a speed of around 5–20 cm min^{-1}". σ_V should be around $\frac{5.3^2}{4} \approx 7\ \text{cm}^2.\text{min}^{-1} \approx 1\ m^2.\text{day}^{-1}$.

According to [72], the diffusion rate σ_P has an order of 20 $m^2.\text{day}^{-1}$. According to [73], σ_P has an order of 1 $m^2.\text{day}^{-1}$. For obvious reasons, we choose the diffusion rate of the predators to be 10 times bigger than the one of the aphids.

- β_{VH}, β_{HV} : transmission rate of the disease.

  Value used : $\beta_{VH} = 0.0379$ and $\beta_{HV} = 0.003\ m^2.\text{individual}^{-1}.\text{day}^{-1}$.

  According to [9], a viruliferous aphid can, directly and via its offspring, contaminate 600 beets. We take an average of 300 beets. For a period of 30 days, an aphid gives birth to roughly 50 aphids (see [10]).

  $\beta_{VH} = -\frac{\sigma_V}{50} \ln(1 - \frac{300}{30H\sigma_V}) \approx 0.0379\ m^2.\text{individual}^{-1}.\text{day}^{-1}$.

  According to Ghislain Malatesta, from the Institut Technique de la Betterave, the proportion of contaminated aphids in the field is around 1% and 2%. Having fixed all of our parameters, and running the simulations, we get approximately this proportion (with no predators) by taking

  $\beta_{HV} = 0.003\ m^2.\text{individual}^{-1}.\text{day}^{-1}$.

- α : recovery rate.

  Value used : $0.0909\ \text{day}^{-1}$.

  According to [10], there are 4 types of viruses and their recovery time varies from 24 hours (non-persistent) to several weeks (persistent). If we want to be very accurate, we should consider 2 viruses, one persistent and one non-persistent, but this would pointlessly complexify the model. A sensitivity analysis shows that the parameter α has a negligible impact on the number of contaminated beets at the end of the spring. We choose to take an α between the 2 possible extreme values ($1/1\ \text{days}^{-1}$ and $1/21\ \text{days}^{-1}$).

  $\alpha = \frac{1}{(1+21)/2} \approx 0.0909\ \text{day}^{-1}$.

- b_V, d_V : birth and death rates of the aphids, so that the Malthusian growth rate r_V is equal to $b_V - d_V$.

  Value used : $b_V = 1.6$ and $d_V = 1.47\ \text{day}^{-1}$.

  According to [9], an aphid gives birth each day to 4 new aphids, so b_V should be equal to $\ln(5) = 1.6$. According to [10], an adult aphid gives birth to 50 larvas on average during his life. With 30 days as a characteristic time of life, $r_V = \ln(50)/30 \approx 0.13$.

  According to [41], r_V should be between 0.11 and $0.15\ \text{day}^{-1}$.

- s_V : saturation rate of the aphids.

  Value used : $0.0011\ m^2.\text{individual}^{-1}.\text{day}^{-1}$.

According to [61], "During 3rd week of March, a peak aphid density of 4.22 aphid/leaf was recorded".

With 24 leaves per beet ([24]), we obtain 101.28 aphids per beet, or $101.28H \approx 1191.5$ aphids.m^{-2}. However, this quantity corresponds better to the peak density of aphids in a confined space. According to Ghislain Malatesta from the Institut Technique de la Betterave, in a large field, we find a maximum of 10 aphids per beet, or $10H \approx 117.647$ aphids.m^{-2}.

$s_V = (r_V/N)\Sigma = \dfrac{0.13}{117.647} \approx 0.0011 m^2.\text{individual}^{-1}.\text{day}^{-1}$.

- b_P, d_P : birth and death rates of the predators, so that the Malthusian growth rate r_P is equal to $b_P - d_P$.

  Value used : $b_P = 0.1562$ and $d_P = 0.1$ day^{-1}.

  According to [36] (Table 1), the average fecundity (for Hippodamia variegata, per individual) is 89.9 eggs, on an average life time of 80 days. r_P should then be equal to $\ln(89.9)/80 \approx 0,0562$ day^{-1}.

  We assume that this value is valid in the refuges, where the predators find food in abundance. In the field, where there should be less food available (except for aphids, which are not taken into account in the value of r_P), we divide this value by 10 : $r_R = 0,0562$ and $r_F = 0,00562$, so that $r_P = (0,0562 - 0,00562)\mathbf{1}_{A_n} + 0,00562$.

- s_P : saturation rate of predators.

  Value used : 0.001 m^2.individual^{-1}.day^{-1}.

  According to [11], we find on average 54 adult Chnootriba similis per square meter. Then $s_P = (r_P/N)\Sigma = \dfrac{0.0562}{54} \approx 0.001\ m^2.\text{individual}^{-1}.\text{day}^{-1}$.

- h : predation rate.

  Value used : 0.0421 m^2.individual^{-1}.day^{-1}.

  According to [21], ladybugs eat until 50 aphids a day. It is important to note that this value corresponds to the maximum amount of aphids a ladybug can eat when the aphids are in abundance. Therefore, we use, for the computation, $s_V = \dfrac{0.13}{1191.5} \approx 0.0001$, which is the value of s_V in a confined space, instead of 0.0011.

  $h = -\dfrac{\sigma_P}{1}\ln(1 - \dfrac{50 s_V}{r_V \sigma_P}) = 0.0421\ m^2.\text{individual}^{-1}.\text{day}^{-1}$.

- γ : Efficiency of predation on predators births.

  Value used : 0.0008.

  According to [75], "L. biplagiata needs 10.4 individuals of 3-d-old A. gossypii for the reproduction of one predator egg". For a generation time of $T = 36,2$ days (same source), we have

  $\gamma = \dfrac{s_P \ln(2)}{10.4 h r_P T} \approx 0.0008$.

2.9 Computation in a one dimensional case

Let $\Omega = [-b, b]$ and $A = [-d, d]$ with $0 < d < b$. Suppose that $r_P = (r_R - r_F)\mathbf{1}_A + r_F$ and $r_V = (r_{V,R} - r_{V,F})\mathbf{1}_A + r_{V,F}$

We are going to solve

$$(-\sigma_V \Delta - r_V + h\frac{r_P}{s_P})\varphi_1 = \lambda_1(A)\varphi_1$$

with the following conditions : $\varphi_1 > 0$ even, $\varphi_1'(0) = \varphi_1'(b) = 0$, and $\varphi \in \mathcal{C}^1(\Omega)$.

Denote $\mu := \dfrac{h}{s_P}(r_R - r_F) - (r_{V,R} - r_{V,F})$, and assume for simplicity that $\mu > 0$.

Denote $\tilde{r_V} := r_{V,F} - \dfrac{h}{s_P} r_F$.

We are now solving

$$\begin{cases} \varphi_1'' = -\dfrac{\lambda_1(A) + \tilde{r_V} - \mu}{\sigma_V}\varphi_1 & \text{on } [0, d] \\ \varphi_1'' = -\dfrac{\lambda_1(A) + \tilde{r_V}}{\sigma_V}\varphi_1 & \text{on } [d, b]. \end{cases}$$

Notice that $-\tilde{r_V} \leq -\tilde{r_V} + \mu\mathbf{1}_A = -r_V + h\dfrac{r_P}{s_P} \leq -\tilde{r_V} + \mu$, hence $\lambda_1(A) \in [-\tilde{r_V}, -\tilde{r_V} + \mu]$.

Denoting $\omega_\mu = \sqrt{-\dfrac{\lambda_1(A) + \tilde{r_V} - \mu}{\sigma_V}}$ and $\omega = \sqrt{\dfrac{\lambda_1(A) + \tilde{r_V}}{\sigma_V}}$, we are thus looking for solutions of the form

$$\varphi_1(x) = (\alpha \cosh(\omega_\mu x) + \beta \sinh(\omega_\mu x))\mathbf{1}_{[0,d)}(x) + \tilde{\alpha}\cos(\omega x + \theta)\mathbf{1}_{[d,b]}(x).$$

Immediately, $\varphi_1'(0) = 0$ gives $\beta = 0$.
$\varphi_1'(b) = 0$ gives $\theta = k\pi - \omega b$ for any $k \in \mathbb{Z}$.
For φ_1 to be $\mathcal{C}^1$, we need to have :

$$\begin{cases} \alpha\cosh(\omega_\mu d) & = \tilde{\alpha}\cos(\omega(d-b) + k\pi) \text{ (continuity of } \varphi_1), \\ \omega_\mu \alpha \sinh(\omega_\mu d) & = -\omega\tilde{\alpha}\sin(\omega(d-b) + k\pi) \text{ (continuity of } \varphi_1') \end{cases}$$

therefore $\alpha = \dfrac{\cos(\omega(d-b) + k\pi)}{\cosh(\omega_\mu d)}\tilde{\alpha}$ and

$$\omega_\mu \frac{\cos(\omega(d-b) + k\pi)}{\cosh(\omega_\mu d)} \sinh(\omega_\mu d) = -\omega\sin(\omega(d-b) + k\pi).$$

If $\cos(\omega(d-b) + k\pi) = 0$, we then would have $\sin(\omega(d-b) + k\pi) = 0$, which is excluded. The last equality can thus be written :

$$\omega_\mu \tanh(\omega_\mu d) = -\omega\tan(\omega(d-b) + k\pi) \text{ for any } k \in \mathbb{Z},$$

hence

$$\omega_\mu \tanh(\omega_\mu d) = \omega\tan(\omega(b-d)),$$

which gives us a unique value of $\lambda_1(A)$: the only λ that nullifies the decreasing hence bijective function

$$\begin{cases} [-r\tilde{V}, -r\tilde{V}+\mu] & \to & \mathbb{R} \\ \lambda & \mapsto & \omega_\mu \tanh(\omega_\mu d) - \omega \tan(\omega(b-d)) \end{cases}$$

(we abusively noted $\omega_\mu = \sqrt{-\dfrac{\lambda + r\tilde{V} - \mu}{\sigma_V}}$ and $\omega = \sqrt{\dfrac{\lambda + r\tilde{V}}{\sigma_V}}$).

So far,

$$\begin{aligned} &\varphi_1(x) \\ &= \tilde{\alpha}\left(\frac{\cos(\omega(d-b)+k\pi)}{\cosh(\omega_\mu d)}\cosh(\omega_\mu x)\mathbf{1}_{[0,d)}(x) + \cos(\omega(x-b)+k\pi)\mathbf{1}_{[d,b]}(x)\right). \end{aligned}$$

The possible values of k only change the sign of φ_1, and we can then choose $\tilde{\alpha} \in \{-1, 1\}$ so that $\varphi_1 > 0$ (notice that $\cos(\omega(d-b)+k\pi) \neq 0$). It follows :

$$\varphi_1(x) = \pm\left(\frac{\cos(\omega(d-b))}{\cosh(\omega_\mu d)}\cosh(\omega_\mu x)\mathbf{1}_{[0,d)}(x) + \cos(\omega(x-b))\mathbf{1}_{[d,b]}(x)\right) > 0.$$

Because φ_1 is even, we finally get :

$$\begin{aligned} \pm\varphi_1(x) = \quad & \cos(\omega(x+b))\mathbf{1}_{[-b,-d)}(x) \\ & + \frac{\cos(\omega(d-b))}{\cosh(\omega_\mu d)}\cosh(\omega_\mu x)\mathbf{1}_{[-d,0)}(x) \\ & + \frac{\cos(\omega(d-b))}{\cosh(\omega_\mu d)}\cosh(\omega_\mu x)\mathbf{1}_{[0,d)}(x) \\ & + \cos(\omega(x-b))\mathbf{1}_{[d,b]}(x). \end{aligned}$$

Let us now suppose that $A := A_n$ has n connected components (and still has the same volume $2d$), evenly distributed on $[-b, b]$:

$$A_n = \bigcup_{k=0}^{n-1}\left[-b + (2k+1)\frac{b}{n} - \frac{d}{n}, -b + (2k+1)\frac{b}{n} + \frac{d}{n}\right] =: \bigcup_{k=0}^{n-1} I_k.$$

We are going to call $(\lambda_1(n, \sigma_V), \varphi_1(n, \sigma_V))$ the unique couple (λ, φ) with $\varphi > 0$ (by Krein-Rutman, see [66]) that verifies

$$\begin{aligned} & (-\sigma_V\Delta - r\tilde{V} + \mu\mathbf{1}_{A_n})\varphi = \lambda\varphi, \\ \text{i.e} \qquad & \Delta\varphi = -\frac{\lambda + r\tilde{V} - \mu\mathbf{1}_{A_n}}{\sigma_V}\varphi. \end{aligned}$$

With this notation, $\varphi_1(1, n^2\sigma_V)$ is a solution of

$$\varphi_1''(1, n^2\sigma_V) = -\frac{\lambda_1(1, n^2\sigma_V) + r\tilde{V} - \mu\mathbf{1}_{A_1}}{n^2\sigma_V}\varphi_1(1, n^2\sigma_V),$$

which is our previously computed φ_1 with $\dfrac{\omega}{n}$, $\dfrac{\omega_\mu}{n}$ instead of ω, ω_μ.

We define

$$\psi(x) := \sum_{k=0}^{n-1}\varphi_1(1, n^2\sigma_V, x - 2kb)\mathbf{1}_{[(2k-1)b,(2k+1)b)}(x)$$

the extension by periodicity on $[-b,(2n-1)b]$ of $\varphi_1(1,n^2\sigma_V)$, and

$$\begin{aligned}
\varphi(x) &:= \psi(nx+(n-1)b) \\
&= \sum_{k=0}^{n-1} \varphi_1(1,n^2\sigma_V, nx+(n-2k-1)b)\mathbf{1}_{[-b+k\frac{2b}{n},-b+(k+1)\frac{2b}{n})}(x) \\
&= \pm\sum_{k=0}^{n-1}\Big[\cos(\omega(x+b-k\tfrac{2b}{n}))\mathbf{1}_{[-b+k\frac{2b}{n},-b+(2k+1)\frac{b}{n}-\frac{d}{n})}(x) \\
&\quad + \frac{\cos(\frac{\omega}{n}(d-b))}{\cosh(\frac{\omega_\mu}{n}d)}\cosh(\omega_\mu(x+b-(2k+1)\tfrac{b}{n}))\mathbf{1}_{I_k}(x) \\
&\quad + \cos(\omega(x+b-(k+1)\tfrac{2b}{n}))\mathbf{1}_{(-b+(2k+1)\frac{b}{n}+\frac{d}{n},-b+(k+1)\frac{2b}{n})}(x)\Big]
\end{aligned}$$

for $x\in[-b,b]$. By construction, $\varphi>0$.
For all $x\in\overset{\circ}{I}_k$,

$$\begin{aligned}
\varphi''(x) &= n^2\psi''(nx+(n-1)b) \\
&= -n^2\frac{\lambda_1(1,n^2\sigma_V)+r\tilde{}_V-\mu}{n^2\sigma_V}\psi(nx+(n-1)b) \\
&= -\frac{\lambda_1(1,n^2\sigma_V)+r\tilde{}_V-\mu}{\sigma_V}\varphi(x).
\end{aligned}$$

For all x on the interiors of the other segments,

$$\begin{aligned}
\varphi''(x) &= n^2\psi''(nx+(n-1)b) \\
&= -n^2\frac{\lambda_1(1,n^2\sigma_V)+r\tilde{}_V}{n^2\sigma_V}\psi(nx+(n-1)b) \\
&= -\frac{\lambda_1(1,n^2\sigma_V)+r\tilde{}_V}{\sigma_V}\varphi(x).
\end{aligned}$$

Hence, we obtained :

$$\varphi'' = -\frac{\lambda_1(1,n^2\sigma_V)+r\tilde{}_V-\mu\mathbf{1}_{A_n}}{\sigma_V}\varphi,$$

$$\text{i.e}\quad (-\sigma_V\Delta - r\tilde{}_V+\mu\mathbf{1}_{A_n})\varphi = \lambda_1(1,n^2\sigma_V)\varphi.$$

By unicity of the principal eigenelements (see [56]),
$\varphi=\varphi_1(n,\sigma_V)$ and $\lambda_1(1,n^2\sigma_V)=\lambda_1(n,\sigma_V)$.
$\lambda_1(n,\sigma_V)$ is then the only λ that nullifies the function

$$\begin{cases}
[-r\tilde{}_V,-r\tilde{}_V+\mu] & \to & \mathbb{R} \\
\lambda & \mapsto & \sqrt{-\dfrac{\lambda+r\tilde{}_V-\mu}{\sigma_V}}\tanh\left(\sqrt{-\dfrac{\lambda+r\tilde{}_V-\mu}{n^2\sigma_V}}d\right) \\
& & -\sqrt{\dfrac{\lambda+r\tilde{}_V}{\sigma_V}}\tan\left(\sqrt{\dfrac{\lambda+r\tilde{}_V}{n^2\sigma_V}}(b-d)\right).
\end{cases}$$

Using the Taylor series of tanh and tan at order 1 :

$$\begin{aligned}
\tanh(x) &= x+o(x^2) \\
\tan(x) &= x+o(x^2),
\end{aligned}$$

we can write, as $n \to +\infty$,

$$\begin{aligned} -\frac{1}{n}.\frac{\lambda + \tilde{r_V} - \mu}{\sigma_V} d - \frac{1}{n}.\frac{\lambda + \tilde{r_V}}{\sigma_V}(b-d) &= o\left(\frac{1}{n^2}\right) \\ \text{i.e} \qquad (\lambda + \tilde{r_V} - \mu)d + (\lambda + \tilde{r_V})(b-d) &= o\left(\frac{1}{n}\right) \\ \text{thus} \qquad \lambda_1(n, \sigma_V) = -\tilde{r_V} + \mu\frac{d}{b} + o\left(\frac{1}{n}\right). & \end{aligned}$$

Pushing the Taylor series at the next order :

$$\begin{aligned} \tanh(x) &= x - \frac{x^3}{3} + o(x^4) \\ \tan(x) &= x + \frac{x^3}{3} + o(x^4), \end{aligned}$$

we can compute C where
$\lambda_1(n, \sigma_V) = -\tilde{r_V} + \mu\frac{d}{b} + \frac{C}{n^2} + o\left(\frac{1}{n^2}\right)$:

$$\begin{aligned} \frac{\mu d - (\lambda + \tilde{r_V})b}{\sigma_V n} - \frac{(\lambda + \tilde{r_V} - \mu)^2 d^3 + (\lambda + \tilde{r_V})^2 (b-d)^3}{3\sigma_V^2 n^3} &= o\left(\frac{1}{n^4}\right), \\ \sigma_V\left(\frac{-bC}{n^2} + o\left(\frac{1}{n^2}\right)\right) & \\ -\frac{1}{3n^2}\left(\mu(\frac{d}{b} - 1) + \frac{C}{n^2} + o\left(\frac{1}{n^2}\right)\right)^2 d^3 & \\ -\frac{1}{3n^2}\left(\mu\frac{d}{b} + \frac{C}{n^2} + o\left(\frac{1}{n^2}\right)\right)^2 (b-d)^3 &= o\left(\frac{1}{n^3}\right), \\ \sigma_V bC + \frac{1}{3}\left(\mu^2(\frac{d}{b} - 1)^2 d^3 + \mu^2\frac{d^2}{b^2}(b-d)^3\right) &= o(1), \\ C = -\frac{\mu^2 d^2 (b-d)^2}{3\sigma_V b^2} + o(1). & \end{aligned}$$

Hence,

$$\lambda_1(n, \sigma_V) = -\tilde{r_V} + \mu\frac{d}{b} - \frac{\mu^2 d^2 (b-d)^2}{3\sigma_V b^2}.\frac{1}{n^2} + o\left(\frac{1}{n^2}\right).$$

Chapter 3

Agro-ecological control of a pest–host system: optimizing the harvest

This article is available on HAL https://hal.science/ [2].

3.1 Abstract

We delve into the interactions between a prey-predator and a vector-borne epidemic system, driven by agro-ecological motivations. This system involves an ODE, two reaction–diffusion PDEs and one reaction–diffusion–advection PDE. It has no complete variational or monotonic structure and features spatially heterogeneous coefficients. Our initial focus is to examine the continuity of a quantity known as "harvest", which depends on the time-integral of infected vectors. We analyze its asymptotic behaviour as the domain becomes homogeneous. Then we tackle a non-standard optimal control problem related to the linearized harvest and conduct an analysis to establish the existence, uniqueness, and properties of optimizers. Finally, we refine the location of optimizers under specific initial conditions.

3.2 Introduction

We are interested in the sugar beet agro-ecosystem, particularly how aphids spread four yellow viruses (BMYV, BChV, BYV, BtMV) in beet fields. Controlling these viruses is crucial, as they can reduce sugar concentration in beets by fifty percent. Pesticides are commonly used but harm biodiversity and health. An alternative approach involves using natural aphid predators like ladybugs (Hippodamia variegata or Chnootriba similis) in flower patches among beet fields. These "biodiversity refuges" can boost predator populations and control aphids, but reduces the total number of beets present in the field. We seek optimal refuge geometry to maximize the harvest of non-infected beets, treating it as an optimal control problem. Many similar agro-ecosystems can benefit from our analysis.

This work is a follow-up analysis from [1], in which one can find a more thorough biological context of our problem in the introduction, as well as comments on the ideal free dispersal strategy of the predators studied in [16]. In our initial paper, we primarily presented numerical arguments regarding the features of harvest optimizers. While a uniform refuge optimizes a linear criterion, we illustrated that its optimality seems not always guaranteed, depending on the initial distribution of infected vectors. For example, when infected vectors are predominantly concentrated in the center of the field, a centrally positioned refuge results in a superior harvest compared to a uniform one. Here, we provide an analytical proof of this phenomenon (Theorem 3.2.2), considering a symmetric, radially decreasing initial condition known as Schwarz rearrangement. However, when infected vectors are, on average, initially homogeneously positioned, a constant refuge is optimal (Theorem 3.2.3). Since having a constant refuge seems biologically unrealistic, we provide a way to approach it through homogenization (Theorem 3.2.1).

Let Ω be an open bounded connected set with Lipschitz boundary $\partial\Omega$ in a Euclidean space $\mathbb{R}^d$. Below is the parabolic–ordinary differential system of interest.

$$\begin{cases} \partial_t I &= \beta_{VH}(H(x)-I)V_i \\ \partial_t V_i &= \sigma_V \Delta V_i + \beta_{HV} I V_s - \alpha V_i - d_V(x)V_i - s_V(V_s+V_i)V_i - hPV_i \\ \partial_t V_s &= \sigma_V \Delta V_s - \beta_{HV} I V_s + \alpha V_i - d_V(x)V_s - s_V(V_s+V_i)V_s - hPV_s \\ & \quad + b_V(x)(V_s+V_i) \\ \partial_t P &= \sigma_P \nabla \cdot \left(r_P(x) \nabla \left(\frac{P}{r_P(x)} \right) \right) + \gamma h (V_s+V_i)P + r_P(x)P - s_P P^2 \end{cases} \tag{3.1}$$

in $\Omega \times \mathbb{R}_+^*$, where we omitted the dependency on (x,t) for I, V_i, V_s and P.

Here, the notations I, V_i, V_s, P stand respectively for the population density of infected hosts, infected vectors, susceptible vectors and predators. The various parameters are all biologically meaningful: $H \in \mathcal{C}^{2+\alpha}(\overline{\Omega}, \mathbb{R}_+^*)$ is the total population of hosts, $\beta_{VH}, \beta_{HV} > 0$ are the transmission rates (from vectors to hosts and vice-versa), $\sigma_V, \sigma_P > 0$ are the diffusion rates of the vectors and predators, respectively, α is the recovery rate of the vectors, $b_V, d_V \in \mathcal{C}^{2+\alpha}(\overline{\Omega}, \mathbb{R}_+^*)$ are the birth rate and death rate of the vectors, respectively, $r_P \in \mathcal{C}^{2+\alpha}(\overline{\Omega}, \mathbb{R}_+^*)$ is the Malthusian growth rate of the predators, $s_V, s_P > 0$ are the saturation rates of vectors and predators, respectively (intraspecific competition for space or resources leading to logistic growth), $h > 0$ is the predation rate and $\gamma > 0$ is a coefficient measuring the efficiency of predation.

We supplement it with initial conditions:

$$(I, V_i, V_s, P)(\cdot, 0) = (0, V_{i,0}, V_{s,0}, P_0) \quad \text{in } \Omega,$$

where $V_{i,0}$, $V_{s,0}$, P_0 are nonnegative functions in $L^\infty(\overline{\Omega})$, and with "no-flux" boundary conditions:

$$\frac{\partial V_i}{\partial n} = \frac{\partial V_s}{\partial n} = \frac{\partial (P/r_P)}{\partial n} = 0 \quad \text{on } \partial\Omega.$$

Note that the condition $\partial_n(P/r_P) = 0$ reduces to $\partial_n P = 0$ under the biologically relevant assumption $\partial_n r_P = 0$, that will be a standing assumption from now on. Hence, we actually have homogeneous Neumann boundary conditions for all three animal populations V_i, V_s and P.

When Ω has a smooth boundary, by [1], the system (3.1) admits a unique classical solution defined in $\overline{\Omega} \times \mathbb{R}_+^*$. In our case, the well-posedness of this system is only a conjecture.

Let $R \in \mathcal{C}^{2+\alpha}(\overline{\Omega}, [0,1])$. We will call the function R the refuge. In the rest of the paper, we assume that the growth rate of the predators and the preys, and the population of hosts are of

the form

$$\begin{aligned} r_P &= (r_P^r - r_P^f)R + r_P^f \\ b_V &= (b_V^r - b_V^f)R + b_V^f \\ d_V &= (d_V^r - d_V^f)R + d_V^f \\ r_V &= b_V - d_V = (r_V^r - r_V^f)R + r_V^f \\ H &= H^0(1-R), \end{aligned}$$

with $r_P^r, r_P^f, b_V^r, b_V^f, d_V^r, d_V^f, r_V^r, r_V^f, H^0 > 0$.

With this set of notations and assumptions, our optimal control problem can be recasted as follows:

Optimal control problem:

Characterize the set of optimal R such that the harvest of healthy beets $\eta = \lim_{t\to+\infty} \int_\Omega H - I(\cdot,t) = \int_\Omega He^{-\beta_{VH}\int_0^{+\infty} V_i(\cdot,t)\mathrm{d}t}$ is maximized.

It is important to highlight that in Section 4, dedicated to optimizing η, Theorem 3.5.3 and 3.5.4 require the shape of the refuge to reside within a subset of $\mathrm{L}^\infty(\Omega)$ for the sake of compactness. We acknowledge that this requirement somewhat sets this result apart from the rest of the paper. Nevertheless, given that the well-posedness of the system should not be an issue when the coefficients are in $\mathrm{L}^\infty(\Omega)$, we believe that this result remains appropriate.

3.2.1 Organization of the paper

In the following subsections, we introduce our notations and present our main results. In Section 2, we investigate the continuity of the harvest and provide partial answers to the question. Section 3 is dedicated to proving our primary homogenization result. Finally, in Section 4, we establish our key findings regarding the location of optimizers based on the properties of $V_{i,0}$.

3.2.2 Notations

- $V_0 = V_{i,0} + V_{s,0}$ and $V = V_i + V_s$.
- $r_V = b_V - d_V$.
- $\overline{\mathcal{L}} = \nabla \cdot \left(r_P \nabla \left(\frac{\cdot}{r_P} \right) \right)$.
- $\mathcal{L}_{V_s} = -\sigma_V \Delta - r_V + h\frac{r_P}{s_P}$.
- $\lambda_1(\mathcal{L}_{V_s})$ the principal eigenvalue of the operator $\mathcal{L}_{V_s}$ with Neumann boundary conditions, associated with the positive principal eigenfunction $\varphi_{s,1}$ (with $\min_\Omega \varphi_{s,1} = 1$):

$$\begin{cases} \mathcal{L}_{V_s}(\varphi_{s,1}) = -\sigma_V \Delta \varphi_{s,1} + (-r_V + h\frac{r_P}{s_P})\varphi_{s,1} = \lambda_1(\mathcal{L}_{V_s})\varphi_{s,1} & \text{in } \Omega \\ \dfrac{\partial \varphi_{s,1}}{\partial n} = 0 & \text{on } \partial\Omega \end{cases}$$

- $I_\infty : x \mapsto \lim_{t\to+\infty} I(x,t)$.
- The harvest $\eta = \int_\Omega H - I_\infty = \int_\Omega He^{-\beta_{VH}\int_0^{+\infty} V_i(\cdot,t)\mathrm{d}t}$.
- The linearized harvest η_L (defined in Section 4).
- If f is a function defined on Ω, $\overline{f} = \max_{\overline{\Omega}} f$ and $\underline{f} = \min_{\overline{\Omega}} f$.

3.2.3 Main result

The idea of our main theorems is the following. The quantities m and ξ are defined in the beginning of section 4.1.

Theorem 3.2.1. *When the frequency of the refuge goes to infinity, the harvest converges to the harvest of the homogenized system.*

Theorem 3.2.2. *If $V_{i,0}$ is symmetric and radially decreasing, the optimal refuge of the linearized harvest is not constant in space, and there exists a symmetric, radially decreasing refuge better than the constant one.*

Theorem 3.2.3. *If (the mean of) $V_{i,0}$ is constant in space, the optimal refuge of (the mean of) the linearized harvest is constant in space and equal to the positive part of* $\dfrac{\sqrt{\beta_{VH}(\xi+m)\mathbb{E}[V_{i,0}]}-\xi}{m}$.

The formal context and notations will be given in Section 3 and 4.

Our homogenization analysis uses an ansatz technique developed by Murat and Tartar [45], which effectively handles the non-trivial aspects of the ideal free dispersal term in the predator equation. The remaining portion of the proof relies on favorable estimates of the solution and the application of the Aubin-Lions theorem on $\Omega \times [0,T]$, and linear estimates previously conducted in [1], which ensures the convergence of the complete time-integral of infected vectors.

The work performed on a Schwarz rearranged initial condition involves the utilization of Talenti inequalities [68], a case of strict inequality in the extended Hardy–Littlewood inequalities [31], and the Pólya–Szegő inequality [67].

3.3 Harvest around $\lambda_1(\mathcal{L}_{V_s}) = 0$

This section deals with the continuity of the harvest η with respect to $\lambda_1(\mathcal{L}_{V_s})$. In [1], it is claimed that η is null when $\lambda_1(\mathcal{L}_{V_s})$ is negative, and positive when $\lambda_1(\mathcal{L}_{V_s})$ is positive. It is trivial that $\lim_{\lambda_1(\mathcal{L}_{V_s})\to 0^-} \eta = 0$. In this section, we establish that the harvest is null when $\lambda_1(\mathcal{L}_{V_s}) = 0$ in a simpler scenario, specifically when $P = r_P/s_P$. If this seems to be a costly assumption regarding the behaviour of the predators, it is, in fact, not: we can arrive at this new system by setting $\gamma = 0$ and $P_0 = r_P/s_P$ in system 3.1. We leave open the question regarding the behaviour of η when $\lambda_1(\mathcal{L}_{V_s})$ approaches 0 from the right. We conjecture that the harvest should be continuous with respect to $\lambda_1(\mathcal{L}_{V_s})$, therefore the right limit should be 0. To support this conjecture, we examine a simpler case when $P = r_P/s_P$ and $-r_V + h\dfrac{r_P}{s_P}$ uniformly converges to 0. For the complete prey-predator system, the maximum principle does not seem to lead anywhere, since the predation term in the prey equation lacks the correct sign, and the best predator supersolution we could obtain is of the form

$$\overline{P}(t) = \frac{\exp\left(t - \dfrac{e^{-\lambda_1(\mathcal{L}_{V_s})t}}{\lambda_1(\mathcal{L}_{V_s})}\right)}{1 + \int_0^t \exp\left(s - \dfrac{e^{-\lambda_1(\mathcal{L}_{V_s})s}}{\lambda_1(\mathcal{L}_{V_s})}\right) \mathrm{d}s},$$

which, while it can be integrated in time, appears to be inadequate in providing insights to the behaviour of $\int_0^{+\infty} V_i$ when $\lambda_1(\mathcal{L}_{V_s})$ approaches 0. Moreover, when the refuge is not constant,

our control over $\lambda_1(\mathcal{L}_{V_s})$ is not explicit, necessitating linear analysis to link this principal eigenvalue to V_i. This, again, does not seem to yield any conclusive results regarding the limit of $\int_0^{+\infty} V_i$ around $\lambda_1(\mathcal{L}_{V_s}) = 0$. Even numerically, as 1) the harvest η can only be approximated by computing $\int_0^T V_i$ for a large T and 2) V_i seems to converge to 0 at a rate similar to $1/t$ when $\lambda_1(\mathcal{L}_{V_s})$ is close to 0, the continuity of η is not clear at all. Some remarks on the numerical behaviour of η around $\lambda_1(\mathcal{L}_{V_s}) = 0$ can be found in Section 4 (see Figure 3.2).

Proposition 3.3.1. *Consider the system*

$$\begin{cases} \partial_t I &= \beta_{VH}(H-I)V_i \\ \partial_t V_i &= \sigma_V \Delta V_i + \beta_{HV} I V_s - \alpha V_i - d_V V_i - s_V(V_s+V_i)V_i - h\dfrac{r_P}{s_P}V_i \\ \partial_t V_s &= \sigma_V \Delta V_s - \beta_{HV} I V_s + \alpha V_i - d_V V_s - s_V(V_s+V_i)V_s - h\dfrac{r_P}{s_P}V_s \\ & \quad + b_V(V_s+V_i) \end{cases} \tag{3.2}$$

with nonnegative initial condition in $\mathrm{L}^\infty(\overline{\Omega})$ *and Neumann boundary conditions (i.e system* (3.1) *with the predators replaced by* r_P/s_P*), with its associated harvest* η*. Suppose that* $V_{i,0} \not\equiv 0$ *and* $\lambda_1(\mathcal{L}_{V_s}) = 0$*.*

Then, $\eta = 0$*.*

Proof. Recall that

$$\eta = \int_\Omega H e^{-\beta_{VH}\int_0^{+\infty} V_i(\cdot,t)\mathrm{d}t}.$$

It is sufficient to prove that the integral $\int_0^{+\infty} V_i(x,t)$ does not converge for any $x \in \Omega$. Let us first deal with the convergence of V_i to 0 when t goes to infinity.

By summing the last two equations of (3.2), V solves the equation

$$\partial_t V - \sigma_V \Delta V = (r_V - h\frac{r_P}{s_P})V - s_V V^2 \tag{3.3}$$

for $(x,t) \in \Omega \times \mathbb{R}_+^*$, with Neumann boundary conditions and initial condition $V(\cdot,0) = V_0$.

Let $\varphi_{s,1}$ be the positive principal eigenvalue associated with $\lambda_1(\mathcal{L}_{V_s})$, and let $\overline{V} = \dfrac{2\varphi_{s,1}}{s_V(t+1)}$. Because $\lambda_1(\mathcal{L}_{V_s})$ is null, $-\Delta\varphi_{s,1} = (r_V - h\frac{r_P}{s_P})\varphi_{s,1}$, hence $\overline{V}$ solves

$$\partial_t \overline{V} - \sigma_V \Delta \overline{V} = \left(r_V - h\frac{r_P}{s_P}\right)\overline{V} - \frac{1}{t+1}\overline{V} \geq \left(r_V - h\frac{r_P}{s_P}\right)\overline{V} - s_V\overline{V}^2$$

and is then a supersolution of the Cauchy–Neumann system (3.3) solved by V (recall that $\min_\Omega \varphi_{s,1} = 1$). We conclude that, for all $x \in \Omega$ and $t > 0$,

$$V_i(x,t) \leq V(x,t) \leq \overline{V}(x,t) \leq \frac{2\overline{\varphi_{s,1}}}{s_V(t+1)} \underset{t\to+\infty}{\longrightarrow} 0,$$

hence the uniform convergence of V_i to 0.

V_i solves, in $\Omega \times \mathbb{R}_+^*$,

$$\partial_t V_i - \sigma_V \Delta V_i = \beta_{HV} I(V - V_i) - \alpha V_i - d_V V_i - s_V V V_i - h\frac{r_P}{s_P}V_i,$$

hence

$$\partial_t V_i - \sigma_V \Delta V_i + (\beta_{HV} I + \alpha + d_V + s_V V + h\frac{r_P}{s_P})V_i = \beta_{HV} I V.$$

Denote $\overline{C} = \beta_{HV}\overline{H} + \alpha + \overline{d_V} + s_V\overline{V} + h\overline{\frac{r_P}{s_P}} > 0$ (we used the global boundedness of V in $\Omega \times \mathbb{R}_+^*$ proved in [1]). Because $V_{i,0} \not\equiv 0$, by [1], there exists $C > 0$ such that $I(x,t) \geq C$ for all $(x,t) \in \Omega \times [1,+\infty)$. Therefore, in $\Omega \times [1,+\infty)$,

$$\partial_t V_i - \sigma_V \Delta V_i + \overline{C} V_i \geq \beta_{HV} C V.$$

Let $T > 1$. Integrating the previous equation on Ω and $[1,T]$, and using the Neumann boundary conditions on V_i, one gets

$$\int_\Omega (V_i(\cdot,T) - V_i(\cdot,1)) + \overline{C} \int_\Omega \int_1^T V_i \geq \beta_{HV} C \int_\Omega \int_1^T V,$$

By the uniform Harnack inequality (see [32], Theorem 2.5), it exists $C' > 0$ independent of T such that $\min_\Omega \int_1^T V_i \geq C' \max_\Omega \int_1^T V_i$. Then, one has, for all $x \in \Omega$,

$$\begin{aligned}
\overline{C} \int_0^T V_i(x,t)\mathrm{d}t &\geq \overline{C} \min_\Omega \int_1^T V_i \\
&\geq \overline{C} C' \max_\Omega \int_1^T V_i \\
&\geq \overline{C} C' |\Omega| \int_\Omega \int_1^T V_i \\
&\geq \beta_{HV} C C' |\Omega| \int_\Omega \int_1^T V + \int_\Omega (V_i(\cdot,1) - V_i(\cdot,T)).
\end{aligned}$$

We have proved that, for an arbitrary $x \in \Omega$, if $V(x,\cdot)$ is not integrable at $+\infty$, then neither is $V_i(x,\cdot)$. It is then sufficient to show that the integral $\int_1^{+\infty} V(x,t)$ does not converge for any $x \in \Omega$.

Let $\underline{V} = \underline{C}\frac{\varphi_{s,1}}{t+1}$, $\underline{C} = 1/(2s_V\overline{\varphi_{s,1}})$. $\underline{V}$ solves

$$\partial_t \underline{V} - \sigma_V \Delta \underline{V} = \left(r_V - h\frac{r_P}{s_P}\right)\underline{V} - \frac{1}{t+1}\underline{V} \leq \left(r_V - h\frac{r_P}{s_P}\right)\underline{V} - s_V\underline{V}^2$$

and is then a subsolution of the Cauchy–Neumann system (3.3) solved by V. We conclude that, for all $x \in \Omega$,

$$\int_1^{+\infty} V(x,t)\mathrm{d}t \geq \int_1^{+\infty} \underline{V}(x,t)\mathrm{d}t = +\infty.$$

□

We now deal with a simpler case of the limit of η when $\lambda_1(\mathcal{L}_{V_s})$ approaches 0 from the right: the case of $-r_V + h\frac{r_P}{s_P}$ uniformly converging to 0. It is clear that it is a sufficient condition for $\lambda_1(\mathcal{L}_{V_s})$ converging to 0, but it is not necessary.

Proposition 3.3.2. *Denote $m = -r_V + h\frac{r_P}{s_P}$. Consider the system (3.2) with its associated harvest η_m. Let $(m_k)_{k\in\mathbb{N}}$ be a nonincreasing sequence (in the sense that $m_k \leq m_{k+1}$ for all $k \in \mathbb{N}$) of nonnegative functions that uniformly converges to 0 as $k \to +\infty$. Suppose that $V_0 \not\equiv 0$. Then,*

$$\lim_{k\to+\infty} \eta_{m_k} = 0.$$

Proof. The same proof as above yields that, for any $x \in \Omega$, if $V(x,\cdot)$ is not integrable, then $V_i(x,\cdot)$ is not integrable. With $\eta_{m_k} = \int_\Omega He^{-\beta_{VH}\int_0^{+\infty} V_i(\cdot,t)\mathrm{d}t}$, by the dominated convergence theorem, it suffices to prove that, for any $x \in \Omega$, $\lim_{k\to+\infty} \int_0^{+\infty} V = +\infty$.

For all $k \in \mathbb{N}$, V^k solves the equation

$$\partial_t V^k - \sigma_V \Delta V^k = -m_k V^k - s_V (V^k)^2 \tag{3.4}$$

for $(x,t) \in \Omega \times \mathbb{R}_+^*$, with Neumann boundary conditions and initial condition $V(\cdot,0) = V_0$. By the comparison principle, and because (m_k) is nonincreasing, (V^k) is nondecreasing.

By [1], for all $\delta > 0$, $\inf_{x\in\Omega} V^0(x,\delta) > 0$. Denote $\underline{V}^k$ the solution of

$$\begin{cases} \underline{V}^k(\cdot,1) = \underline{V}_1 := \inf\limits_{x\in\Omega} (V^0)(x,1) > 0 & \text{in } \Omega \\ \partial_t \underline{V}^k - \sigma_V \Delta \underline{V}^k = -\overline{m}_k \underline{V}^k - s_V (\underline{V}^k)^2 & \text{in } \Omega \times [1,+\infty) \\ \dfrac{\partial \underline{V}^k}{\partial n} = 0 & \text{on } \partial\Omega \times [1,+\infty). \end{cases}$$

which is a subsolution of the Cauchy–Neumann problem solved by V^k on $\Omega \times [1,+\infty)$. We deduce, for all $t > 1$,

$$V^k(\cdot,t) \geq \underline{V}^k(t) = \frac{-\overline{m}_k}{s_V} \left(1 + \left(\frac{-\overline{m}_k}{s_V \underline{V}_1} - 1\right) e^{\overline{m}_k t}\right)^{-1}.$$

By assumption, $\overline{m}_k := \|m_k\|_\infty$ converges to 0 when $k \to +\infty$. For all $x \in \Omega$,

$$\begin{aligned} \int_0^{+\infty} V^k(x,t)\mathrm{d}t &\geq \frac{\overline{m}_k}{s_V} \int_1^{+\infty} \left(-1 + \left(\frac{\overline{m}_k}{s_V \underline{V}_1} + 1\right) e^{\overline{m}_k t}\right)^{-1} \mathrm{d}t \\ &= \frac{\overline{m}_k}{s_V} \int_1^{+\infty} e^{-\overline{m}_k t} \left(\frac{\overline{m}_k}{s_V \underline{V}_1} + 1 - e^{-\overline{m}_k t}\right)^{-1} \mathrm{d}t \\ &= \frac{1}{s_V} \left[\ln\left(\frac{\overline{m}_k}{s_V \underline{V}_1} + 1 - e^{-\overline{m}_k t}\right)\right]_1^{+\infty} \\ &= \frac{1}{s_V} \ln\left(\frac{\overline{m}_k/(s_V \underline{V}_1) + 1}{\overline{m}_k/(s_V \underline{V}_1) + 1 - e^{-\overline{m}_k}}\right) \underset{k\to+\infty}{\longrightarrow} +\infty. \end{aligned}$$

□

3.4 Homogenization of the refuges

In this section, we prove our primary homogenization result. In order to define properly a "refuge of higher frequency", we assume that Ω is a hyperrectangle in $\mathbb{R}^d$. In the example of the beet field, one can take $d = 2$.

We can periodically extend a refuge $R \in \mathrm{L}^\infty(\Omega, [0,1])$ in $\mathbb{R}^d$ and define $R_n : x \mapsto R(nx)$ the refuge of frequency n.

For a function $f \in \mathrm{L}^\infty(\Omega)$, we denote

$$\langle f \rangle_\Omega = \frac{1}{|\Omega|} \int_\Omega f$$

the average of f over Ω.

Denote $\mathcal{R} := \langle R \rangle_\Omega$ and $\mathcal{R}_2 := \langle R^2 \rangle_\Omega$. One can easily verify that for all $n \in \mathbb{N}^*$, $\langle R_n \rangle_\Omega = \mathcal{R}$ and $\langle R_n^2 \rangle_\Omega = \mathcal{R}_2$.

For such a refuge, we denote

$$\begin{aligned}
H_n &= H^0(1-R_n)\\
b_V^n &= (b_V^r - b_V^f)R_n + b_V^f\\
d_V^n &= (d_V^r - d_V^f)R_n + d_V^f\\
r_V^n &= b_V^n - d_V^n\\
r_P^n &= (r_P^r - r_P^f)R_n + r_P^f.
\end{aligned}$$

We consider a similar Cauchy–Neumann problem as (3.1) with a refuge R_n, for which the system rewrites itself

$$\begin{cases}
\partial_t I &= \beta_{VH}(H_n - I)V_i\\
\partial_t V_i &= \sigma_V \Delta V_i + \beta_{HV} I V_s - (\alpha + d_V^n + s_V(V_s+V_i) + hP)V_i\\
\partial_t V_s &= \sigma_V \Delta V_s + (\alpha + b_V^n)V_i + (r_V^n - \beta_{HV} I - s_V(V_s+V_i) - hP)V_s\\
\partial_t P &= \sigma_P \nabla \cdot \left(r_P^n \nabla \left(\frac{P}{r_P^n} \right) \right) + (\gamma h(V_s+V_i) + r_P^n - s_P P)P.
\end{cases} \tag{3.5}$$

with nonnegative initial condition $(I, V_i, V_s, P)(\cdot, 0) = (I_0^n, V_{i,0}^n, V_{s,0}^n, P_0^n) \quad \text{in } \Omega.$

Denote (I_n, V_i^n, V_s^n, P_n), the unique solution of this new problem, and

$$\eta_n = \left(\int_\Omega H - I_\infty \right)_n = \int_\Omega H_n e^{-\beta_{VH} \int_0^{+\infty} V_i^n}$$

the associated harvest.

We also denote

$$\begin{aligned}
H_\infty &= \langle H_n \rangle_\Omega &&= H^0(1-\mathcal{R})\\
b_V^\infty &= \langle b_V^n \rangle_\Omega &&= (b_V^r - b_V^f)\mathcal{R} + b_V^f\\
d_V^\infty &= \langle d_V^n \rangle_\Omega &&= (d_V^r - d_V^f)\mathcal{R} + d_V^f\\
r_V^\infty &= \langle r_V^n \rangle_\Omega &&= b_V^\infty - d_V^\infty\\
r_P^\infty &= \langle r_P^n \rangle_\Omega &&= (r_P^r - r_P^f)\mathcal{R} + r_P^f\\
(r_P^\infty)_2 &= \langle (r_P^n)^2 \rangle_\Omega &&= (r_P^r - r_P^f)^2 \mathcal{R}_2 + 2(r_P^r - r_P^f) r_P^f \mathcal{R} + (r_P^f)^2,
\end{aligned}$$

and $r^* \in \mathcal{M}_d(\mathbb{R})$ the so-called "homogenized conductivity" defined in [4].

The homogenized Cauchy–Neumann problem is the following:

$$\begin{cases}
\partial_t I &= \beta_{VH}(H_\infty - I)V_i\\
\partial_t V_i &= \sigma_V \Delta V_i + \beta_{HV} I V_s - (\alpha + d_V^\infty + s_V(V_s+V_i) + hP)V_i\\
\partial_t V_s &= \sigma_V \Delta V_s + (\alpha + b_V^\infty)V_i + (r_V^\infty - \beta_{HV} I - s_V(V_s+V_i) - hP)V_s\\
\partial_t P &= \sigma_P \nabla \cdot \left(r^* \nabla \left(\frac{P}{r_P^\infty} \right) \right) + (\gamma h(V_s+V_i) + \frac{(r_P^\infty)_2}{r_P^\infty} - s_P \frac{(r_P^\infty)_2}{(r_P^\infty)^2} P)P.
\end{cases} \tag{3.6}$$

with nonnegative initial condition $(I, V_i, V_s, P)(\cdot, 0) = (I_0^\infty, V_{i,0}^\infty, V_{s,0}^\infty, P_0^\infty)$ in Ω. We assume the weak convergence in $\mathrm{L}^2(\Omega)$ of I_0^n, $V_{i,0}^n$, $V_{s,0}^n$, P_0^n to I_0^∞, $V_{i,0}^\infty$, $V_{s,0}^\infty$, P_0^∞, respectively.

Denote $(I^\infty, V_i^\infty, V_s^\infty, P^\infty)$, the unique solution of this problem, and

$$\eta_\infty = \left(\int_\Omega H - I_\infty \right)_\infty = \int_\Omega H_\infty e^{-\beta_{VH} \int_0^{+\infty} V_i^\infty}$$

the associated harvest.

Remark: The classical homogenization techniques, as developed by Murat and Tartar [45], elaborated upon in books like [6], and well comprehensively explained by Allaire [4], are applicable in this context, particularly for the fourth equation in (3.5). As for the first three equations in (3.5), given that the parameter n solely appears in the reaction term, straightforward estimates lead to the strong convergence in $\mathrm{L}^2(\Omega \times [0,T])$ of the solutions toward those of the homogenized problem. However, the presence of r_P^n in the divergence term of the fourth equation in (3.5) hinders a straightforward limit transition without further considerations. In fact, unlike the sequences (I_n), (V_i^n), and (V_s^n), the sequence (P_n) converges only weakly in $\mathrm{L}^2(\Omega \times [0,T])$.

Lemma 3.4.1. *The sequences (H_n), (b_V^n), (d_V^n), (r_V^n) and (r_P^n) weakly converge to, respectively, H_∞, b_V^∞, d_V^∞, r_V^∞ and r_P^∞ in $\mathrm{L}^2(\Omega)$.*

Proof. The weak convergence of the five sequences comes from the weak convergence of the sequence (R_n) to $x \mapsto \mathcal{R}$. Indeed, say $\Omega = [0,L]$ and let $\mathbf{1}_{[a,b]}$ be an indicator function. A change of variable yields

$$\int_a^b R_n = \frac{1}{n}\int_{na}^{nb} R.$$

For $k \in \mathbb{N}^*$, if $kL \leq n(b-a) \leq (k+1)L$, the segment $[na, nb]$ intersects at least k intervals of size L, and at best $k+1$, therefore

$$\frac{k}{n}L\mathcal{R} \leq \frac{1}{n}\int_{na}^{nb} R \leq \frac{k+1}{n}L\mathcal{R},$$

thus

$$\left(b-a-\frac{L}{n}\right)\mathcal{R} \leq \frac{1}{n}\int_{na}^{nb} R \leq \left(b-a+\frac{L}{n}\right)\mathcal{R}$$

and

$$\frac{1}{n}\int_{na}^{nb} R \underset{n\to+\infty}{\longrightarrow} (b-a)\mathcal{R} = \int_\Omega \mathbf{1}_{[a,b]}\mathcal{R}.$$

With a very similar proof, this is also true when Ω is a rectangle in $\mathbb{R}^d$, and trivially for any step function. We deduce the weak convergence of (R_n) by density of the space of step functions in $\mathrm{L}^2(\Omega)$. □

We then need to assess the strong convergence almost everywhere in $\Omega \times [0,T]$ for $T > 0$ of the solutions when $n \to +\infty$.

Lemma 3.4.2. *Let $T > 0$ be arbitrary. Consider the Cauchy–Neumann problem (3.5) for $(x,t) \in \Omega \times [0,T]$, and call, for $n \in \mathbb{N}$, (I_n, V_i^n, V_s^n, P_n) the unique solution. Then, the sequences (I_n), (V_i^n), (V_s^n) and (P_n/r_P^n) strongly converge in $\mathrm{L}^2(\Omega \times [0,T])$ and almost everywhere in $\Omega \times [0,T]$ to, respectively, (I_∞), (V_i^∞), (V_s^∞) and (P_∞/r_P^∞), and P_∞ is the weak limit in $\mathrm{L}^2(\Omega \times [0,T])$ of (P_n).*

Proof. This proof is very much inspired by [20].

First of all, by [1], for all $n \in \mathbb{N}$, $(I_n, V_i^n, V_s^n, P_n/r_P^n)$ are bounded in $\mathrm{L}^\infty(\Omega \times [0,T])$ by a constant $C > 0$ independent of n.

Multiplying the second equation by V_i and integrating over Ω, one gets

$$\begin{aligned}\frac{1}{2}\frac{\partial}{\partial t}\textstyle\int_\Omega (V_i^n)^2 + \sigma_V \int_\Omega |\nabla V_i^n|^2 &= \textstyle\int_\Omega \beta_{HV} I_n V_s^n V_i^n \\ &\quad - \textstyle\int_\Omega (\alpha + d_V + s_V(V_s^n + V_i^n) + hP_n)(V_i^n)^2 \\ &\leq |\Omega|\beta_{HV}C^3.\end{aligned}$$

Integrating this over $[0,T]$ yields the existence of a constant $C' > 0$ independent of n such that

$$\int_0^T \int_\Omega |\nabla V_i^n|^2 \leq C',$$

hence the boundedness of the $L^2([0,T], H^1(\Omega))$-norm of V_i^n.

Similarly, multiplying the first equation by I and integrating over Ω and $[0,T]$, multiplying the third equation by V_s and integrating over Ω and $[0,T]$, and multiplying the fourth equation by P/r_P and integrating over Ω and $[0,T]$ yields the boundedness of the $L^2([0,T], H^1(\Omega))$-norm of I_n, V_s^n and P_n/r_P^n.

Let $\zeta \in L^2([0,T], H^1(\Omega))$ be arbitrary. Multiplying the second equation by ζ and integrating over $\Omega \times [0,T]$, one gets

$$\begin{array}{rl} & \int_0^T \int_\Omega \partial_t V_i^n \zeta + \sigma_V \int_0^T \int_\Omega \nabla V_i^n \cdot \nabla \zeta \\ = & \int_0^T \int_\Omega (\beta_{HV} I_n V_s^n - (\alpha + d_V + s_V(V_s^n + V_i^n) + hP_n) V_i^n)\zeta, \end{array}$$

hence

$$\begin{array}{rl} \left| \int_0^T \int_\Omega \partial_t V_i^n \zeta \right| & \leq \sigma_V \sqrt{C'} \sqrt{\int_0^T \int_\Omega |\nabla \zeta|^2} + C'' \sqrt{\int_0^T \int_\Omega \zeta^2} \\ & \leq \max(\sigma\sqrt{C'}, C'') \|\zeta\|_{L^2([0,T], H^1(\Omega))}, \end{array}$$

where C'' is a positive constant independent of n. By the arbitrariness of ζ, this shows that $\|\partial_t V_i^n\|_{L^2([0,T],(H^1(\Omega))')} \leq \max(\sigma\sqrt{C}, C'')$.

Similarly, multiplying the first, second and third equation by ζ and integrating over $\Omega \times [0,T]$ yields bounds for the $L^2([0,T], (H^1(\Omega))')$-norm of $\partial_t I_n$, $\partial_t V_s^n$ and $\partial_t(P_n/r_P^n)$ (recall that r_P is independent of time).

By the Aubin-Lions theorem, the sequences (I_n), (V_i^n) (V_s^n) and (P_n/r_P^n) are precompact in $L^2(\Omega \times [0,T])$.

Then, up to extraction, we obtain strong convergence of the four sequences in $L^2(\Omega \times [0,T])$ and almost everywhere in $\Omega \times [0,T]$. Denote $\overline{I}$, $\overline{V_i}$, $\overline{V_s}$ and $\overline{P_r}$ the respective limits. In the following, we denote again by (I_n), (V_i^n) (V_s^n) and (P_n/r_P^n) the extracted sequences. Recall that the initial conditions converge weakly in $L^2(\Omega)$ of the initial conditions of the homogenized system.

Let $\varphi \in \mathcal{C}^2(\Omega \times [0,T])$ verifying the Neumann boundary conditions in Ω and such that $\varphi(\cdot, T) = 0$. Multiplying the first equation of (3.5) by φ and integrating over $\Omega \times [0,T]$ yields

$$\int_0^T \int_\Omega \varphi \partial_t I_n = \beta_{VH} \int_0^T \int_\Omega \varphi(H_n - I_n) V_i^n. \tag{3.7}$$

Moreover,

$$\begin{array}{rl} \int_0^T \int_\Omega \varphi \partial_t I_n & = \int_\Omega \left([\varphi I_n]_0^T - \int_0^T \partial_t \varphi I_n \right) \\ & = -\int_\Omega \left(\varphi(\cdot,0) I_0 + \int_0^T \partial_t \varphi I_n \right), \end{array}$$

$$\begin{array}{rl} & \left| \int_0^T \int_\Omega \partial_t \varphi I_n - \int_0^T \int_\Omega \partial_t \varphi \overline{I} \right| \\ \leq & \left| \int_\Omega \varphi(\cdot,0)(I_0^\infty - I_0^n) \right| + \sqrt{\int_0^T \int_\Omega (\partial_t \varphi)^2} \|I_n - I\|_{L^2(\Omega \times [0,T])} \\ & \underset{n \to +\infty}{\longrightarrow} 0, \end{array}$$

$$\begin{aligned} & \left|\int_0^T\int_\Omega \varphi H_n V_i^n - \int_0^T\int_\Omega \varphi H_\infty \overline{V_i}\right| \\ = & \left|\int_0^T\int_\Omega \varphi H_n (V_i^n - \overline{V_i}) + \int_0^T\int_\Omega \varphi (H_n - H_\infty)\overline{V_i}\right| \\ \leq & \sqrt{\int_0^T\int_\Omega \varphi^2 H_n^2}\|V_i^n - \overline{V_i}\|_{\mathrm{L}^2(\Omega\times[0,T])} \\ & + \left|\int_0^T\int_\Omega (H_n - H_\infty)\varphi\overline{V_i}\right| \\ & \underset{n\to+\infty}{\longrightarrow} 0 \end{aligned}$$

and

$$\begin{aligned} & \left|\int_0^T\int_\Omega \varphi I_n V_i^n - \int_0^T\int_\Omega \varphi \overline{I V_i}\right| \\ = & \left|\int_0^T\int_\Omega \varphi (I_n - \overline{I}) V_i^n + \int_0^T\int_\Omega \varphi \overline{I}(V_i^n - \overline{V_i})\right| \\ \leq & T\max(r_V^r, r_V^f)/s_V \sqrt{\int_0^T\int_\Omega \varphi^2}\|I_n - I\|_{\mathrm{L}^2(\Omega\times[0,T])} \\ & + \sqrt{\int_0^T\int_\Omega \varphi^2 \overline{I}^2}\|V_i^n - \overline{V_i}\|_{\mathrm{L}^2(\Omega\times[0,T])} \\ & \underset{n\to+\infty}{\longrightarrow} 0. \end{aligned}$$

Therefore, letting n go to $+\infty$ in (3.7), one gets

$$\int_0^T\int_\Omega \varphi\partial_t\overline{I} = \beta_{VH}\int_0^T\int_\Omega \varphi(H_\infty - \overline{I})\overline{V_i}.$$

Similarly, multiplying the second and third equation of (3.5) by φ, and letting n go to $+\infty$, also using the following convergence:

$$\begin{aligned} \left|\int_0^T\int_\Omega \varphi\Delta V_i^n - \int_0^T\int_\Omega \varphi\Delta\overline{V_i}\right| &= \left|\int_0^T\int_\Omega \Delta\varphi(V_i^n - \overline{V_i})\right| \\ &\leq \sqrt{\int_0^T\int_\Omega (\Delta\varphi)^2}\|V_i^n - \overline{V_i}\|_{\mathrm{L}^2(\Omega\times[0,T])} \\ &\underset{n\to+\infty}{\longrightarrow} 0, \end{aligned}$$

one gets:

$$\int_0^T\int_\Omega \varphi\partial_t\overline{V_i} = \int_0^T\int_\Omega \varphi(\sigma_V\Delta\overline{V_i} + \beta_{HV}\overline{IV_s} - (\alpha + d_V^\infty + s_V(\overline{V_s} + \overline{V_i}) + h\overline{P})\overline{V_i})$$

and

$$\int_0^T\int_\Omega \varphi\partial_t\overline{V_s} = \int_0^T\int_\Omega \varphi(\sigma_V\Delta\overline{V_s} + (\alpha + b_V^\infty)\overline{V_i} + (r_V^\infty - \beta_{HV}\overline{I} - s_V(\overline{V_s} + \overline{V_i}) - h\overline{P})\overline{V_s})$$

(where $\overline{P}$ is the weak limit of P_n, whose existence will be justified hereafter). We deal with the fourth equation by applying the change of variable $\tilde{P} = P/r_P^n$:

$$r_P^n\partial_t\tilde{P} = \sigma_P\nabla\cdot\left(r_P^n\nabla\tilde{P}\right) + (\gamma h(V_s + V_i) + r_P^n - s_P r_P^n\tilde{P})r_P^n\tilde{P}$$

and by carrying out a classical two-scale asymptotic expansion (also called an ansatz, cf [4]), we find that (P_n/r_P^n) converges weakly in $\mathrm{L}^2([0,T],\mathrm{H}^1(\Omega))$ to the solution (in the weak sense) of

$$r_P^\infty\partial_t\tilde{P} = \sigma_P\nabla\cdot\left(r^*\nabla\tilde{P}\right) + (\gamma h r_P^\infty(\overline{V_s} + \overline{V_i}) + (r_P^\infty)_2 - s_P(r_P^\infty)_2\tilde{P})\tilde{P}. \tag{3.8}$$

We voluntarily elude the computations to lighten the proof, as they are almost identical to the examples given in [4].

By uniqueness of the limit, $\overline{P_r}$ solves equation (3.8). Moreover,

$$P_n = r_P^n(P_n/r_P^n) \underset{n\to+\infty}{\longrightarrow} r_P^\infty \overline{P_r} =: \overline{P} \text{ weakly in } \mathrm{L}^2(\Omega\times[0,T]).$$

By plugging $\overline{P}$ in (3.8), one gets (in the weak sense)

$$\partial_t \overline{P} = \sigma_P \nabla\cdot\left(r^*\nabla\left(\frac{\overline{P}}{r_P^\infty}\right)\right) + (\gamma h(\overline{V_s}+\overline{V_i}) + \frac{(r_P^\infty)_2}{r_P^\infty} - s_P\frac{(r_P^\infty)_2}{(r_P^\infty)^2}\overline{P})\overline{P}.$$

The weak Neumann boundary condition follows easily from the weak convergence of the gradient of the sequences.

By uniqueness of the weak solution of (3.6),

$$(\overline{I},\overline{V_i},\overline{V_s},\overline{P}) = (I_\infty, V_i^\infty, V_s^\infty, P_\infty),$$

and we obtain the strong convergence in $\mathrm{L}^2(\Omega\times[0,T])$ and almost everywhere in $\Omega\times[0,T]$ of the non-extracted sequences (I_n), (V_i^n), (V_s^n) and (P_n/r_P^n) and the weak convergence in $\mathrm{L}^2(\Omega\times[0,T])$ of the non-extracted sequence (P_n).

□

Theorem 3.4.3 (Theorem 3.2.1). *Suppose that* $\lambda_1(\mathcal{L}_{V_s}) > 0$.

The harvest $\eta_n = \left(\int_\Omega H - I_\infty\right)_n$ *converges to* $\eta_\infty = \left(\int_\Omega H - I_\infty\right)_\infty$ *as* $n\to+\infty$.

Proof. For all $T>0$, by Lemma 3.4.2, the sequence (V_i^n) strongly converges in $\mathrm{L}^2(\Omega\times[0,T])$ to V_i^∞. By positivity of $\lambda_1(\mathcal{L}_{V_s})$, since $n\mapsto\lambda_1^n(\mathcal{L}_{V_s})$ is increasing and converges to the principal eigenvalue associated to the constant refuge $\mathcal{R}$ we denote $\lambda_1^\infty(\mathcal{L}_{V_s})$, by [1], for a small enough $\varepsilon>0$, there exists a constant $C>0$ and $t_0>0$ such that, for all $x\in\Omega$, $t\geq t_0$ and $n\in\mathbb{N}$ large enough,

$$V_i^n(x,t) \leq Ce^{-(\lambda_1^n(\mathcal{L}_{V_s})-h\varepsilon)(t-t_0)} \leq Ce^{-(\lambda_1(\mathcal{L}_{V_s})-h\varepsilon)(t-t_0)}$$

and

$$V_i^\infty(x,t) \leq Ce^{-(\lambda_1^\infty(\mathcal{L}_{V_s})-h\varepsilon)(t-t_0)} \leq Ce^{-(\lambda_1(\mathcal{L}_{V_s})-h\varepsilon)(t-t_0)}.$$

Let $x\in\Omega$, $T\geq t_0$ such that $\dfrac{2C|\Omega|}{\lambda_1(\mathcal{L}_{V_s})-h\varepsilon}e^{-(\lambda_1(\mathcal{L}_{V_s})-h\varepsilon)(T-t_0)} \leq \varepsilon/2$ and $n\in\mathbb{N}$ verifying the above inequality, and such that $\|V_i^n - V_i^\infty\|^2_{\mathrm{L}^2(\Omega\times[0,T])} \leq \dfrac{\varepsilon}{2|\Omega|T}$.

$$\begin{aligned}
&\int_\Omega\left|\int_0^{+\infty}(V_i^n(x,t)-V_i^\infty(x,t))\mathrm{d}t\right|\mathrm{d}x\\
\leq\ &\int_\Omega\left|\int_0^{T}(V_i^n(x,t)-V_i^\infty(x,t))\mathrm{d}t\right|\mathrm{d}x\\
&+\int_\Omega\left|\int_T^{+\infty}(V_i^n(x,t)-V_i^\infty(x,t))\mathrm{d}t\right|\mathrm{d}x\\
\leq\ &\|V_i^n-V_i^\infty\|^2_{\mathrm{L}^2(\Omega\times[0,T])}|\Omega|T + 2C\int_\Omega\int_T^{+\infty}e^{-(\lambda_1(\mathcal{L}_{V_s})-h\varepsilon)(t-t_0)}\mathrm{d}t\mathrm{d}x\\
\leq\ &\varepsilon/2 + \frac{2C|\Omega|}{\lambda_1(\mathcal{L}_{V_s})-h\varepsilon}e^{-(\lambda_1(\mathcal{L}_{V_s})-h\varepsilon)(T-t_0)}\\
\leq\ &\varepsilon.
\end{aligned}$$

We have shown the convergence of $\int_0^{+\infty} V_i^n(\cdot,t)\mathrm{d}t$ to $\int_0^{+\infty} V_i^\infty(\cdot,t)\mathrm{d}t$ in $\mathrm{L}^1(\Omega)$. Up to extraction, the sequence $(\int_0^{+\infty} V_i^n)$ hereby converges almost everywhere in Ω to $\int_0^{+\infty} V_i^\infty$. By positivity of the sequence, and by the dominated convergence theorem, we obtain the convergence of $e^{-\beta_{VH}\int_0^{+\infty} V_i^n}$ to $e^{-\beta_{VH}\int_0^{+\infty} V_i^\infty}$ in $\mathrm{L}^1(\Omega)$.

Let $n \in \mathbb{N}$ be large enough so that $\|e^{-\beta_{VH}\int_0^{+\infty} V_i^n} - e^{-\beta_{VH}\int_0^{+\infty} V_i^\infty}\|_{\mathrm{L}^1(\Omega)} \leq \varepsilon/(2H^0)$ and $\left|\int_\Omega (H_n - H_\infty)e^{-\beta_{VH}\int_0^{+\infty} V_i^\infty}\right| \leq \varepsilon/2$.

$$\begin{aligned}
& \left|\int_\Omega H_n e^{-\beta_{VH}\int_0^{+\infty} V_i^n} - \int_\Omega H_\infty e^{-\beta_{VH}\int_0^{+\infty} V_i^\infty}\right| \\
= & \left|\int_\Omega H_n (e^{-\beta_{VH}\int_0^{+\infty} V_i^n} - e^{-\beta_{VH}\int_0^{+\infty} V_i^\infty}) + \int_\Omega (H_n - H_\infty)e^{-\beta_{VH}\int_0^{+\infty} V_i^\infty}\right| \\
\leq & H^0 \int_\Omega |e^{-\beta_{VH}\int_0^{+\infty} V_i^n} - e^{-\beta_{VH}\int_0^{+\infty} V_i^\infty}| + \left|\int_\Omega (H_n - H_\infty)e^{-\beta_{VH}\int_0^{+\infty} V_i^\infty}\right| \\
\leq & \varepsilon.
\end{aligned}$$

Hence the convergence of η_n to η_∞.

□

3.5 Optimizers of the linearized harvest

We devote the next section to the computation of what we call the linearized harvest η_L. We would like to justify the necessity of utilizing a linearized version of η by briefly examining a straightforward scenario within our problem, wherein all spatial variables remain constant and specific parameter values are applied. Even in this case, the explicit computation of the solution for V (let alone V_i) remains unattainable. When we combine the equations for V_i and V_s, we obtain the following prey–predator system.

$$\begin{cases} \partial_t V - \sigma_V \Delta V = r_V(x)V - s_V V^2 - hPV \\ \partial_t P - \sigma_P \overline{\mathcal{L}}(P) = r_P(x)P - s_P P^2 + \gamma hPV \end{cases} \tag{3.9}$$

Now, assume that R is constant in space, so that r_V and r_P are constant, and assume that V_0 and P_0 are constant. To simplify even further, assume that $r_V = r_P = s_V = s_P = 1$ and $(\gamma - 1)h = -2$ (for instance, $\gamma = 1/2$ and $h = 4$). The system now writes:

$$\begin{cases} V' = V - V^2 - hPV \\ P' = P - P^2 + \gamma hPV \end{cases} \tag{3.10}$$

Denote $u = V + P$. u solves

$$\begin{aligned} u' &= u - (V^2 + P^2) + (\gamma - 1)hPV \\ &= u - u^2 + 2PV + (\gamma - 1)hPV \\ &= u - u^2, \end{aligned}$$

which yields, for all $t > 0$,

$$u(t) = \frac{1}{1 + \left(\frac{1}{V_0 + P_0} - 1\right)e^{-t}},$$

which means V solves

$$\begin{aligned} V' &= V - V^2 - h(u-V)V \\ &= (1-hu)V + (h-1)V^2. \end{aligned}$$

Although this equation is entirely decorrelated with the variable P, it remains too hard to compute explicitly or to calculate its time integral from 0 to $+\infty$. As a result, we lack information regarding the derivative of V with respect to R, and thus, we also lack information on the derivative of η with respect to R. To the best of our knowledge, this renders the nonlinear optimization problem too complicated to address directly via η. However, we can assume that R is constant, V_0 and $P_0 = r_P/s_P$ constant, and $\gamma = 0$, so that $P(t) = r_P/s_P$ for all $t > 0$, hence V solves

$$V' = (r_V - h\frac{r_P}{s_P})V - s_V V^2$$

and one can compute, denoting $\hat{m} = hr_P/s_P - r_V$, for all $t > 0$

$$V(t) = \frac{\hat{m}}{s_V}\left(\left(\frac{\hat{m}}{s_V V_0} + 1\right)e^{\hat{m}t} - 1\right)^{-1}$$

and, if $\hat{m}$ is positive,

$$\begin{aligned} \int_0^{+\infty} V(t)\mathrm{d}t &= \frac{1}{s_V}\left[\ln\left(\frac{\hat{m}}{s_V V_0} + 1 - e^{-mt}\right)\right]_0^{+\infty} \\ &= \frac{1}{s_V}\ln\left(1 + \frac{s_V V_0}{\hat{m}}\right), \end{aligned}$$

hence a sub-estimation of the harvest, that we call η_V:

$$\begin{aligned} \eta_V &= \int_\Omega H e^{-\beta_{VH}\int_0^{+\infty} V} \\ &= H|\Omega|\left(1 + \frac{s_V V_0}{\hat{m}}\right)^{-\beta_{VH}/s_V}. \end{aligned}$$

We can make explicit the R-dependency by plugging the expressions of H and $\hat{m}$ in function of $R \in [0,1]$:

$$\eta_V = H^0|\Omega|(1-R)\left(1 + \frac{s_V V_0}{\tilde{\xi} + \tilde{m}R}\right)^{-\beta_{VH}/s_V},$$

where $\tilde{\xi} = hr_P^f/s_P - r_V^f$ and $\tilde{m} = h(r_P^r - r_P^f)/s_P - r_V^r + r_V^f$. We plot this function in Figure 3.1.

A simple computation yields the optimal R of η_V we call R_{opt}^V:

$$\begin{aligned} R_{\text{opt}}^V = \; & \frac{1}{2\tilde{m}^2}\left(\sqrt{\tilde{m}^2(2\tilde{\xi} + s_V V_0 - \beta_{VH}V_0)^2 - 4\tilde{m}^2(\tilde{\xi}^2 + s_V V_0\tilde{\xi} - \beta_{VH}\tilde{m}V_0)}\right. \\ & \left. + \tilde{m}\left(\beta_{VH}V_0 - 2\tilde{\xi} - s_V V_0\right)\right). \end{aligned}$$

Here, $R_{\text{opt}}^V \approx 0,19$.

Comment: By doing a Taylor expansion of η_V around $V_0 = 0$, one gets

$$\eta_V = H^0|\Omega|(1-R)\left(1 - \frac{\beta_{VH}V_0}{\tilde{\xi} + \tilde{m}R}\right) + o(V_0),$$

which is an expression similar to that of the linearized harvest in the constant case, that will be computed later on in Remark 1.

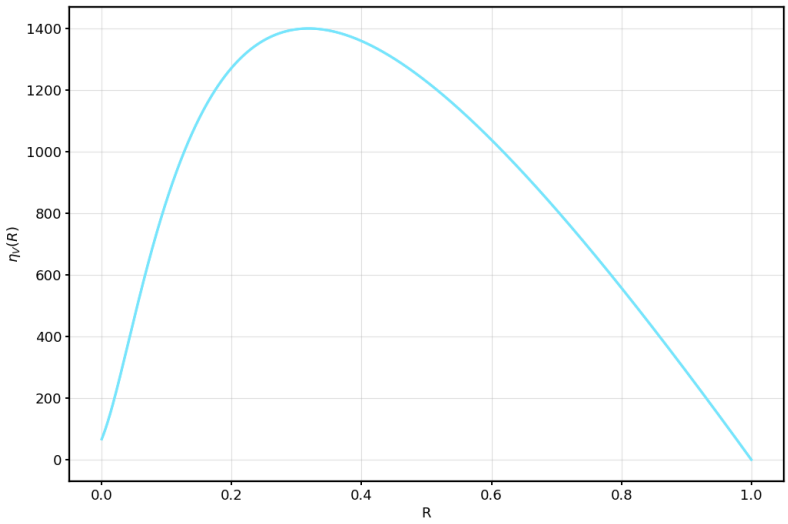

Figure 3.1: Sub-estimate of the harvest in function of a constant R (with biologically consistent parameters, see [1]).

3.5.1 Computation of η_L

Let us now delve into the linearization. We suppose in the following that $\lambda_1(\mathcal{L}_{V_s})$, the principal eigenvalue of $-\sigma_V\Delta + \dfrac{h}{s_P}r_P - r_V$ is positive, so that V converges to 0 exponentially fast uniformly in Ω as $t \to +\infty$, as well as the exponential convergence of P to r_P/s_P (see [1]). This ensures the boundedness of V, P in $\Omega \times \mathbb{R}_+^*$, and the existence of $\displaystyle\int_\Omega \int_0^{+\infty} \max(V, P - r_P/s_P)$.

Let us define some useful constants to lighten the writing:

- $m = \dfrac{h}{s_P}(r_P^r - r_P^f) + d_V^r - d_V^f$,
- $\xi = \alpha + d_V^f + \dfrac{h}{s_P}r_P^f > 0$.

We suppose in the following that m is positive. This will ensure that placing refuges in the field increases $\lambda_1(\mathcal{L}_{V_s})$, and therefore is beneficial for a quicker eradication of the population V. In the case $m \leq 0$, the optimisation problem is trivial: $R = 0$ yields the best harvest (which is 0 in the case $\lambda_1(\mathcal{L}_{V_s}) < 0$).

Denote $\tilde{P} = P - r_P/s_P$ and

$$o(\|(V,\tilde{P})\|) = \underset{\|(V,\tilde{P})\|_{\mathrm{L}^\infty(\Omega\times\mathbb{R}_+^*)}\to 0}{o}\left(\|(V,\tilde{P})\|_{\mathrm{L}^\infty(\Omega\times\mathbb{R}_+^*)}\right).$$

We have

$$\frac{\|IV_s\|_{\mathrm{L}^\infty(\Omega\times\mathbb{R}_+^*)}}{\|(V,\tilde{P})\|_{\mathrm{L}^\infty(\Omega\times\mathbb{R}_+^*)}} \leq \|I\|_{\mathrm{L}^\infty(\Omega\times\mathbb{R}_+^*)},$$

and this quantity converges to 0 as $\|(V,\tilde{P})\|_{\mathrm{L}^\infty(\Omega\times\mathbb{R}_+^*)}$ goes to 0, since

$$I(x,t) = H(x)\left(1-\exp\left(-\beta_{VH}\int_0^t V_i(x,s)\mathrm{d}s\right)\right)$$

Therefore, $IV_s = o(\|(V,\tilde{P})\|)$. Similarly, $VV_i = o(\|(V,\tilde{P})\|)$ and $\tilde{P}V_i = o(\|(V,\tilde{P})\|)$.

The population V_i satisfies

$$\begin{aligned}\partial_t V_i &= \sigma_V\Delta V_i - (\alpha+d_V)V_i + \beta_{HV}IV_s - s_V VV_i - hPV_i\\ &= \sigma_V\Delta V_i - (\alpha+d_V+h\frac{r_P}{s_P})V_i + \beta_{HV}IV_s - s_V VV_i - h\tilde{P}V_i\\ &= \sigma_V\Delta V_i - (\alpha+d_V+h\frac{r_P}{s_P})V_i + o(\|(V,\tilde{P})\|)\\ &= \sigma_V\Delta V_i - (\xi+mR)V_i + o(\|(V,\tilde{P})\|).\end{aligned}$$

Denote

$$o\left(\int_0^{+\infty}\max(V,\tilde{P})\right) = \underset{\|(V,\tilde{P})\|_{\mathrm{L}^\infty(\Omega\times\mathbb{R}_+^*)}\to 0}{o}\left(\int_0^{+\infty}\max(V,\tilde{P})\right)$$

and

$$o\left(\int_\Omega\int_0^{+\infty}\max(V,\tilde{P})\right) = \underset{\|(V,\tilde{P})\|_{\mathrm{L}^\infty(\Omega\times\mathbb{R}_+^*)}\to 0}{o}\left(\int_\Omega\int_0^{+\infty}\max(V,\tilde{P})\right).$$

We have

$$\left\|\frac{\int_0^{+\infty}IV_s}{\int_0^{+\infty}\max(V,\tilde{P})}\right\|_{\mathrm{L}^\infty(\Omega)} \leq \|I\|_{\mathrm{L}^\infty(\Omega\times\mathbb{R}_+^*)},$$

therefore, $\int_0^{+\infty}IV_s = o\left(\int_0^{+\infty}\max(V,\tilde{P})\right)$.

Similarly,

$$\int_0^{+\infty}VV_i = o\left(\int_0^{+\infty}\max(V,\tilde{P})\right)$$

and

$$\int_0^{+\infty}\tilde{P}V_i = o\left(\int_0^{+\infty}\max(V,\tilde{P})\right).$$

The same work can be done when integrating over Ω.

Integrating in time between 0 and $+\infty$, and because $V \underset{t\to+\infty}{\longrightarrow} 0$,

$$-V_{i,0} = \sigma_V\Delta\int_0^{+\infty}V_i - (\xi+mR)\int_0^{+\infty}V_i + o\left(\int_0^{+\infty}\max(V,\tilde{P})\right).$$

Integrating over Ω,

$$\begin{aligned}-\int_\Omega V_{i,0} = \;& \sigma_V\int_\Omega\Delta\int_0^{+\infty}V_i - \xi\int_\Omega\int_0^{+\infty}V_i - m\int_\Omega\left(R\int_0^{+\infty}V_i\right)\\ &+o\left(\int_\Omega\int_0^{+\infty}\max(V,\tilde{P})\right).\end{aligned}$$

Because of the Neumann boundary conditions,

$$\int_\Omega\Delta\int_0^{+\infty}V_i = \left[\nabla\int_0^{+\infty}V_i\right]_{\partial\Omega} = 0.$$

As a consequence,

$$m\int_\Omega\left(R\int_0^{+\infty}V_i\right)=\int_\Omega V_{i,0}-\xi\int_\Omega\int_0^{+\infty}V_i+o\left(\int_\Omega\int_0^{+\infty}\max(V,\tilde{P})\right).$$

Denote

$$o\left(\int_0^{+\infty}V_i\right)=\underset{\|(V,\tilde{P})\|_{\mathrm{L}^\infty(\Omega\times\mathbb{R}_+^*)}\to 0}{o}\left(\int_0^{+\infty}V_i\right).$$

On the other hand, using a Taylor expansion of the exponential function, the harvest verifies

$$\begin{aligned}\int_\Omega H-I_\infty&=\int_\Omega He^{-\beta_{VH}\int_0^{+\infty}V_i}\\&=\int_\Omega H\left(1-\beta_{VH}\int_0^{+\infty}V_i+o\left(\int_0^{+\infty}V_i\right)\right)\\&=\int_\Omega H-\beta_{VH}\int_\Omega\left(H\int_0^{+\infty}V_i\right)+o\left(\int_0^{+\infty}V_i\right),\end{aligned}$$

where we used the boundedness of Ω and H to get

$$\int_\Omega Ho\left(\int_0^{+\infty}V_i\right)=o\left(\int_0^{+\infty}V_i\right).$$

With $H=H^0(1-R)$,

$$\begin{aligned}&\int_\Omega H-I_\infty\\=\;&|\Omega|H^0-H^0\int_\Omega R-\beta_{VH}H^0\int_\Omega\left(\int_0^{+\infty}V_i\right)\\&+\beta_{VH}H^0\int_\Omega\left(R\int_0^{+\infty}V_i\right)+o\left(\int_0^{+\infty}V_i\right)\\=\;&|\Omega|H^0-H^0\int_\Omega R-\beta_{VH}H^0\int_\Omega\left(\int_0^{+\infty}V_i\right)\\&+\frac{\beta_{VH}H^0}{m}\left(\int_\Omega V_{i,0}-\xi\int_\Omega\int_0^{+\infty}V_i+o\left(\int_\Omega\int_0^{+\infty}\max(V,\tilde{P})\right)\right)\\&+o\left(\int_0^{+\infty}V_i\right)\\=\;&|\Omega|H^0-H^0\int_\Omega R+\frac{\beta_{VH}H^0}{m}\int_\Omega V_{i,0}\\&-\beta_{VH}H^0(1+\frac{\xi}{m})\int_\Omega\left(\int_0^{+\infty}V_i\right)+o\left(\int_0^{+\infty}V_i\right).\end{aligned}$$

We have used the uniform Harnack inequality (see [32], Theorem 2.5) to get

$$o\left(\int_\Omega\int_0^{+\infty}\max(V,\tilde{P})\right)=o\left(\int_0^{+\infty}V_i\right),$$

which also gives

$$-\sigma_V\Delta\int_0^{+\infty}V_i+(\xi+mR)\int_0^{+\infty}V_i=V_{i,0}+o\left(\int_0^{+\infty}V_i\right).$$

For a test function $\varphi \in \mathcal{C}^{2+\alpha}(\Omega)$ satisfying $\partial_n \varphi = 0$, after integrating by part,

$$\int_\Omega \left((-\sigma_V \Delta \varphi + (\xi + mR)\varphi) \int_0^{+\infty} V_i \right) = \int_\Omega \varphi V_{i,0} + o\left(\int_0^{+\infty} V_i \right).$$

We now look for solutions of

$$-\sigma_V \Delta \varphi + (\xi + mR)\varphi = 1$$

supplemented with Neumann boundary conditions.

By theorem 6.31 of [25] there exists a unique solution in $\mathcal{C}^{2+\alpha}(\Omega)$. Denote φ_R this solution. Injecting

$$\int_\Omega \left(\int_0^{+\infty} V_i \right) = \int_\Omega \varphi_R V_{i,0} + o\left(\int_0^{+\infty} V_i \right).$$

in the equation of the harvest, one gets

$$\begin{aligned} & \int_\Omega H - I_\infty + o\left(\int_0^{+\infty} V_i \right) \\ = \; & |\Omega| H^0 - H^0 \int_\Omega R + \frac{\beta_{VH} H^0}{m} \int_\Omega V_{i,0} - \beta_{VH} H^0 (1 + \frac{\xi}{m}) \int_\Omega \varphi_R V_{i,0} \\ = \; & H^0 \left(|\Omega| - \int_\Omega R \right) + \frac{\beta_{VH} H^0}{m} \left(\int_\Omega V_{i,0} - (\xi + m) \int_\Omega \varphi_R V_{i,0} \right). \end{aligned}$$

From now on, we denote

$$\eta_L(R, V_{i,0}) = H^0 \left(|\Omega| - \int_\Omega R \right) + \frac{\beta_{VH} H^0}{m} \left(\int_\Omega V_{i,0} - (\xi + m) \int_\Omega \varphi_R V_{i,0} \right),$$

the linearized harvest.

Important note: The domain of applicability for the preceding computations leading to the linearized harvest, specifically the range of parameters denoted as X where $\int_0^{+\infty} V_i$ is "sufficiently small", remains uncertain. For all the results presented in this paper, we assume that X encompasses the entire set of admissible parameters where $\lambda_1(\mathcal{L}_{V_s})$ is positive. This assumption is likely flawed, as we conjectured that $\int_0^{+\infty} V_i$ diverges as $\lambda_1(\mathcal{L}_{V_s})$ approaches zero. We acknowledge that this assumption severs the connection between the linearized harvest and the actual harvest. Nevertheless, our results (with different boundary) should still hold within a closed, convex, and bounded set. Furthermore, we know that X is not empty, as evidenced by the case where $V_0 = 0$ resulting in $\int_0^{+\infty} V_i = 0$. Supposing that X possesses non-empty interior within the space of all admissible parameters, then X contains a closed, convex, and bounded region. We hope that the existence of this region renders the assumption more acceptable. Moreover, in numerical experiments involving a biologically consistent parameter set (details available in [1] for the sources and values of the chosen parameters, except for h that we take three times smaller in order to have $\lambda_1(\mathcal{L}_{V_s})$ negative when $R = 0$), the harvest and linearized harvest are very close when $\lambda_1(\mathcal{L}_{V_s})$ is positive (even when it is small), as shown in Figure 3.2. This suggests that X covers a significant portion of the entire set of admissible parameters within the subset where $\lambda_1(\mathcal{L}_{V_s})$ is positive. In the following sections, we look for optimizers of the linearized harvest, and we hope that the numerical simulations provided suffice to convince the relevance of studying this quantity instead of the real harvest. As seen in Figures 3.3 and 3.4, when the transmission rates are larger, the two harvests become further apart, which is consistent with the fact that $\int_0^{+\infty} V_{i,0}$ becomes larger as $\beta_{HV}, \beta_{VH} \to +\infty$.

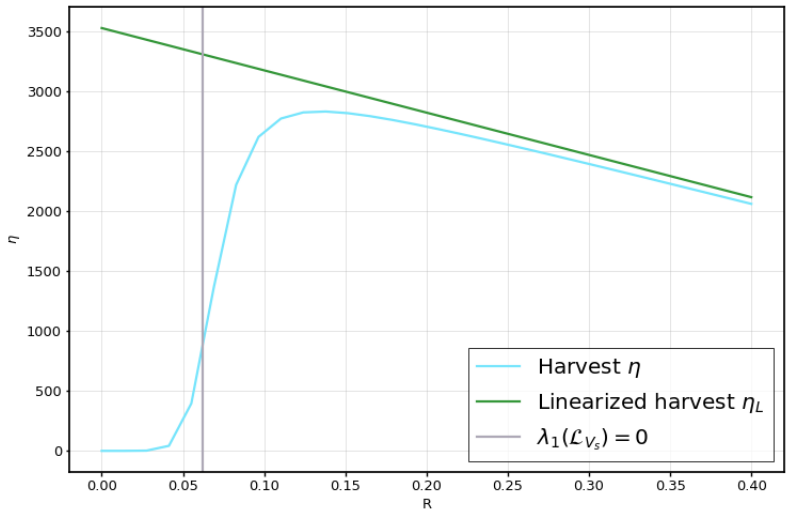

Figure 3.2: Harvest and linearized harvest in function of a constant R (with biologically consistent parameters, see [1], and h three times smaller). Explicit formula for η_L can be found in Remark 1.

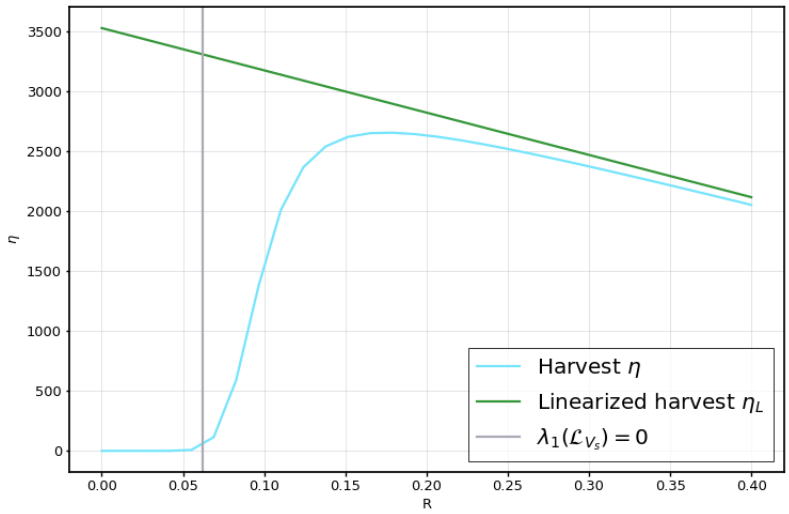

Figure 3.3: Harvest and linearized harvest in function of a constant R (with h three times smaller and β_{HV} twice as big).

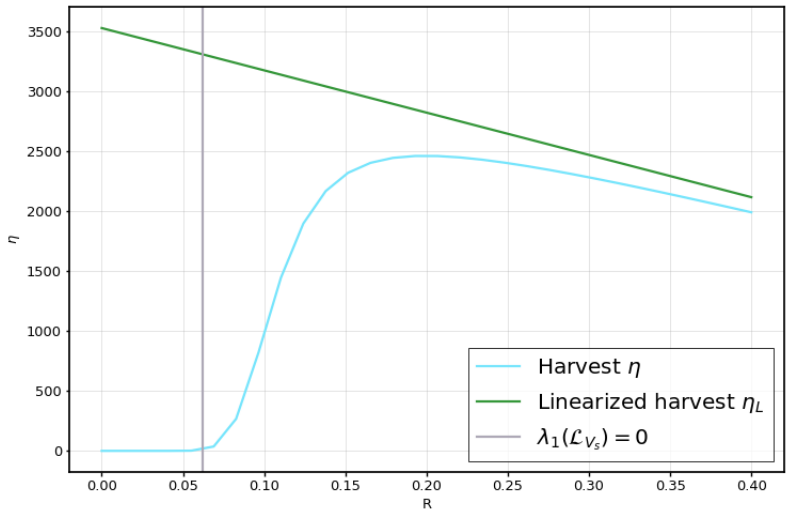

Figure 3.4: Harvest and linearized harvest in function of a constant R (with h three times smaller and β_{VH} twice as big).

Remark 1: In figure 3.2, we compute the harvest η and linearized harvest η_L in the case where R and $V_{i,0}$ are constant in space. Here, η_L is explicit since φ_R can be computed: $\varphi_R = 1/(\xi + mR)$ yields

$$\begin{aligned}\eta_L(R, V_{i,0}) &= H^0\left(|\Omega| - \int_\Omega R\right) + \frac{\beta_{VH}H^0}{m}\left(1 - \frac{\xi + m}{\xi + mR}\right)\int_\Omega V_{i,0} \\ &= H^0|\Omega|\,(1 - R) + \frac{\beta_{VH}H^0}{m}\left(\frac{mR - m}{\xi + mR}\right)|\Omega|V_{i,0} \\ &= H^0|\Omega|(1 - R)\left(1 - \frac{\beta_{VH}V_{i,0}}{\xi + mR}\right).\end{aligned}$$

Although it looks like a linear function of R, it is not. With our parameter values (see [1] for some details), $\eta_L(R) \approx 3529(1 - R)\left(1 - \frac{5.10^{-5}}{1.64 + 0,7R}\right)$. We have taken an initial condition $V_{i,0}$ of one percent of the carrying capacity of V.

Remark 2: One can observe that the harvest is positive for some negative values of $\lambda_1(\mathcal{L}_{V_s})$. This is, to our understanding, due to numerical imprecisions: when $\lambda_1(\mathcal{L}_{V_s})$, while still negative, becomes very close to 0, V_i diverges to $+\infty$ much slower (at a rate that is roughly $e^{-\lambda_1(\mathcal{L}_{V_s})t}$), therefore $e^{-\int_0^{+\infty} V_i}$ (that we approximate by computing $e^{-\int_0^T V_i}$ for a large T) becomes at a greater distance from 0. This phenomenon is less visible when we increase T, as can be observed in Figure 3.5.

We denote $\mathcal{C}_b^{2+\alpha}(\Omega)$ the space of bounded $\mathcal{C}^{2+\alpha}$ functions defined on Ω. In the proofs of Lemma 3.5.1 and Theorem 3.5.5, we use differential calculus in Banach spaces (in $\mathrm{L}^\infty(\Omega)$ and in $\mathcal{C}_b^{2+\alpha}(\Omega)$). As the computation of the partial derivative of φ_R or η_L with respect to R is usual, we freely use it without delving into its details.

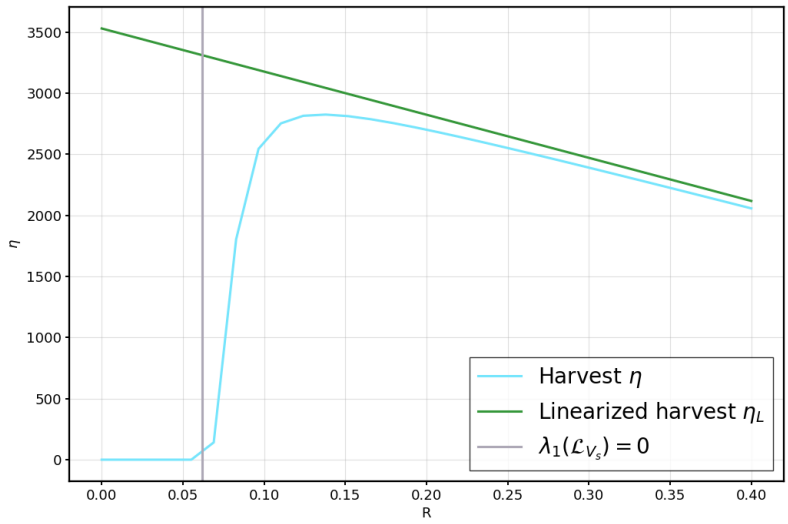

Figure 3.5: Harvest and linearized harvest in function of a constant R (with h three times smaller and T ten times bigger).

In the context of the optimization problem, the first crucial lemma is the concavity of the application $R \mapsto \eta_L(R, V_{i,0})$:

Lemma 3.5.1. *Fix $V_{i,0} \in \mathcal{C}^{2+\alpha}(\Omega)$. Then, the application*

$$\begin{cases} \mathcal{C}_b^{2+\alpha}(\Omega) & \to & \mathbb{R} \\ R & \mapsto & \eta_L(R, V_{i,0}) \end{cases}$$

is concave and coercive : $\eta_L(R, V_{i,0}) \underset{\|R\|_{\mathcal{C}_b^{2+\alpha}(\Omega)} \to +\infty}{\longrightarrow} -\infty$.

Proof. By Lemma 1.4 of Chapter 3 of [54] applied on

$$-\sigma_V \Delta \varphi_R + (\xi + mR)\varphi_R = 1,$$

the function φ_R is positive in Ω.

By the same lemma, we obtain consequently the negativity of $\partial_R \varphi_R$, solving

$$-\sigma_V \Delta \partial_R \varphi_R + (\xi + mR)\partial_R \varphi_R = -m\varphi_R,$$

and the positivity of $\partial_R^2 \varphi_R$ in Ω. The application $R \mapsto \eta_L(R, V_{i,0})$ is hereby concave.

The linearized harvest has the following form:

$$\eta_L(R, V_{i,0}) = C_1 + C_2 \int_\Omega V_{i,0} - C_3 \int_\Omega R - C_4 \int_\Omega \varphi_R V_{i,0},$$

with $C_1, C_2, C_3, C_4 > 0$. Hence, to prove its coercivity, it suffices to show the boundedness of $\int_\Omega \varphi_R V_{i,0}$ when $\|R\|_{\mathcal{C}_b^{2+\alpha}(\Omega)} \to +\infty$. By nonnegativity of m and R, $1/\xi$ is a supersolution of the Neumann system solved by φ_R, hence $\varphi_R \leq 1/\xi$ and the coercivity of η_L follows.

□

Comment: The concavity of $R \mapsto \eta_L(R, V_{i,0})$ gives interesting insights on the optimal refuge, $R^L_{\text{opt}} := \underset{R \in \mathcal{C}^{2+\alpha}(\Omega,[0,1])}{\text{argmax}} \eta_L(R, V_{i,0})$. For instance, there exists β_{VH} small enough such that

$$\partial_R \eta_L = -H^0 \int_\Omega \cdot - \beta_{VH} H^0 (1 + \frac{\xi}{m}) \int_\Omega \partial_R \varphi_R V_{i,0}.$$

is negative, and in this case $R^L_{\text{opt}} \equiv 0$. Conversely, there exists β_{VH} large enough such that $\partial_R \eta_L$ is positive (by negativity of $\partial_R \varphi_R$), and in this case $R^L_{\text{opt}} \not\equiv 0$. The same comment can be made with $\|V_{i,0}\|$ instead of β_{VH}.

A natural question can arise on the convergence of the linearized harvest when the frequency of the refuge goes to infinity. We answer the question in the following proposition.

Proposition 3.5.2. *In the context of the homogenization problem (see Section 3 for the details),*

$$\eta_L(R_n, V_{i,0}) \underset{n \to +\infty}{\longrightarrow} \eta_L(\mathcal{R}, V_{i,0}).$$

Proof. The proof lies in the fact that $\int_\Omega \varphi_{R_n} V_{i,0} \underset{n \to +\infty}{\longrightarrow} \int_\Omega \varphi_{\mathcal{R}} V_{i,0}$.

Integrating

$$-\sigma_V \Delta \varphi_{R_n} + (\xi + m R_n) \varphi_{R_n} = 1,$$

one gets

$$\begin{aligned} \xi \int_\Omega \varphi_{R_n} &= |\Omega| - m \int_\Omega R_n \varphi_{R_n} \\ &\leq |\Omega|. \end{aligned}$$

Multiplying the equation on φ_{R_n} by φ_{R_n} and integrating over Ω, one gets

$$\sigma_V \int_\Omega |\nabla \varphi_{R_n}|^2 + \int_\Omega (\xi + m R_n) \varphi_{R_n}^2 = \int_\Omega \varphi_{R_n} \leq |\Omega|/\xi,$$

hence the uniform boundedness of $\|\varphi_{R_n}\|_{\mathrm{H}^1(\Omega)}$. A direct application of the Rellich–Kondrachov theorem yields, up to extraction, the strong L^2-convergence of φ_{R_n} to $\overline{\varphi}$.

Let $\psi \in \mathcal{C}^{2+\alpha}(\Omega)$. Multiplying the equation on φ_{R_n} by ψ and integrating over Ω, one gets

$$-\sigma_V \int_\Omega \psi \Delta \varphi_{R_n} + \int_\Omega (\xi + m R_n) \psi \varphi_{R_n} = \int_\Omega \psi$$

and two integration by parts followed by passing to the limit $n \to +\infty$ yields

$$-\sigma_V \int_\Omega \Delta \psi \overline{\varphi} + \int_\Omega (\xi + m \mathcal{R}) \psi \overline{\varphi} = \int_\Omega \psi.$$

By uniqueness of the weak solution of this equation, $\overline{\varphi} = \varphi_{\mathcal{R}}$. □

3.5.2 Schwarz rearrangement

In this section, we assume that $\Omega \subset \mathbb{R}^d$ is symmetric. In order to alleviate the proofs, we will further assume that $d = 1$, hence $\Omega = [-L, L]$, $L > 0$. However, it is not, as far as we know, a necessary assumption. For an arbitrary $f \in \mathrm{L}^\infty(\Omega)$, we will denote by f_* the decreasing Schwarz rearrangement of f, which is a symmetric, radially nonincreasing function that preserves the measures of the level sets of f (see [67] and [68] for a thorough definition of the Schwarz rearrangement). With our assumptions on Ω, f_* also belongs in $\mathrm{L}^\infty(\Omega)$.

We call the increasing Schwarz rearrangement of f, and denote f^*, the application

$$f^* : \left\{ \begin{array}{ccc} \Omega & \to & \mathbb{R} \\ x & \mapsto & f_*(L - |x|). \end{array} \right.$$

Our main theorem states that, if $V_{i,0}$ is its own decreasing Schwarz rearrangement and is decreasing, then the optimal refuge for the linearized harvest is not constant, and there exists a refuge that is its own decreasing Schwarz rearrangement which yields a better linearized harvest than the constant refuge. The same proof also works if $V_{i,0}$ is its own increasing Schwarz rearrangement and is increasing, and the result would be that the optimal refuge for the linearized harvest is not constant, and there exists a refuge that is its own increasing Schwarz rearrangement which yields a better linearized harvest than the constant refuge.

Theorem 3.5.3 (Theorem 3.2.2)**.** *Denote, for $c > 0$,*
$\mathcal{M}_c(\Omega) = \{f \in \mathcal{C}^{2+\alpha}(\overline{\Omega}, [0,1]),\ \|f\|_{\mathrm{L}^1} = c\}$.
Fix $V_{i,0} \in \mathcal{C}^{2+\alpha}(\Omega)$ and $\mathcal{R} > 0$. Let us assume that $V_{i,0} = (V_{i,0})_*$ and is radially decreasing. Then,

$$\eta_L(\mathcal{R}, V_{i,0}) \neq \max_{R \in \mathcal{M}_{|\Omega|\mathcal{R}}(\Omega)} \eta_L(R, V_{i,0}).$$

Moreover, there exists $R \in \mathcal{M}_{|\Omega|\mathcal{R}}(\Omega)$ such that $R = R_*$ and $\eta_L(R, V_{i,0}) > \eta_L(\mathcal{R}, V_{i,0})$.

Proof. Recall that

$$\eta_L(R, V_{i,0}) = H^0\left(|\Omega| - \int_\Omega R\right) + \frac{\beta_{VH} H^0}{m}\left(\int_\Omega V_{i,0} - (\xi + m)\int_\Omega \varphi_R V_{i,0}\right),$$

hence the quantity we aim to minimize is

$$\int_\Omega \varphi_R V_{i,0}$$

with

$$-\sigma_V \varphi_R'' + (\xi + mR)\varphi_R = 1.$$

Let $\tilde{R} \in \mathcal{M}_0(\Omega)$. Denote $\psi : \varepsilon \mapsto \varphi_{\mathcal{R}+\varepsilon\tilde{R}} \in \mathcal{C}^2([0, +\infty), \mathcal{M}_{|\Omega|\mathcal{R}}(\Omega))$ and $u = \psi'(0)$. Then, for all $\varepsilon > 0$, $\varphi_{\mathcal{R}+\varepsilon\tilde{R}} = \varphi_{\mathcal{R}} + \varepsilon u + o(\varepsilon)$. With $\varphi_{\mathcal{R}} = 1/(\xi + m\mathcal{R})$, injecting this Taylor expansion in the equation of $\varphi_{\mathcal{R}+\varepsilon\tilde{R}}$, one gets, at first order,

$$-\sigma_V(\varphi_{\mathcal{R}} + \varepsilon u)'' + (\xi + m(\mathcal{R} + \varepsilon\tilde{R}))(\varphi_{\mathcal{R}} + \varepsilon u) = 1,$$

hence, dividing by ε and letting it go to 0,

$$-\sigma_V u'' + (\xi + m\mathcal{R})u = -m\tilde{R}/(\xi + m\mathcal{R}).$$

By Schwarz theorem, $u_{|\partial\Omega} = \dfrac{\partial}{\partial\varepsilon}((\varphi_{\mathcal{R}+\varepsilon\tilde{R}})_{|\partial\Omega})(0)$. Solving this ordinary differential equation with Neumann boundary conditions on $\Omega = [-L, L]$ with $\tilde{R}(x) = \cos\left(\dfrac{\pi}{L}x\right)$, one gets

$$u(x) = \frac{-m}{(\xi + m\mathcal{R})(\xi + m\mathcal{R} + \sigma_V(\pi/L)^2)}\cos\left(\frac{\pi}{L}x\right).$$

By symmetry of u and $V_{i,0}$,

$$\int_\Omega u V_{i,0} = 2\int_0^{L/2} u V_{i,0} + 2\int_{L/2}^{L} u V_{i,0}.$$

Because $u(L/2-x) = -u(L/2+x)$ for all $x \in [0, L/2]$, after a change of variable, one gets

$$\int_0^{L/2} uV_{i,0} = -\int_{L/2}^{L} u(x)V_{i,0}(L-x)\mathrm{d}x$$

and therefore, because $V_{i,0}$ is decreasing on $[0, L]$,

$$\int_\Omega uV_{i,0} = 2\int_{L/2}^{L} u(x)(V_{i,0}(x) - V_{i,0}(L-x))\mathrm{d}x < 0.$$

Moreover,

$$\int_\Omega \varphi_{\mathcal{R}+\varepsilon\tilde{R}}V_{i,0} = \int_\Omega \varphi_{\mathcal{R}}V_{i,0} + \varepsilon\int_\Omega uV_{i,0} + o(\varepsilon),$$

hence for a small enough ε, $\int_\Omega \varphi_{\mathcal{R}+\varepsilon\tilde{R}}V_{i,0} < \int_\Omega \varphi_{\mathcal{R}}V_{i,0}$, i.e $\eta_L(\mathcal{R}+\varepsilon\tilde{R}, V_{i,0}) > \eta_L(\mathcal{R}, V_{i,0})$. One can easily verify that $\mathcal{R}+\varepsilon\tilde{R} \in \mathcal{M}_{|\Omega|\mathcal{R}}(\Omega)$ and $(\mathcal{R}+\varepsilon\tilde{R})_* = \mathcal{R}+\varepsilon\tilde{R}$.

□

The next corollary is similar: if we fix the refuge R, and if R is its own Schwarz rearrangement, then the optimal $V_{i,0}$ for the linearized harvest is its own Schwarz rearrangement.

Corollary 3.5.4. *Fix $R \in \mathcal{C}^{2+\alpha}(\Omega)$.*
Denote, for $c_1, c_2 > 0$, $\mathcal{M}_{c_1,c2}(\Omega) = \{f \in \mathrm{L}^\infty(\Omega),\ \|f\|_{\mathrm{L}^1} = c_1,\ \|f\|_{\mathrm{L}^\infty} \leq c_2\}$. The quantities

$$m_V := \min_{V_{i,0}\in\mathcal{M}_{c_1,c_2}(\Omega)} \eta_L(R, V_{i,0})$$

and

$$M_V := \max_{V_{i,0}\in\mathcal{M}_{c_1,c_2}(\Omega)} \eta_L(R, V_{i,0})$$

exist. Moreover, if $R = R_*$ and is not constant, then

$$\{V_{i,0} \in \mathcal{M}_{c_1,c2}(\Omega),\ \eta_L(R, V_{i,0}) = m_V\} \subset \{V_{i,0} \in \mathcal{M}_{c_1,c2}(\Omega),\ V_{i,0} = (V_{i,0})^*\}$$

and

$$\{V_{i,0} \in \mathcal{M}_{c_1,c2}(\Omega),\ \eta_L(R, V_{i,0}) = M_V\} \subset \{V_{i,0} \in \mathcal{M}_{c_1,c2}(\Omega),\ V_{i,0} = (V_{i,0})_*\}.$$

Proof. With this set of constraints, one optimizes η_L by optimizing the quantity $\int_\Omega \varphi_R V_{i,0}$. Let $(\underline{V}_n)$ be a minimizing sequence, and $(\overline{V}_n)$ be a maximizing sequence of $V \mapsto \int_\Omega \varphi_R V$. The set $\mathcal{M}_{c_1,c_2}(\Omega)$ is a closed, convex and bounded subset of $\mathrm{L}^\infty(\Omega)$, therefore it is weakly compact. Hence, up to an extraction, the sequences converge to $\underline{V}_\infty, \overline{V}_\infty \in \mathcal{M}_{c_1,c_2}$ minimizing and maximizing η_L.

Let us suppose that $R = R_*$. By positivity of the principal eigenvalue of $-\sigma_V\Delta + \xi + mR$, the energy

$$\mathcal{E} : \left\{ \begin{array}{rcl} \mathcal{C}^{2+\alpha}(\Omega, \mathbb{R}_+) & \to & \mathbb{R} \\ u & \mapsto & \frac{1}{2}\left(\int_\Omega \sigma_V|\nabla u|^2 + (\xi + mR)u^2\right) - \int_\Omega u \end{array} \right.$$

is coercive, therefore φ_R is the unique minimizer of $\mathcal{E}$.

Moreover, by the general rearrangement inequality (see e.g Theorem 3.4 of [12]), for all $u \in \mathcal{C}^{2+\alpha}(\Omega, \mathbb{R}_+)$ and for a large constant $C > 0$,

$$\int_\Omega (C-R)^*(u^*)^2 \geq \int_\Omega (C-R)u^2.$$

By the fifth property of part 3 of [68] (page 10),

$$\int_\Omega (u^*)^2 = \int_\Omega u^2,$$

which yields

$$\int_\Omega R(u^*)^2 \leq \int_\Omega Ru^2.$$

By the Pólya–Szegő inequality (see [67]), for all $u \in \mathcal{C}^{2+\alpha}(\Omega, \mathbb{R}_+)$,

$$\int_\Omega |\nabla u^*|^2 \leq \int_\Omega |\nabla u|^2.$$

The previous inequalities yield, for all $u \in \mathcal{C}^{2+\alpha}(\Omega, \mathbb{R}_+)$,

$$\mathcal{E}(u^*) \leq \mathcal{E}(u),$$

hence, by uniqueness of the minimizer of $\mathcal{E}$, $\varphi_R = \varphi_R^*$.

By Talenti inequalities [67], for all $V_{i,0} \in \mathcal{M}_{c_1,c_2}(\Omega)$,

$$\int_\Omega \varphi_R V_{i,0} \leq \int_\Omega \varphi_R (V_{i,0})^*$$

and

$$\int_\Omega \varphi_R V_{i,0} \geq \int_\Omega \varphi_R (V_{i,0})_*.$$

Let $V_{i,0} \in \mathcal{M}_{c_1,c_2}(\Omega)$ such that $\eta_L(R, V_{i,0}) = m_V$. Then $V_{i,0}$ maximizes the quantity $\int_\Omega \varphi_R V_{i,0}$. By the first inequality above,

$$\int_\Omega \varphi_R V_{i,0} = \int_\Omega \varphi_R (V_{i,0})^*.$$

By our assumption on R, φ_R is increasing. By [31], $V_{i,0} = (V_{i,0})^*$. The case $\eta_L(R, V_{i,0}) = M_V$ is treated identically, with φ_R being decreasing. □

3.5.3 Explicit optimizers in the homogeneous case

In this section, we assume that, for all $x \in \Omega$, $V_{i,0}(x)$ follows a given probability distribution $\mathbb{P}_x$ on $\mathbb{R}_+$, such that its mean $x \mapsto \mathbb{E}[V_{i,0}(x)]$ is known and homogeneous in space. Since this section is not intended to focus on probability concepts, we intentionally refrain from delving into a rigorous definition of this probability distribution. The biological rationale for this approximation is as follows: the primary provenance of aphids in the field is wind dispersal. Aphids transported by the wind cover distances significantly greater than the size of an average beet field, making it reasonable to employ a uniform mean for initially infected vectors.

The mean of the linearized harvest is

$$\begin{aligned} & \mathbb{E}[\eta_L(R, V_{i,0})] \\ = \; & H^0 \left(|\Omega| - \int_\Omega R \right) + \frac{\beta_{VH} H^0}{m} \left(\int_\Omega \mathbb{E}[V_{i,0}] - (\xi + m) \int_\Omega \varphi_R \mathbb{E}[V_{i,0}] \right) \end{aligned}$$

We prove in the following that the constant refuge $\mathcal{R}$ is optimal, for the mean of the linearized harvest $\mathbb{E}[\eta_L]$, in the space of real bounded $\mathcal{C}^{2+\alpha}$ functions defined on Ω we denote $\mathcal{C}_b^{2+\alpha}(\Omega, \mathbb{R})$. Note that rather than assuming a constant mean for $V_{i,0}$ in space, an alternative approach is to assume $V_{i,0}$ itself to be constant. This would yield a similar result, asserting that a constant refuge maximizes the linearized harvest. The choice of using the mean is purely biological; it renders the assumption about the initial condition more realistic, since having $V_{i,0}$ constant in space appears highly unlikely in real-life scenarios.

Theorem 3.5.5 (Theorem 3.2.3)**.** *Suppose that $x \mapsto \mathbb{E}[V_{i,0}]$ is constant. Let $\mathcal{R} = \left(\frac{\sqrt{\beta_{VH}(\xi + m)\mathbb{E}[V_{i,0}]} - \xi}{m} \right)^+$. Then*

$$\mathbb{E}[\eta_L(\mathcal{R}, V_{i,0})] = \max_{R \in \mathcal{C}_b^{2+\alpha}(\Omega, \mathbb{R})} \mathbb{E}[\eta_L(R, V_{i,0})]$$

Proof. First of all, by Lemma 3.5.1, the application $R \mapsto \eta_L(R, V_{i,0})$ is concave and coercive, which immediately yields the existence and uniqueness of the maximizer of η_L, which nullifies $\partial_R \mathbb{E}[\eta_L(R, V_{i,0})] = \partial_R \eta_L(R, \mathbb{E}[V_{i,0}])$.

Let $R \in \mathcal{C}_b^{2+\alpha}(\Omega, \mathbb{R})$ so that $\partial_R \mathbb{E}[\eta_L(R, V_{i,0})] = 0$, and let $\zeta \in \mathcal{C}_b^{2+\alpha}(\Omega, \mathbb{R})$. We have

$$\begin{aligned} \partial_R \mathbb{E}[\eta_L(R, V_{i,0})] \cdot \zeta &= -H^0 \textstyle\int_\Omega \zeta - \beta_{VH} H^0 (1 + \frac{\xi}{m}) \mathbb{E}[V_{i,0}] \int_\Omega \partial_R \varphi_R \zeta \\ &= 0, \end{aligned}$$

hence

$$\int_\Omega \partial_R \varphi_R \zeta = -\frac{m}{\beta_{VH}(\xi + m)\mathbb{E}[V_{i,0}]} \int_\Omega \zeta$$

Denote $C = -\frac{m}{\beta_{VH}(\xi + m)\mathbb{E}[V_{i,0}]}$. There exists a sequence of step functions (ψ_k) such that $\|\psi_k - \partial_R \varphi_R \zeta\|_{\mathrm{L}^2} \to 0$. Let h be a function in $\mathrm{L}^2(\Omega)$.

$$\begin{aligned} |\textstyle\int_\Omega (\psi_k - C)h| &= |\textstyle\int_\Omega (\psi_k - \partial_R \varphi_R \zeta + \partial_R \varphi_R \zeta - C)h| \\ &= |\textstyle\int_\Omega (\psi_k - \partial_R \varphi_R \zeta)h| \\ &\leq \|\psi_k - \partial_R \varphi_R \zeta\|_{\mathrm{L}^2} \sqrt{\textstyle\int_\Omega h^2} \\ &\underset{k \to +\infty}{\longrightarrow} 0. \end{aligned}$$

We have shown the weak convergence in L^2 of (ψ_k) to C. By uniqueness of the limit,

$$\partial_R \varphi_R \zeta = C.$$

By differentiating the equation on φ_R with respect to R, one gets

$$-\sigma_V \Delta \partial_R \varphi_R \zeta + (\xi + mR)\partial_R \varphi_R \zeta = -m \varphi_R \zeta,$$

therefore

$$\varphi_R = \frac{\xi + mR}{\beta_{VH}(\xi + m)\mathbb{E}[V_{i,0}]}.$$

Plugging the expression of φ_R into its equation, it yields

$$\begin{cases} -\sigma_V m \Delta R + (\xi + mR)^2 = \beta_{VH}(\xi + m)\mathbb{E}[V_{i,0}] \\ \partial_n R = 0. \end{cases}$$

By uniqueness of the solution of this elliptic problem with Neumann boundary conditions (see e.g Section 3.3 of [54]), we deduce

$$R = \frac{\sqrt{\beta_{VH}(\xi + m)\mathbb{E}[V_{i,0}]} - \xi}{m}.$$

Reciprocally, if $R = \dfrac{\sqrt{\beta_{VH}(\xi+m)\mathbb{E}[V_{i,0}]}-\xi}{m}$, following the proof backwards, it is clear that $\partial_R \mathbb{E}[\eta_L(R, V_{i,0})] = 0$. If this quantity is negative, i.e if $\beta_{VH}(\xi+m)\mathbb{E}[V_{i,0}] < \xi^2$, then a straightforward computation yields

$$\partial_R \mathbb{E}[\eta_L(0, V_{i,0})] \cdot \zeta = -H^0 \int_\Omega \zeta + \beta_{VH} H^0 (1 + \frac{\xi}{m}) \mathbb{E}[V_{i,0}] \frac{m}{\xi^2} \int_\Omega \zeta < 0.$$

Therefore, in this case, the optimal refuge is 0. □

Remark: We just proved that, if $V_{i,0}$ is constant, then $\partial_R \eta_L = 0 \iff R = \mathcal{R}$. With a very similar proof, we can obtain that, if R is constant, then $\partial_R \eta_L = 0 \iff V_{i,0} = \dfrac{(\xi+mR)^2}{\beta_{VH} m(1+\xi/m)}$. We deduce that, if R is constant and $V_{i,0}$ is not constant, then $\eta_L(R, V_{i,0})$ is not optimal.

Chapter 4

Spreading properties of the solutions of an ODE-PDE agro-ecological model in a spatially periodic one-dimensional crop field

4.1 Introduction

In this mostly heuristic chapter, we consider the same system of equations as before but in a spatially extended one-dimensional crop field with periodically arranged refuges. Spatially extended frameworks are best suited to investigate the spreading properties of solutions of reaction–diffusion models. In our case, spreading occurs when the agro-ecological control strategy fails and the aphids proliferate. From the viewpoint of applications, the field should be spatially two-dimensional instead of one-dimensional, yet it is well-known that a good understanding of the one-dimensional case is a prerequisite for the multi-dimensional case regarding spreading properties. In fact, it will be clear after reading the forthcoming discussion that the one-dimensional case is already rich enough to warrant a specific discussion.

One of our main goals is to investigate for a new quantitative criterion, namely spreading speeds, the optimality of the homogenized crop field control strategy.

Rigorous results in this chapter are sparse and it should be understood instead as an informal discussion on what to expect. The system under consideration mixes several technical difficulties – degenerate ellipticity, spatial periodicity, non-monotonicity, shifting reaction terms, to name just a few – which make the rigorous analysis quite complex. In this PhD manuscript it is left as a perspective.

4.1.1 The model

More precisely, we consider the following system, where all the parameters are either positive constants or 1-periodic positive functions in $\mathcal{C}^{2+\alpha}(\mathbb{R})$ (whenever their $x-$dependency is speci-

fied):

$$\left\{\begin{array}{lcl} \partial_t I &=& \beta_{VH}(H(x)-I)V_i, \\ \partial_t V_i &=& \sigma_V \partial_{xx} V_i + \beta_{HV} I(V-V_i) - \alpha V_i - d_V(x)V_i - s_V V V_i - hPV_i, \\ \partial_t V &=& \sigma_V \partial_{xx} V + r_V(x)V - s_V V^2 - hPV, \\ \partial_t P &=& \sigma_P \partial_x \left(r_P(x) \partial_x \left(\dfrac{P}{r_P(x)} \right) \right) + \gamma hPV + r_P(x)P - s_P P^2, \end{array}\right. \tag{4.1}$$

in $\mathbb{R} \times \mathbb{R}_+^*$, where we omitted the dependency on (x,t) for I, V_i, V and P, with initial conditions:

$$(I, V_i, V, P)(\cdot, 0) = (0, V_{i,0}, V_0, P_0) \quad \text{in } \mathbb{R}.$$

4.1.2 Standing assumptions

Since we are interested in solutions starting from perturbations of the vector-free equilibrium $(0,0,0,r_P/s_P)$, we set $P = r_P/s_P + \tilde{P}$, $P_0 = r_P/s_P + \tilde{P}_0$, and rewrite accordingly the system:

$$\left\{\begin{array}{lcl} \partial_t I &=& \beta_{VH}(H(x)-I)V_i, \\ \partial_t V_i &=& \sigma_V \partial_{xx} V_i + \beta_{HV} I(V-V_i) - \alpha V_i - d_V(x)V_i - s_V V V_i \\ && - \frac{hr_P(x)}{s_P} V_i - h\tilde{P}V_i, \\ \partial_t V &=& \sigma_V \partial_{xx} V + r_V(x)V - s_V V^2 - \frac{hr_P(x)}{s_P} V - h\tilde{P}V, \\ \partial_t \tilde{P} &=& \sigma_P \partial_x \left(r_P(x) \partial_x \left(\dfrac{\tilde{P}}{r_P(x)} \right) \right) + \frac{\gamma h r_P(x)}{s_P} V + \gamma h \tilde{P} V \\ && - s_P \tilde{P} \left(\frac{r_P(x)}{s_P} + \tilde{P} \right). \end{array}\right. \tag{4.2}$$

It is known [7] that the equation

$$\sigma_V \partial_{xx} V + \left(r_V(x) - \frac{hr_P(x)}{s_P} \right) V - s_V V^2 = 0.$$

admits a positive 1-periodic solution $V_* \in \mathcal{C}^2(\mathbb{R})$ if, and only if, the periodic principal eigenvalue of the linearized operator at $V = 0$ is negative, namely

$$\lambda_1 \left(-\sigma_V \partial_{xx} - \left(r_V(x) - \frac{hr_P(x)}{s_P} \right) \right) < 0.$$

Moreover, in such a case, the positive solution is unique. In our model, by straightforward analogy with the Neumann case studied in [1], this condition is the necessary and sufficient condition for the non-extinction of V. Therefore in this chapter it is a standing assumption.

We can now make the assumptions on the initial conditions precise: we assume that V_0, $V_{i,0}$ and $\tilde{P}_0$ are compactly supported and satisfy the following bounds:

$$0 \leq V_{i,0} \leq V_0 \leq V_*, \quad 0 \leq \tilde{P}_0.$$

Moreover, in order to study a nontrivial epidemiological situation, we assume $V_{i,0} \neq 0$. Under such conditions, it is expected that V_i, V and $\tilde{P}$ spread in the field.

4.1.3 The long-time behavior, locally in space

The long-time behavior of (4.1) (or, equivalently, (4.2)) in, say, a fixed compact subset K of $\mathbb{R}$ is elusive. Adapting to the space periodic framework the proofs of [1], we could readily establish the following:

$$\liminf_{t \to +\infty} \inf_{x \in K} V(x,t) \geq \liminf_{t \to +\infty} \inf_{x \in K} V_i(x,t) > 0,$$

$$\liminf_{t\to+\infty} \inf_{x\in K} \tilde{P}(x,t) > 0,$$
$$\lim_{t\to+\infty} \sup_{x\in K} |I(x,t) - H(x)| = 0.$$

Actually, apart from I, the convergence is far from clear. It is indeed well-known that predator–prey systems lead in some cases to stable time-periodic oscillations, and that spatial diffusion tends to transform time periodic cycles into space-time periodic wave trains.

This is why we introduce in the next subsection an approach of spreading properties compatible with loose persistence properties, that does not require convergence to a steady state in the wake of the front. This approach is now standard in reaction–diffusion theory.

4.1.4 Definition of the spreading speed and formula in the space periodic KPP case

Let $u(x,t)$ be a nonnegative function for $x \in \mathbb{R}$, $t > 0$. We define the *spreading speed* of u as, when it exists, the number $c^u_* \in \mathbb{R}$ such that:

1. For every $c > c^u_*$,
$$\lim_{t\to+\infty} \sup_{|x|>ct} [u(x,t)] = 0,$$
2. For every $c < c^u_*$,
$$\liminf_{t\to+\infty} \inf_{|x|<ct} [u(x,t)] > 0.$$

We refer to [71, 8] for greater details on the construction of c^u_* in the case where u is the solution of a Fisher-KPP type equation with space periodic coefficients. In this case, for example when u is a solution with compactly supported initial value of

$$\partial_t u - \sigma \partial_{xx} u = r(x)u - su^2,$$

then

$$c^u_* = \min_{\mu>0} \frac{-\lambda_1(\mathcal{L}_\mu)}{\mu},$$

where $\lambda_1(\mathcal{L}_\mu)$ designates the principal eigenvalue of the operator

$$\mathcal{L}_\mu = -\sigma\partial_{xx} + 2\sigma\mu\partial_x - \sigma\mu^2 - r(x).$$

This formula is indeed a KPP-type formula: when r is actually constant, it reduces to:

$$c^u_* = \min_{\mu>0} \frac{\sigma\mu^2 + r}{\mu} = 2\sqrt{\sigma r}.$$

4.2 Conjectures for the spreading speeds of the populations

In the following, the *ecological invasion* refers to the invasion of the vector population density V and to the afferent change in predator population density P. In contrast, the *epidemiological invasion* refers to the invasion of the infected vector population V_i and infected host population I.

From (4.1) or (4.2), it is clear that the problem has a triangular structure: the ecological invasion is independent from the epidemiological invasion. It is therefore convenient to consider the ecological invasion first.

4.2.1 The ecological invasion

The system solved by (V, P) is the following:

$$\begin{cases} \partial_t V - \sigma_V \partial_{xx} V &= r_V(x)V - s_V V^2 - hPV, \\ \partial_t P - \sigma_P \overline{\mathcal{L}}(P) &= r_P(x)P - s_P P^2 + \gamma hVP, \end{cases} \tag{4.3}$$

where $\overline{\mathcal{L}}(P) = \partial_x \left(r_P \partial_x (P/r_P) \right)$.

By the initial condition on P (see [1]), $P \geq r_P/s_P$, *i.e.* $\tilde{P} \geq 0$, hence V admits a supersolution $\overline{V}$ solving a Fisher-KPP type equation

$$\partial_t \overline{V} - \sigma_V \partial_{xx} \overline{V} = r_V(x)\overline{V} - s_V \overline{V}^2 - h r_P(x)/s_P \overline{V}$$

with compactly supported initial value. This yields the rigorous estimate $c_*^V \leq c_*^{\overline{V}}$ (provided c_*^V exists indeed), where, by [71, 8],

$$c_*^{\overline{V}} = \min_{\mu > 0} \frac{-\lambda_1(-\sigma_V \partial_{xx} + 2\sigma_V \mu \partial_x - \sigma_V \mu^2 - r(x) + h r_P(x)/s_P)}{\mu}.$$

In the spatially homogeneous case, Pan and Lin [53, Lemma 4] state that the predator population increases with the prey population, and that the prey population invades at its linearly determined speed. More precisely, if all coefficients in (4.3) are constant, then the following equalities are all true:

$$c_*^V = c_*^{\tilde{P}} = c_*^{\overline{V}} = 2\sqrt{\sigma_V (r_V - h r_P/s_P)}.$$

Having in mind the formula presented above for the spreading speed of a scalar KPP-type equation in space periodic media, this leads to our first conjecture.

Conjecture 4.2.1. *The spreading speeds c_*^V and $c_*^{\tilde{P}}$ are well-defined and satisfy:*

$$c_*^V = c_*^{\tilde{P}} = \min_{\mu > 0} \frac{-\lambda_1(-\sigma_V \partial_{xx} + 2\sigma_V \mu \partial_x - \sigma_V \mu^2 - r(x) + h r_P(x)/s_P)}{\mu}.$$

Let us point out that Madec et al. [47] studied the existence of traveling waves for a related type of prey-predator interaction with homogeneous coefficients.

4.2.2 The epidemiological invasion

The idea is to use, as in [43], the fact that V is now a function relatively well understood, combined with the underlying cooperative interaction between I and V_i.

In order to ease the reading, we set:

$$W = \begin{pmatrix} I \\ V_i \end{pmatrix}.$$

A straightforward computation yields

$$\begin{aligned} \partial_t W = \; & \begin{pmatrix} 0 & 0 \\ 0 & \sigma_V \end{pmatrix} \partial_{xx} W + \begin{pmatrix} 0 & \beta_{VH} H \\ \beta_{HV} V & -\alpha - d_V - s_V V - \frac{h r_P}{s_P} - h\tilde{P} \end{pmatrix} W \\ & - \begin{pmatrix} \beta_{VH} V_i \\ \beta_{HV} I \end{pmatrix} \circ W, \end{aligned} \tag{4.4}$$

where $\circ : \mathbb{R}^2 \times \mathbb{R}^2 \to \mathbb{R}^2$ denotes the multiplication coordinate by coordinate (also known as the Hadamard product).

Neglecting second-order terms, we find a space-time heterogeneous linear system:

$$\partial_t W = \begin{pmatrix} 0 & 0 \\ 0 & \sigma_V \end{pmatrix} \partial_{xx} W + \begin{pmatrix} 0 & \beta_{VH} H \\ \beta_{HV} V & -\alpha - d_V - s_V V - \frac{h r_P}{s_P} - h\tilde{P} \end{pmatrix} W. \tag{4.5}$$

This linear system is cooperative at every (x,t). Since the second-order terms in (4.4) are negative, we can use the solution W of (4.4) as a sub-solution for (4.5) and deduce that the solution $\overline{W}$ of (4.5) satisfies, globally in time and space, $\overline{W} \geq W$. Consequently, if both spreading speeds are well-defined, then $c_*^W \leq c_*^{\overline{W}}$ is a rigorous estimate.

Nevertheless, (4.5) has two quite different regimes:

- where $\frac{|x|}{t} > c_*^V + \varepsilon$, $V \sim 0$, $\tilde{P} \sim 0$, and the cooperative system is triangular;
- where $\frac{|x|}{t} < c_*^V - \varepsilon$, $V \gg 0$, $\tilde{P} \gg 0$, and the cooperative system is *fully coupled*, that is the coupling between I and V_i is irreducible.

Hence it is not straightforward to derive its spreading properties. Indeed this problem is related to climate change reaction–diffusion models that have been the object of an ongoing literature for more than a decade. Due to the loss of irreducibility in $\frac{|x|}{t} > c_*^V + \varepsilon$, it is not even clear at this point that I and V_i spread indeed at the same speed.

To argue in favor of a joint invasion at a unique speed, we have to consider the periodic principal eigenvalues. It turns out that in the triangular regime, it can be expressed simply:

$$\lambda_1 \left[-\begin{pmatrix} 0 & 0 \\ 0 & \sigma_V \end{pmatrix} \partial_{xx} - \begin{pmatrix} 0 & \beta_{VH} H \\ 0 & -\alpha - d_V - \frac{h r_P}{s_P} \end{pmatrix} \right] = 0.$$

In view of this, heuristically, the population density W should not grow in the triangular regime. But if it is able to grow only in the fully coupled regime, then, in view of the literature on fully coupled cooperative systems, both components of W should grow simultaneously, and then invade at the same speed. We refer for instance to [26] where the spreading properties of another non-cooperative system with fully coupled cooperative linearization are studied. This leads to our second conjecture.

Conjecture 4.2.2. *The spreading speeds $c_*^I = c_*^{V_i} = c_*^W$ are well-defined.*

To analyze the problem further, it is now convenient for the discussion to remind that $V_i \leq V$, so that $c_*^W \leq c_*^V$, which leads to the distinction between three space-time zones:

- Zone 1, in the wake of the epidemiological invasion, that is in the wake of the W front, or in other words where $|x|/t < c_*^W - \varepsilon$;
- Zone 2, between the W front and the $(V, \tilde{P})$ front, where $c_*^W + \varepsilon < |x|/t < c_*^V - \varepsilon$;
- Zone 3, ahead of the ecological invasion, where $c_*^V + \varepsilon < |x|/t$.

These are summarized in Figure 4.1.

Note that since the equality $c_*^W = c_*^V$ cannot be ruled out (at least at this point of the analysis), the Zone 2 might be empty.

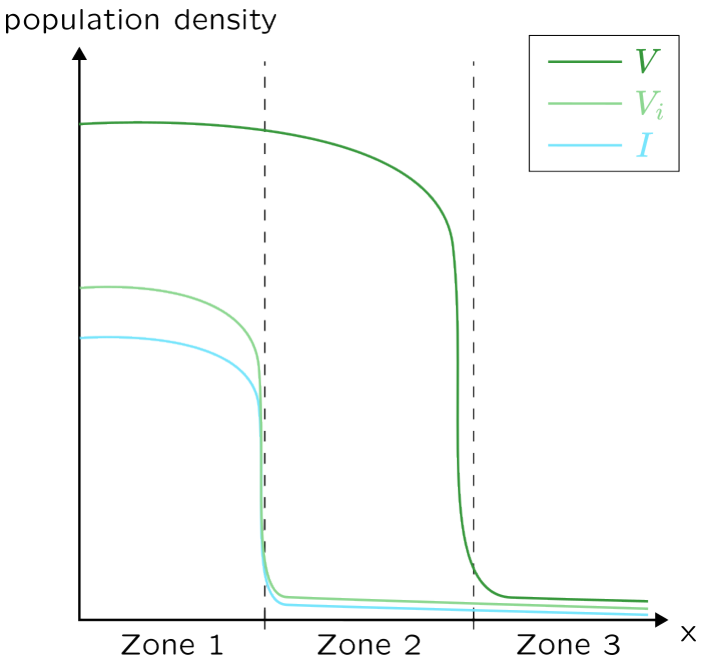

Figure 4.1: The three potential different zones

Now we turn to estimates of c_*^W. Of course, if c_*^W is well-defined and if the Zone 2 is empty, then $c_*^W = c_*^V$ – this is referred to as a *locked front*. So the remaining case is $c_*^W < c_*^V$, with a nonempty Zone 2.

In the Zone 2, as explained before, the exact behaviors of V and $\tilde{P}$ are unknown. But it is known that they are uniformly positive bounded, say $0 < \frac{1}{C} \leq V, \tilde{P} \leq C$ for some $C > 0$. In order to carry on the discussion, we assume that $(V, \tilde{P})$ converges in the Zones 2 and 3 to a 1-periodic equilibrium $(V^*, \tilde{P}^*)$.

In such a case, the periodic principal eigenvalue of the linearized system in the Zone 2 is the principal eigenvalue of the operator

$$-\begin{pmatrix} 0 & 0 \\ 0 & \sigma_V \end{pmatrix} \partial_{xx} - A$$

where A is the following 1-periodic cooperative pointwise irreducible matrix:

$$A = \begin{pmatrix} 0 & \beta_{VH} H \\ \beta_{HV} V^* & -\alpha - d_V - s_V V^* - \frac{h r_P}{s_P} - h P^* \end{pmatrix}.$$

The main issue with this operator is that one of its diffusion rates is zero. In the case of bounded domains with homogeneous Dirichlet boundary conditions, the existence of a principal eigenvalue has been proved by Liang, Zhang and Zhao [42]. It should remain true in the periodic case with analogous arguments. For the solution W_l of the linearized system, the conjecture arising from works on fully coupled cooperative systems [26, 30] is the following.

Conjecture 4.2.3.

$$c_*^{W_l} = \min_{\mu > 0} \frac{-\lambda_1(\mathcal{L}_\mu)}{\mu} \tag{4.6}$$

where $\lambda_1(\mathcal{L}_\mu)$ designates the principal eigenvalue of the operator

$$\mathcal{L}_\mu = -\begin{pmatrix} 0 & 0 \\ 0 & \sigma_V \end{pmatrix} \partial_{xx} + 2\mu \begin{pmatrix} 0 & 0 \\ 0 & \sigma_V \end{pmatrix} \partial_x - \mu^2 \begin{pmatrix} 0 & 0 \\ 0 & \sigma_V \end{pmatrix} - A.$$

However, and this is quite important, the second-order terms of the semilinear system are not, this time, negative. Indeed, (4.4) is rewritten as:

$$\begin{aligned} \partial_t W = & \begin{pmatrix} 0 & 0 \\ 0 & \sigma_V \end{pmatrix} \partial_{xx} W + AW \\ & + \begin{pmatrix} -\beta_{VH} V_i I \\ (\beta_{HV} - s_V)(V - V^*)V_i - h(\tilde{P} - \tilde{P}^*)V_i - \beta_{HV} I V_i \end{pmatrix} \end{aligned}$$

Even if V_0 and $\tilde{P}_0$ are chosen small in such a way that $V - V^\star \leq 0$ and $\tilde{P} - \tilde{P}^* \leq 0$ remain true globally in time and space, the second order-term might change sign. Hence the linear determinacy of the spreading speed c_*^W is unclear and its spreading front might actually be, for instance, pushed.

Conjecture 4.2.4. *Under some parameter conditions, the spreading speed of W is linearly determined:*

$$c_*^{W_l} = c_*^W.$$

Conjecture 4.2.5. *Under some (different) parameter conditions, the spreading speed of W is not linearly determined, and when this is the case it satisfies the inequality*

$$c_*^{W_l} < c_*^W.$$

The following subsection argues in favor of these last two conjectures.

4.2.3 Known results on a similar epidemiological invasion

Lin, Wang, and Zhao [43] have recently published a paper dealing with a very similar system. The differences with our system is the homogeneity in space of the coefficients, the absence of predators, the diffusion of the host population, the recovery of the host population, the non-recovery of the vector population, and the non-death of the vector population. We also refer to [70] for some analysis on the spreading speeds of a very similar system. Using our notations, their system is the following:

$$\left\{ \begin{array}{lcl} \partial_t I & = & \sigma_I \partial_{xx} I + \beta_{VH}(H(x) - I)V_i - \alpha I \\ \partial_t V_i & = & \sigma_V \partial_{xx} V_i + \beta_{HV} I(V - V_i) - s_V V V_i \\ \partial_t V & = & \sigma_V \partial_{xx} V + r_V(x)V - s_V V^2 \end{array} \right. \tag{4.7}$$

They define $V_s = V - V_i$, along with several constants:

$$\mathcal{R}_0 = \frac{H\beta_{VH}\beta_{HV}}{s_V \alpha},$$

$$c_{kpp} = 2\sqrt{\sigma_V r_V},$$

$$c_* = \inf_{\mu > 0} \frac{\sigma_V \mu^2 - \alpha - r_V + \sqrt{(\sigma_V \mu^2 - r_V + \alpha)^2 + 4 r_V \alpha \mathcal{R}_0}}{2\mu},$$

attained at a unique μ_*,

$$c_{**} = \inf_{\mu>0} \frac{\sigma_V \mu^2 - \alpha + \sqrt{(\sigma_V \mu^2 + \alpha)^2 + 4 r_V \alpha \mathcal{R}_0}}{2\mu}.$$

attained at a unique μ_{**}.

Their main results are:

Theorem 4.2.6. *Assume that $\mathcal{R}_0 > 1$. If $c_* < c_{kpp}$, then*

1. *for any $c > \min(c_{**}, c_{kpp})$, we have*

$$\lim_{t\to+\infty} \sup_{|x|\geq ct} [V_i + I](x,t) = 0,$$

if $c_{**} < c_{kpp}$ also holds, then for any $c_{**} < c_1 < c_2 < c_{kpp}$, any $c_3 > c_{kpp}$, we have

$$\begin{aligned} \lim_{t\to+\infty} \sup_{c_1 t\leq|x|\leq c_2 t} |V_s(x,t) - r_V/s_V| + \lim_{t\to+\infty} \sup_{|x|\geq c_3 t} V_s(x,t) \\ + \lim_{t\to+\infty} \sup_{|x|\geq c_1 t} [V_i + I](x,t) = 0; \end{aligned}$$

2. *if $c_{**} < c_{kpp}$ and*

$$\frac{\mu_*}{\mu_{**}} < \frac{c_{kpp} - c_{**}}{c_{kpp} - c_*}, \tag{4.8}$$

then for any $c_* < c_1 < c_2 < c_{kpp}$, any $c_3 > c_{kpp}$, we have

$$\begin{aligned} \lim_{t\to+\infty} \sup_{c_1 t\leq|x|\leq c_2 t} |V_s(x,t) - r_V/s_V| + \lim_{t\to+\infty} \sup_{|x|\geq c_3 t} V_s(x,t) \\ + \lim_{t\to+\infty} \sup_{|x|\geq c_1 t} [V_i + I](x,t) = 0; \end{aligned}$$

3. *for any $c \in [0, c_*)$,*

$$\begin{aligned} \lim_{t\to+\infty} \sup_{|x|\leq ct} \left| V_s(x,t) - \frac{r_V}{s_V \mathcal{R}_0} \right| + \left| V_i(x,t) - \frac{r_V(\mathcal{R}_0 - 1)}{s_V \mathcal{R}_0} \right| \\ + \left| I(x,t) - \frac{r_V(\mathcal{R}_0 - 1)}{\beta_{HV}} \right| = 0. \end{aligned}$$

This theorem asserts that, when I and V_i are slower than V, the spreading speed of the population V is c_{kpp}, while the spreading speed of I and V_i is bounded between c_* and c_{**}. Under the condition 4.8, the spreading speed of I and V_i is actually c_*. This condition allows them to construct a supersolution for the populations I and V_i, demonstrating that the upper limit on their spreading speed is c_*. We can interpret condition 4.8 in the following manner: ahead of the front of I and V_i (in zones 2 and 3), certain non-local pulling effects may occur (see [39] and [27]), causing the spreading speed of the populations in zone 1 to exceed the anticipated speed c_*, although it never surpasses the speed c_{**}. When condition 4.8 is met, the non-local pulling effects are not strong enough to elevate the spreading speed of I and V_i.

Theorem 4.2.7. *Assume that $\mathcal{R}_0 > 1$. If $c_{kpp} < c_*$, then*

1. *for any* $c > c_{kpp}$, *we have*
$$\lim_{t\to+\infty} \sup_{|x|\geq ct} [V_s + V_i + I](x,t) = 0,$$

2. *for any* $c \in [0, c_{kpp})$,
$$\lim_{t\to+\infty} \sup_{|x|\leq ct} \left| V_s(x,t) - \frac{r_V}{s_V \mathcal{R}_0} \right| + \left| V_i(x,t) - \frac{r_V(\mathcal{R}_0 - 1)}{s_V \mathcal{R}_0} \right| + \left| I(x,t) - \frac{r_V(\mathcal{R}_0 - 1)}{\beta_{HV}} \right| = 0.$$

This theorem asserts that, in the case when the three population spread at the same pace, their spreading speed is c_{kpp}.

Theorem 4.2.8. *Assume that* $\mathcal{R}_0 \leq 1$. *Then,*

1. *uniformly for* $x \in \mathbb{R}$, *we have*
$$\lim_{t\to+\infty} [V_i + I](x,t) = 0,$$

2. *for any* $c > c_{kpp}$,
$$\lim_{t\to+\infty} \sup_{|x|\geq ct} V_s(x,t) = 0$$

3. *for any* $c \in [0, c_{kpp})$,
$$\lim_{t\to+\infty} \sup_{|x|\leq ct} |V_s(x,t) - r_V/s_V| = 0.$$

This theorem asserts that, when $\mathcal{R}_0 \leq 1$, the disease goes extinct along with the populations I and V_i, while V spreads at the speed c_{kpp}.

Here, their spreading speed c_* corresponds to our spreading speed c_*^W, the spreading speed of the infected population. In a more general case, with non-homogenous periodic coefficient, this spreading speed would be
$$c_* = \min_{\mu>0} \frac{-\lambda_1(\mathcal{L}_\mu)}{\mu}$$
where $\lambda_1(\mathcal{L}_\mu)$ designates the principal eigenvalue of the operator
$$\mathcal{L}_\mu = -\begin{pmatrix} \sigma_I & 0 \\ 0 & \sigma_V \end{pmatrix} \partial_{xx} + 2\mu \begin{pmatrix} \sigma_I & 0 \\ 0 & \sigma_V \end{pmatrix} \partial_x - \mu^2 \begin{pmatrix} \sigma_I & 0 \\ 0 & \sigma_V \end{pmatrix} - A.$$

If the generalisation to the non-homogeneous periodic case is true, and if their result extend to our system with $\sigma_I = \alpha = 0$ (the presence of $\alpha + d_V$ at the bottom right of the matrix does not change its nature and is therefore not important), then we find again formula (4.6) for the spreading speed of the population W.

4.3 Homogenization

Let $n \in \mathbb{N}^*$. In this section, we assume that the space-dependent parameters H, d_V, r_V and r_P are $1-$periodic, and we denote $H^n(x) = H(nx)$, $d_V^n(x) = d_V(nx)$, $r_V^n(x) = r_V(nx)$ and $r_P^n(x) = r_P(nx)$. We are interested in studying the behaviour of the spreading speeds of the solution of

(3.1) at "high frequency", i.e when n goes to infinity. El Smaily, Hamel and Roques [64] have worked on this matter in the scalar case, Griette and Matano [30] have proved homogenization formulas for a cooperative system, when the diffusion matrix is positive. We also refer to [28] on the homogenization of the principal eigenvalue of a periodic cooperative non scalar operator.

We denote $\langle f \rangle = n \int_0^{1/n} f = \int_0^1 f$, the average of a $1/n-$periodic function f. According to [64], we have

$$c_*^V(n), c_*^P(n) \underset{n\to+\infty}{\longrightarrow} 2\sqrt{\sigma_V \langle r_V \rangle}.$$

If we can extend the results of Griette and Matano to a non-positive diffusion matrix (which is far from trivial, given that the homogenized diffusive matrix has harmonic mean coefficients), we can conjecture that

$$c_*^W(n) \underset{n\to+\infty}{\longrightarrow} \inf_{\mu>0} \frac{-\lambda_1(\mathcal{L}_\mu^W(\infty))}{\mu},$$

where $\lambda_1(\mathcal{L}_\mu^W(\infty))$ designates the principal eigenvalue of the operator

$$\begin{aligned}\mathcal{L}_\mu^W(\infty) = & -\begin{pmatrix} 0 & 0 \\ 0 & \sigma_V \end{pmatrix} \partial_{xx} + 2\mu \begin{pmatrix} 0 & 0 \\ 0 & \sigma_V \end{pmatrix} \partial_x \\ & - \begin{pmatrix} 0 & \beta_{VH} \langle H \rangle \\ \beta_{HV} \langle V_* \rangle & -\alpha - \langle d_V \rangle - s_V \langle V_* \rangle - h \langle P_* \rangle + \sigma_V \mu^2 \end{pmatrix}.\end{aligned}$$

By uniqueness, $-\lambda_1(\mathcal{L}_\mu^W(\infty))$ reduces to the Perron–Frobenius eigenvalue of the irreducible matrix with constant coefficients,

$$\begin{pmatrix} 0 & \beta_{VH} \langle H \rangle \\ \beta_{HV} \langle V_* \rangle & -\alpha - \langle d_V \rangle - s_V \langle V_* \rangle - h \langle P_* \rangle + \sigma_V \mu^2 \end{pmatrix}.$$

Hence, denoting $\delta = \alpha + \langle d_V \rangle + s_V \langle V_* \rangle + h \langle P_* \rangle$,

$$c_*^W(n) \underset{n\to+\infty}{\longrightarrow} \inf_{\mu>0} \frac{\sigma_V \mu^2 - \delta + \sqrt{(\sigma_V \mu^2 - \delta)^2 + 4\beta_{VH}\beta_{HV} \langle H \rangle \langle V_* \rangle}}{2\mu}.$$

Grégoire Nadin [51] also provided insights on the variations of the spreading speeds as a function of the period. According to their Proposition 4.1, the application $L \mapsto c_*^L$ is nondecreasing, where L designates the period of the parameters. To mitigate the spread of the disease, i.e., minimize the spreading speed c_*^L, the optimal strategy is then to opt for the smallest possible period, or the highest frequency, for the parameters. This aligns with the findings of [1] concerning the monotonicity of a specific principal eigenvalue with respect to the period (with the shared goal of limiting the spread of the disease).

Chapter 5

Numerical simulations

Through numerical simulations of our model, we can visualize the swift dynamics of the populations, which validate our assumption of an eternal Spring, observe the monotonicity of the harvest with respect to the parameters, and compute the spreading speeds of the different population conjectured in Chapter 4.

Let $\Omega \in \mathbb{R}^d$, $d \in \{1,2\}$. Our model of interest, for which we conduct all the numerical simulations, is the following.

$$\begin{cases} \partial_t I = & \beta_{VH}(H-I)V_i \\ \partial_t V_i = & \sigma_V \Delta V_i + \beta_{HV} I V_s - \alpha V_i - d_V V_i - s_V(V_s+V_i)V_i - hPV_i \\ \partial_t V_s = & \sigma_V \Delta V_s - \beta_{HV} I V_s + \alpha V_i - d_V V_s - s_V(V_s+V_i)V_s - hPV_s \\ & + b_V(V_s+V_i) \\ \partial_t P = & \sigma_P \nabla \cdot \left(r_P \nabla \left(\frac{P}{r_P} \right) \right) + \gamma h (V_s+V_i)P + r_P P - s_P P^2, \end{cases}$$

with positive coefficients in $L^\infty(\Omega)$, nonnegative initial conditions in $L^\infty(\Omega)$ and Neumann boundary conditions.

In the simulation we run, σ_V, σ_P, β_{VH}, β_{HV}, α, d_V, s_V, s_P, h and γ are constant, and H, b_V and r_P are indicator functions with two values: a value in the refuge and a value in the field.

The details of the discretization scheme and the parameter values used are presented in Chapter 2, supplementary materials. We use a finite differences scheme, and we solve the diffusive part implicitely using the python package scipy, and the reaction part explicitely. We deal with the potential degenerative behaviour of the diffusion term $\nabla \cdot (r_P \nabla (P/r_P))$ by making the change of variable $\tilde{P} = P/r_P$. The parameters values are summarized in the tables 5.1 and 5.2.

Parameter	Value	Unit	Reference
H (refuge)	0	m^{-2}	$\emptyset$
H (field)	11.7647	m^{-2}	Fields of Laon
σ_V	1	$m^2.day^{-1}$	[55]
σ_P	10	$m^2.day^{-1}$	[72, 73]
β_{VH}	0.0379	$m^2.individual^{-1}.day^{-1}$	[9]
β_{HV}	0.003	$m^2.individual^{-1}.day^{-1}$	ITB

Table 5.1: Parameter values used for the numerical simulation

Parameter	Value	Unit	Reference
α	0.0909	day^{-1}	[10]
b_V (refuge)	1.483	day^{-1}	[9, 10, 41]
b_V (field)	1.6	day^{-1}	[9, 10, 41]
d_V	1.47	day^{-1}	[10, 41]
s_V	0.0011	$\text{m}^2.\text{individual}^{-1}.\text{day}^{-1}$	[61], ITB
r_P (refuge)	0.0562	day^{-1}	[36]
r_P (field)	0.00562	day^{-1}	[36]
s_P	0.001	$\text{m}^2.\text{individual}^{-1}.\text{day}^{-1}$	[11]
h	0.0421	$\text{m}^2.\text{individual}^{-1}.\text{day}^{-1}$	[21]
γ	0.0008	No unit	[75]

Table 5.2: Parameter values used for the numerical simulation

We present snapshots of the simulations first in a two-dimensional rectangle ($\Omega = [0, L]^2$), and then in an interval ($\Omega = [0, L]$). For computing time reasons, we use the one-dimensional variant of our script to run longer simulation.

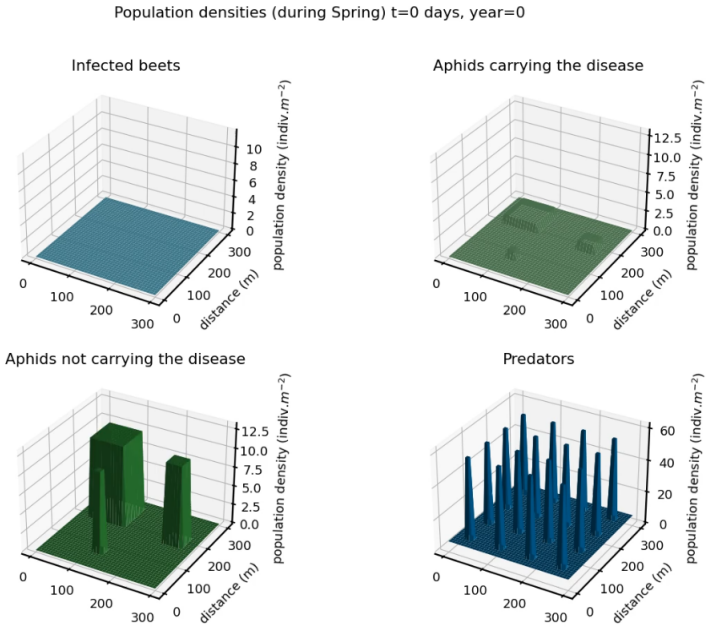

Figure 5.1: Snapshots of the simulation at different days

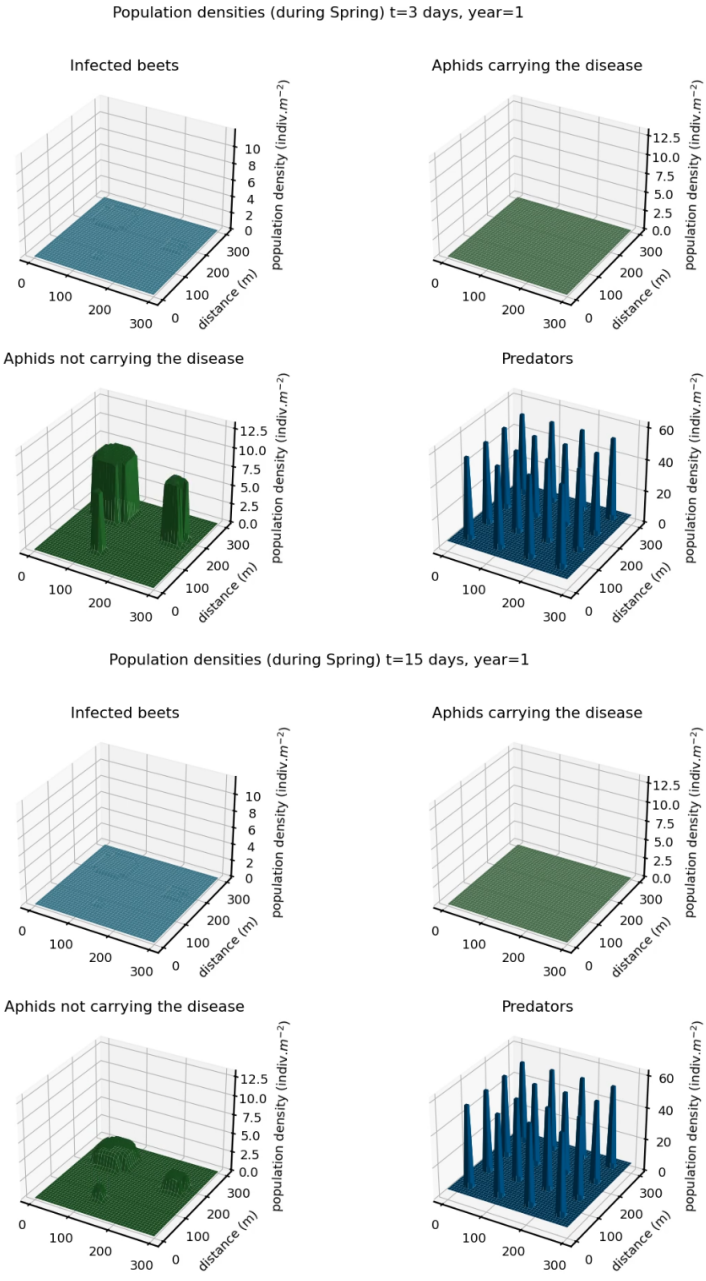

Figure 5.2: Snapshots of the simulation at different days

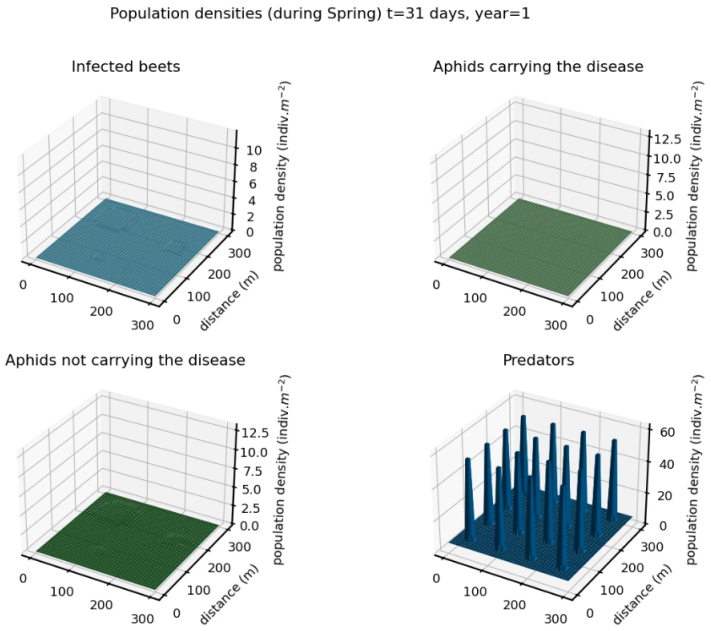

Figure 5.3: Snapshots of the simulation at different days

The populations are represented using distinct colors: the infected beets (I) in light blue, the infected vectors (V_i) in light green, the susceptible vectors (V_s) in dark green, and the predators (P) in dark blue. We use a refuge with a frequency of 4, generating 16 uniformly distributed refuge patches in the 2-dimensional field and 4 patches in the 1-dimensional field, with a total area of one-fifth the area of the field. Initial conditions, displayed in the snapshot at day 0, feature 3 compact patches for populations $V_{i,0}$ and $V_{s,0}$, along with $P_0 = r_P/s_P$ (which has the additional benefit of showing the refuge patch positions).

We observe a remarkably fast dynamic: within a month, the populations reach their respective steady states. This numerical phenomenon aligns with our mathematical approximation of "eternal Spring", which led us to assume time-independent coefficients. We hope that this suffices to make the mathematical harvest η (defined in the first chapters) close to the real-life harvest.

Next, we examine the monotonicity of the harvest with respect to the different parameters by conducting simulations across a range of values, spanning from a fraction to several times their biologically consistent values found in the tables 5.1 and 5.2.

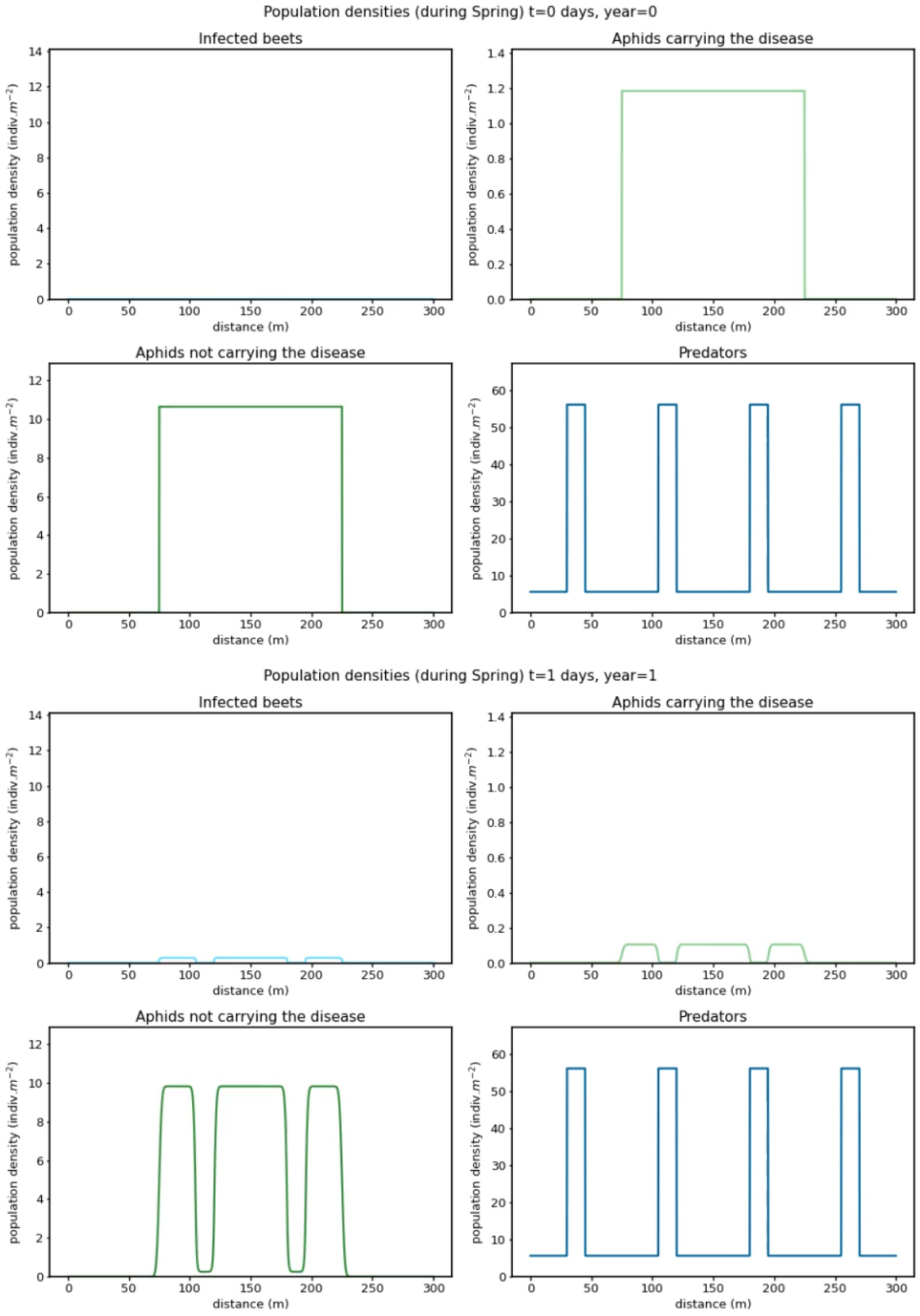

Figure 5.4: Snapshots of the simulation at different days

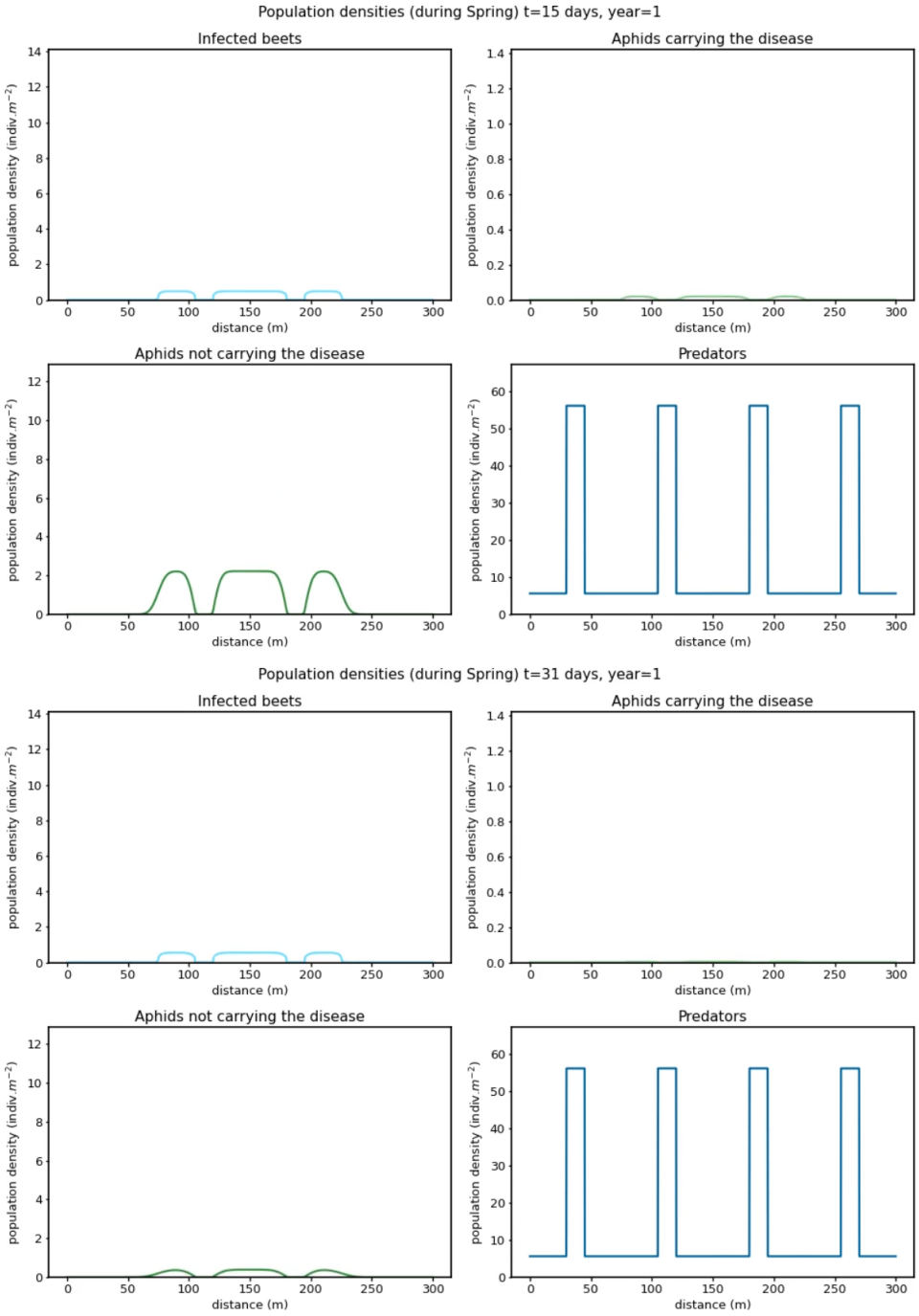

Figure 5.5: Snapshots of the simulation at different days

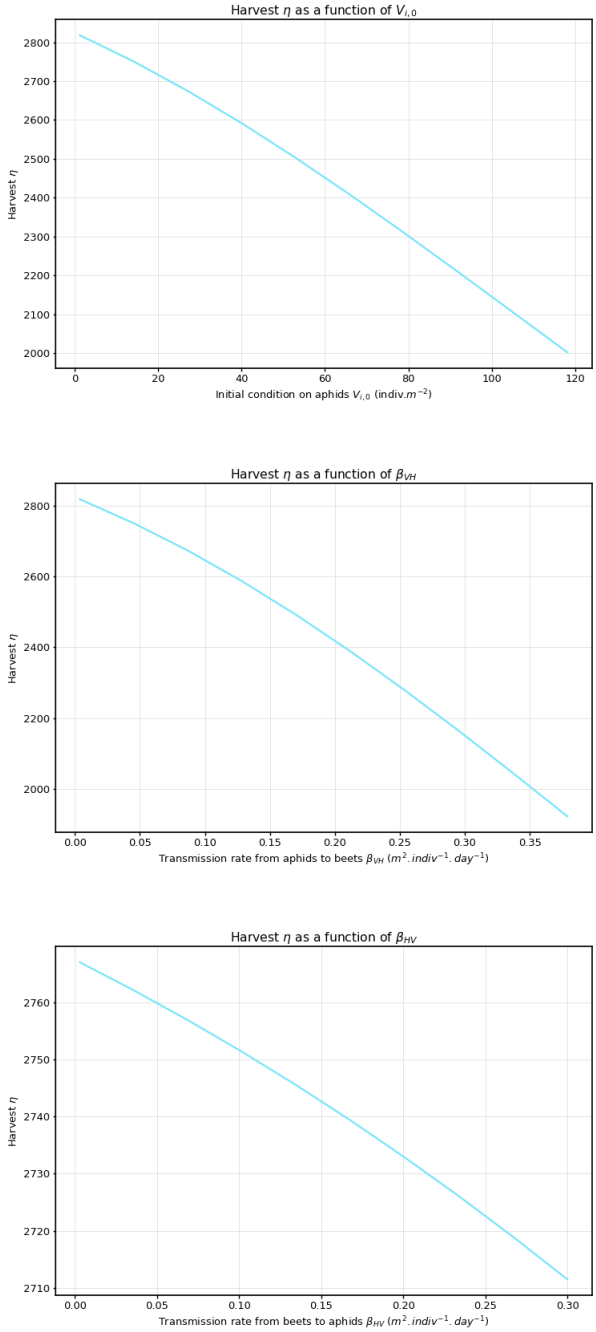

Figure 5.6: Final harvest as a function of different parameters. $V_{i,0}$ is the initial condition on infected aphids, β_{VH} and β_{HV} are transmission rates of the disease, from aphids to beets and from beets to aphids, respectively.

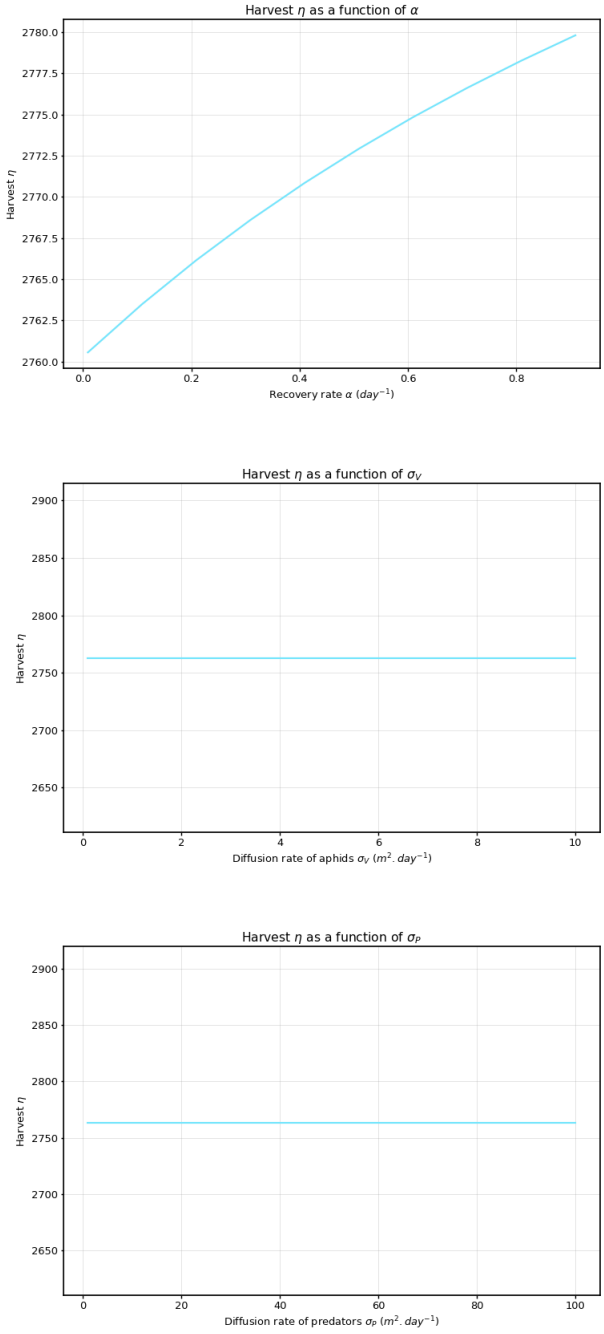

Figure 5.7: Final harvest as a function of different parameters. α is the recovery rate of the disease, σ_V and σ_P are diffusion rates of aphids and predators, respectively.

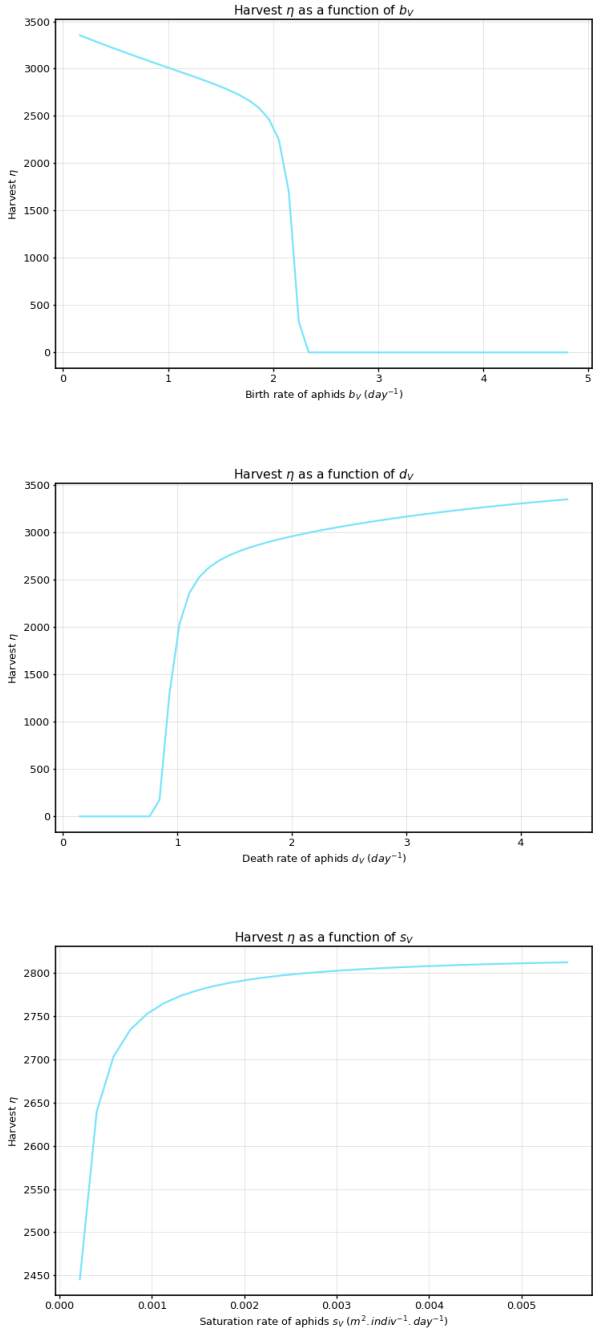

Figure 5.8: Final harvest as a function of different parameters. b_V, d_V, and s_V are birth, death, and saturation rates of aphids, respectively.

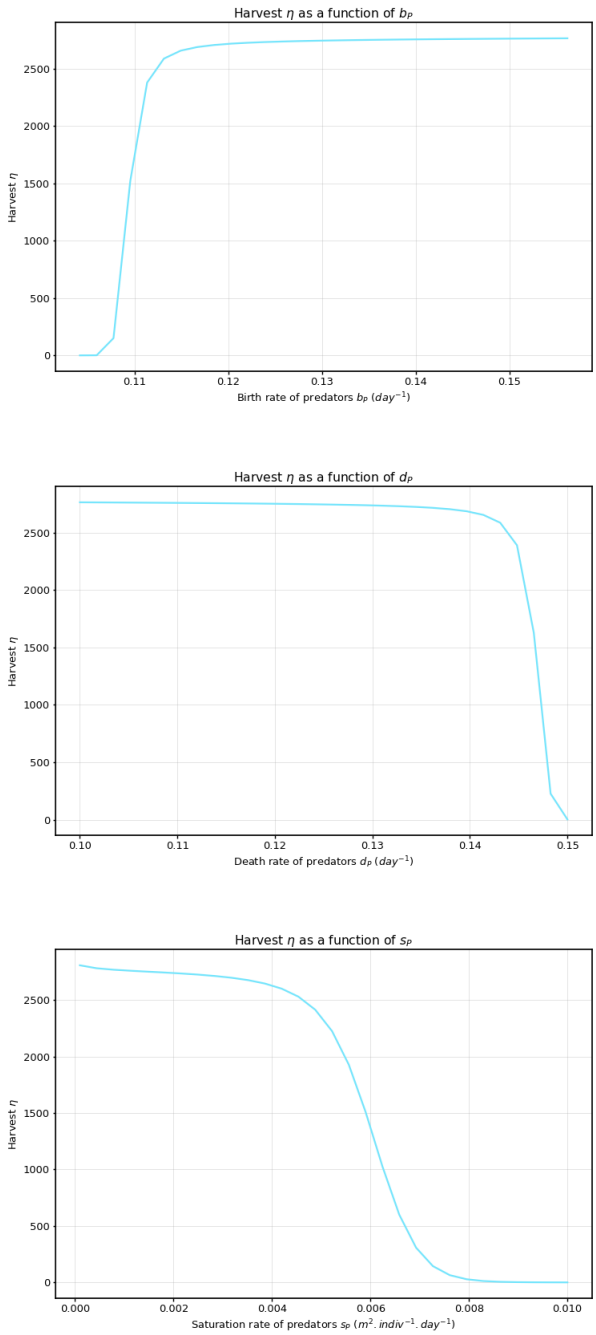

Figure 5.9: Final harvest as a function of different parameters. b_P, d_P, and s_P are birth, death, and saturation rates of predators, respectively.

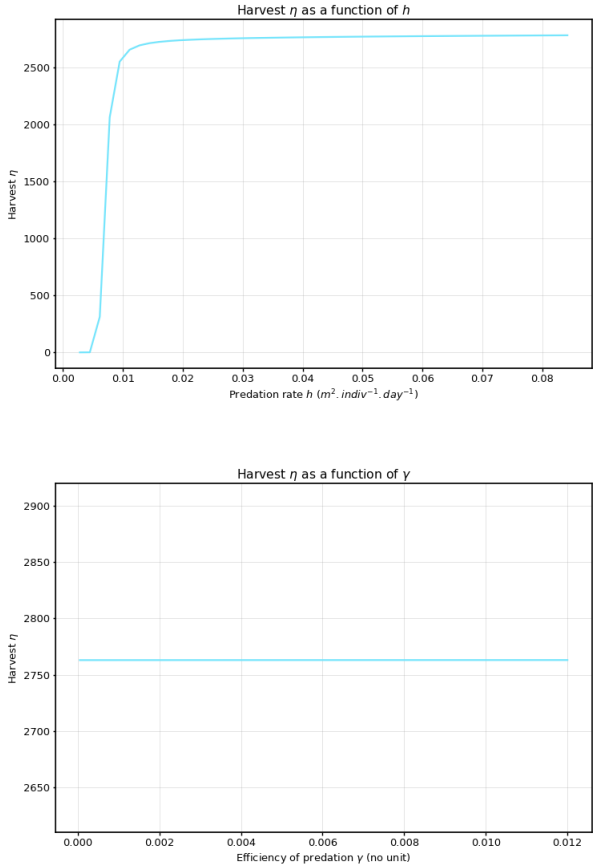

Figure 5.10: Final harvest as a function of different parameters. h is the predation rate and γ is the efficiency of predation.

Among our parameters, which exhibit the anticipated monotonicity, some have a negligible impact on the quantity of healthy beets. Notably influential parameters include b_V, d_V, b_P, d_P, s_P, and h. The initial aphid condition, along with β_{VH} and s_V, also exerts a significant influence. Conversely, β_{HV} and α demonstrate almost negligible effects on the harvest, as do σ_V, σ_P, and γ.

As a concrete illustration of the conjectures presented in Chapter 4, we conducted simulations 5.11 using the parameters detailed in Tables 5.1 and 5.2. However, with this set of parameters, the aphids cannot invade the field as $\lambda_1(\mathcal{L}_{V_s})$ is positive. Therefore, we deliberately made specific modifications to the parameters, namely setting b_V (refuge) $= 1.579$ and b_V (field) $= 2.56$. These adjustments enhance the propagation of aphids, ensuring that $\lambda_1(\mathcal{L}_{V_s})$ becomes negative and the traveling waves of I, V_i and V spread in the field. In regions where a refuge is placed (four patches distributed uniformly in the field), beets cannot grow, resulting in $I = 0$ in these areas. Starting from a single patch at the left boundary of the domain, the aphids progressively invade the field, contaminating all beets in their path. The wave of the population $\tilde{P}$ follows, starting from 0 to its steady state in the presence of aphids.

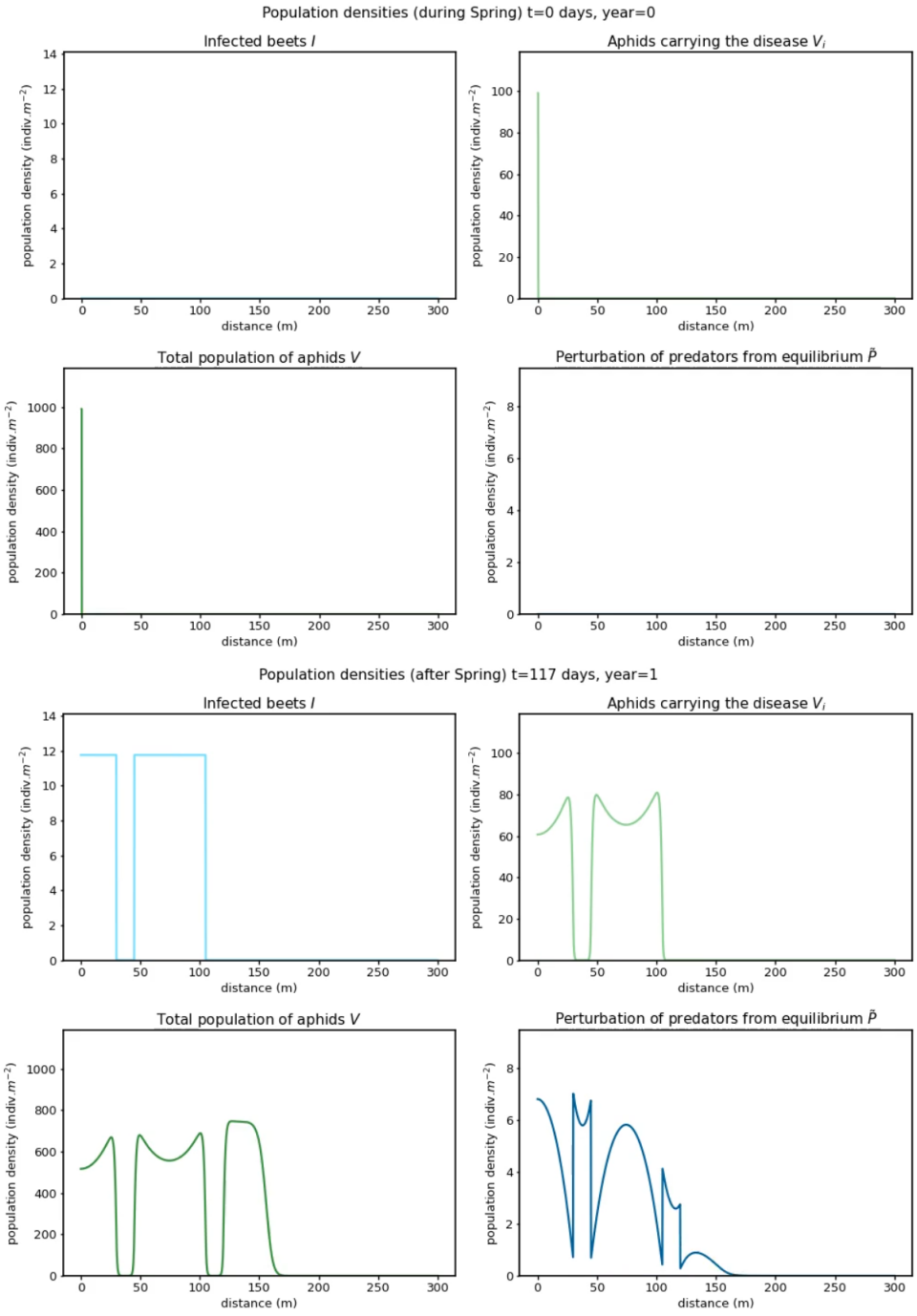

Figure 5.11: Snapshots of the traveling waves of the different populations

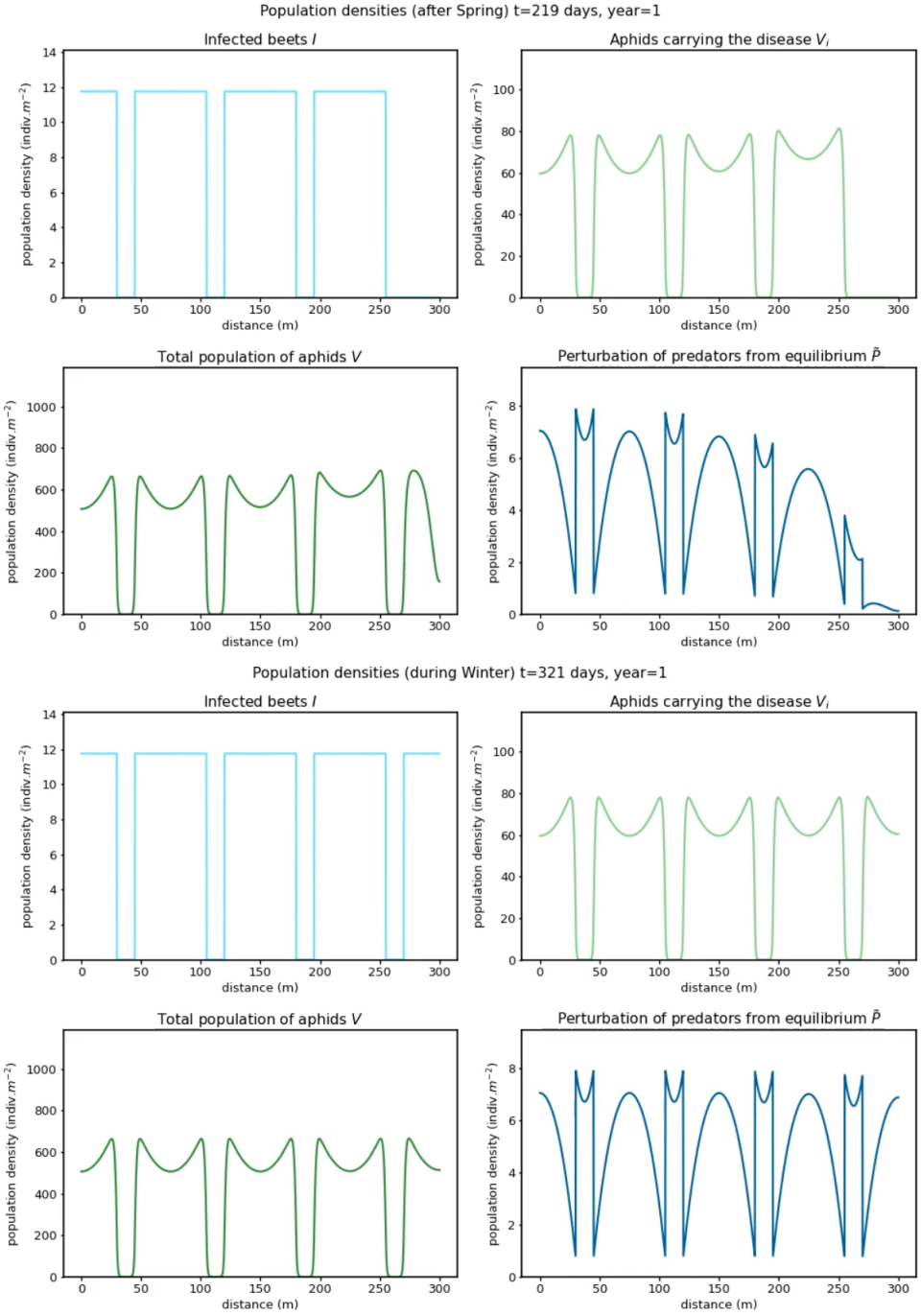

Figure 5.12: Snapshots of the traveling waves of the different populations

As anticipated from the analysis in Chapter 4, we identify two spreading speeds: the spreading speed c_*^W of the populations I and V_i, and the (greater) spreading speed c_*^V (or $c_*^{\tilde{P}}$) of the populations V and $\tilde{P}$. Here, c_*^V appears to be very close to c_*^W, indicating a *locked front* (refer to Chapter 4). Figure 5.13 illustrates the positions of the fronts for the four populations I, V_i, V and $\tilde{P}$ as a function of time. Apart from minor shifts due to the presence of the refuge patches, the four speeds are nearly identical. However, under a different set of parameters (specifically, when the transmission rates are smaller), the waves of the populations I and V_i propagate noticeably slower than those of V and $\tilde{P}$. We conducted an additional simulation with $\beta_{VH} = 0.00758$ (one-fifth of its original value), maintaining b_V (refuge) $= 1.579$ and b_V (field) $= 2.56$, and observed this anticipated behaviour, as depicted in Figure 5.14.

Theoretically (see Chapter 4), the spreading speed of V and $\tilde{P}$ converges to $c_*^\infty = 2\sqrt{\sigma_V \langle r_V \rangle}$ when the frequency of the refuge goes to infinity. Here, with the chosen values of parameters, we have $c_*^\infty = 2\sqrt{\sigma_V \langle r_V \rangle} \approx 1.89$ meters per day. Numerically, we can compute this limit by setting a constant refuge of $1/5$ (which correspond to the homogenized refuge of an area equal to one-fifth the area of the field): we find that $c_*^\infty \approx 1.767$ meters per day.

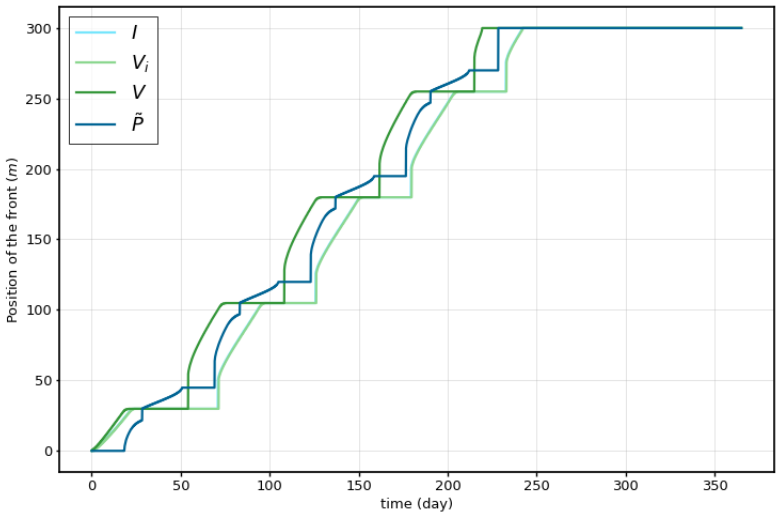

Figure 5.13: Position of the fronts of the four populations I, V_i, V, $\tilde{P}$ as a function of time.

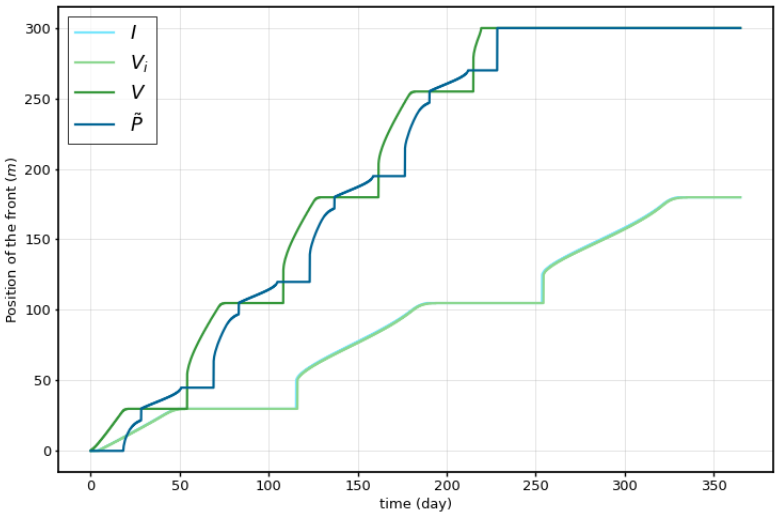

Figure 5.14: Position of the fronts of the four populations I, V_i, V, $\tilde{P}$ as a function of time (with $\beta_{VH} = 0,00758$, one-fifth of its original value).

The numerical simulations displaying the population densities over time validate our assumption of an eternal Spring. Moreover, the consistent monotonicity of the parameters aligns with their biological interpretation and highlights the most sensible parameters. These parameters necessitate precise biological data to accurately determine their values for consistent simulations. Finally, simulations on traveling waves indicate that both conjectured scenarios (locked front or not) are possible depending on parameter values. They also provide a numerical estimate for the spreading speed c_*^∞ close to the theoretical prediction.

Chapter 6

Discussion

6.1 Optimalité du champ homogénéisé

Dans cette thèse, nous avons exploré l'utilisation des prédateurs comme moyen de contrôle de la population de pucerons dans un champ de betteraves. Nous nous sommes concentrés sur la manipulation de la géométrie spatiale d'un «refuge de biodiversité», tel que des allées de fleurs, afin d'introduire de l'hétérogénéité dans le champ. La principale mesure pour évaluer l'efficacité de cette approche était la «récolte», représentant la quantité de betteraves saines restantes à la fin de la saison.

Dans notre premier article [1], notre objectif était d'entraver complètement la propagation des pucerons en exerçant un contrôle sur la valeur propre principale λ_1 de l'opérateur $-\sigma_V \Delta - r_V + h r_P / s_P$. Un λ_1 positif garantit la convergence uniforme de la population de pucerons vers zéro. Notre étude a généré des estimations de la récolte basées sur des évaluations de la population de pucerons infectés, révélant que les bornes augmentent en fonction de λ_1. La formulation variationnelle de cette valeur propre principale a mis en évidence sa monotonie en fonction de la fréquence spatiale de certains paramètres, à savoir H, b_V, d_V, et r_P. Des calculs explicites dans un cas unidimensionnel ont même démontré que λ_1 converge vers son supremum à une vitesse de $1/n^2$, n étant la fréquence. Sachant qu'une fonction périodique converge faiblement vers sa moyenne lorsque sa période tend vers zéro, nous avons établi un lien avec une géométrie de refuge potentiellement optimale : le champ homogénéisé.

Bien que le champ homogénéisé optimise la valeur propre principale λ_1, des questions subsistaient quant à son optimalité globale. Pour répondre à cette incertitude, notre deuxième article [2] a introduit un autre critère : la récolte linéarisée. En considérant la récolte linéarisée, nous avons préservé des informations cruciales sur la condition initiale des pucerons infectés $V_{i,0}$. L'examen a révélé des propriétés intrigantes de la géométrie optimale du refuge, en particulier l'impact de la centralité de la condition initiale.

Il est surprenant de constater que, bien que λ_1 augmente avec la fréquence des refuges, ce n'est pas le cas de la récolte linéarisée. Un unique refuge connexe et centré est plus performant qu'une multitude de petits refuges déconnectés et uniformément distribués lorsque la condition initiale $V_{i,0}$ est principalement centrée. Cependant, dans les cas où $V_{i,0}$ présente une homogénéité spatiale, le champ homogénéisé est apparu comme la géométrie de refuge optimale pour la récolte linéarisée. Nous avons rigoureusement établi la convergence de la récolte du système lorsque la fréquence du refuge tend vers l'infini vers la récolte du système homogénéisé.

Notre étude a mis en évidence le rôle central de la condition initiale sur la récolte. Dans les

scénarios pratiques où la prévision des lieux d'arrivée exacts des pucerons s'avère difficile, nous avons proposé de supposer une distribution de probabilité sur $\mathbb{R}_+$ pour chaque $V_{i,0}(x), x \in \Omega$. En supposant que les pucerons transportés par le vent couvrent des distances nettement supérieures à la taille d'un champ de betteraves moyen, nous avons estimé que la moyenne de chaque $V_{i,0}(x)$ ne dépendait pas de x. Dans ce cadre, le champ homogénéisé apparaît à nouveau comme la géométrie de refuge optimale, cette fois pour la moyenne de la récolte linéarisée.

En conclusion de l'exploration des vitesses de propagation dans notre chapitre heuristique, nous avons introduit un troisième critère pour l'optimisation de la récolte : la vitesse de propagation de la population de pucerons. Bien que spéculatifs à l'heure actuelle, les résultats existants [51] suggèrent l'efficacité d'un champ homogénéisé pour entraver la vitesse de propagation des pucerons. Ainsi, nos résultats suggèrent que le champ homogénéisé excelle dans l'optimisation de trois critères : la valeur propre principale λ_1, la récolte linéarisée (sous certaines hypothèses strictes mais naturelles concernant la condition initiale $V_{i,0}$), et la vitesse de propagation de la population de pucerons.

6.2 Perspectives sur l'optimisation de la récolte

6.2.1 La forme primitive optimale du refuge

L'approche optimale pour configurer la forme du refuge est la suivante : opter pour une forme connexe et la disperser en de nombreuses petites formes déconnectées et uniformément réparties dans le champ. Toutefois, une question subsiste : quelle forme primitive faut-il choisir ? Par exemple, un disque est-il plus efficace qu'un carré ou un triangle ? Cette question reste sans réponse à la fin de cette thèse, ce qui la laisse comme une perspective à explorer à l'avenir. Bien qu'il semble trop difficile de s'attaquer directement à ce problème et d'obtenir des informations sur la *forme* optimale, nous pouvons néanmoins apporter une réponse partielle à la question en déterminant le *volume* optimal de cette forme primitive. Dans les situations où $V_{i,0}$ est constant en espace, notre deuxième article [2] répond entièrement à la question en fournissant la valeur explicite du refuge constant optimal. Dans les cas où aucune information n'est donnée sur $V_{i,0}$, les résultats de [2] impliquent que la valeur propre principale λ_1^n de l'opérateur $-r_V^n + hr_P^n/s_P$ (qui est la valeur propre principale du système comportant un refuge de fréquence n) converge, lorsque n tend vers l'infini, vers $\lambda_1^\infty := \langle -r_V + hr_P/s_P \rangle_\Omega$ la valeur propre principale de l'opérateur homogénéisé. Selon les conclusions de notre premier article [1], si cette valeur est négative, les pucerons envahiront le champ, entraînant ainsi une récolte nulle. Par conséquent, pour que cette stratégie ait une chance de préserver au moins partiellement le rendement, λ_1^∞ doit être positif. Compte tenu des hypothèses que nous avons faites concernant la dépendance des paramètres par rapport au refuge, r_V et r_P présentent deux valeurs distinctes : l'une dans le refuge (r_V^R et r_P^R) et l'autre dans le champ (r_V^F et r_P^F). Donc, en appelant $\mathcal{R}$ le volume du refuge,

$$\begin{aligned}\lambda_1^\infty &= -(r_V^R\mathcal{R} + r_V^F(|\Omega| - \mathcal{R})) + h/s_P(r_P^R\mathcal{R} + r_P^F(|\Omega| - \mathcal{R})) \\ &= (-r_V^R + hr_P^R/s_P)\mathcal{R} + (-r_V^F + hr_P^F/s_P)(|\Omega| - \mathcal{R}) \\ &= \lambda_1^R\mathcal{R} + \lambda_1^F(|\Omega| - \mathcal{R})\end{aligned}$$

où nous avons noté $\lambda_1^R = -r_V^R + hr_P^R/s_P$ et $\lambda_1^F = -r_V^F + hr_P^F/s_P$. Bien entendu, pour que notre stratégie soit efficace, il faut que $\lambda_1^R > \lambda_1^F$ (si ce n'est pas le cas, cela signifie que la propagation des pucerons est mieux entravée dans le champ que dans le refuge, ce qui suggère que la stratégie optimale consiste à supprimer tout refuge). Par conséquent, trois scénarios potentiels se présentent :

1. Scénario 1: $\lambda_1^R, \lambda_1^F < 0$. Dans ce scénario, la récolte sera toujours nulle, indépendamment de la présence d'un refuge. C'est le scénario que nous avons choisi pour notre simulation de fronts de propagation dans le chapitre 5.

2. Scénario 2: $\lambda_1^R, \lambda_1^F > 0$. Nous soulignons ici qu'avec les valeurs de paramètres choisies pour notre simulation numérique (voir chapitre 5), nous tombons dans ce scénario. Ici, même sans placer de refuge dans le champ, la population de pucerons converge vers 0. Bien que l'augmentation du volume des refuges puisse être avantageuse pour la récolte, une réponse quantitative à la question du volume optimal dépasse le cadre de cette thèse. Cependant, les estimations de récolte dans [1] offrent une limite inférieure à la récolte, essentiellement $H(|\Omega| - \mathcal{R})e^{-\beta_{VH}/\lambda_1^n}$, sans tenir compte de certaines constantes multiplicatives. Une première étape vers la recherche d'un volume optimal consisterait à déterminer
$$\text{argmax}_{\mathcal{R}\in[0,|\Omega|]} H(|\Omega| - \mathcal{R})e^{-\beta_{VH}/\lambda_1^n}$$
(rappelons que λ_1^n dépend de $\mathcal{R}$ et est croissant).

3. Scénario 3: $\lambda_1^R > 0$ et $\lambda_1^F < 0$. Ce scénario est similaire au précédent, à la différence près que la récolte peut être nulle si le volume du refuge est trop faible, et que nous pouvons fournir une limite inférieure à ce seuil. La condition
$$\lambda_1^\infty = \lambda_1^R \mathcal{R} + \lambda_1^F(|\Omega| - \mathcal{R}) < 0$$
est équivalente à
$$\mathcal{R} < \frac{-\lambda_1^F}{\lambda_1^R - \lambda_1^F}|\Omega| =: \mathcal{T}.$$
Si le volume $\mathcal{R}$ est inférieur à $\mathcal{T}$, la récolte sera nulle. Par conséquent, dans ce scénario, pour obtenir une récolte positive, il est nécessaire d'avoir $\mathcal{R} \geq \mathcal{T}$. Une fois cette condition remplie, la stratégie d'homogénéisation peut être employée, permettant à λ_1^n de tendre vers $\lambda_1^\infty \geq 0$ et d'empêcher la propagation des pucerons.

6.2.2 La récolte linéarisée

Dans notre deuxième article [2], nous avons approfondi l'examen d'un paramètre η_L appelé la récolte linéarisée. Nos observations numériques ont indiqué sa forte proximité avec la récolte réelle η. Cependant, malgré cette corrélation empirique, un lien formel et rigoureux entre ces deux quantités reste à établir. Plus précisément, une perspective intéressante serait de travailler à fournir des estimations robustes sur la différence $\eta - \eta_L$ et d'établir un lien concluant.

Le raisonnement derrière l'utilisation de la récolte linéarisée est clair : la récolte η dépend de manière non linéaire de l'intégrale temporelle de la population V_i, ce qui rend beaucoup plus difficile la dérivation de propriétés précises concernant ses optimiseurs. Néanmoins, il pourrait être possible de contourner le besoin d'utiliser les propriétés de la récolte linéarisée et de prouver directement des théorèmes concernant les optimiseurs de η, bien que nous ne soyons pas certains que cela soit faisable actuellement.

Dans une perspective plus accessible, nous proposons également d'explorer la monotonie de la fonction $n \mapsto \eta_L(R_n, V_{i,0})$, représentant la récolte linéarisée associée à un refuge de fréquence n. Par analogie avec la valeur propre principale $\lambda_1(\mathcal{L}V_s)$, nous prévoyons que cette fonction soit croissante, dans le cas où la condition initiale sur les pucerons infectés $Vi, 0$ est spatialement homogène.

6.3 Perspectives biostatistiques

Pour compléter le cadre numérique, une incorporation judicieuse de méthodologies statistiques peut améliorer de manière significative le réalisme du modèle. Cela est particulièrement pertinent dans le contexte actuel du changement climatique, où les changements de température et les altérations des configurations de la biodiversité peuvent induire des ajustements phénologiques notables dans le calendrier d'arrivée des populations. Notamment, les données d'observation que nous avons recueillies en suivant les jours d'arrivée de diverses familles d'insectes dans différents pays illustrent clairement une tendance perceptible à des arrivées plus précoces, potentiellement liée à l'évolution des conditions environnementales.

Dans notre quête d'une compréhension plus nuancée du système agro-écologique de la betterave sucrière, nous avons exploité et adapté la base de code de [3], couplée à la bibliothèque rgbif, pour extraire et analyser méticuleusement les données collectées à partir de la source réputée gbif.org. Le but de notre analyse serait de pouvoir, dans le futur, incorporer une dépendance temporelle dans notre système, en fonction de l'évolution des dates d'arrivées des différentes populations dans le champ. Le jeu de données comprend les dates d'arrivée de plusieurs espèces de coccinelles, notamment *Adalia bipunctata*, *Coccinella septempunctata*, *Adalia decempunctata*, *Psyllobora vigintiduopunctata*, ainsi que d'autres espèces telles que la punaise *Anthocoris nemorum*, le perce-oreille *Forficula auricularia Linnaeus*, la mouche *Mikiola fagi* et la chrysope *Chrysoperla carnea*. Couvrant une période complète de 1960 à 2016, l'ensemble des données comprend des observations provenant de divers pays européens, à savoir l'Allemagne, la France, la Suède, le Royaume-Uni, la Belgique et les Pays-Bas. Nos choix d'espèces et de pays ont été principalement motivés par la présence de données abondantes.

Afin de tirer des enseignements significatifs de ce riche ensemble de données, nous avons utilisé un modèle linéaire pour saisir et quantifier les changements phénologiques observés chez ces espèces. Les résultats de notre analyse statistique sont illustrés dans la figure 6.1, offrant une représentation de la dynamique temporelle, en jours par an, intrinsèque aux populations observées.

Cette approche statistique permet non seulement d'approfondir notre étude, mais offre également une perspective précieuse pour analyser et comprendre l'interaction complexe des facteurs environnementaux affectant le comportement phénologique de ces espèces. L'introduction d'une dépendance temporelle dans notre modèle afin d'intégrer ces changements pourrait améliorer son réalisme. Cependant, rétrospectivement, les valeurs obtenues dans notre analyse sont très probablement incompatibles avec une prévision sur le long terme. Par exemple, un décalage de 6 jours par an en Allemagne pour *Adalia bipunctata* implique un décalage de près d'un an sur 50 ans. Une analyse plus complète, utilisant potentiellement un modèle linéaire plus raffiné, est donc nécessaire pour intégrer efficacement ces données dans un cadre numérique.

6.4 Améliorations du modèle

Dans un premier temps, nous avons dérivé du modèle d'EDO de [50] :

$$\begin{cases} I' &= \beta_{VH}(H-I)V_i - \alpha_I I \\ V_i' &= \beta_{HV} I V_s - d_V V_i - s_V(V_s+V_i)V_i - hPV_i \\ V_s' &= -\beta_{HV} I V_s - d_V V_s - s_V(V_s+V_i)V_s - hPV_s + b_V(V_s+V_i) \\ P' &= \gamma h(V_s+V_i)P - d_P P \end{cases}$$

le modèle d'EDP, en tenant compte de l'hétérogénéité spatiale potentielle du champ de betteraves :

$$\begin{cases} \partial_t I &= \beta_{VH}(H(x)-I)V_i \\ \partial_t V_i &= \sigma_V \Delta V_i + \beta_{HV} I V_s - \alpha V_i - d_V(x)V_i - s_V(V_s+V_i)V_i - hPV_i \\ \partial_t V_s &= \sigma_V \Delta V_s - \beta_{HV} I V_s + \alpha V_i - d_V(x)V_s - s_V(V_s+V_i)V_s - hPV_s \\ & \quad + b_V(x)(V_s+V_i) \\ \partial_t P &= \sigma_P \nabla \cdot \left(r_P(x) \nabla \left(\frac{P}{r_P(x)} \right) \right) + \gamma h (V_s+V_i)P + r_P(x)P - s_P P^2. \end{cases}$$

Ici, nous avons introduit une stratégie idéale de dispersion libre pour la population de prédateurs, exprimée par le terme $\nabla \cdot (r_P(x) \nabla (P/r_P(x)))$. Cette addition, au-delà de sa signification mathématique, représente à notre avis une avancée vers un modèle plus réaliste. Cependant, à mesure qu'un modèle devient plus réaliste, l'obtention d'informations sur ses solutions analytiques à l'aide de la théorie des équations aux dérivées partielles devient de plus en plus difficile. Nous suggérons plusieurs améliorations du modèle qui, tout en posant des défis mathématiques techniques pour la reproduction des résultats de [1] et [2], pourraient ouvrir la voie à l'exploration de nouveaux problèmes complexes intéressants.

L'amélioration la plus simple consiste à incorporer une dépendance temporelle pour certains paramètres, en tenant compte de facteurs tels que la saisonnalité, le changement climatique et d'autres altérations potentielles de l'environnement. L'introduction d'un terme source dépendant du temps pourrait mieux rendre compte des arrivées tardives de pucerons dans le champ, remplaçant ainsi l'arrivée unique modélisée par la condition initiale.

En outre, [2] a souligné l'importance de la condition initiale $V_{i,0}$. Un modèle plus raffiné pourrait adopter une variable aléatoire comme condition initiale, suivant une loi de probabilité approximée par de préalables analyses statistiques. À l'heure actuelle, il n'est pas certain que ce cadre s'aligne sur la théorie connue des équations différentielles partielles stochastiques. Indépendamment de ses implications mathématiques, cette approche pourrait améliorer de manière significative la précision des résultats concernant la géométrie optimale du refuge sans nécessiter d'hypothèses drastiques sur $V_{i,0}$.

Enfin, l'intégration d'un modèle de chimiotaxie qui guide les prédateurs vers les vecteurs de maladies représente une amélioration significative de la stratégie de dispersion employée dans notre modèle actuel. Le défi mathématique consiste à intégrer la stratégie idéale de dispersion libre avec un terme de Keller-Segel similaire à $\nabla \cdot (P \nabla V)$ et à obtenir un système biologiquement cohérent et mathématiquement bien posé.

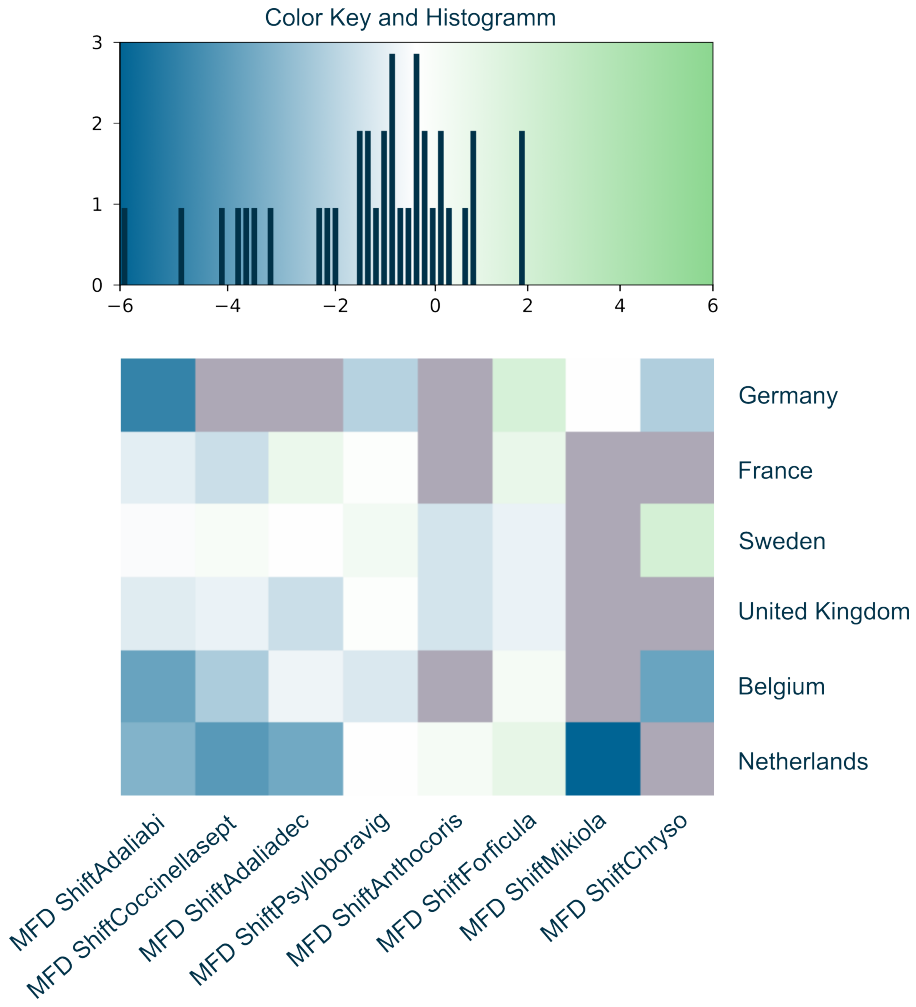

Figure 6.1: Carte thermique des changements phénologiques de diverses familles d'insectes (jours par an). Une valeur de $+2$ (respectivement -2) signifie une arrivée en retard (respectivement en avance) de 2 jours par rapport à l'année d'avant.

Discussion (English version)

6.5 Optimality of the homogenized field

In this thesis, we delved deeply into the utilization of predators as a mean to control the aphid population in a beet field. We focused on the manipulation of the spatial geometry of a "biodiversity refuge", such as flower alleys, to inject heterogeneity in the field. The primary metric for assessing the effectiveness of this approach was the "harvest", representing the quantity of healthy beets remaining at the end of the season.

In our first paper [1], our objective was to achieve complete prevention of aphid spread by exerting control over the principal eigenvalue λ_1 of the operator $-\sigma_V \Delta - r_V + h r_P / s_P$. A positive λ_1 ensured the uniform convergence of the aphid population to zero. Our study derived estimates on the harvest based on estimates on the infected aphid population, revealing that the bounds are increasing with respect to λ_1. The variational formulation of this principal eigenvalue showcased its monotonicity as a function of the spatial frequency of certain parameters, namely H, b_V, d_V, and r_P. Explicit computations in a one-dimensional case even showed that λ_1 converges to its supremum at a rate $1/n^2$, n being the frequency. Knowing that a periodic function weakly converges to its average as its period approaches zero, we established a link to a potential optimal refuge geometry: the homogenized field.

Although the homogenized field optimizes the principal eigenvalue λ_1, questions lingered about its global optimality. To address this uncertainty, our second paper [2] introduced another criterion: the linearized harvest. By considering the linearized harvest, we preserved crucial information about the initial condition on infected aphids $V_{i,0}$. The examination unveiled intriguing properties of the optimal refuge geometry, particularly the impact of the initial condition's centrality.

Surprisingly, while λ_1 increases with refuge frequency, the linearized harvest does not. A uniquely centered connected refuge outperforms a multitude of small, disconnected, uniformly distributed refuges when the initial condition $V_{i,0}$ is primarily centered. However, in cases where $V_{i,0}$ exhibited spatial homogeneity, the homogenized field emerged as the optimal refuge geometry for the linearized harvest. We rigorously established the convergence of the harvest of the system when the refuge frequency approaches infinity to the harvest of the homogenized system.

Our study emphasized the pivotal role of the initial condition on the harvest. In practical scenarios where predicting the exact arrival locations of aphids proves challenging, we proposed assuming a probability distribution on $\mathbb{R}_+$ for each $V_{i,0}(x), x \in \Omega$. Under the assumption that wind-transported aphids cover distances significantly greater than an average beet field's size, we approximated that the mean of each $V_{i,0}(x)$ did not depend on x. Within this framework, the homogenized field once again emerges as the optimal refuge geometry, this time for the mean of the linearized harvest.

In a concluding exploration of spreading speeds in our heuristic chapter, we introduced

a third criterion for harvest optimization: the spreading speed of the aphid population. Although currently speculative, existing results [51] hinted at the efficacy of a homogenized field in impeding aphid spreading speed. Hence, our findings suggested that the homogenized field excelled in optimizing three criteria: the principal eigenvalue λ_1, the linearized harvest (under certain strict yet natural assumptions about the initial condition $V_{i,0}$), and the spreading speed of the aphid population.

6.6 Perspectives on the optimization of the harvest

6.6.1 The optimal primitive shape of the refuge

The optimal approach for configuring the refuge shape is as follows: opt for a connected shape and disperse it into numerous small, disconnected, uniformly distributed shapes across the field. However, a question remains unanswered: what primitive shape should be chosen? For instance, is a disk more effective than a square or a triangle? This question remains unanswered at the conclusion of this thesis, leaving it as a perspective for future exploration. Although it seems too hard to tackle this problem directly and get information on the optimal *shape*, we can nonetheless provide a partial response to the matter by determining the optimal *volume* of this primitive shape. In situations where $V_{i,0}$ is constant in space, our second paper [2] fully addresses the matter by providing the explicit value of the optimal constant refuge. In cases where no information is given on $V_{i,0}$, the results from [2] imply that the principal eigenvalue λ_1^n of the operator $-r_V^n + hr_P^n/s_P$ (which is the principal eigenvalue of the system featuring a refuge of frequency n) converges, as n goes to infinity, to $\lambda_1^\infty := \langle -r_V + hr_P/s_P \rangle_\Omega$—the principal eigenvalue of the homogenized operator. According to the findings of our first paper [1], if this value is negative, aphids will invade the field, resulting in a null harvest. Therefore, for this strategy to have any chance of preserving the yield at least partially, λ_1^∞ must be positive. Given the assumptions we made regarding the parameter dependency on the refuge, r_V and r_P exhibit two distinct values: one in the refuge (r_V^R and r_P^R) and another in the field (r_V^F and r_P^F). Thus, calling $\mathcal{R}$ the volume of the refuge,

$$\begin{aligned}\lambda_1^\infty &= -(r_V^R\mathcal{R} + r_V^F(|\Omega| - \mathcal{R})) + h/s_P(r_P^R\mathcal{R} + r_P^F(|\Omega| - \mathcal{R})) \\ &= (-r_V^R + hr_P^R/s_P)\mathcal{R} + (-r_V^F + hr_P^F/s_P)(|\Omega| - \mathcal{R}) \\ &= \lambda_1^R\mathcal{R} + \lambda_1^F(|\Omega| - \mathcal{R})\end{aligned}$$

where we denoted $\lambda_1^R = -r_V^R + hr_P^R/s_P$ and $\lambda_1^F = -r_V^F + hr_P^F/s_P$. Of course, for our strategy to be effective, we require $\lambda_1^R > \lambda_1^F$ (if this is not the case, it implies that the spread of aphids is better hampered in the field than in the refuge, suggesting the optimal strategy is to remove any refuge altogether). Consequently, three potential scenarios arise:

1. Scenario 1: $\lambda_1^R, \lambda_1^F < 0$. In this scenario, the harvest will always be null, regardless of the presence of a refuge. This is the scenario we selected for our simulation of traveling waves in Chapter 5.

2. Scenario 2: $\lambda_1^R, \lambda_1^F > 0$. We point out here that, with the parameter values selected for our numerical simulation (refer to Chapter 5), we fall into this scenario. Here, even without placing any refuge in the field, the aphid population converges to 0. While increasing the refuge volume might still be advantageous for the harvest, providing a quantitative answer to the question of optimal volume is beyond the scope of this thesis. However, harvest estimates in [1] offer a lower bound to the harvest, essentially $H(|\Omega| - \mathcal{R})e^{-\beta_{VH}/\lambda_1^n}$,

disregarding some multiplicative constants. An initial step towards finding an optimal volume would involve determining

$$\text{argmax}_{\mathcal{R}\in[0,|\Omega|]} H(|\Omega| - \mathcal{R}) e^{-\beta_{VH}/\lambda_1^n}$$

(recall that λ_1^n depends on $\mathcal{R}$ and is increasing).

3. Scenario 3: $\lambda_1^R > 0$ and $\lambda_1^F < 0$. This scenario is similar to the previous one, with the primary distinction being that the harvest can be null if the refuge volume is too small, and we can provide a lower bound to this threshold. The condition

$$\lambda_1^\infty = \lambda_1^R \mathcal{R} + \lambda_1^F (|\Omega| - \mathcal{R}) < 0$$

is equivalent to

$$\mathcal{R} < \frac{-\lambda_1^F}{\lambda_1^R - \lambda_1^F} |\Omega| =: \mathcal{T}.$$

If the volume $\mathcal{R}$ is below $\mathcal{T}$, the harvest will be null. Therefore, in this scenario, to achieve a positive harvest, it is necessary to have $\mathcal{R} \geq \mathcal{T}$. Once this condition is met, the homogenization strategy can be employed, causing λ_1^η to approach $\lambda_1^\infty \geq 0$ and impeding the spread of aphids.

6.6.2 The linearized harvest

In our second paper [2], we delved into the examination of a parameter η_L called the linearized harvest. Our numerical observations strongly indicated its proximity to the actual harvest η. However, despite this empirical correlation, a formal and rigorous connection between these two quantities remains to be established. Specifically, an interesting perspective would be to work towards providing robust estimates on the difference $\eta - \eta_L$ and establishing a conclusive link.

The rationale behind the utilization of the linearized harvest is clear: the harvest η is non-linearly dependent on the time integral of the population V_i, making it significantly more challenging to derive precise properties concerning its optimizers. Nevertheless, it might be feasible to circumvent the need of using the properties of the linearized harvest and directly prove theorems regarding the optimizers of η, although we are uncertain whether this is currently doable.

In a more accessible perspective, we also propose the exploration of the monotonicity of the function $n \mapsto \eta_L(R_n, V_{i,0})$, representing the linearized harvest associated with a refuge of frequency n. Analogous to the principal eigenvalue $\lambda_1(\mathcal{L}_{V_s})$, we anticipate this function to be increasing, in the case where the initial condition on the infected aphids $V_{i,0}$ is spatially homogeneous.

6.7 Biostatistical perspectives

To complement the numerical framework, a judicious incorporation of statistical methodologies can significantly enhance the model's realism. Particularly pertinent in the current context of climate change, where shifts in temperatures and alterations in biodiversity configurations might induce noticeable phenological adjustments in the timing of population arrivals. Notably, the observational data we have gathered from tracking the arrival days of diverse bug

families across various countries vividly illustrates a discernible trend towards earlier arrivals, potentially linked to evolving environmental conditions.

In our pursuit of a more nuanced understanding of the sugar-beet agro-ecological system, we leveraged and adapted the codebase from [3], coupled with the rgbif library, to extract and meticulously analyze data collected from the reputable source gbif.org. The aim of our analysis would be to be able, in the future, to incorporate a time dependency into our system, based on the evolution of the arrival dates of the different populations in the field. The dataset encompasses the arrival dates of several ladybug species, including *Adalia bipunctata*, *Coccinella septempunctata*, *Adalia decempunctata*, *Psyllobora vigintiduopunctata*, along with other species such as the flowerbug *Anthocoris nemorum*, the earwig *Forficula auricularia Linnaeus*, the fly *Mikiola fagi*, and the lacewing *Chrysoperla carnea*. Spanning a comprehensive timeline from 1960 to 2016, the dataset includes observations from diverse European countries, namely Germany, France, Sweden, the United Kingdom, Belgium, and the Netherlands. Our choices of species and countries were mostly driven by the presence of abundant data.

In order to distill meaningful insights from this rich dataset, we employed a linear model to capture and quantify the observed phenological shifts across these species. The outcomes of our statistical analysis are illustrated in Figure 6.2, offering a representation of the temporal dynamics, in days per year, intrinsic to the observed populations.

This statistical approach not only deepens our investigation but also offers a valuable perspective to analyze and understand the complex interaction of environmental factors affecting the phenological behavior of these species. Introducing time dependency to our model to incorporate these shifts could enhance its realism. However, in retrospect, the values obtained in our analysis are most likely inconsistent with a long-term forecast. For instance, a shift of 6 days per year in Germany for *Adalia bipunctata* implies that over 50 years, it would shift by almost one year. A more comprehensive analysis, potentially employing a more refined linear model, is therefore necessary to integrate this data effectively into a numerical framework.

6.8 Improvements of the model

Initially, we derived our model from the ODE model of [50]:

$$\begin{cases} I' &= \beta_{VH}(H-I)V_i - \alpha_I I \\ V_i' &= \beta_{HV} I V_s - d_V V_i - s_V(V_s+V_i)V_i - hPV_i \\ V_s' &= -\beta_{HV} I V_s - d_V V_s - s_V(V_s+V_i)V_s - hPV_s + b_V(V_s+V_i) \\ P' &= \gamma h(V_s+V_i)P - d_P P \end{cases}$$

to the PDE model, accounting for the potential spatial heterogeneity of the field of beets:

$$\begin{cases} \partial_t I &= \beta_{VH}(H(x)-I)V_i \\ \partial_t V_i &= \sigma_V \Delta V_i + \beta_{HV} I V_s - \alpha V_i - d_V(x)V_i - s_V(V_s+V_i)V_i - hPV_i \\ \partial_t V_s &= \sigma_V \Delta V_s - \beta_{HV} I V_s + \alpha V_i - d_V(x)V_s - s_V(V_s+V_i)V_s - hPV_s \\ & \quad + b_V(x)(V_s+V_i) \\ \partial_t P &= \sigma_P \nabla \cdot \left(r_P(x) \nabla \left(\frac{P}{r_P(x)} \right) \right) + \gamma h(V_s+V_i)P + r_P(x)P - s_P P^2. \end{cases}$$

Here, we introduced an ideal free dispersal strategy for the predator population, expressed as the term $\nabla \cdot (r_P(x) \nabla (P/r_P(x)))$. This addition, beyond its mathematical significance, represents in our opinion a step towards a more realistic model. However, as a model becomes more realistic, obtaining informations on its analytical solutions using PDE theory becomes

increasingly challenging. We suggest several enhancements to the model, which, while posing technical mathematical challenges for reproducing the results of [1] and [2], could open avenues for addressing new interesting complex problems.

The most straightforward improvement is incorporating time dependency for certain parameters, considering factors such as seasonality, climate change, and other potential environmental alterations. Introducing a time-dependent source term could better capture the later arrivals of aphids in the field, replacing the single arrival modeled by the initial condition.

Furthermore, [2] highlighted the significance of the initial condition $V_{i,0}$. A more refined model could adopt a random variable as the initial condition, following a probability law approximated by preliminary statistical analyses. Currently, it remains uncertain whether this framework aligns with known stochastic partial differential equation theory. Regardless of its mathematical implications, this approach could significantly improve the precision of results concerning the optimal refuge geometry without necessitating drastic assumptions about $V_{i,0}$.

Finally, incorporating a chemotaxis model that guides predators toward disease vectors represents a significant enhancement to the dispersal strategy employed in our current model. The mathematical challenge lies in integrating the ideal free dispersal strategy with a Keller-Segel term similar to $\nabla \cdot (P \nabla V)$ and get a biologically consistent and mathematically well-posed system.

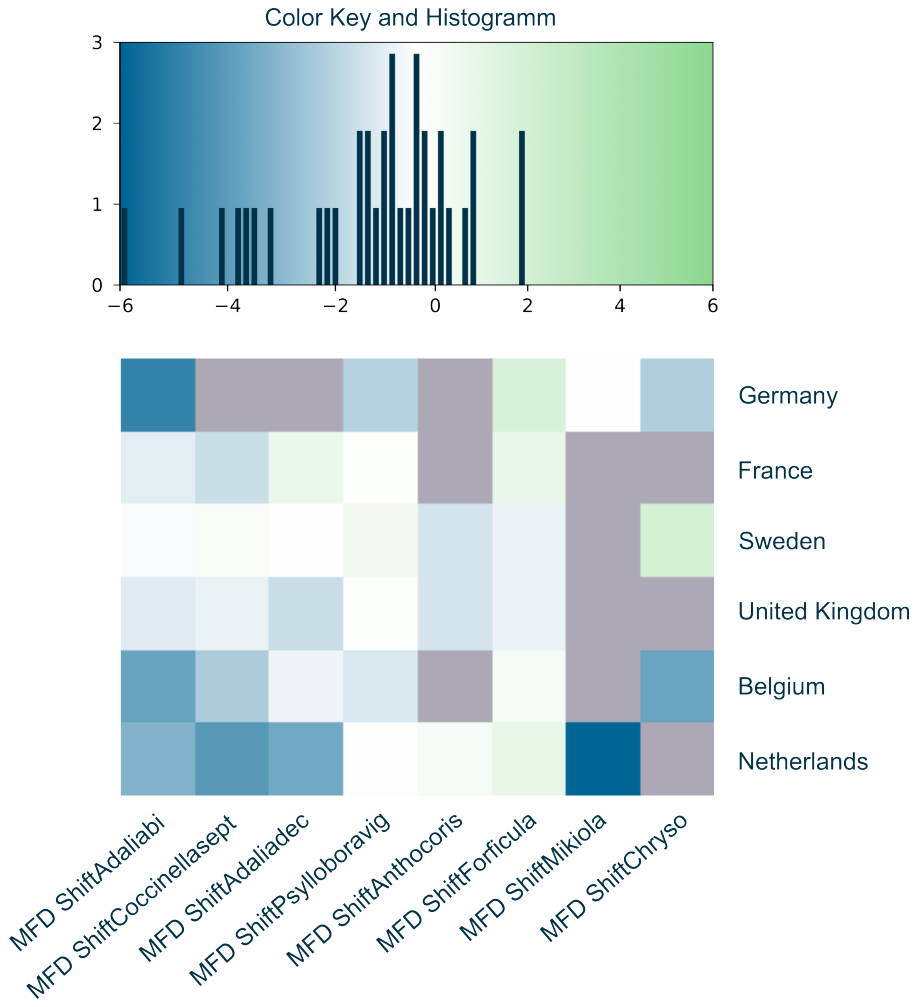

Figure 6.2: Heatmap of the phenological shifts of various families of bugs (days per year). A value of $+2$ (respectively -2) indicates a late arrival (respectively early arrival) of 2 days compared to the previous year.

Author's articles

[1] Léo Girardin and Baptiste Maucourt. "Agro-ecological control of a pest-host system: preventing spreading". In: *SIAM Journal on Applied Mathematics* (2023).

[2] Baptiste Maucourt. "Agro-ecological control of a pest-host system: optimizing the harvest". In: *Preprint* (2024).

Bibliography

[3] François Duchenne et. al. "Phenological shifts alter the seasonal structure of pollinator assemblages in Europe". In: *Nature ecology and evolution* (2020).

[4] Grégoire Allaire. *Lecture 1 Introduction to homogenization theory*. 2010.

[5] Ivo Babuška. "Homogenization and its application. Mathematical and computational problems". In: *Numerical solution of partial differential equations–III*. Elsevier, 1976.

[6] Nikolai Bakhvalov and Grigory Panasenko. *Homogenization: Averaging Processes in Periodic Media*. Kluwer, 1989.

[7] Henri Berestycki, François Hamel, and Lionel Roques. "Analysis of the periodically fragmented environment model : I – Species persistence". In: *Journal of Mathematical Biology* (2005).

[8] Henri Berestycki, François Hamel, and Lionel Roques. "Analysis of the periodically fragmented environment model : II – Biological invasions and pulsating traveling waves". In: *Journal de Mathématiques Pures et Appliquées (9)* (2005).

[9] Institut Technique de la Betterave. "F. A. Q. Betterave sucrière, pucerons verts, jaunisse et néonicotinoïdes". In: *Institut Technique de la Betterave* (2020).

[10] Institut Technique de la Betterave. "Les jaunisses virales et leurs pucerons vecteurs". In: *Institut Technique de la Betterave* (2020).

[11] Yibrah Beyene, Trond Hofsvang, and Ferdu Azerefegne. "Population dynamics of tef epilachna (Chnootriba similis Thunberg) (Coleoptera, Coccinellidae) in Ethiopia". In: *Crop Protection* (2007).

[12] Herm Jan Brascamp, Elliott Hershel Lieb, and Joaquin Mazdak Luttinger. "A General Rearrangement Inequality for Multiple Integrals". In: *Journal of functional analysis* (1974).

[13] Bogusław Buszewski et al. "A holistic study of neonicotinoids neuroactive insecticides properties, applications, occurrence, and analysis". In: *Environmental Science and Pollution Research* 26 (2019).

[14] Robert Stephen Cantrell and Chris Cosner. *Spatial Ecology via Reaction-Diffusion Equations*. Wiley, 2004.

[15] Robert Stephen Cantrell, Chris Cosner, and Yuan Lou. "Approximating the ideal free distribution via reaction–diffusion–advection equations". In: *Department of Mathematics, University of Miami and Ohio State University, USA* (2008).

[16] Robert Stephen Cantrell, Chris Cosner, and Yuan Lou. "Evolution of dispersal and the ideal free distribution". In: *Department of Mathematics, University of Miami and Ohio State University, USA* (2010).

[17] Xinfu Chen and Yuan Lou. “Effects of diffusion and advection on the smallest eigenvalue of an elliptic operator and their applications”. In: *Indiana University Mathematics Journal* (2012).

[18] Andria M. Cimino et al. “Effects of Neonicotinoid Pesticide Exposure on Human Health: A Systematic Review”. In: *Environmental Health Perspectives* (2017).

[19] C Cosner. “Reaction–diffusion equations and ecological modeling”. In: *Tutorials in Mathematical Biosciences IV: Evolution and Ecology*. Springer, 2008.

[20] Edward Norman Dancer et al. “Spatial segregation limit of a competition–diffusion system”. In: *Euro. Journal of Applied Mathematics* (1999).

[21] Esther. http://www.blog.naturoptic.com/2011/02/25/le-puceron-vert-myzus-persica/. 2011.

[22] Lawrence C. Evans. *Partial Differential Equations*. American Mathematical Society, 1998.

[23] Ronald Aylmer Fisher. “The wave of advance of advantageous genes”. In: *Annals of eugenics* 7.4 (1937).

[24] Sarah Garre. https://www.researchgate.net/. 2018.

[25] David Gilbarg and Neil Trudinger. *Elliptic partial differential equations of second order*. Springer, 2001.

[26] Léo Girardin. “Persistence, extinction and spreading properties of non-cooperative Fisher-KPP systems in space-time periodic media”. In: *Preprint* (2023).

[27] Léo Girardin and King-Yeung Lam. “Invasion of open space by two competitors: spreading properties of monostable two-species competition-diffusion systems”. In: *Proceedings of the London Mathematical Society* (2019).

[28] Léo Girardin and Idriss Mazari. “Generalized principal eigenvalue of space-time periodic, weakly coupled, cooperative, parabolic systems”. In: *Preprint* (2022).

[29] Louise Friot Giroux. “Méthodes de reconstruction avancées en tomographie dentaire par faisceau conique”. In: *INSA de Lyon* (2023).

[30] Quentin Griette and Hiroshi Matano. “Propagation dynamics of solutions to spatially reaction-diffusion systems with hybrid nonlinearity”. In: *Preprint* (2021).

[31] Hichem Hajaiej. “Cases of equality and strict inequality in the extended Hardy–Littlewood inequalities”. In: *Proceedings of the Royal Society of Edinburgh* (2004).

[32] Juraj Húska. “Harnack inequality and exponential separation for oblique derivative problems on Lipschitz domains”. In: *Journal of Differential Equations* (2006).

[33] Hervé Jactel et al. “Alternatives to neonicotinoids”. In: *Environmental International* (2019).

[34] Doris Klingelhöfer et al. “Neonicotinoids: A critical assessment of the global research landscape of the most extensively used insecticide”. In: *Environmental Research* (2022).

[35] A Kolmogorov, I Petrovskii, and N Piskunov. “A Study of the Diffusion Equation with Increase in the Amount of Substance, and its Application to a Biological Problem. Übersetzung aus: Bulletin of the Moscow State University Series A 1: 1-26, 1937”. In: *Selected Works of AN Kolmogorov* 1 ().

[36] D.C. Kontodimas and G.J. Stathas. “Phenology, fecundity and life table parameters of the predator Hippodamia variegata reared on Dysaphis crataegi”. In: *Biocontrol* (2005).

[37] Mark Grigor’evich Krein and Mark A Rutman. “Linear operators leaving invariant a cone in a Banach space”. In: *Uspekhi mat. nauk* 3.1 (1948).

[38] Ajaz Ahmad Kundoo et al. “Role of neonicotinoids in insect pest management: A review”. In: *Journal of Entomology and Zoology Studies* 6.1 (2018).

[39] King-Yeung Lam and Xiao Yu. “Asymptotic spreading of KPP reactive fronts in heterogeneous shifting environments”. In: *Journal de Mathematiques Pures et Appliquees* (2021).

[40] Jay Ram Lamichhane et al. “Toward a Reduced Reliance on Conventional Pesticides in European Agriculture”. In: *Plant Disease* 100.1 (2016).

[41] J.-M. Legay and L. De Reggi. “Longévité et fécondité chez Myzus persicae Sulzer, élevé au laboratoire”. In: *Publications de la Société Linnéenne de Lyon* (1964).

[42] Xing Liang, Lei Zhang, and Xiao-Qiang Zhao. “The principal eigenvalue for degenerate periodic reaction-diffusion systems”. In: *SIAM* (2017).

[43] Guo Lin, Xinjian Wang, and Xiao-Qiang Zhao. “Propagation Phenomena of a Vector-Host Disease Model”. In: *Journal of Differential Equations* (2023).

[44] Pierre-Louis Lions and Panagiotis E Souganidis. “Homogenization of degenerate second-order PDE in periodic and almost periodic environments and applications”. In: *Annales de l’IHP Analyse non linéaire*. Vol. 22. 5. 2005.

[45] François Murat et Luc Tartar. “H-convergence”. In: *Séminaire Analyse Fonctionnelle et Numérique de l’Université d’Alger* (1977).

[46] Gabriel Maciel et al. “Evolutionarily stable movement strategies in reaction-diffusion models with edge behavior”. In: *Department of Mathematics and Statistics, and Department of Biology, University of Ottawa, University of Miami* (2019).

[47] Sten Madec et al. “Bistability induced by generalist natural enemies can reverse pest invasions”. In: *Journal of Mathematical Biology* (2021).

[48] Rajesh Mahadevan. “A note on a non-linear Krein–Rutman theorem”. In: *Nonlinear Analysis: Theory, Methods & Applications* 67.11 (2007).

[49] Anna Marciniak-Czochra. “Reaction-diffusion models of pattern formation in developmental biology”. In: *Mathematics and life sciences*. De Gruyter, 2012.

[50] Sean Moore, Elizabeth Borer, and Parviez Hosseini. “Predators indirectly control vector-borne disease: linking predator–prey and host–pathogen models”. In: *Journal of the Royal Society Interface* (2010).

[51] Grégoire Nadin. “The effect of the Schwarz rearrangement on the periodic principal eigenvalue of a nonsymmetric operator”. In: *SIAM journal on mathematical analysis* 41.6 (2010).

[52] E-C Oerke. “Crop losses to pests”. In: *The Journal of Agricultural Science* 144.1 (2006).

[53] Shuxia Pan and Guo Lin. “Invasion Speed of the Prey in a Predator-Prey System”. In: *Bulletin of the Malaysian Mathematical Sciences Society* (2021).

[54] Chia-Ven Pao. *Nonlinear Parabolic and Elliptic Equations*. Springer US, 1993.

[55] Hazel R Parry. “Cereal aphid movement: general principles and simulation modelling”. In: *Parry Movement Ecology* (2013).

[56] Murray H. Protter and Hans F. Weinberger. *Maximum Principles in Differential Equations*. Springer-Verlag, 1984.

[57] Zexin Qi. “An Application of a Nonlinear Krein-Rutman Theorem to a Semi-linear Elliptic System.” In: *Results in Mathematics* 70 (2016).

[58] D Quesada. “Dispersion of Pollutants based on a Reaction–Diffusion model”. In: ().

[59] Alex Roxin and Anders Ledberg. “Neurobiological models of two-choice decision making can be reduced to a one-dimensional nonlinear diffusion equation”. In: *PLoS Computational Biology* 4.3 (2008).

[60] Maj Rundlöf et al. “Neonicotinoid Insecticides and Their Impacts on Bees: A Systematic Review of Research Approaches and Identification of Knowledge Gaps”. In: *PLOS ONE* (2015).

[61] Ahmad-ur-Rahman Saljoqi. “Population dynamics of Myzus Persicae (Sulzer) and its associated natural enemies in Spring potato crop, Peshawar-Pakistan”. In: *Sarhad J. Agric. Vol.25, No.3* (2009).

[62] Christoph Schwab. “Krein-Rutman theorem and the principal eigenvalue”. In: *Numerical Methods for Elliptic and Parabolic PDEs (Lecture Notes)* (2005).

[63] Irmi Seidl and Clem A Tisdell. “Carrying capacity reconsidered: from Malthus’ population theory to cultural carrying capacity”. In: *Ecological economics* 31.3 (1999), pp. 395–408.

[64] Mohammad El Smaily, François Hamel, and Lionel Roques. “Homogenization and influence of fragmentation in a biological invasion model”. In: *Preprint* (2009).

[65] Ivar Stakgold. “Reaction-diffusion problems in chemical engineering”. In: *Nonlinear Diffusion Problems: Lectures given at the 2nd 1985 Session of the Centro Internazionale Matermatico Estivo (CIME) held at Montecatini Terme, Italy June 10–June 18, 1985* (2006).

[66] Peter Takac. “A short elementary proof of the Krein-Rutman theorem”. In: *Houston Journal of Mathematics, Volume 20, No. 1* (1994).

[67] Giorgio Talenti. “Inequalities in rearrangement invariant function spaces”. In: *Nonlinear analysis, function spaces and applications* (1994).

[68] Giorgio Talenti. “The Art of Rearranging”. In: *Milan Journal of Mathematics* (2016).

[69] Vitaly A Volpert. *Elliptic partial differential equations*. Vol. 1. Springer, 2011.

[70] Xinjian Wang and Guo Lin. “Spreading speeds and traveling wave solutions of diffusive vector-borne disease models without monotonicity”. In: *Proceedings of the Royal Society of Edinburgh* (2021).

[71] Hans Weinberger. “On spreading speeds and traveling waves for growth and migration models in a periodic habitat”. In: *Journal of Mathematical Biology* (2002).

[72] Wopke Van Der WERF, Edward Walter EVANS, and James POWELL. “Measuring and modelling the dispersal of Coccinella septempunctata (Coleoptera: Coccinellidae) in alfalfa field”. In: *Wageningen, Utah* (2000).

[73] Richard E. Wetzler and Stephen J. “Experimental Studies of Beetle Diffusion in Simple and Complex Crop Habitats”. In: *Journal of Animal Ecology* (1984).

[74] Angelika Wilkowska and Marek Biziuk. “Determination of pesticide residues in food matrices using the QuEChERS methodology”. In: *Food chemistry* 125.3 (2011).

[75] Jih-Zu Yu, Hsin Chi, and Bing-Huei Chen. “Life Table and Predation of Lemnia biplagiata (Coleoptera: Coccinellidae) Fed on Aphis gossypii (Homoptera: Aphididae) with a Proof on Relationship Among Gross Reproduction Rate, Net Reproduction Rate, and Preadult Survivorship”. In: *Ecology and population Biology* (2005).

Contrôle agro-écologique d'un système parasite-hôte spatio-temporel
Prévention de la propagation et optimisation de la récolte

Résumé : Cette thèse est consacrée à l'exploration du système agro-écologique de la betterave sucrière, à sa modélisation grâce à des équations aux dérivées partielles, et à l'optimisation de l'utilisation d'une méthode de protection sans pesticide contre le virus de la jaunisse de la betterave. Ce virus se propage au sein des champs de betteraves sucrières par des pucerons, et constitue une menace pour le rendement des champs. Dans notre modèle, nous introduisons des prédateurs naturels des pucerons afin de contrôler leur population, et plaçons des «refuges» de biodiversité à l'intérieur du champ, désormais hétérogène en espace (c'est-à-dire dont les propriétés dépendent de la position). Au chapitre 2, notre premier article se penche sur ce système, en étudiant la valeur propre principale d'un opérateur spécifique représentant l'évolution de la population de pucerons. Si celle-ci est strictement positive, la population de pucerons converge uniformément vers 0, et la population de prédateurs converge uniformément vers leur capacité de charge strictement positive. Nous fournissons alors des estimations pour la population de pucerons et la récolte restante. Inversement, lorsque cette valeur propre principale est strictement négative, les pucerons persistent en tout point de l'espace et du temps, ce qui se traduit par une récolte nulle. Au chapitre 3, le deuxième article explore le même système, établissant la convergence de la récolte vers celle du système homogénéisé lorsque la fréquence des refuges tend vers l'infini. Nous étudions l'optimalité d'un refuge homogénéisé pour maximiser une quantité appelée récolte linéarisée sous des hypothèses spécifiques concernant la condition initiale de la population de pucerons infectés. Lorsqu'elle est constante, nous identifions une valeur explicite pour le refuge homogénéisé optimal. Le chapitre 4 présente des idées et des conjectures sur les vitesses de propagation de toutes les populations au cours d'une invasion de pucerons, ainsi qu'un résultat d'homogénéisation potentiel lié à ces vitesses de propagation. La discussion s'appuie sur des résultats établis sur les ondes progressives. Le dernier chapitre 5 fournit des valeurs numériques biologiquement cohérentes et dérivées des expériences de la littérature pour les paramètres. Cela nous permet d'effectuer des simulations numériques du système, illustrant l'évolution de la population et les calculs de récolte pour une gamme de paramètres.

Mots clés: réaction–diffusion; environnements hétérogènes; distribution libre idéale; contrôle optimal; système proie-prédateur; maladie à transmission vectorielle.

Crédit image en couverture : Intelligence artificielle (Dall-E).

UNIVERSITÉ DE LYON